

ไฮโดรจีเนชันของยางธรรมชาติเร่งปฏิกิริยาด้วย $\text{OsHCl}(\text{CO})(\text{O}_2)(\text{PCy}_3)_2$ และ
 $[\text{Ir}(\text{cod})(\text{PCy}_3)(\text{py})]\text{PF}_6$



นางสาว นพิตา หิญาธิระนันท์

วิทยานิพนธ์นี้เป็นส่วนหนึ่งของการศึกษาตามหลักสูตรปริญญาวิทยาศาสตรดุษฎีบัณฑิต

สาขาวิชาเคมีเทคนิค ภาควิชาเคมีเทคนิค


คณะวิทยาศาสตร์ จุฬาลงกรณ์มหาวิทยาลัย

ปีการศึกษา 2547

ISBN 974-17-6454-5

ลิขสิทธิ์ของจุฬาลงกรณ์มหาวิทยาลัย

HYDROGENATION OF NATURAL RUBBER CATALYZED BY $\text{OsHCl}(\text{CO})(\text{O}_2)(\text{PCy}_3)_2$ AND
 $[\text{Ir}(\text{cod})(\text{PCy}_3)(\text{py})]\text{PF}_6$



Miss Napida Hinchiranan

สถาบันวิทยบริการ
จุฬาลงกรณ์มหาวิทยาลัย

A Dissertation Submitted in Partial Fulfillment of the Requirements
for the Degree of Doctor of Philosophy in Chemical Technology

Department of Chemical Technology

Faculty of Science

Chulalongkorn University

Academic year 2004

ISBN 974-17-6454-5

นพิตา วิทยาระนันท์ : ไฮโดรจิเนชันของยางธรรมชาติเร่งปฏิกิริยาด้วย $\text{OsHCl}(\text{CO})(\text{O}_2)(\text{PCy}_3)_2$ และ $[\text{Ir}(\text{cod})(\text{PCy}_3)(\text{py})]\text{PF}_6$. (HYDROGENATION OF NATURAL RUBBER CATALYZED BY $\text{OsHCl}(\text{CO})(\text{O}_2)(\text{PCy}_3)_2$ AND $[\text{Ir}(\text{cod})(\text{PCy}_3)(\text{py})]\text{PF}_6$) อ. ที่ปรึกษา : ศ.ดร.ภัทรพรรณ ประศาสน์สารกิจ, อ. ที่ปรึกษา ร่วม : Prof. Garry L. Rempel 157 หน้า. ISBN 974-17-6454-5.

โครงสร้างของยางธรรมชาติประกอบด้วยซิส-1,4-พอลิไอโซพรีนเป็นองค์ประกอบหลัก ซึ่งมีความต้านทานต่ำต่อออกซิเดชันและการสลายตัวด้วยโอโซนและความร้อนเนื่องจากพันธะคู่ของคาร์บอน - คาร์บอนในโครงสร้างหลักของพอลิเมอร์ ปฏิกิริยาไฮโดรจิเนชันถูกนำมาใช้เพื่อเพิ่มความต้านทานของพอลิเมอร์ต่อการสลายตัวด้วยความร้อนและออกซิเดชันโดยการลดปริมาณความไม่อิ่มตัวในไดอีนพอลิเมอร์หลายชนิด จุดประสงค์ของงานวิจัยนี้เพื่อศึกษาไฮโดรจิเนชันของยางธรรมชาติเร่งปฏิกิริยาด้วย $\text{OsHCl}(\text{CO})(\text{O}_2)(\text{PCy}_3)_2$ หรือ $[\text{Ir}(\text{cod})(\text{PCy}_3)(\text{py})]\text{PF}_6$ ระดับการเกิดไฮโดรจิเนชันได้จากการวัดด้วยเทคนิคทางโปรตอนนิวเคลียร์แมกเนติกเรโซแนนซ์สเปคโตรสโคปี ข้อมูลทางจลนพลศาสตร์ในเทอมของปริมาณแก๊สไฮโดรเจนที่ถูกใช้ไปเป็นฟังก์ชันกับเวลาได้จากเครื่องแก๊สอ็อปเทค ผลการทดลองทางจลนพลศาสตร์แสดงให้เห็นว่าไฮโดรจิเนชันของยางธรรมชาติซึ่งถูกเร่งด้วยตัวเร่งปฏิกิริยาทั้งสองชนิดนั้นเป็นปฏิกิริยาอันดับหนึ่งขึ้นกับความเข้มข้นของตัวเร่งปฏิกิริยาและเป็นปฏิกิริยาผกผันกับความเข้มข้นของยางธรรมชาติเนื่องจากสิ่งปนเปื้อนในยาง ค่าพลังงานกระตุ้นของปฏิกิริยาไฮโดรจิเนชันของยางธรรมชาติเร่งปฏิกิริยาด้วย $\text{OsHCl}(\text{CO})(\text{O}_2)(\text{PCy}_3)_2$ และ $[\text{Ir}(\text{cod})(\text{PCy}_3)(\text{py})]\text{PF}_6$ มีค่า 122.8 และ 75.6 กิโลจูล/โมลตามลำดับ ข้อมูลทางจลนพลศาสตร์นำไปสู่การเสนอกลไกของปฏิกิริยาไฮโดรจิเนชัน การเติมกรดบางชนิดและสารประกอบไนโตรเจนมีผลกับอัตราการเกิดไฮโดรจิเนชัน เสถียรภาพเชิงความร้อนของยางธรรมชาติถูกปรับปรุงด้วยปฏิกิริยาไฮโดรจิเนชันโดยไม่มีผลกระทบต่ออุณหภูมิคล้ายแก้วของยางผลิตภัณฑ์ น้ำหนักโมเลกุลและการกระจายน้ำหนักโมเลกุลของยางธรรมชาติไฮโดรจิเนตไม่เปลี่ยนแปลงหลังจากการทำปฏิกิริยาไฮโดรจิเนชัน นอกจากนี้ยังได้ศึกษาสมบัติเชิงกลและความต้านทานต่อโอโซนของยางธรรมชาติไฮโดรจิเนตหลังผ่านกระบวนการวัลคาไนเซชันอีกด้วย

ภาควิชา	เคมีเทคนิค	ลายมือชื่อนิติ.....
สาขาวิชา	เคมีเทคนิค	ลายมือชื่ออาจารย์ที่ปรึกษา.....
ปีการศึกษา	2547	ลายมือชื่ออาจารย์ที่ปรึกษาร่วม.....

4373819123 : MAJOR CHEMICAL TECHNOLOGY

KEY WORD: HYDROGENATION / NATURAL RUBBER / HOMOGENEOUS CATALYST / OSMIUM / IRIDIUM

NAPIDA HINCHIRANAN : HYDROGENATION OF NATURAL RUBBER CATALYZED BY $\text{OsHCl}(\text{CO})(\text{O}_2)(\text{PCy}_3)_2$ AND $[\text{Ir}(\text{cod})(\text{PCy}_3)(\text{py})]\text{PF}_6$.
 THESIS ADVISOR : PROF. PATTARAPAN PRASASSARAKICH, THESIS COADVISOR : PROF. GARRY L. REMPEL , 157 pp. ISBN 974-17-6454 -5.

The structure of natural rubber (NR) is comprised of cis-1,4-polyisoprene as the major component which has poor resistance to oxidation and degradation by ozone and long term heating due to the presence of carbon-carbon double bonds in the polymer backbone. Hydrogenation is normally utilized to enhance the resistance of polymers to thermal and oxidative degradation by reducing the amount of unsaturation in various diene polymers. The purpose of the present work is to study the hydrogenation of NR in the presence of $\text{OsHCl}(\text{CO})(\text{O}_2)(\text{PCy}_3)_2$ or $[\text{Ir}(\text{cod})(\text{PCy}_3)(\text{py})]\text{PF}_6$ as a catalyst. The level of hydrogenation was determined via a $^1\text{H-NMR}$ spectroscopic technique. Kinetic data were collected using a computer controlled gas-uptake apparatus in terms of hydrogen consumption as a function of time. The kinetic results indicated that the hydrogenation of NR catalyzed by both catalysts exhibited a first-order behavior with respect to catalyst concentration and an inverse behavior dependence on rubber concentration due to impurities present in the rubber. The apparent activation energy for NR hydrogenation catalyzed by $\text{OsHCl}(\text{CO})(\text{O}_2)(\text{PCy}_3)_2$ and $[\text{Ir}(\text{cod})(\text{PCy}_3)(\text{py})]\text{PF}_6$ were 122.8 and 75.6 kJ/mol, respectively. Mechanistic aspects of NR hydrogenation were derived from the kinetic results. The addition of some acids and certain nitrogen containing materials exhibited an effect on the hydrogenation rate. The thermal stability of NR was improved by hydrogenation without affecting its glass transition temperature. The molecular weight and molecular weight distribution of hydrogenated NR were not changed during hydrogenation. In addition, a study of mechanical properties and ozone resistance of hydrogenated NR after vulcanization process was also investigated.

Department	Chemical Technology	Student's signature.....
Field of study	Chemical Technology	Advisor's signature.....
Academic year	2004	Co-advisor' signature.....

ACKNOWLEDGEMENTS

The author would like to express her gratitude to supervisor, Prof. Pattarapan Prasassarakich, and co-supervisor, Prof. Garry L. Rempel for their encouraging guidance, supervision and helpful suggestion throughout this research. The author also would like to acknowledge Assoc. Prof. Tharapong Vitidsant, Assoc. Prof. Amorn Petsom, Assist. Prof. Krisda Suchiva and Assist. Prof. Khantong Soontarapa for serving as chairman and members of thesis committee, respectively.

The author wishes to express her thankfulness to all people in the associated institutions and companies for their kind assistance and collaboration: Dr. Neil T. McManus for his encouragement and helpful suggestion during this research at University of Waterloo, Canada; Mr. Sarat Chittasonthi, director of Thai Rubber Latex Corporation (Thailand) Public Co., Ltd., the supply of natural rubber throughout this thesis; Mr. Pattanapong Sanguanrak, production technical assist. manager of Pan Innovation Limited, for his suggestion and the chemical supply of rubber vulcanization, Mr. Parin Udomsak, chief engineer of Apollo (Thailand) Co., Ltd., for providing the praffinic oil in blending process, Dr. Kitikorn Charmondusit, Mr. Aungsuthorn Mahittikul and Mr. Natthapong Ngampradit for their assistance during the period of this research.

Many thanks are going to technicians of the Department of Chemical Engineering, University of Waterloo for helping in maintaining the equipment, technicians of the Department of Chemical Technology, Chulalongkorn University, and Rubber Research Institute for assisting in polymer characterization.

Thanks go towards Golden Jubilee Scholarship (Thailand Research Fund) and Natural Science and Engineering Research Council of Canada (NSERC) for financial support of this research.

Finally, the author wishes to express her deep gratitude to her family for their love, support, and encouragement throughout the tenure of her Ph.D. program.

CONTENTS

	PAGE
ABSTRACT (in Thai)	iv
ABSTRACT (in English)	v
ACKNOWLEDGEMENTS	vi
CONTENTS.....	vii
LIST OF TABLES	xi
LIST OF FIGURES	xiii
NOMENCLATURES	xix
CHAPTER 1: INTRODUCTION	1
1.1 Natural Rubber	1
1.2 Chemical Modification via Hydrogenation Diene – Based Polymers.....	5
1.3 Homogeneous Hydrogenation in the Presence of 5d Metal Complexes... ..	8
1.3.1 Catalytic Hydrogenation in the Presence of OsHCl(CO)(PR ₃) ₂ (1a, R = Cy; 1b, R = i-Pr)	9
1.3.2 Catalytic Hydrogenation in the Presence of [Ir(cod)(PCy ₃)(py)]PF ₆ (Crabtree’s Catalyst).....	14
1.4 Catalytic Hydrogenation of Natural Rubber and Synthetic Cis-1,4-Polyisoprene	17
1.5 Vulcanization and Properties of Hydrogenated Rubbers	21
1.6 Objective and Scope	23
CHAPTER 2: EXPERIMENTAL AND CHARACTERIZATION	24
2.1 Materials	24
2.2 Catalyst Preparation	25
2.2.1 OsHCl(CO)(O ₂)(PCy ₃) ₂	25
2.2.2 [Ir(cod)(PCy ₃)(py)]PF ₆	28
2.3 Hydrogenation in Gas Uptake Apparatus.....	29
2.4 Typical Procedure of Kinetic Experiment.....	30
2.5 Typical Hydrogenation Method in 2 Liters Parr Reactor.....	32
2.6 Blend and Vulcanization Process of Rubbers	33
2.7 Characterization Methods.....	33
2.7.1 Fourier Transform Infrared Spectroscopic Analysis.....	33
2.7.2 ¹ H-NMR and ¹³ C-NMR Analysis	33

CONTENTS (continued)

	PAGE
2.7.3 Gel Permeation Chromatography (GPC)	34
2.7.4 Viscosity Measurement.....	34
2.7.5 Thermogravimetric Analysis (TGA).....	34
2.7.6 Differential Scanning Calorimetry (DSC)	35
2.7.7 Cure Characterization	35
2.7.8 Dynamic Mechanical Analysis (DMA)	35
2.7.9 Mechanical Properties.....	35
2.7.10 Ozone Resistance Test	36
2.8 Degree of Hydrogenation Determination	36
CHAPTER 3: HYDROGENATION OF NATURAL RUBBER IN THE	
 PRESENCE OF OsHCl(CO)(O₂)(PCy₃)₂	37
3.1 Structure Characterization Using FTIR and NMR Spectroscopy	38
3.2 Kinetic Experimental Design for Natural Rubber Hydrogenation.....	42
3.2.1 Statistical Analysis Using Two-Level Factorial	
Design Experiments	44
3.2.2 Univariate Kinetic Experiments.....	47
3.2.2.1 Dependence on Catalyst Concentration.....	49
3.2.2.2 Dependence on Rubber Concentration	49
3.2.2.3 Dependence on Hydrogen Pressure.....	52
3.2.2.4 Dependence on Reaction Temperature.....	53
3.2.2.5 Dependence on Solvents.....	56
3.2.3 Effect of Acid Addition on the Catalytic Activity	57
3.3 Mechanistic Interpretation of the Kinetic Data	61
3.4 Relative Viscosity of Hydrogenated Natural Rubber.....	64
CHAPTER 4: HYDROGENATION OF NATURAL RUBBER IN THE	
 PRESENCE OF [Ir(cod)(PCy₃)(py)]PF₆	67
4.1 Structure characterization using FTIR and NMR spectroscopy.....	69
4.2 Kinetic Experiments of Natural Rubber Hydrogenation Compared	
with Synthetic Cis-1,4-Polyisoprene Hydrogenation.....	72
4.2.1 Effect of Catalyst Concentration.....	76

CONTENTS (continued)

	PAGE
4.2.2 Effect of Hydrogen Pressure	77
4.2.3 Effect of Rubber Concentration	79
4.2.4 Effect of Reaction Temperature	80
4.2.5 Effect of Solvents	82
4.2.6 Effect of Acid Addition on the Catalytic Activity	83
4.3 Reaction Mechanism and Rate Law	86
4.4 Relative Viscosity of Hydrogenated Natural Rubber	90
CHAPTER 5: THERMAL ANALYSIS OF HYDROGENATED NATURAL	
RUBBER	93
5.1 Glass Transition Temperature	94
5.2 Decomposition Temperature	96
5.3 Decomposition Kinetics by Thermogravimetry Analysis	98
CHAPTER 6: PHYSICAL AND MECHANICAL PROPERTIES OF	
HYDROGENATED NATURAL RUBBER	105
6.1 Hydrogenation of Natural Rubber in 2-Liter Batch Reactor	105
6.2 Molecular Weight and Molecular Weight Distribution of Hydrogenated Natural Rubber	108
6.3 Blend and Vulcanization Process of Hydrogenated Natural Rubber	110
6.3.1 Blend of Rubbers with Curing Agent	112
6.3.2 Cure Characterization and Color of Vulcanizates	112
6.4 Mechanical Properties of Vulcanized Hydrogenated Natural Rubber	116
6.5 Dynamic Mechanical Properties of Vulcanized Hydrogenated Natural Rubber	119
6.6 Ozone resistance of Vulcanized Hydrogenated Natural Rubber	123
CHAPTER 7: CONCLUSIONS AND RECOMMENDATIONS	129
7.1 Conclusions	129
7.1.1 Hydrogenation of Natural Rubber Catalyzed by $\text{OsHCl}(\text{CO})(\text{O}_2)(\text{PCy}_3)_2$	129
7.1.2 Hydrogenation of Natural Rubber Catalyzed by $[\text{Ir}(\text{cod})(\text{PCy}_3)(\text{py})]\text{PF}_6$	129

CONTENTS (continued)

PAGE

7.1.3 Thermal Analysis of Hydrogenated Natural Rubber	130
7.1.4 Physical and Mechanical Properties of Hydrogenated Natural Rubber	131
7.2 Recommendations	132
REFERENCES	133
APPENDICES	141
Appendix A: The Overall Compositions of Rubbers	142
Appendix B: Calculation of Level of Hydrogenation	143
Appendix C: Derivation of the Rate Law from the Proposed Kinetic Model.....	148
Appendix D: Calculation of Decomposition Kinetic Parameters by Thermogravimetry	149
Appendix E: Steps of Rubber Blending	154
Appendix F: Mechanical Properties of Vulcanizates	155
VITA.....	157

สถาบันวิทยบริการ
จุฬาลงกรณ์มหาวิทยาลัย

LIST OF TABLES

TABLE	PAGE
1.1 Production of Natural Rubber in 2002	2
1.2 Net Exports of Natural Rubber in 2001	2
1.3 Typical Composition of Fresh Latex and Dry Rubber.....	2
3.1 Results from 2 ³ Factorial Design Experiment for NR Hydrogenation	45
3.2 Yate's Algorithm Calculation of the 2 ³ Factorial Experiment.....	46
3.3 Calculation of Effects and Standard Errors for 2 ³ Factorial Design Experiment	47
3.4 Univariate Kinetic Data of NR Hydrogenation Catalyzed by OsHCl(CO)(O ₂)(PCy ₃) ₂	48
3.5 Effect of Nitrogenous Substances on Hydrogenation Rate of Synthetic <i>Cis</i> -1,4-Polyisoprene (PIP)	52
3.6 Effect of Solvent on the NR Hydrogenation.....	56
3.7 Effect of Acid Types and Acid Concentration on the Rate of NR Hydrogenation	58
3.8 Effect of Acid Addition on the Hydrogenation Rate of Synthetic <i>Cis</i> -1,4-Polyisoprene.....	59
4.1 Kinetic Results of Univariate Experiments for NR Hydrogenation Catalyzed by [Ir(cod)(PCy ₃)(py)]PF ₆	75
4.2 Effect of Solvent on Hydrogenation of <i>Cis</i> -1,4-Polyisoprene and Natural Rubber	83
4.3 Effect of Acid Addition on the Rate of Hydrogenation of <i>Cis</i> -1,4-Polyisoprene and Natural Rubber	87
5.1 Analysis of Glass Transition Temperature and Decomposition Temperature of Rubber Samples under the Nitrogen Atmosphere.....	95
5.2 % Mass Loss of Isothermal Degradation of Rubbers Under Nitrogen and Air Atmosphere.....	98
5.3 Decomposition Temperature at Constant % Mass Loss at Various Heating Rate.....	99

LIST OF TABLES (continued)

TABLE	PAGE
5.4 Values of Non-Isothermal Kinetic Parameters for the Thermal Degradation of Rubbers	104
6.1 Effect of Agitator Speed and State of Catalyst on %Hydrogenation.....	107
6.2 Molecular Weight and Molecular Weight Distribution of Natural Rubber and Hydrogenated Natural Rubber at Various %Hydrogenation	110
6.3 Formulation of Mixes for Vulcanization using Brabender Plasticorder.....	113
6.4 Cure Characteristics of Vulcanizates Using Oscillating Disk Rheometer.....	115
6.5 Physical Properties of Vulcanized Rubber Samples.....	117
6.6 Value of Tg, $\tan\delta$ at Tg and Storage Modulus (E') at 30°C of Vulcanized Rubbers	122
6.7 Classification of Cracking on Rubber Surface (Nishi and Nagano, 1983).....	125
6.8 Ozone Cracking of Vulcanized HNR Compared with NR and EPDM	126
A-1 Properties of Standard Thai Rubber 5L (STR-5L)	142
A-2 Properties of Ethylene-Propylene-Diene Copolymer	142
D-1 Degradation Temperatures of Hydrogenated Natural Rubber with 95.6% Hydrogenation at Various Heating Rates	150
D-2 Numerical Integral Constants	152
E-1 Steps of Blending for Each Formulation in Brabender Plasticorder.....	154
F-1 Tensile Strength of Vulcanizates.....	155
F-2 Ultimate Elongation of Vulcanizates	155
F-3 Hardness of Vulcanizates	156

LIST OF FIGURES

FIGURE	PAGE
1.1 Chemical structure of natural rubber	3
1.2 Typical molecular weight distribution of commercial Hevea rubbers.....	3
1.3 Schematic representation of gel phase in rubber	4
1.4 Characterized reactions of OsHCl(CO)(PR ₃) ₂ (1a, R = Cy; 1b, R = <i>i</i> -Pr).....	9
1.5 Coordination mechanism of H ₂ and O ₂ to OsHCl(CO)(PiPr ₃) ₂	10
1.6 Catalytic cycle for the hydrogenation of phenylacetylene to styrene.....	11
1.7 Coordination of hydrogen molecule to OsHCl(CO)(L)(PR ₃) ₂ (1a: R = Cy; 1b: R = <i>i</i> -Pr)	12
1.8 The cationic adduct <i>cis</i> -[IrH ₂ (cod)L ₂] ⁺	16
1.9 Preparation of <i>cis, trans</i> -[IrH ₂ (cod)L ₂]PF ₆ via <i>cis</i> -[IrH ₂ (cod)L ₂]PF ₆	16
1.10 The reaction for producing the cation <i>cis</i> -[IrH ₂ (cod)(PR ₃)py]PF ₆	16
1.11 General structure of natural rubber before and after hydrogenation process....	18
2.1 ¹ H-NMR and ³¹ P{ ¹ H} NMR spectra of OsHCl(CO)(PCy ₃) ₂	26
2.2 ¹ H-NMR, ³¹ P{ ¹ H} NMR and FTIR spectra of OsHCl(CO)(O ₂)(PCy ₃) ₂	27
2.3 ¹ H-NMR spectrum of [Ir(cod)(PCy ₃)(py)]PF ₆	28
2.4 Schematic of gas uptake apparatus	30
3.1 FTIR spectra of (a) NR and (b) HNR catalyzed by OsHCl(CO)(O ₂)(PCy ₃) ₂	39
3.2 ¹ H-NMR spectra of (a) NR and (b) HNR catalyzed by OsHCl(CO)(O ₂)(PCy ₃) ₂	40
3.3 ¹³ C-NMR spectra of (a) NR and (b) HNR catalyzed by OsHCl(CO)(O ₂)(PCy ₃) ₂	41
3.4 Hydrogenation profile of NR obtained from gas uptake apparatus: olefin conversion profiles and (b) first-order ln plot (----- model from linear regression). [Os] = 60 μM (◆) and 100 μM (○); [C=C] = 260 mM; P _{H₂} = 6.9 bar; T = 140°C in monochlorobenzene	43

LIST OF FIGURES (continued)

FIGURE	PAGE
3.5 Effect of catalyst concentration on the rate of NR hydrogenation compared with PIP hydrogenation (Charmondusit et al., 2003). For NR: $[C=C] = 260 \text{ mM}$; $P_{H_2} = 6.9 (\diamond)$, $27.6 (O)$ and $41.4 (+)$ bar; $T = 140^\circ\text{C}$ in monochlorobenzene. For PIP (\bullet): $[C=C] = 260 \text{ mM}$; $P_{H_2} = 20.7 \text{ bar}$ and $T = 130^\circ\text{C}$ in toluene	50
3.6 Effect of rubber concentration on the rate of NR hydrogenation compared with PIP hydrogenation (Charmondusit et al., 2003). For NR (O): $[Os] = 100 \mu\text{M}$; $P_{H_2} = 27.6 \text{ bar}$; $T = 140^\circ\text{C}$ in monochlorobenzene For PIP (\blacksquare): $[Os] = 70 \mu\text{M}$; $P_{H_2} = 20.7 \text{ bar}$; $T = 130^\circ\text{C}$ in toluene	50
3.7 (a) Effect of hydrogen pressure on the rate of NR hydrogenation and the plot of $1/P_{H_2}$ versus the rate constant (2.1-6.9 bar). $[Os] = 100 \mu\text{M}$; $[C=C] = 260 \text{ mM}$; $T = 140^\circ\text{C}$ in monochlorobenzene	54
3.8 (a) Arrhenius plots and (b) Eyring plot for the NR hydrogenation. $[Os] = 100 \mu\text{M}$; $[C=C] = 260 \text{ mM}$ and $P_{H_2} = 27.6 \text{ bar}$	55
3.9 NR hydrogenation conversion profiles of non-acid addition (\blacklozenge) and acid addition systems: $[3\text{-CPA}]/[Os] = 3/1 (\blacktriangle)$ and $[3\text{-CPA}]/[Os] = 12/1 (O)$. $[Os] = 100 \mu\text{M}$; $[C=C] = 260 \text{ mM}$; $P_{H_2} = 27.6 \text{ bar}$; $T = 140^\circ\text{C}$ in toluene.....	59
3.10 Effect of acid type and acid concentration on the NR hydrogenation: the effect of 3-chloropropionic and (b) the effect of p-toluenesulfonic acid in toluene (\blacklozenge) and monochlorobenzene (O). $[Os] = 100 \mu\text{M}$; $[C=C] = 260 \text{ mM}$ and $P_{H_2} = 27.6 \text{ bar}$	60
3.11 Proposed catalytic mechanism for NR hydrogenation in the presence of $OsHCl(CO)(O_2)(PCy_3)_2$	61

LIST OF FIGURES (continued)

FIGURE	PAGE
3.12 (a) Relative viscosity (η_{rel}) of HNR as a function of total metal loading (72.7 - 98.3% hydrogenation): $P_{H_2} = 27.6$ bar, $[C=C] = 260$ mM, $T = 140^\circ C$; (b) Relative viscosity of HNR as a function of rubber concentration (95 - 98% hydrogenation): $[Os] = 100$ μM , $P_{H_2} = 27.6$ bar, $T = 140^\circ C$; (c) Relative viscosity of HNR as a function of hydrogen pressure (93 - 96% hydrogenation): $[Os] = 100$ μM , $[C=C] = 260$ mM, $T = 140^\circ C$; (d) Relative viscosity of HNR as a function of acid-catalyst ratio (95 - 98% hydrogenation): $[Os] = 100$ μM , $[C=C] = 260$ mM, $P_{H_2} = 27.6$ bar, $T = 140^\circ C$ in toluene (Relative viscosity of NR (\square) = 7.54)	65
4.1 FTIR spectra of PIP and NR before and after hydrogenation catalyzed by $[Ir(cod)(PCy_3)(py)]PF_6$	70
4.2 1H -NMR spectra of PIP and NR before and after hydrogenation catalyzed by $[Ir(cod)(PCy_3)(py)]PF_6$	71
4.3 Hydrogenation profile of PIP and NR obtained from gas uptake apparatus: olefin conversion profiles and (b) first-order \ln plot (----- model from linear regression). PIP hydrogenation (\diamond): $[Ir]_T = 90$ μM , $[C=C] = 259.8$ mM; $P_{H_2} = 27.6$ bar at $130^\circ C$ and NR hydrogenation (\blacktriangle): $[Ir]_T = 105$ μM , $[C=C] = 151.9$ mM; $P_{H_2} = 27.6$ bar at $140^\circ C$ in monochlorobenzene	73
4.4 Effect of catalyst concentration on hydrogenation rate. PIP hydrogenation (Charmondusit, 2002) (\blacklozenge): $P_{H_2} = 27.6$ bar, $[C=C] = 246$ mM; $T = 130^\circ C$ and NR hydrogenation (\square): $P_{H_2} = 27.6$ bar, $[C=C] = 152$ mM; $T = 140^\circ C$	77
4.5 Effect of hydrogen pressure on hydrogenation rate. PIP hydrogenation (Charmondusit, 2002) (\blacklozenge): $[Ir] = 90$ μM ; $[C=C] = 246$ mM; $T = 130^\circ C$ and NR hydrogenation (\square): $[Ir] = 105$ μM ; $[C=C] = 152$ mM; $T = 140^\circ C$	78
4.6 Effect of rubber concentration on hydrogenation rate. PIP hydrogenation (Charmondusit, 2002) (\blacklozenge): $[Ir] = 90$ μM ; $P_{H_2} = 27.6$ bar; $T = 130^\circ C$ and NR hydrogenation (\square): $[Ir] = 105$ μM ; $P_{H_2} = 27.6$ bar; $T = 140^\circ C$	80

LIST OF FIGURES (continued)

FIGURE	PAGE
4.7 (a) Arrhenius plot and (b) Eyring plot for PIP and NR hydrogenation. PIP hydrogenation (Charmondusit, 2002) (◆): [Ir] = 90 μM; P _{H₂} = 27.6 bar; [C=C] = 246 mM; T = 120-140°C and NR hydrogenation (□): [Ir] = 105 μM; P _{H₂} = 27.6 bar; [C=C] = 152 mM; T = 130-150°C	81
4.8 Comparison NR hydrogenation conversion profiles between non-acid addition (◆) and acid addition systems: [3-CPA]/[Ir] = 21/1 (▲) and [p-TSA]/[Ir] = 20/1 (○). [Ir] = 105 μM; [C=C] = 152 mM; P _{H₂} = 27.6 bar; T = 140°C in monochlorobenzene	84
4.9 Proposed catalytic mechanism for PIP hydrogenation in the presence of [Ir(cod)(py)(PCy ₃)]PF ₆	88
4.10 Proposed catalytic mechanism for NR hydrogenation in the presence of [Ir(cod)(py)(PCy ₃)]PF ₆	88
4.11 (a) Relative viscosity as a function of total metal loading, HPIP: P _{H₂} = 27.6 bar; [C=C] = 246 mM; T = 130°C and HNR: P _{H₂} = 27.6 bar; [C=C] = 152 mM; T = 140°C. (b) Relative viscosity as a function of polymer loading, HPIP: [Ir] = 90 μM; P _{H₂} = 27.6 bar; T = 130°C and HNR: [Ir] = 105 μM; P _{H₂} = 27.6 bar; T = 140°C. (c) Influence of hydrogen pressure on relative viscosity, HPIP: [Ir] = 90 μM; [C=C] = 246 mM; T = 130°C and HNR: [Ir] = 105 μM; [C=C] = 152 mM; T = 140°C	91
5.1 DSC thermograms of NR and HNR catalyzed by OsHCl(CO)(O ₂)(PCy ₃) ₂ at various % hydrogenation. (a) 0.0%; (b) 37.9%; (c) 52.2%; (d) 79.1%; (e) 91.9% and (f) 99.7%	95
5.2 TGA thermograms of NR and HNR catalyzed by OsHCl(CO)(O ₂)(PCy ₃) ₂ at various % hydrogenation. (a) 0.0%; (b) 37.9%; (c) 52.2%; (d) 79.1%; (e) 91.9% and (f) 99.7%	97

LIST OF FIGURES (continued)

FIGURE	PAGE
5.3 (a) Nonisothermal kinetics and (b) Arrhenius plot of heating rate versus the reciprocal decomposition temperature of NR	101
5.4 (a) Nonisothermal kinetics and (b) Arrhenius plot of heating rate versus the reciprocal decomposition temperature of HNR (95.6% hydrogenation) ..	102
5.5 (a) Nonisothermal kinetics and (b) Arrhenius plot of heating rate versus the reciprocal decomposition temperature of EPDM (Keltan 314)	103
6.1 Effect of catalyst and acid types on %hydrogenation: Os/3-CPA: [NR]/[Os] = 6398 and [3-CPA]/[Os] = 47 in toluene; Ir/p-TSA: [NR]/[Ir] = 4976 and [p-TSA]/[Ir] = 40 in chlorobenzene; Os/p-TSA: [NR]/[Os] = 6398 and [p-TSA]/[Os] = 30 in toluene ($P_{H_2} = 27.6$ bar at 140°C)	107
6.2 Surface color of hydrogenated natural rubber from each system ((b) – (d) captured by CCD camera): (a) natural rubber, (b) Os/3-CPA (82.1% hydrogenation), (c) Ir/p-TSA (43.9% hydrogenation) and (d) Os/p-TSA (85.0% hydrogenation)	108
6.3 GPC chromatograms of natural rubber samples before and after hydrogenation at various %hydrogenation	110
6.4 Rheographs of vulcanizates: (a) pure rubbers and (b) rubber blends between HNR90 and NR	115
6.5 Color of vulcanized rubbers cured by (1) CBS/TMTD system and (2) MBT/TMTD system.....	116
6.6 Mechanical properties before and after heat aging at 100°C for 22 h of hydrogenated natural rubber compared with natural rubber and EPDM (Keltan 509x100).....	118
6.7 Temperature dependence of (a) the storage modulus (E') and (b) the loss tangent ($\tan \delta$) for hydrogenated natural rubber at various level of hydrogenation (ca. 60%, 80% and 90% hydrogenation) compared with natural rubber and EPDM after vulcanization using MBT/TMTD as accelerators	120

LIST OF FIGURES (continued)

FIGURE		PAGE
6.8	Storage modulus behaviors as the function of temperature for various structural changes in polymers.....	122
6.9	Possible reactions following ozonolysis of a diene-containing polymer.....	123
6.10	Surface of rubbers vulcanized by CBS/TMTD curing system after exposure to ozone at 40°C for 48 h: (a) NR and (b) HNR at 94±3% hydrogenation	126
6.11	Surface of rubbers vulcanized by MBT/TMTD curing system after exposure to ozone for 48 h (captured by CCD camera).....	126


 สถาบันวิทยบริการ
 จุฬาลงกรณ์มหาวิทยาลัย

NOMENCLATURES

A	:	Pre-Exponential Factor
CBS	:	<i>N</i> -Cyclohexylbenzthiazylsulphenamide
CCD Camera	:	Charge Coupled Devices Camera
cod	:	1,5-cyclooctadiene
3-CPA	:	3-Chloropropionic acid
DMA	:	Dynamic Mechanical Analysis
DSC	:	Differential Scanning Calorimetry
E'	:	Storage or Elastic Modulus
E''	:	Loss or viscous Modulus
EPDM	:	Ethylene – Propylene Copolymer
FTIR	:	Fourier Transform Infrared Spectroscopy
GPC	:	Gel Permeation Chromatography
HNR	:	Hydrogenated Natural Rubber
HPIP	:	Hydrogenated <i>Cis</i> -1,4-Polyisoprene
HSBR	:	Hydrogenated Styrene – Butadiene Rubber
Ir	:	Iridium
k'	:	Pseudo-First-Order Rate Constant
MBT	:	2 - Mercaptobenzothiazole
MCB	:	Monochlorobenzene
MWD	:	Molecular Weight Distribution
NBR	:	Acrylonitrile – Butadiene Rubber
NMR	:	Nuclear Magnetic Resonance Spectroscopy
NR	:	Natural Rubber
ODR	:	Oscillating Disk Rheometer
Os	:	Osmium
PBD	:	Polybutadiene
PCy ₃	:	Tricyclohexylphosphine
Pd	:	Palladium
PIP	:	Synthetic <i>Cis</i> -1,4-Polyisoprene
PiPr ₃	:	Triisopropylphosphine
pphm	:	Part Per Hundred Million

NOMENCLATURES (continued)

p-TSA	:	<i>p</i> -Toluenesulfonic acid
Rh	:	Rhodium
Ru	:	Ruthenium
SBR	:	Styrene – Butadiene Rubber
T _g	:	Glass Transition Temperature
T _{id}	:	Initial Decomposition Temperature
T _{max}	:	Maximum Decomposition Temperature
tan δ	:	Loss angle or ratio of E'' to E'
TGA	:	Thermogravimetric Analysis
TMTD	:	Tetramethyl thiuram disulphide
x	:	Extent of Hydrogenation
X	:	Impurities in Natural Rubber
ZnO	:	Zinc Oxide
α	:	Mass Loss Value (% Mass Loss/100)
β	:	Heating Rate (K/min)
η _{rel}	:	Relative Viscosity

CHAPTER 1

INTRODUCTION

1.1 Natural Rubber

Natural rubber is an important industrial material for a variety of applications; especially in the tire industry. The most common source of natural rubber is obtained by tapping the *Hevea brasiliensis* or Para rubber tree, indigenous to forests in the Amazon valley. Although natural rubber can be obtained from more than 200 different species of plants, none could compete with Hevea rubber in yield, frequency of tapping, or longevity (Morton, ed., 1987). Southeast Asia has become a dominant producer of natural rubber since 1913 (Morton, ed., 1999). Thailand has been the world's leader in natural rubber production and exportation during the last decade followed by Indonesia and Malaysia as shown in Table 1.1 and 1.2.

Natural rubber latex consists of particles of rubber hydrocarbon and non-rubber components suspended in an aqueous phase. A typical composition of a natural rubber latex and dry rubber is shown in Table 1.3. The major polymer structure component of natural rubber determined by using infrared, nuclear magnetic resonance (NMR) and X-ray is polyisoprene with the isoprene unit being *cis*-1,4 configuration of about 94%. The major contaminants in natural rubber are proteins (ca. 2.2%) and lipids (ca. 3.4%). Tanaka (2001) reported that the rubber chain is composed of unidentified initiating terminal groups, two *trans* isoprene units and a long chain of *cis*-isoprene units terminated with unidentified chain end groups. The unidentified initiating and chain end groups are possibly an oligopeptide (ω') and a fatty acid ester (α'), respectively. The chemical structure of natural rubber is presented in Figure 1.1.

Table 1.1 Production of Natural Rubber in 2002 (Thai Rubber Association, 2003)

Country	January	February	March	Total
Thailand	226.0	209.0	194.0	629.0
Indonesia	127.2	125.6	141.5	394.3
Malaysia	56.8	51.1	38.6	146.5
Vietnam	33.0	32.0	27.0	92.0
Others	147.0	112.3	108.9	368.2
Total	630	570	550	1750.0

Unit: thousand tons

Table 1.2 Net Exports of Natural Rubber in 2001 (Thai Rubber Association, 2003)

Country	Jan.	Feb.	Mar.	Apr.	May	Jun.	Jul.	Aug.	Sep.	Oct.	Nov.	Dec.	Total
Thailand	146.4	178.0	165.2	130.1	157.0	180.8	180.0	195.0	155.6	200.0	190.0	180.0	2059.2
Indonesia	97.3	104.7	112.5	104.7	138.3	96.0	140.0	176.7	127.7	118.8	83.0	120	1419.7
Malaysia	13.3	-0.8	30.4	17.2	2.7	0.6	-17.2	16.4	19.5	32.4	28.7	18.8	162.1
Vietnam	23.0	240	24.0	25.0	250	250	260	25.0	24.0	24.0	24.0	24.0	293.0
Sri Lanka	3.0	2.7	3.6	2.7	2.7	2.1	2.5	3.4	2.8	1.5	2.0	2.5	31.5
Others	87.0	101.4	84.3	90.3	94.3	95.5	108.7	93.5	100.4	73.3	72.3	54.7	1054.5
Total	370	410	420	370	420	400	440	510	430	450	400	400	5020

Unit: thousand tons

Table 1.3 Typical Composition of Fresh Latex and Dry Rubber (Morton, ed., 1999)

	Latex, %	Dry Rubber, %
Rubber hydrocarbon	36	93.7
Proteins	1.4	2.2
Carbohydrates	1.6	0.4
Neutral lipids	1.0	2.4
Glycolipids + phospholipids	0.6	1.0
Inorganic constituents	0.5	0.2
Others	0.4	0.1
Water	58.5	-

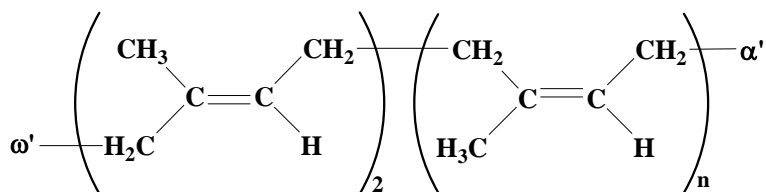


Figure 1.1 Chemical structure of natural rubber.

Hevea rubber is a high molecular weight polymer with broad molecular weight distribution. The molecular weight of *Hevea* rubber analyzed by gel permeation chromatography (GPC) shows a bimodal distribution (Tanaka, 1989). The difference in molecular weight distribution (MWD) of commercial *Hevea* rubbers is shown in Figure 1.2. The distributions of various clonal *Hevea* rubbers are classified into three types:

Type A: distinctly bimodal distribution with nearly equal peak height.

Type B: bimodal distribution with small low molecular weight peak

Type C: skewed unimodal distribution with a shoulder.

The high molecular weight peak in the MWD appears around $1 - 2.5 \times 10^6$, while the peak at around $1 - 2 \times 10^5$ is attributed to the low molecular weight component. The average molecular weight is $M_w = 1.6 - 2.3 \times 10^6$ and $M_n = 2.0 - 5.2 \times 10^5$. The polydispersity index is very wide ranging from 2.8 to 10.

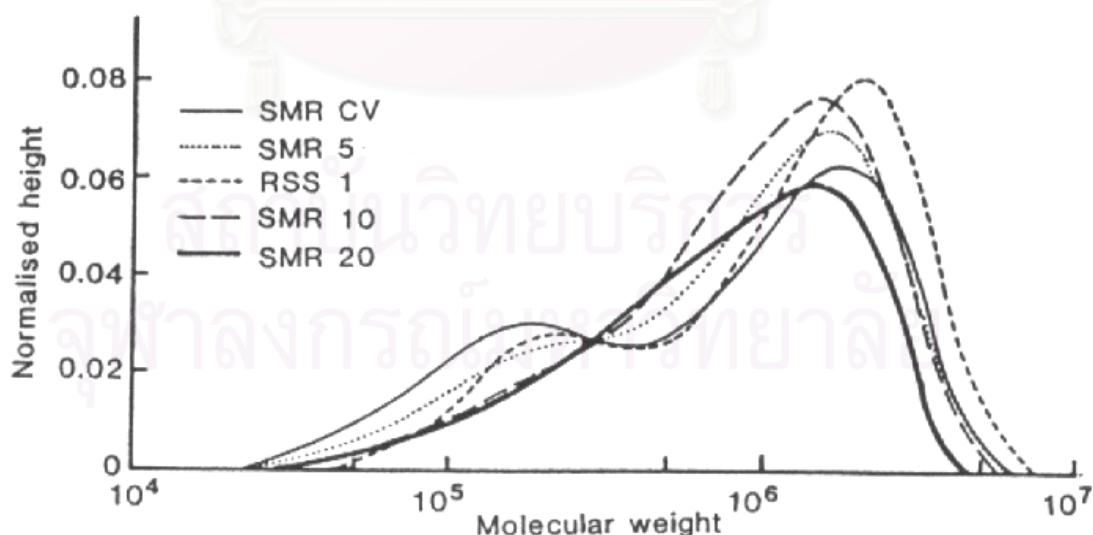


Figure 1.2 Typical molecular weight distribution of commercial *Hevea* rubbers (Subramaniam, 1975 cited in Tanaka, 1989).

The broad MWD of *Hevea* rubber is presumed to be associated with branching and crosslinking of some functional groups within natural rubber. Generally, natural rubber is composed of two components called “sol” and “gel”. The sol phase relates to the rubber fraction that can be dissolved easily in good solvents such as cyclohexane, toluene, tetrahydrofuran, etc., without much preliminary swelling, while the gel phase contains the rubber part that swells without dissolving. *Hevea* rubber contains 5 – 50% gel phase, depending on the clonal origin of the rubber, processing conditions and the time and temperature of storage (Tanaka, 1989). Allen et al. (1963) reported that the true gel phase in natural rubber consists of small crosslinked latex particles or microgels, which are combined into a matrix with the sol fraction and then form an apparent gel phase as shown in Figure 1.3. The gel is a result of branching which occurs from abnormal functional groups inside the natural rubber such as aldehydes, epoxides and lactones. The nitrogenous components might have an important role in formation of crosslinking points in the gel fraction via hydrogen bonding (Sehhar, 1962; Burfield, 1974; Gregg and Macey, 1973 cited in Tankpakdee and Tanaka, 1997).

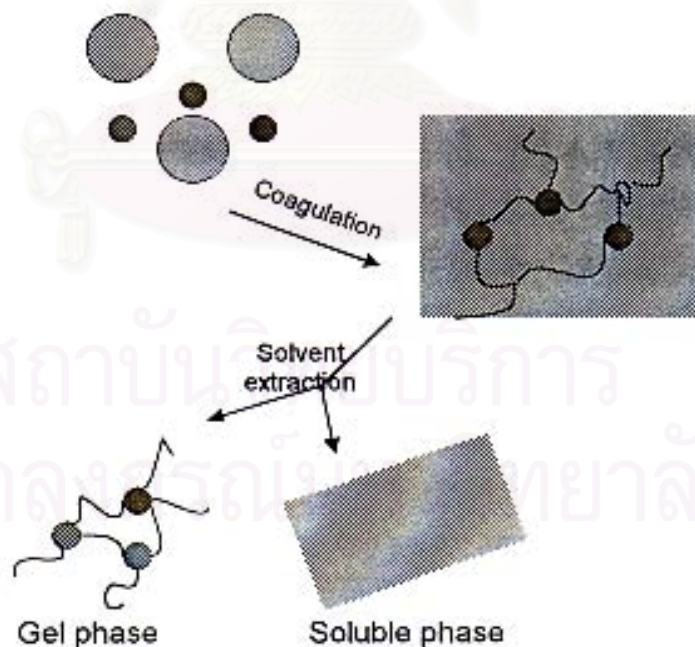


Figure 1.3 Schematic representation of gel phase in rubber. (Allen et al., 1963).

Nowadays, the demand for natural rubber in the commercial market receives competition from synthetic rubbers such as styrene-butadiene rubber and synthetic polyisoprene since it is not possible to control the quality of natural rubber during its polymerization process unlike that of synthetic rubbers which have the specific pendent groups to improve some physical and chemical properties of rubbers. However, natural rubber is still used in many applications due to the following reasons: superior building tack, green stock strength, superior processing, high strength in nonblack formulations, hot tear resistance, retention of strength at elevated temperature, high resilience, low hysteresis, excellent dynamic properties, and general fatigue resistance (Morton, ed., 1987). Due to the unsaturation of carbon – carbon double bonds of the isoprene backbone, natural rubber deteriorates when exposed to sunlight, ozone and oxygen. Thus, it is necessary to improve natural rubber to have better chemical resistance properties so that it might be competitive with synthetic rubbers.

1.2 Chemical Modification via Hydrogenation of Diene – Based Polymers

The chemical modification of polymers has been an interesting method to improve or produce novel polymeric materials, which are inaccessible or difficult to prepare by conventional polymerization processes. Chemical modifications such as crosslinking, grafting, degradation, oxidation, isomerization, and cyclization have been studied for altering and optimizing the physical and mechanical properties of polymers (Bhowmick and Stephens, eds., 1988; McManus and Rempel, 1995). Diene-based polymers e.g., polyisoprene (PI), polybutadiene (PBD), nitrile butadiene rubber (NBR) including natural rubber (NR) have the presence of unsaturated carbon – carbon double bond in the backbone structure. The residual carbon – carbon double bonds in the polymer structure is susceptible to thermal and oxidative degradation when exposed to harsh operating systems, resulting in a decline of the structural properties of the polymers.

Hydrogenation, one type of chemical modification of unsaturated polymers, is an important method to reduce the amount of unsaturation; consequently, the structure of the hydrogenated polymer has better resistance to thermal and oxidative degradation. Significant examples of hydrogenated polymer products in the

commercial synthetic rubber market are hydrogenated styrene-butadiene rubber (HSBR) produced by Shell under the tradename “Kraton” and hydrogenated acrylonitrile-butadiene rubber (HNBR) manufactured by Zeon Chemicals and Bayer Inc. under the tradename “Therban”. Both of these hydrogenated rubbers have excellent high temperature stability and resistance to oxygen, ozone and ultraviolet radiation, which are far superior to those of the parent rubbers (McManus and Rempel, 1995).

Hydrogenation of polymers can be performed by both catalytic and non-catalytic methods. There are also some research reports involving the non-catalytic hydrogenation by using diimide reduction, which is generated from *p*-toluenesulfonylhydrazide (Nang et al., 1975). The advantage of this method over others is not to require specialized hydrogenation reactor and high pressure hydrogen (McManus and Rempel, 1995). However, hydrogenation via diimide reduction is not able to completely saturate the 1,4-double bond and it also promotes *cis-trans* isomerization of the residual 1,4 units. In addition, depolymerization and cyclization of *cis*-1,4-polyisoprene have been observed by using this method. To avoid these side reaction problems, catalytic hydrogenation, via heterogeneous and homogeneous catalysts, has been more widely studied for diene based polymers. Heterogeneous hydrogenation catalysts use insoluble transition metals e.g. Pd to promote the hydrogen addition to the carbon double bond. Good catalysts provide fair high conversion and they are easier to remove from the product than homogeneous hydrogenation catalysts. However, heterogeneous catalysts reaction rates are generally slower than that of homogeneous ones in solution system. Many of the new developments in the field of catalytic hydrogenation have involved the use of homogeneous catalysts because they have higher selectivity and do not have the macroscopic diffusion problems. In addition, the performance of homogeneous catalyst are more easily explained and understood on the molecular level (Bhaduri and Mukesh, 2000). The selection of an optimum catalyst for a given system is dependent on the selectivity of the catalyst to specific functional groups in the polymer chain, e.g., selective hydrogenation of C=C without any reduction of CN or CO₂H groups. Moreover, ease of handling the catalyst and its cost are also important factors to be considered for choosing a suitable catalyst for a particular system (McManus and Rempel, 1995).

There are many research reports for the hydrogenation of synthetic diene-based polymers such as polybutadiene, styrene-butadiene copolymers (SBR) and acrylonitrile-butadiene copolymers (NBR). Such reactions are catalyzed by homogeneous catalysts composed of transition metal complexes containing Rh, Ru, Pd or Os as well as metallocenes including Ziegler-Natta type catalysts.

The Wilkinson's catalyst, $\text{RhCl}(\text{PPh}_3)_3$, has been well known to be an effective catalyst with high selectivity for hydrogenation of olefins containing other functional groups such as $-\text{CN}$ or $>\text{C}=\text{O}$. $\text{RhCl}(\text{PPh}_3)_3$ can be produced in high yield and it is easy to handle because of its excellent air stability as a dry solid. Mohammadi and Rempel (1989) studied the kinetics of polybutadiene hydrogenation catalyzed by $\text{RhCl}(\text{PPh}_3)_3$. The kinetic data for the hydrogenation were obtained using automated gas-uptake apparatus (Mohammadi and Rempel, 1987). They found that the polybutadiene hydrogenation exhibited a first-order dependence on carbon-carbon double bond concentration, catalyst and hydrogen concentration. In 1996, the kinetics of hydrogenation of NBR catalyzed by $\text{RhCl}(\text{PPh}_3)_3$ and $\text{RhH}(\text{PPh}_3)_4$ was investigated by Parent et al. (1996). The results indicated that the hydrogenation reaction was inverse first-order with respect to nitrile concentration. Moreover, another advantage of these Rh complexes for NBR hydrogenation is that the relative viscosity of hydrogenated product was constant when the polymer and catalyst loading was increased (Parent et al., 2001). This viscosity result implies that these complexes did not promote crosslinking or gel formation of NBR. Although Rh complexes are excellent catalysts for hydrogenation, a major practical drawback is the high cost of Rh. In order to achieve quantitative hydrogenation of $\text{C}=\text{C}$ in the presence of $\text{RhCl}(\text{PPh}_3)_3$, the hydrogenation process needs to have an excess of PPh_3 to prevent the formation of a binuclear Rh complex which is inactive for the hydrogenation.

Ruthenium complexes are potentially practical alternative for catalytic hydrogenation of unsaturated polymers because the cost of Ru is ca. one-thirtieth that of Rh. Rao et al. (2001) reported that $\text{RuCl}_2(\text{PPh}_3)_3$ was an effective catalyst for polybutadiene hydrogenation. Unlike in the case of the $\text{RhCl}(\text{PPh}_3)_3$, the $\text{RuCl}_2(\text{PPh}_3)_3$ was able to catalyze the hydrogenation, without PPh_3 addition, and maintain the catalytic activity. Martin et al. (1997) studied the kinetics of NBR hydrogenation catalyzed by $\text{Ru}(\text{X})\text{Cl}(\text{CO})\text{L}_2$ where $\text{X} = \text{H}$ or β -styryl ($\text{CH}=\text{CH}(\text{Ph})$)

and L was a bulky phosphine such as tricyclohexyl or triisopropyl-phosphine. In addition, Ru complexes have been found to be active for direct use in the hydrogenation of NBR emulsions without the step of NBR precipitation after emulsion polymerization process. This represents a possible economic advantage for industrial production of hydrogenated NBR (Guo and Rempel, 1997). Although Ru complexes are efficient catalysts for polymer hydrogenation, their activity is less than that of analogous Rh complexes for hydrogenation of internal C=C; therefore, it is necessary to operate the reaction under higher temperature and pressure. Moreover, Ru catalysts can promote gel formation in NBR hydrogenation due to very slight reduction of the -CN group to secondary amines (Braun et al., 1988 cited in McManus and Rempel, 1995).

1.3 Homogeneous Hydrogenation in the Presence of 5d Metal Complexes

Generally, the Groups VIII 4d transition metals in the second row of the periodic table, namely Rh, Ru and Pd, are well known to be used as catalysts for hydrogenation of unsaturated polymers. The potential reactivity of 5d transition metals in the third row of the periodic table, for homogeneous catalytic transformation has hitherto been little exploited. Presumably, the reactions typically confirming catalytic cycles such as Lewis base addition-elimination, oxidative addition-reductive elimination, insertion-deinsertion of the third row metal complexes are slower than their 4d congeners because 5d metals usually form more stable catalytic complexes. A judicious choice of the metal-ligand system may lead to highly efficient catalyst (Delgado et al., 1995). Certain osmium and iridium complexes have been found to be high efficient catalysts for hydrogenation of alkene and alkyne substrates as well as diene-based elastomers.

1.3.1 Catalytic Hydrogenation in the Presence of $\text{OsHCl}(\text{CO})(\text{PR}_3)_2$ (1a, R = Cy; 1b, R = *i*-Pr)

The square – pyramidally pentacoordinated osmium complex, $\text{OsHCl}(\text{CO})(\text{PR}_3)_2$, has been discovered by Moers (1971). Figure 1.4 shows the structure of osmium complexes with the bulky phosphines *trans* positioned within a plane shared by Cl and CO. It has been shown that the osmium centre lies essentially in the basal plane of 1a and the other ligands such as O_2 , H_2 , olefin and –CN can coordinate to the Os metal at the vacant coordination site *trans* to the hydride to give the six-coordinate complexes (Moers, 1984; Esteruelas and Werner, 1986). There is no evidence for the coordination of a third phosphine or a phosphite ligand to either 1a or 1b (Moers, 1971; Esteruelas and Werner, 1986).

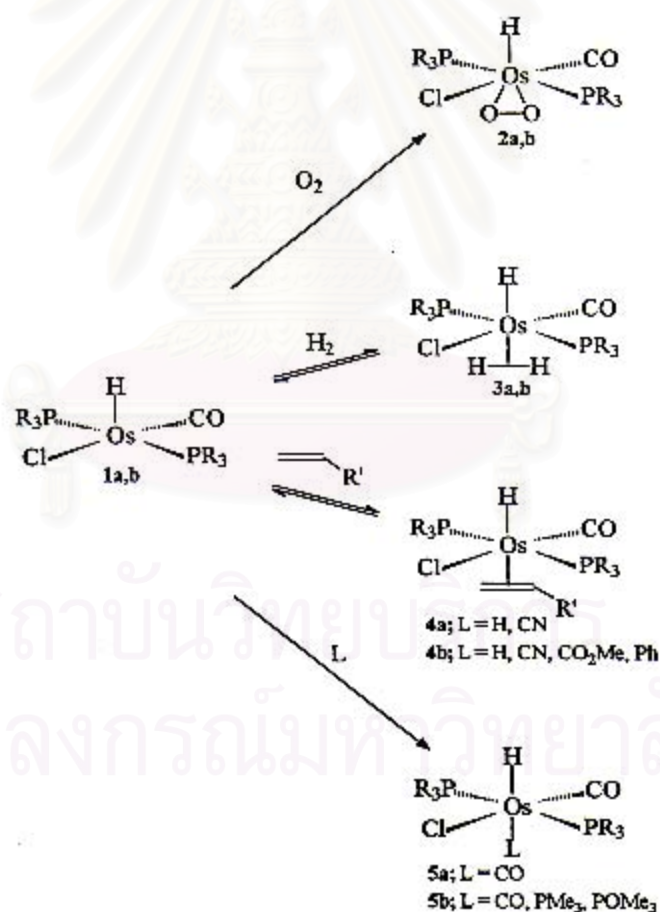


Figure 1.4 Characterized reactions of $\text{OsHCl}(\text{CO})(\text{PR}_3)_2$ (1a, R = Cy; 1b, R = *i*-Pr) (Moers, 1971).

As shown in Figure 1.4, the solid form of 1a and 1b binds the small (diatomic) molecules, H_2 and O_2 , to osmium. The osmium complex, $\text{OsHCl}(\text{CO})(\text{P}i\text{Pr}_3)_2$, was found to react with H_2 or O_2 under ambient conditions (25°C , 1 bar) in benzene as shown in Figure 1.5 (Esteruelas et al., 1988). In both cases, the initially red benzene solution of $\text{OsHCl}(\text{CO})(\text{P}i\text{Pr}_3)_2$ changed rapidly to colorless. The infrared spectrum of the benzene solution of this osmium complex indicated a strong absorption for a CO stretching vibration at 1913 cm^{-1} , which was shifted by ca. 25 cm^{-1} to higher wavenumbers compared with that of $\text{OsHCl}(\text{CO})(\text{P}i\text{Pr}_3)_2$. Upon removal of the H_2 atmosphere, $\text{OsHCl}(\eta^2\text{-H}_2)(\text{CO})(\text{P}i\text{Pr}_3)_2$ slowly transformed back into the original complex; however, this reaction occurs very rapidly under vacuum. To suspend $\text{OsHCl}(\text{CO})(\text{P}i\text{Pr}_3)_2$ in 2-propanol under air or oxygen atmosphere, the dioxygen ligand resulted in displacement of H_2 from $\text{OsHCl}(\eta^2\text{-H}_2)(\text{CO})(\text{P}i\text{Pr}_3)_2$ to $\text{OsHCl}(\eta^2\text{-O}_2)(\text{CO})(\text{P}i\text{Pr}_3)_2$. The infrared spectra of $\text{OsHCl}(\eta^2\text{-O}_2)(\text{CO})(\text{P}i\text{Pr}_3)_2$ showed an absorption band $\nu(\text{O-O})$ at 837 cm^{-1} , suggesting the possibility of a η^2 -peroxo coordination mode (Andriollo et al., 1989). This dioxygen ligand is very strongly bound. It indicates that the dioxygen osmium complex has stability even under high vacuum. The *trans* position of O_2 is relative to the hydride ligand. The O_2 ligand is a very good σ donor; thus, it is probably responsible for this strong binding (Esteruelas et al., 1988).

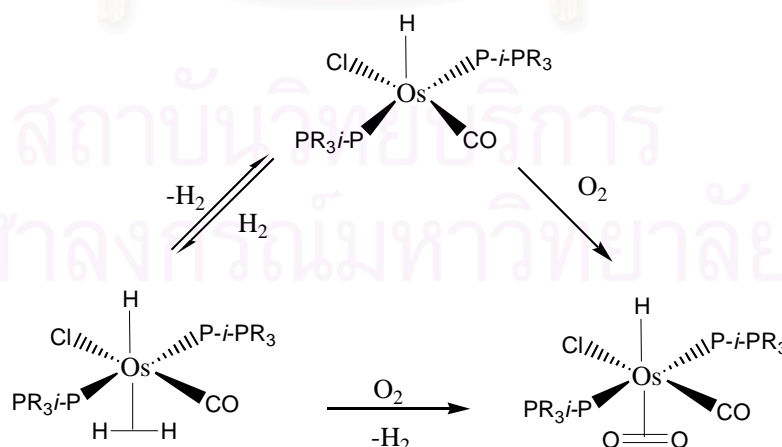


Figure 1.5 Coordination mechanism of H_2 and O_2 to $\text{OsHCl}(\text{CO})(\text{P}i\text{Pr}_3)_2$ (Esteruelas et al., 1988).

Andriollo et al. (1989) studied the kinetics and investigated the mechanism of the sequential hydrogenation of phenylacetylene catalyzed by $\text{OsHCl}(\text{CO})(\text{PR}_3)_2$ [$\text{PR}_3 = \text{PMe-}t\text{-Bu}_2$ and $\text{P-}i\text{-Pr}_3$]. The dioxygen adducts, $\text{OsHCl}(\eta^2\text{-O}_2)(\text{CO})(\text{PR}_3)_2$, were applied as the catalytic precursors for this system. Kinetic data indicated that a trishydrido(alkene)osmium or trihydrido(alkyne)osmium complex occurred as intermediate via an insertion reaction to give an alkyl or vinyl species. The catalytic cycle for the hydrogenation of phenylacetylene to styrene in the presence of $\text{OsHCl}(\eta^2\text{-H}_2)(\text{CO})(\text{PR}_3)_2$ is shown in Figure 1.6.

The osmium complexes, $\text{OsHCl}(\text{CO})(\text{PR}_3)_2$, is not only active for hydrogenation of small molecule olefins, but it is also an efficient catalyst for hydrogenation of diene-based polymers such as acrylonitrile-butadiene rubber (NBR) and synthetic polyisoprene.

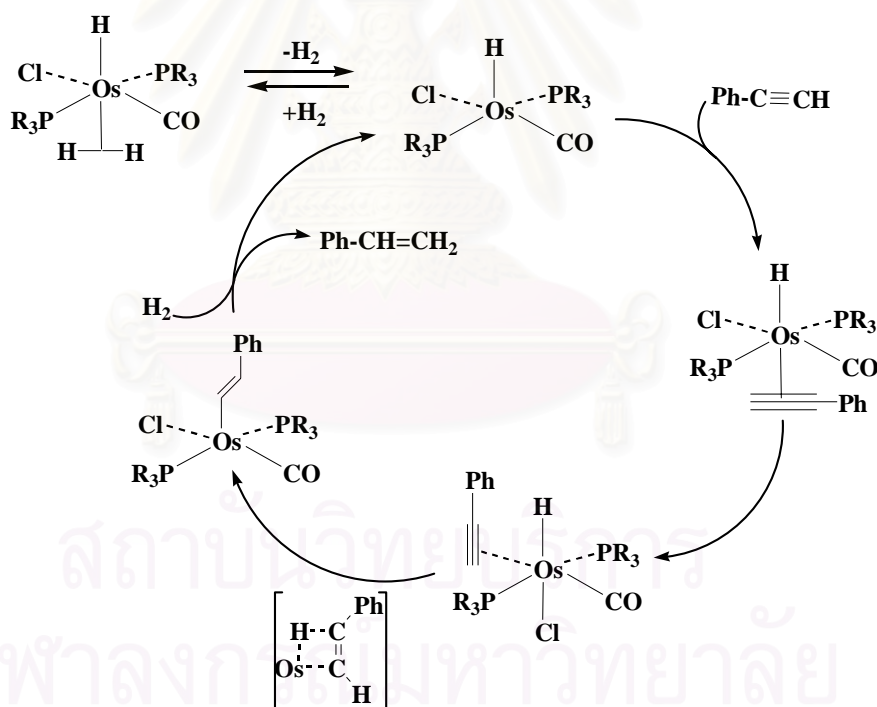


Figure 1.6 Catalytic cycle for the hydrogenation of phenylacetylene to styrene (Andriollo et al., 1989).

Parent et al. (1998a) have discovered that the complexes, $\text{OsHCl}(\text{CO})\text{L}(\text{PR}_3)_2$ ($\text{L} = \text{vacant}, \text{O}_2$; $\text{R} = \text{Cy}, i\text{-Pr}$), are highly catalytically active for selective hydrogenation of NBR. These complexes were much more highly efficient than Ru, Rh and Pd systems under industrial conditions normally used in the hydrogenated NBR industry ($P > 20 \text{ bar}, T > 100^\circ\text{C}$). They found that nitrile within NBR was not only able to inhibit the reactivity of catalyst due to a competitive coordination of nitrile to the metal center but also generated an unprecedented sensitivity of the process to pressure. The NBR hydrogenation reaction showed a first order dependence on the carbon double bond concentration and catalyst concentration, implying that the active complex is mononuclear. The second order behavior observed with respect to hydrogen concentration, which diminished toward a zero order dependence at pressures higher than 60 bar was induced by nitrile coordination to the metal center. In contrast, hydrogenation of substrates without nitrile functional group such as SBR and decene was independent of hydrogen pressure. The proposed catalytic mechanism of NBR hydrogenation was involved the dissociation of O_2 and the addition of H_2 and $\text{R}'\text{CN}$ to $\text{OsHCl}(\text{CO})\text{L}(\text{PR}_3)_2$ (1a: $\text{R} = \text{Cy}$; 1b: $\text{R} = i\text{-Pr}$). Under 24 bar of hydrogen pressure, the dioxygen ligand of $\text{OsHCl}(\text{CO})\text{L}(\text{PR}_3)_2$ was displaced by η^2 -coordination of H_2 to produce the *trans*-hydridodihydrogen complexes, $\text{OsHCl}(\eta^2\text{-H}_2)(\text{CO})\text{L}(\text{PR}_3)_2$ (3a,b), as shown in Figure 1.7. Complexes 1a,b reacted reversibly with aryl and alkyl nitriles to produce the isolable complexes, $\text{OsHCl}(\text{CO})(\text{R}'\text{CN})(\text{PR}_3)_2$. It is also reported that the phosphine ligand exchanged with unbound, bulky alkyl phosphine caused the slow reaction rate (Parent et al., 1998a).

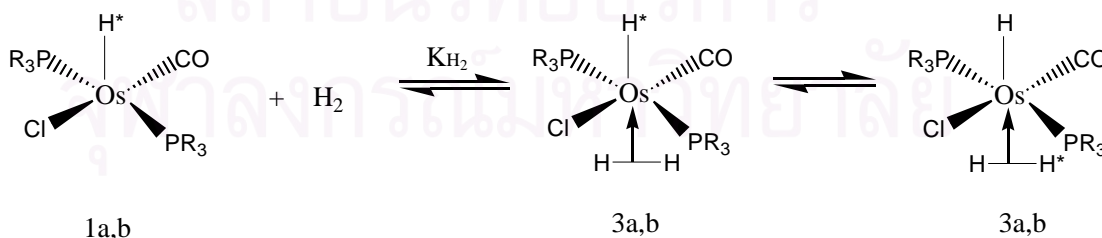


Figure 1.7 Coordination of hydrogen molecule to $\text{OsHCl}(\text{CO})\text{L}(\text{PR}_3)_2$ (1a: $\text{R} = \text{Cy}$; 1b: $\text{R} = i\text{-Pr}$) (Parent et al., 1998a).

Mao and Rempel (2000) studied the effect of various phosphine ligands on osmium complexes, $\text{OsHCl}(\text{CO})(\text{O}_2)(\text{PR}_3)_2$, on the catalytic activity for NBR hydrogenation. The complexes studied were classified into three classes. Class I was the bulky monophosphines with Tolman's cone angle $\geq 160^\circ$ such as $\text{P-}i\text{-Pr}_3$, PCy_3 and PCy_2Ph . Class II involved smaller monophosphines such as PPh_3 and $\text{P}(m\text{-C}_6\text{H}_4\text{Me})_3$ and Class III involved diphosphine such as $\text{Ph}_2\text{P}(\text{CH}_2)_3\text{PPh}_2$ (dppp). Class I showed the highest catalytic activity due to the ease of dissociation of ligand from an 18-electron complex to produce a 16-electron species. The activity of complexes in class I increased in the order: $\text{PCy}_2\text{Ph} \ll \text{P-}i\text{-Pr}_3 < \text{PCy}_3$. This activity trend was not related with the steric effect based on Tolman's cone angle, but the results agreed with the electronic effect which was evaluated based on the infrared ν_{CO} values of these complexes. The decrease in ν_{CO} values, which is consistent with an increase in the donor power of phosphine ligands, caused the increase in catalytic activity. The results indicated that the activity of osmium complexes was dependent on the electronic properties of phosphines. Complexes containing the chelating phosphine ligand would be a poor catalyst, whereas complexes coordinated with bulky, strong σ -donor and weak π -acceptor phosphines exhibited a high catalytic activity.

The selectivity of the $\text{OsHCl}(\text{CO})(\text{O}_2)(\text{PCy}_3)_2$ catalyzed hydrogenation of NBR rubber has also been studied by Parent et al. (2001). The results showed that this process produced the undesirable crosslinking reaction that was not observed in the presence of the rhodium complex, $\text{RhCl}(\text{PPh}_3)_3$. The extent of crosslinking was dependent on the process conditions and could be reduced by using low catalyst concentration and high hydrogen pressure.

1.3.2 Catalytic Hydrogenation in the Presence of $[\text{Ir}(\text{cod})(\text{PCy}_3)(\text{py})]\text{PF}_6$ (Crabtree's Catalyst)

Schrock and Osborn (1976, cited in Crabtree, 1979) observed that cationic rhodium (I) complexes having two phosphines per rhodium were active hydrogenation catalysts. These experiments were carried out by using coordinating solvents such as ethanol, acetone or tetrahydrofuran. The active species in each case were found to be the isolable solvates, $[\text{M}(\text{cod})\text{L}_2]\text{ClO}_4$ ($\text{M} = \text{Rh}$ or Ir ; $\text{cod} = 1,5$ -cyclooctadiene; $\text{L} =$ tertiary phosphine). Before the olefin substrate can access the active site, a solvent or phosphine ligand is required to dissociate. This process was relatively rapid for the rhodium complexes, but displacement occurred more slowly for the analogous iridium complexes (Shapley et al., 1968 and 1970 cited in Crabtree, 1979). To allow the substrate free access to the active site, the effect of irreversibly creating active sites in a noncoordinating solvent was examined. Schrock and Osborn (1971 cited in Crabtree et al., 1977) found that the iridium complexes, $[\text{Ir}(\text{cod})\text{L}_2]\text{PF}_6$, were less effective in noncoordinating solvents such as benzene, toluene or hexane because catalytically inactive precipitates were formed under hydrogen. Then, Crabtree et al. (1977) discovered that the cationic iridium catalysts, $[\text{Ir}(\text{cod})\text{L}_2]\text{PF}_6$ and $[\text{Ir}(\text{cod})\text{L}(\text{py})]\text{PF}_6$, were effective catalysts for alkene hydrogenation in the presence of noncoordinating chlorinated solvents, CHCl_3 , $\text{C}_6\text{H}_5\text{Cl}$ and CH_2Cl_2 . Presumably, they all have high polarity but negligible coordinating power. Normally, CHCl_3 and CH_2Cl_2 can oxidize and deactivate the low valent catalysts involved in hydrogenation. Nevertheless, both iridium catalytic precursors were later found that they are stable to oxidizing reagents such as O_2 or EtI .

The iridium catalysts, $[\text{Ir}(\text{cod})\text{L}_2]\text{PF}_6$ (Ia: $\text{L} = \text{PMePh}_2$; Ib: $\text{L} = \text{PPh}_3$) and $[\text{Ir}(\text{cod})\text{L}(\text{py})]\text{PF}_6$ (IIa: $\text{L} = \text{P-}i\text{-Pr}_3$; IIb: $\text{L} = \text{PPh}_3$; IIc: $\text{L} = \text{PCy}_3$) were examined to be the hydrogenation catalyst and found that their catalytic activity showed much smaller rates differences between mono-, di-, tri- and tetra- substituted alkene and the reaction rate were also greater than that of other homogeneous hydrogenation systems (Crabtree et al., 1977). Both catalysts can be deactivated by a number of functional groups such as amines, which totally deactivate the catalysts by deprotonation, ketones, alcohols and carboxylic acids which can cause the deactivation by coordination. Ester groups, chlorinated solvents and even molecular oxygen do not

appear to deteriorate the catalysts. Some chlorinated solvents such as 1,1-dichloroethylene and carbon tetrachloride are found to fail to dissolve the catalytic precursors I and II, even under hydrogen. In addition, the catalyst solutions of Ia and Ib are deactivated by triethylamine (NEt_3) which leads to the formation of a white solid, $[\text{IrH}_5\text{L}_2]$, known to be a poor catalyst.

Dihydrido-olefin complexes have been discovered as intermediates in the homogeneous hydrogenation of olefins. Dolcetti and Hoffman (1974, cited in Crabtree et al., 1979) studied the routes for the formation of dihydrido-olefin complexes in the catalytic cycles for homogeneous hydrogenation in the presence of $\text{RhCl}(\text{PPh}_3)_3$ or similar compounds. They reported that there are two routes, a hydride route and an unsaturated route, involved in the catalytic cycle. The hydride route involves the attack of an olefin on a dihydrido complex, while the unsaturated route involves with the attack of H_2 on a metal-olefin complex. Generally, an olefin, as an electron-withdrawing substituent, should deactivate a metal center for oxidative addition of hydrogen and thus the hydrido route has been widely proposed as the major mechanistic path for many catalysts of the dihydride type. Two isomeric series of dihydrido-diolefin complexes cations, *cis*- and *trans*- $[\text{IrH}_2(\text{cod})\text{L}_2]\text{PF}_6$ were studied by Crabtree et al. (1979). They found that the red solution of $[\text{Ir}(\text{cod})\text{L}_2]\text{PF}_6$ ($\text{L} = \text{PPh}_3$) turned colorless under hydrogen and the catalyst quickly became active for hydrogenation, but the red color of the initial solution was partially restored if hydrogen was pumped away within the first minute of the experiment. At -80°C the colorless intermediate was stable for several hours even in air. The $^1\text{H-NMR}$ spectrum at this temperature showed that the product was the simple cationic adduct *cis*- $[\text{IrH}_2(\text{cod})\text{L}_2]^+$, which was the first example known of a dihydrido olefin complex (Crabtree, 1979) as shown in Figure 1.8. Then, the initial mole of (cod) coordinated to the metal was hydrogenated via a new *cis*- $[\text{IrH}_2(\text{cod})\text{L}_2]^+$ to produce *cis*, *trans*- $[\text{IrH}_2(\text{cod})\text{L}_2]\text{PF}_6$ and cyclooctene (coe) as presented in Figure 1.9. The (cod) ligand derived from excess (cod) present in the system was used as substrate for the catalyst. In addition, the *cis*, *trans*- $[\text{IrH}_2(\text{cod})\text{L}_2]\text{PF}_6$ could be prepared by the displacement of acetone from $[\text{IrH}_2(\text{acetone})_2\text{L}_2]^+$ by (cod).

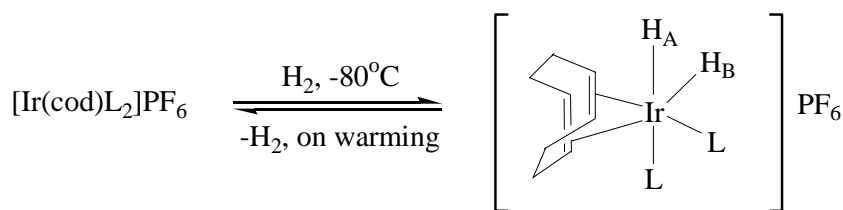


Figure 1.8 The cationic adduct $\text{cis-}[\text{IrH}_2(\text{cod})\text{L}_2]^+$ (Crabtree et al. 1979).

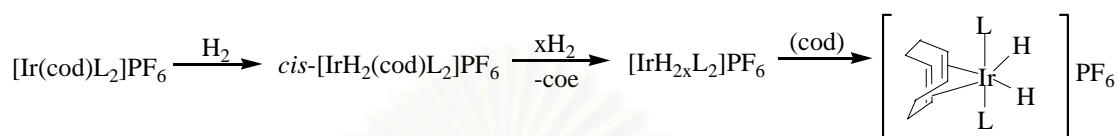


Figure 1.9 Preparation of $\text{cis, trans-}[\text{IrH}_2(\text{cod})\text{L}_2]\text{PF}_6$ via $\text{cis-}[\text{IrH}_2(\text{cod})\text{L}_2]\text{PF}_6$ (Crabtree, 1979).

To investigate the catalytic activity of two isomeric series of dihydrido-diolefin complex cations, cis- and $\text{cis, trans-}[\text{IrH}_2(\text{cod})\text{L}_2]\text{PF}_6$, Crabtree et al. (1979) found that the cis- isomers transferred hydrogen to the coordinated (cod) much more rapidly than the cis, trans isomers. The different properties of the two complexes involved with the metal hydride insertion into the cis metal-olefin group due to the coplanarity of this $\text{M}(\text{C}=\text{C})\text{H}$ system in the cis complex, $\text{cis-}[\text{IrH}_2(\text{cod})\text{L}_2]^+$ leads to facile insertion in this isomer (Crabtree, 1979). Crabtree et al. (1979) also found that the complexes $[\text{Ir}(\text{cod})(\text{PR}_3)\text{py}]\text{PF}_6$ ($\text{PR}_3 = \text{PCy}_3, \text{P-}i\text{-Pr}_3$), which were the most active hydrogenation catalysts, particularly for tri- and tetra-substituted olefins, reacted with H_2 at 0°C in CH_2Cl_2 in the presence of excess cod to generate the cis- dihydrido-diolefin complexes as represented in Figure 1.10. There was no evidence that $[\text{IrH}_2(\text{cod})(\text{PR}_3)\text{py}]\text{PF}_6$ was produced directly from the activation of H_2 by $[\text{Ir}(\text{cod})(\text{PR}_3)\text{py}]\text{PF}_6$ without the excess of (cod) such as probably occurs when $[\text{Ir}(\text{cod})(\text{PR}_3)\text{py}]\text{PF}_6$ was used as a catalyst for hydrogenation.

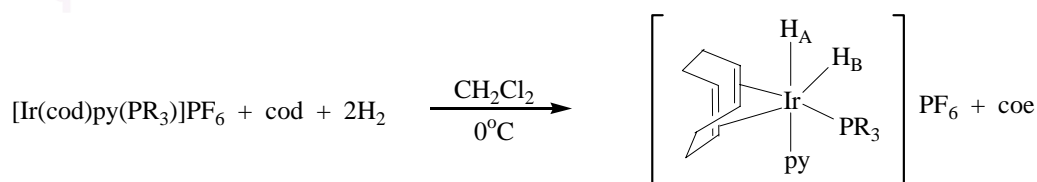


Figure 1.10 The reaction for producing the cation $\text{cis-}[\text{IrH}_2(\text{cod})(\text{PR}_3)\text{py}]\text{PF}_6$ (Crabtree et al., 1979).

There are some research reports involving the hydrogenation of diene - based polymer catalyzed by iridium catalysts. Gilliom (1989) and Gilliom and Honnell (1992) studied the catalytic hydrogenation of polybutadiene and butadiene-styrene triblock copolymer by using $[\text{Ir}(\text{cod})(\text{PMePh}_2)_2]\text{PF}_6$ as a catalyst in the absence of solvent under moderate conditions ($0 - 100$ psig at $60 \pm 1^\circ\text{C}$). The iridium catalyst showed faster initial hydrogen consumption; however, the reaction had a higher degree of conversion when $\text{RhCl}(\text{PPh}_3)_3$ was used. In both cases, the reaction could reach greater than 80% of theoretical capacity within 70 h. Hu (2000) studied the kinetics of hydrogenation of nitrile-butadiene rubber using $[\text{Ir}(\text{cod})(\text{py})(\text{PCy}_3)]\text{PF}_6$ as the hydrogenation catalyst. The kinetic results indicated that the rate constant exhibited a first order dependence on catalyst and hydrogen concentration, while an inverse proportionality appeared when nitrile concentration increased. From the viscometry analysis, the results showed that crosslinking was caused by the residual catalyst in the hydrogenated product. This crosslinking could be eliminated by increasing the process temperature.

1.4 Catalytic Hydrogenation of Natural Rubber and Synthetic *Cis*-1,4-Polyisoprene

Any polymer with unsaturated hydrocarbon groups, present either in the backbone or within the side chain, can be hydrogenated. The most recent work for polymer hydrogenation has produced excellent products, such as hydrogenated NBR and hydrogenated SBR that have better resistance of thermal and oxidative degradation. In addition, hydrogenation is an alternative way to produce some polymer structures which are difficult to access via conventional polymerization, such as alternating ethylene-propylene copolymer from the hydrogenation of polyisoprene or natural rubber and hydrogenated block copolymers such as poly(styrene-co-butadiene-co-styrene), poly(1,4-butadiene-co-1,2-butadiene) and poly(1,4-butadiene-co-1,4-isoprene-co-1,4-butadiene). Hydrogenation of these block copolymers forms thermoplastic elastomers with crystalline and amorphous segments, which are different from those of their unsaturated counterparts (Mark et al., 1994).

As described above, hydrogenation catalyzed by homogeneous catalysts is more favorable to study for the hydrogenation of diene-based polymers containing various functional groups than heterogeneous system because it has higher catalytic activity and selectivity and it can also overcome the diffusion problem. Bhattacharjee et al. (1993) reported the hydrogenation of epoxidized natural rubber in the presence of a homogeneous palladium acetate catalyst. The hydrogenated product retained the epoxy content of the polymer. Thus, it indicated that this catalyst was highly selective to saturate carbon-carbon double bonds in the presence of epoxy groups. The competition between carbon double bonds and oxygen atoms of the epoxy group led to a decrease in the reaction rate due to the coordination of epoxy group to metal center. The kinetics of natural rubber hydrogenation catalyzed by a homogeneous catalyst prepared from nickel 2-ethylhexanoate and triisobutylaluminum has been studied by Gan et al. (1996). They found that the reaction kinetics showed an overall second-order with respect to hydrogen concentration as well as the carbon-carbon double bond concentration. The activation energy of this reaction was calculated as 26.0 kJ/mol. The impurities in the rubber slightly affected the catalytic activity.

The well known homogeneous hydrogenation catalyst, Wilkinson's catalyst ($\text{RhCl}(\text{PPh}_3)_3$), has been examined as a catalyst for natural rubber hydrogenation (Singha et al., 1997). They reported the kinetics of natural rubber hydrogenation by measuring the pressure drop of hydrogen versus the reaction time. Hydrogen consumption plots indicated an apparent first-order rate dependence on the concentration of carbon-carbon double bond. The apparent activation energy for this system was calculated to be about 29.1 kJ/mol. The level of hydrogenation increased with hydrogen pressure and then leveled off when hydrogen pressure was higher than 40 kg/cm². This system also showed that the extent of hydrogenation increased with catalyst concentration. However, the high concentration of triphenylphosphine could decrease the rate of hydrogenation. The effect of solvents on the rate of hydrogenation was also studied. They observed that the extent of hydrogenation of natural rubber decreased as a function of solvent in the order of toluene > chlorobenzene > benzene. The important factors for the catalyst were the nature of solvated rhodium hydride complex and the interaction of solvent with polymer. This system reached 88% hydrogenation within 20 h. in the presence of 1.18 mM of $[\text{RhCl}(\text{PPh}_3)_3]$ and toluene

under 30 kg/cm² of H₂ at 100°C. In addition, the thermal degradation properties of hydrogenated natural rubber were investigated. It can be concluded that the hydrogenation enhanced the thermal stability of natural rubber while retaining its glass transition temperature.

Tangthongkul (2003) studied the kinetics of the hydrogenation of synthetic *cis*-1,4-polyisoprene, natural rubber and natural rubber latex in the presence of Ru(CH=CH(Ph))Cl(CO)(PCy₃)₂. It was observed that the hydrogenation rate of these rubbers followed pseudo first order kinetics in carbon-carbon double bond concentration under all sets of reaction conditions studied. The kinetic results suggested that the hydrogenation reaction of isoprene rubbers showed a first-order behavior with respect to total catalyst concentration and hydrogen pressure. An inverse first-order dependence on added PCy₃ was also observed. The apparent activation energy of *cis*-1,4-polyisoprene hydrogenation was estimated as 51.1 kJ/mol over the temperature range of 130 to 180°C, whereas it was 25.3 kJ/mol for natural rubber hydrogenation and 29.2 kJ/mol for natural rubber latex hydrogenation (over the temperature range of 140 to 160°C). The addition of a small amount of *p*-toluenesulfonic acid to the system could substantially increase the rate of reaction. The impurities in the natural rubber showed the severely reduced the catalytic activity. The main polymer chain length and molecular weight was decreased during the hydrogenation due to the reaction conditions employed.

The use of the 5d metal complexes, OsHCl(CO)(O₂)(PCy₃)₂ and [Ir(cod)(PCy₃)(py)]PF₆, as the catalyst for hydrogenation of synthetic *cis*-1,4-polyisoprene and natural rubber has been investigated by Charmondusit (2002). The kinetics of homogeneous hydrogenation of *cis*-1,4-polyisoprene catalyzed by OsHCl(CO)(O₂)(PCy₃)₂ and [Ir(cod)(PCy₃)(py)]PF₆ has been studied by monitoring the amount of hydrogen consumed during the reaction. Both catalysts were effective for hydrogenation of isoprene rubbers providing a high level of hydrogenation (> 95% hydrogenation) could be obtained within 20 minutes. This study showed that the hydrogenation of *cis*-1,4-polyisoprene in the presence of OsHCl(CO)(O₂)(PCy₃)₂ had a first order dependence on the carbon-carbon double bond concentration. A second order behavior with respect to hydrogen concentration at low concentration shifts to a zero order dependence as the hydrogen pressure was increased. The apparent

activation energy over the temperature range of 115 – 140°C was calculated as 109.3 kJ/mol. The kinetic study of the hydrogenation of *cis*-1,4-polyisoprene catalyzed by [Ir(cod)(PCy₃)(py)]PF₆ differs from the osmium complex with respect to the effect of hydrogen pressure. The hydrogenation catalyzed by the iridium system was first order with respect to hydrogen pressure and high catalyst concentration trended to produce dimerization or trimerization of the catalyst, which decreased the catalytic activity. An apparent activation energy for hydrogenation in the presence of the iridium catalyst of 79.8 kJ/mol was obtained. The relative viscosity of hydrogenated rubber catalyzed by both catalysts indicated that no side reaction such as degradation or crosslinking occurred over the range of experimental conditions used. Natural rubber could be quantitatively hydrogenated using OsHCl(CO)(O₂)(PCy₃)₂ in the presence of acid addition. The presence of a strong acid and the high coordinating power of the reaction solvent increased the catalytic activity for the hydrogenation process.

1.5 Vulcanization and Properties of Hydrogenated Rubbers

Vulcanization involves chemical bonding or crosslinking of rubber chains, usually by the reaction of sulfur and accelerators under pressure at elevated temperature to form three-dimensional structures. During this process, the rubber or stock changes its structure from an essentially plastic material to either a predominantly elastic final product or a hard material. As a result, its inherent deformation resistance is enhanced in terms of its strength, resilience (bounciness) and toughness. Moreover, the vulcanized rubber loses its tackiness and becomes insoluble in solvents (Morton, 1999).

Due to the excellent potential of thermal and oxidative resistance of hydrogenated rubbers, hydrogenated synthetic rubbers such as hydrogenated NBR (Therban from Bayer) and hydrogenated SBR (Kraton from Shell) have been commercialized. For hydrogenated NBR, the compounding formulations of Therban show the differences from those of NBR because hydrogenated NBR has high saturated structure. Thus, the selection of other ingredients (antioxidants, fillers and plasticizers) is important as well as vulcanizing agents (Koch, ed., 1993). The peroxide vulcanization is recommended for fully saturated and partially unsaturated grades. 1,4-bis(tert-butylperoxyisopropyl)benzene is used as accelerator to give good

results. An effective crosslinking (coagent) activator at relatively low temperatures for peroxide curing of hydrogenated NBR is N, N'-m-phenylenedimaleimide used for increasing the crosslink density and reducing the compression set. The typical sulfur vulcanization can be used for partially unsaturated grades of hydrogenated NBR. The higher level of sulfur together with a thiazole and a dithiocarbamate as principle accelerators can be used. This formulation is similar to those used for ethylene-propylene copolymer (EPDM) and isoprene-isobutylene rubber (IIR). To achieve the good compression set resistance at high temperature and excellent hot air aging, 0.5 – 1 pbw (part by weight) of thiuram as accelerator for sulfur vulcanization is added. The physical properties of hydrogenated NBR have been reported by Bhattacharjee et al. (1992). It was found that the stress at a particular strain increased and the elongation at break decreased with increasing the degree of hydrogenation because of strain-induced crystallization. The shear viscosity of hydrogenated NBR also decreased when shear rate and shear stress increased. The die swell decreased along with an increase in the degree of hydrogenation for all shear rates.

In the case of hydrogenated natural rubber, the limited scale of its preparation has precluded the measurement of any technological properties and this also results in difficulties in vulcanizing it in the conventional manner (Bhowmick and Stephen, ed., 1988). However, the physical properties of vulcanizates of synthetic *cis*-1,4-polyisoprene hydrogenated via diimide reduction have been investigated by Nang et al. (1976). The hydrogenated rubbers were compounded with curing agents, according to the following method; rubber (10 g), zinc stearate (0.2 g), zinc oxide (0.6 g), zinc dimethyl dithiocarbamate (0.06 g) and sulfur (0.2 g). The vulcanizing characteristics such as scorch time (T_{10}), cure time (T_{90}) and physical properties of hydrogenated rubber compound were observed. The results showed that T_{10} and T_{90} increased with increase in the hydrogenation level. It means that higher degree of hydrogenation tended to decrease the vulcanization rate. The physical properties in terms of tensile strength, elongation and hardness of vulcanizates from the hydrogenated rubbers were poorer than those of their parent rubber owing to the depolymerization during the hydrogenation reaction.

1.6 Objectives and Scope

Due to the drastic competition between natural rubber and synthetic rubbers in the world commercial market, natural rubber requires improvement of some of its properties in order to be used for a wider range of applications and increase the monetary value of natural rubber. Chemical modification of diene-based polymers is an alternative method to modify polymers to obtain the desired properties.

The thermal and oxidative degradation of natural rubber caused by unsaturated carbon-carbon double bonds in the backbone structure is a serious problem for application in many fields. Therefore, the present study focuses on the possibility to use hydrogenation for eliminating this disadvantage of natural rubber. Two homogeneous catalytic systems, $\text{OsHCl}(\text{CO})(\text{O}_2)(\text{PCy}_3)_2$ and $[\text{Ir}(\text{cod})(\text{PCy}_3)(\text{py})]\text{PF}_6$, were applied to catalyze the hydrogenation of natural rubber. The kinetics of both systems were carried out using an automatic gas uptake apparatus. The influence of reaction parameters was evaluated by using a two-level factorial design in order to find the main and interaction effects of these systems. Univariate experiments were used to study the effect of each parameter on the hydrogenation rate. Then, the reaction mechanism of both catalytic systems was proposed from the kinetic data.

According to the change of the polymer structure after the hydrogenation process, the relative viscosity, molecular weight and molecular weight distribution including the thermal properties such as glass transition temperature and decomposition temperature were examined and compared with the parent polymer. Subsequently, the vulcanization process for hydrogenated natural rubber was also investigated and physical properties of vulcanized hydrogenated natural rubber in terms of tensile strength, hardness and ozone resistance were also studied. Finally, important conclusions from this thesis and recommendations for future work are reported.

CHAPTER 2

EXPERIMENTAL AND CHARACTERIZATION

2.1 Materials

$\text{OsHCl}(\text{CO})(\text{O}_2)(\text{PCy}_3)_2$ was prepared by refluxing osmium (III) chloride trihydrate ($\text{OsCl}_3 \cdot 3\text{H}_2\text{O}$) with tricyclohexylphosphine (PCy_3), which were obtained from Strem Chemicals (Newburyport, MA, USA), as described in the procedure of Esteruelas et al. (1986, 1988). The Crabtree's catalyst, $[\text{Ir}(\text{cod})(\text{PCy}_3)(\text{py})]\text{PF}_6$, was synthesized from chloro-1,5-cyclooctadiene iridium (I) dimer, $[\text{IrCl}(\text{cod})]_2$ (Strem Chemicals) as described in the literature (Stork and Kahne, 1983). The 99.99% oxygen-free hydrogen gas for the hydrogenation experiments was supplied by Praxair Inc. (Kitchener, ON, Canada). Monochlorobenzene and methanol from Fischer Scientific Ltd. (Fair Lawn, NJ, USA), toluene, xylene, hexane and 2-methoxyethanol from EM Science (Darmstadt, Germany), tetrahydrofuran and pyridine from Calendon Laboratories Ltd. (Georgetown, ON, Canada) were all reagent grade and used as received. 3-Chloropropionic acid and *p*-toluenesulfonic acid were purchased from Aldrich Chemical Company, Inc. (Milwaukee, WI, USA). Hexylamine was obtained from BDH Chemicals (Toronto, ON, Canada) and hexadecylacrylamide was synthesized in our laboratory. The natural rubber (STR-5L) was provided by Chalong Latex Industry Co., Ltd. (Songkhla, Thailand). The composition of natural rubber is summarized in Appendix A (Table A-1). High molecular weight *cis*-1,4-polyisoprene with 97% *cis* configuration (Natsyn) was obtained from Bayer, Inc. (Sania, Canada).

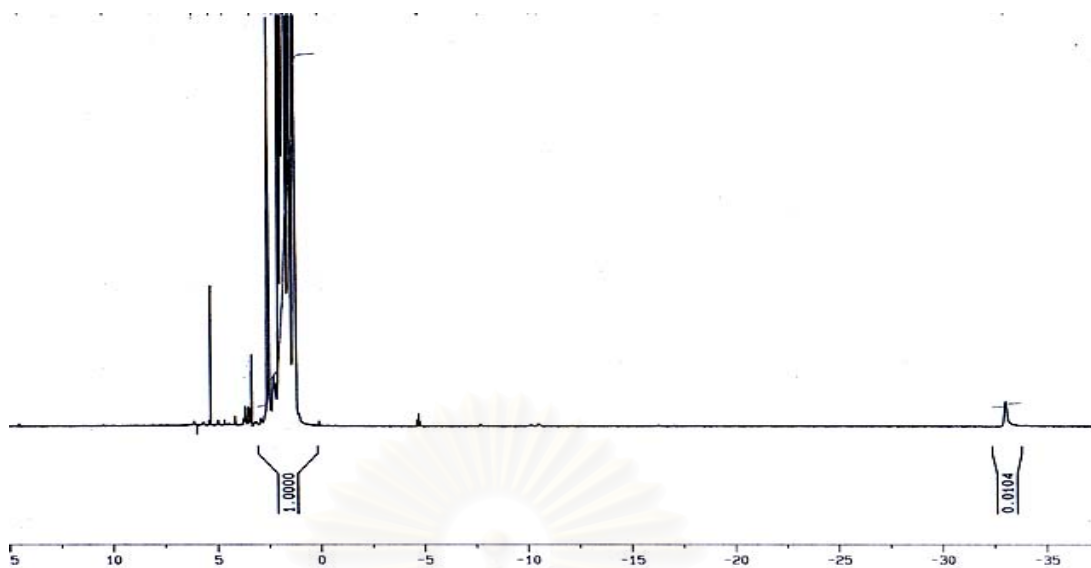
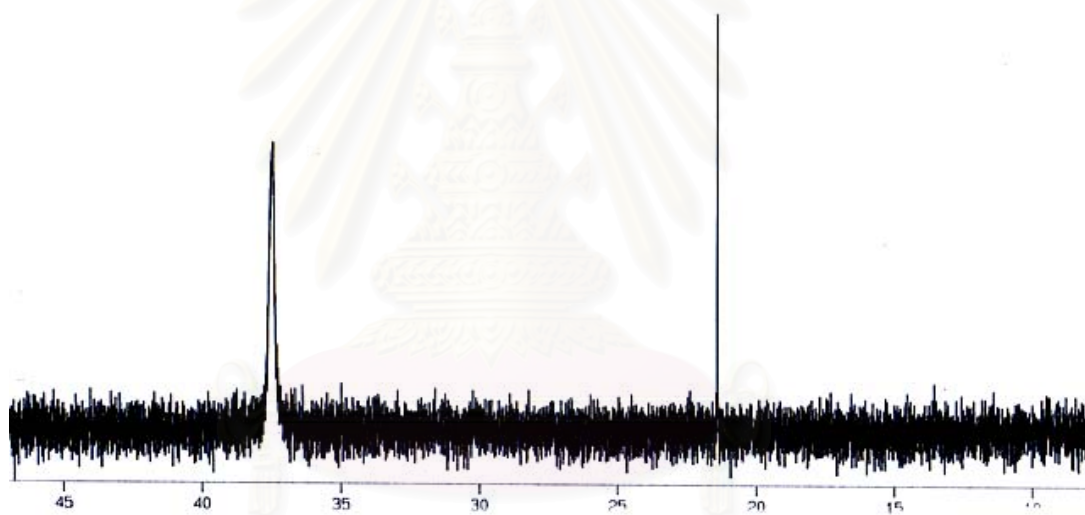
The rubber chemicals for the vulcanization process, such as zinc oxide from Utids Enterprise Co. Ltd. (Bangkok, Thailand), stearic acid from Imperial Industrial Chemicals (Thailand) Co. Ltd. (Pathumthani, Thailand), sulfur from Siam Chemical Industry Co. Ltd. (Samutprakarn, Thailand), *N*-cyclohexylbenzothiazole-2-sulfenamide (CBS) from Flexsys (Monsanto) (Antwerp, Belgium), tetramethylthiuram disulfide (TMTD) from Flexsys (Monsanto) (Cologne, Germany), 2-mercaptobenzothiazole (MBT) from Kawaguchi Chemicals (Tokyo, Japan) and

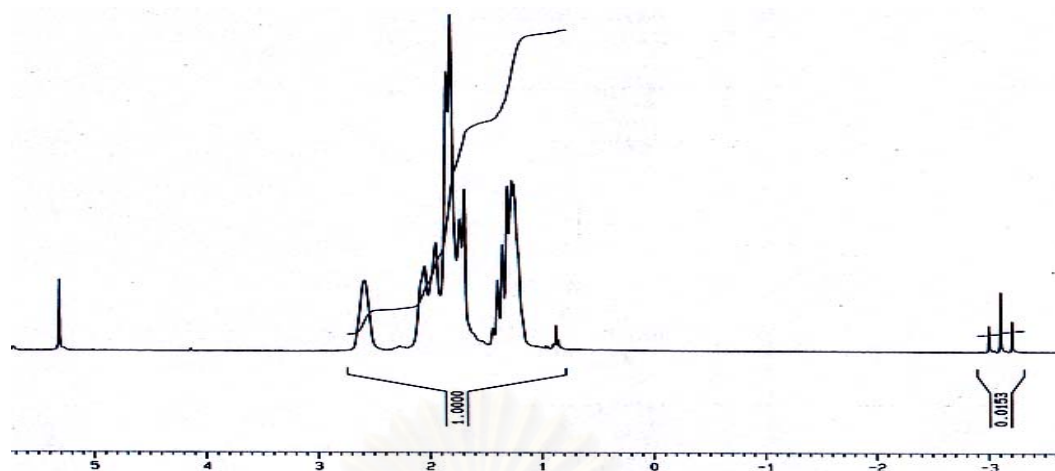
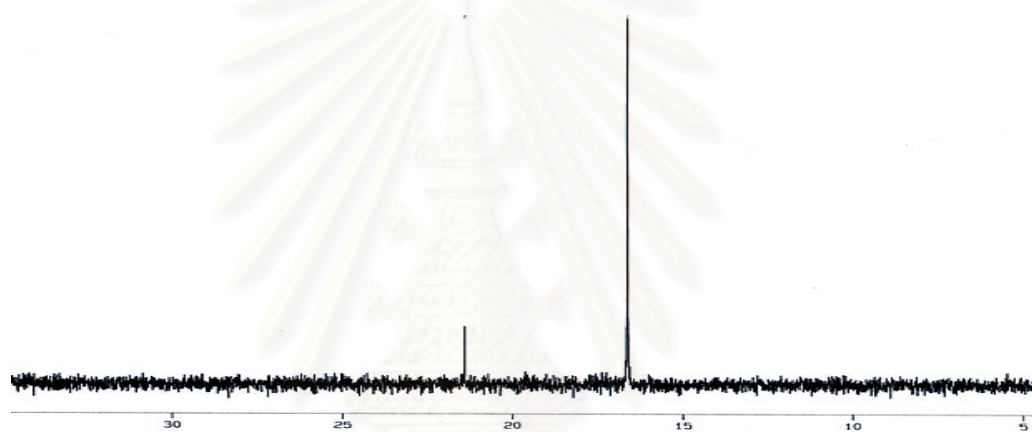
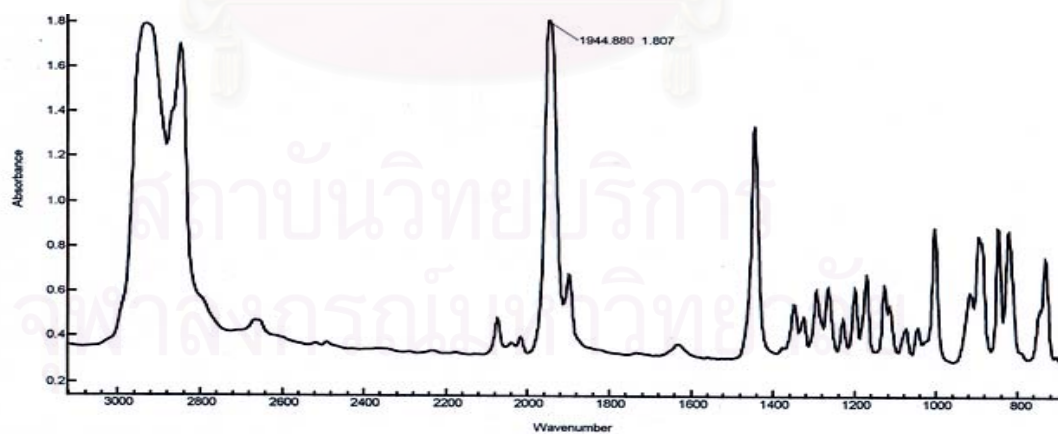
paraffinic oil in grade Diana process oil PS 32 T from Apollo (Thailand) Co., Ltd. (Bangkok, Thailand) were all commercial grade. Ethylene-propylene rubber (EPDM) of grade Keltan 509 x 100 (100 parts paraffinic extender oil with 8.7% diene content) and Keltan 314 obtained from DSM Elastomer (Sittard, Netherlands) were used for properties comparison. The information properties for these EPDM are summarized in Appendix A (Table A-2).

2.2 Catalyst Preparation

2.2.1 OsHCl(CO)(O₂)(PCy₃)₂

OsHCl(CO)(O₂)(PCy₃)₂ was prepared by refluxing OsCl₃*H₂O (1 g) with tricyclohexylphosphine (5 g) in degassed 2-methoxyethanol (100 mL) in a 500 mL bottom flask with gas inlet tube under a nitrogen atmosphere for 24 h and then cooled down to room temperature. After that, the red-orange crystalline product, OsHCl(CO)(PCy₃)₂, was collected and washed with degassed methanol (15 mL) 2 times. OsHCl(CO)(PCy₃)₂ was kept under a nitrogen atmosphere until it was dried. OsHCl(CO)(PCy₃)₂ was analyzed by NMR spectroscopy and the ¹H and ³¹P spectra obtained are shown in Figure 2.1: ¹H-NMR (CD₂Cl₂): δ -33.06 (br.), ³¹P{¹H} NMR (CD₂Cl₂): δ 37.5 (s). OsHCl(CO)(O₂)(PCy₃)₂ was synthesized by exposing a degassed hexane (50 mL) suspension of the species OsHCl(CO)(PCy₃)₂ to pure oxygen gas until a white product was obtained. OsHCl(CO)(O₂)(PCy₃)₂ was filtered using normal filtration since this osmium complex is air-stable. The product was washed with hexane 2 times and dried in vacuum overnight. The NMR and FTIR spectra of the final product are illustrated in Figure 2.2: ¹H-NMR (CD₂Cl₂): δ -2.99 (t), ³¹P{¹H}NMR (CD₂Cl₂): δ 16.63 (s), IR: ν(CO) 1945 cm⁻¹. The spectrum obtained from ¹H-NMR spectroscopy showed a triplet at -2.99 ppm, attributed to the metal-hydride peaks, and peaks for various cyclohexyl protons of the complex appeared in the region from 2.5 to 0.8 ppm. The integration of the hydride and cyclohexyl protons gave a ratio of approximately 66 to 1 which is consistent with the structural formula OsHCl(CO)(O₂)(PCy₃)₂.

(a) ^1H -NMR(b) $^{31}\text{P}\{^1\text{H}\}$ NMR**Figure 2.1** ^1H -NMR and $^{31}\text{P}\{^1\text{H}\}$ NMR spectra of $\text{OsHCl}(\text{CO})(\text{PCy}_3)_2$.

(a) $^1\text{H-NMR}$ (b) $^{31}\text{P}\{^1\text{H}\}$ NMR

(C) FTIR

Figure 2.2 $^1\text{H-NMR}$, $^{31}\text{P}\{^1\text{H}\}$ NMR and FTIR spectra of $\text{OsHCl}(\text{CO})(\text{O}_2)(\text{PCy}_3)_2$.

2.2.2 [Ir(cod)(PCy₃)(py)]PF₆

A degassed mixture of pyridine (3 mL), acetone (20 mL), ethanol (10 mL) and water (2 mL) was added to 1.4 g of [IrCl(cod)]₂ and 0.8 g of KPF₆. The solution was stirred under a nitrogen atmosphere for 30 min. Then, the solvent was removed and the resulting yellow crystals, [Ir(cod)(py)₂]PF₆, were dried under vacuum. The crystalline product was washed with degassed water to remove KCl and then subsequently dried. The above dipyridyl complex was stirred at room temperature into CH₂Cl₂ for 10 min. and a slight excess of just over 1 equiv of PCy₃ was added in the solution. Finally, solvent was removed and the obtained complex was recrystallized from CH₂Cl₂-ether and then vacuum dried overnight to obtain the orange crystal product, [Ir(cod)(PCy₃)(py)]PF₆. Figure 2.3 shows the ¹H-NMR spectrum of [Ir(cod)(PCy₃)(py)]PF₆ dissolved in CH₂Cl₂. The peaks in region of 3.9 to 4.1 are attributed to cod-vinyl. The peaks of pyridine and PCy₃ appear in the region of 7.6 to 8.7 ppm and 1.0 to 2.4 ppm, respectively (Crabtree and Morris, 1977).

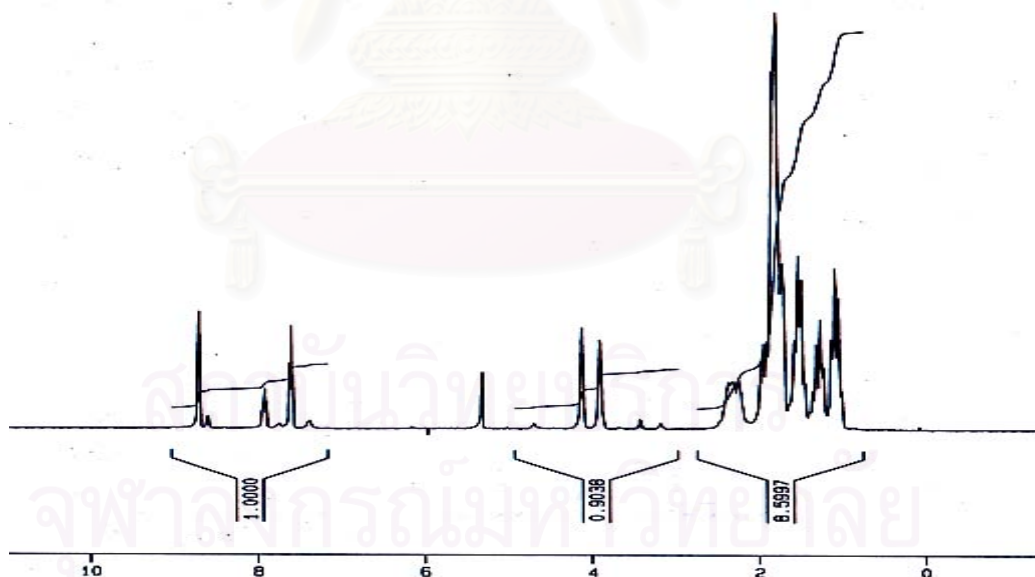


Figure 2.3 ¹H-NMR spectrum of [Ir(cod)(PCy₃)(py)]PF₆.

2.3 Hydrogenation in an Automated Gas Uptake Apparatus

The automated gas uptake apparatus is a reactor facility used to collect experimental kinetic data for the reaction by measuring the amount of hydrogen consumption as a function of time and the temperature of the rubber solution throughout the course of reaction. The high-pressure variation of this apparatus, developed by Mohammadi and Rempel (1987), has proven to be capable of monitoring the reaction process in real time. A schematic of the gas uptake apparatus is provided in Figure 2.4. The description of this high pressure reactor has been given by Martin et al. (1997).

The apparatus can maintain isothermal and isobaric conditions while it is monitoring hydrogen consumption. A drop in the autoclave pressure relative to the reference bomb RB-1 is detected by the differential pressure transducer PT-1. This error signal serves as the input for the control algorithm residing within a personal computer. To control the constant pressure in the autoclave, the PC activates the pneumatic control valve via an i/p converter to release hydrogen gas from a supply cell to recharge the autoclave. This control system can control the pressure in the reactor to no less than 0.3 psi below its set point. PT-2 detects the amount of hydrogen lost from the supply cell during the reaction by monitoring the pressure drop in the supply cell relative to RB-2 due to the hydrogen transfer to the autoclave. The amount of hydrogen lost during the reaction is an integrated measure of the hydrogenation rate. PT-2 converts the conversion of the signal generated to millimoles of hydrogen gas by calibrating its output voltage against the conversion of a known amount of substrate. This technique assumes that a change in pressure is linearly proportional to the hydrogen lost from the supply cell.

Although this gas uptake can efficiently control the reactor pressure, autoclave temperature fluctuations of $\pm 1^\circ\text{C}$ create pressure swings to which the pressure controller responds. This is especially problematic at operating pressures higher than 40 bar where pressure is increasingly sensitive to autoclave temperature variations. To further overcome this problem, a cooling system with oil circulation is installed to control the temperature to $\pm 1^\circ\text{C}$ of the set point. Before starting the reaction, the autoclave is stabilized at the desired temperature for 45 min.

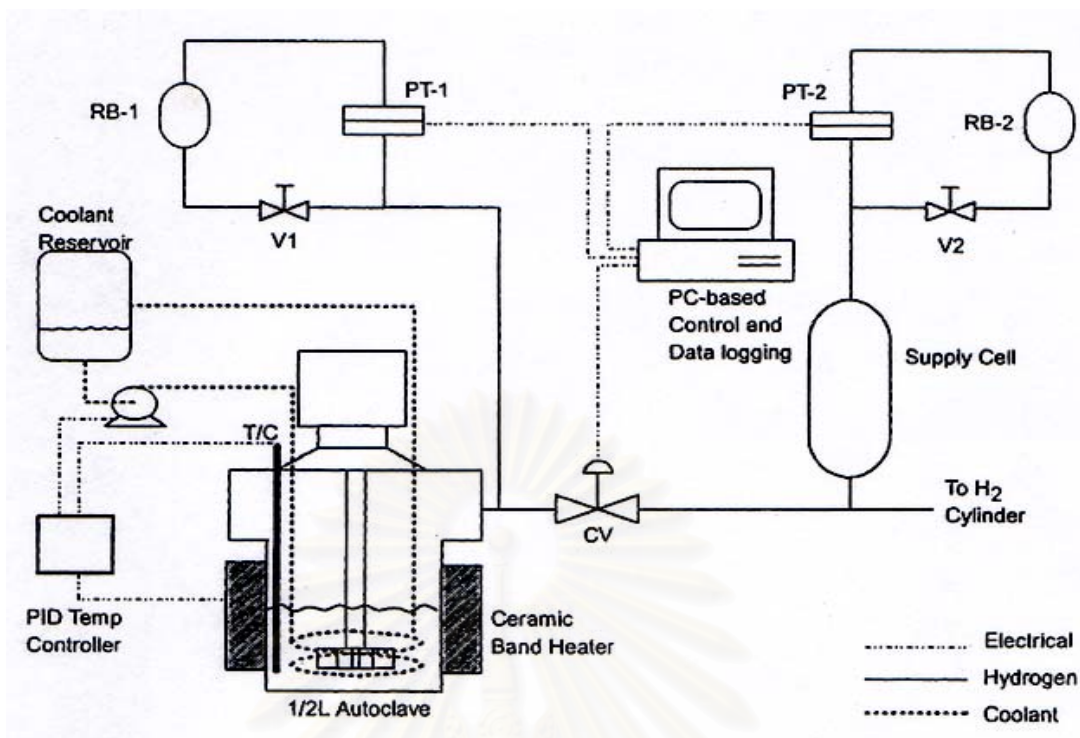


Figure 2.4 Schematic of gas uptake apparatus.

2.4 Typical Procedure for Kinetic Experiments

The kinetic data for the hydrogenation of natural rubber in the presence of $\text{OsHCl}(\text{CO})(\text{O}_2)(\text{PCy}_3)_2$ and $[\text{Ir}(\text{cod})(\text{PCy}_3)(\text{py})]\text{PF}_6$ were obtained by measuring the hydrogen consumed as a function of time using a gas uptake apparatus. The hydrogenation conditions can be controlled at a constant temperature $\pm 1^\circ\text{C}$ and pressure ± 0.02 bar from the target point throughout the reaction. Typically, natural rubber was prepared by dissolving the desired mass in monochlorobenzene within a 100 mL volumetric flask. This step took approximately 24 h. and this flask was placed in the dark. Then, this rubber solution was transferred into the autoclave and the flask was rinsed with 50 mL of chlorobenzene to make a total solution volume of 150 mL. The required mass of catalyst precursor was weighed into a small glass bucket and then it was loaded into a catalyst chamber positioned within the reactor head. The autoclave, containing the rubber solution and the catalyst bucket positioned within the reactor head, was then assembled.

Due to the sensitiveness of the catalyst to air when it is in a solution form, the system is required to eliminate air by rigorously purging with hydrogen gas (H_2). Three cycles of charging the reactor with the H_2 at 14 bar and venting were performed without agitation. Then, the agitator was started at 200 rpm and the autoclave was immersed in an ice-water bath until the temperature inside the autoclave dropped to below $10^\circ C$ in order to reduce the vapor pressure of the solvent. Subsequently, the reactor pressure was vented and recharged with H_2 continuously at 14 bar for ca. 20 min. while agitation speed was increased to 1,200 rpm to ensure that any residual oxygen in the reactor was removed. After that, the ceramic band heater was installed. To achieve the desired reaction conditions, the reactor was pressurized to approximately 80% of the target value and heating was initiated through the temperature controller. The increase in the temperature of the sealed autoclave provided the remaining 20% of the pressure of the desired set point. Once the system reached the desired conditions, it was allowed a minimum of 45 min. to equilibrate.

The H_2 uptake monitoring program employed two user-specified, data logging intervals. The first was of short duration and was designed to monitor the reaction during its initial stages where the reaction rates are greatest. The second interval was initiated by the operator to avoid the unnecessary collection of data during periods of slow hydrogenation. Once activated, the program waited one logging interval before starting to record the time, reaction temperature and amount of H_2 consumed. At this point, the reference isolation valves V1 and V2 were closed and the catalyst bucket was dropped. For dispersing the catalyst powder in the rubber solution, the agitator speed was adjusted to 1,200 rpm.

After the reaction for each experiment was terminated, the reactor was cooled down to below $50^\circ C$ using the cooling unit and blowing with air before releasing the pressure of the reactor. Then, the autoclave was disassembled and the hydrogenated product was precipitated with ethanol and dried under vacuum. The residue of product in the reactor was removed by using toluene. After that the reactor containing toluene was reassembled and heated at ca. $120^\circ C$ with 200 rpm of agitation speed and then the reactor was blown dry with air before starting the next hydrogenation run. The final degree of olefin conversion obtained via gas uptake measurement was confirmed by 1H -NMR spectroscopy.

2.5 Typical Hydrogenation Method in 2 Liters Parr Reactor

In order to test the physical properties of the hydrogenated natural rubber after the vulcanization process, it is necessary to produce the hydrogenated rubber in a scale-up reactor (2 liters). In a typical experiment, a specific amount of the rubber was weighed (ca. 55 g/batch) and placed in toluene (total volume 1 liter) and shaken in the dark for 3 days. Then, the rubber solution was transferred into the reactor and the 1 liter flask was rinsed with 250 mL of toluene which was also added to the reactor. The desired mass of catalyst was weighed (ca. 0.11 g/batch) into a small glass bucket and placed in the catalyst addition port or prepared in a glovebox by dissolving the catalyst in the 25 mL of degassed toluene and transferred into the catalyst addition device. The acids such as 3-chloropropionic acid and *p*-toluenesulfonic acid were used to increase the rate of hydrogenation as described later. If 3-chloropropionic acid was used in the reaction system, it was weighed and dissolved in 50 mL of toluene and then poured into the reactor containing the rubber solution. For the acid, *p*-toluenesulfonic acid, it was weighed and added directly into the rubber solution. The total rubber solution volume of both systems was adjusted to 1,300 mL by addition of further toluene as required. The reactor was then assembled. The system was purged with hydrogen gas through the rubber solution by venting and recharging for 10 times at 14 bar without agitation. Then, the system was purged continuously by bubbling the hydrogen gas at 14 bar for 40 min. with a 200 rpm agitation rate. Heating was then initiated to the desired temperature and the agitation speed was changed to 600 rpm. Once the temperature of the system was stabilized, the hydrogenation reaction was initiated by charging the catalyst into the rubber solution at the desired hydrogen pressure. The hydrogenation progress was observed by collecting the hydrogenated sample at various reaction times. When the reaction ceased, the hydrogenated product (ca. 50 g/batch) was isolated by precipitation in ethanol and then dried under vacuum. The degree of hydrogenation in each sample was determined using $^1\text{H-NMR}$ spectroscopy.

2.6 Blend and Vulcanization Process of Rubbers

To study the mechanical properties of the hydrogenated natural rubber (HNR) compared with natural rubber (NR) and ethylene-propylene rubber (EPDM), all rubbers (15 g/batch) were blended with the desired amount of ingredients in a Brabender Plasticorder with 30 rpm of rotor speed at mixing temperature of 70°C for blending of NR and compounds of NR/HNR in order to avoid the overcure of NR in rubber mixtures and 100°C for blending of pure HNR and EPDM. In the vulcanization process, zinc oxide and stearic acid were both used as the activator. The curing agents used for this step were composed of sulfur and accelerators such as *N*-cyclohexylbenzothiazole-2-sulfenamide (CBS), tetramethylthiuram disulfide (TMTD) and 2-mercaptobenzothiazole (MBT) which were added to reduce the cure time for the vulcanization step. The recipe of blending will be given in Chapter 6. Subsequently, three or four batches of each rubber mixed with ingredients were blended together using a two-roll mill at 70°C in order to obtain a fairly homogeneous rubber compounds and eliminate the air bubble inside them. Then, these compounds were left at room temperature overnight and vulcanized in an electrically heated compression mould at 150°C for NR and 160°C for HNR, EPDM and NR/HNR. The optimum cure time could be investigated using an oscillating disk rheometer (ODR) before vulcanizing the rubber compounds.

2.7 Characterization Methods

2.7.1 Fourier Transform Infrared Spectroscopic Analysis

Infrared spectra were collected on a Bio-Rad FTS 3000X spectrometer. Samples for FTIR analyses were prepared by casting thin films of rubber on sodium chloride plates.

2.7.2 ¹H-NMR and ¹³C-NMR Analysis

The final degree of olefin conversion was investigated by NMR spectroscopic analysis. ¹H-NMR and ¹³C-NMR spectra were obtained by dissolving 0.01 g of rubbers in CDCl₃ and recording the spectra using an Avance 300 MHz spectrometer, Bruker.

2.7.3 Gel Permeation Chromatography (GPC)

Molecular weights were obtained using a GPC system which consisted of a Water 590 Programmable HPLC pump, a laser photometer DAWN DSP-F and a Waters 410 refractive index detector (RID). ASTRA software (Wyatt Technology Corporation) was used for data collection and processing. Three 300 x 7.5 mm columns, PL gel 10 μm mixed-B, were used for separation. Tetrahydrofuran at a flow rate of 1 mL/min was used as the mobile phase. The samples of 0.1% (w/v) rubber solutions were filtered through a 0.45 μm pore size filter and then 200 μL of the filtrated samples were injected in the mobile phase. The measurements were carried out at room temperature. Due to the insoluble part of rubbers and unavailable refractive index increment (dn/dc) for hydrogenated natural rubber in any handbooks, the processing parameters were assumed as 100% mass recovery. To obtain the rather precise values of molecular weight and molecular weight distribution of rubbers for gross changes in the chain length after hydrogenation, the gel content present in each rubber sample was evaluated to obtain the exact mass injected.

2.7.4 Viscosity Measurement

The relative viscosity representative of the molecular weight of the hydrogenated natural rubber was investigated by dissolving 0.12500 ± 0.00015 g of HNR samples in 25 mL of toluene at 35°C and then transferring the solution to an Ubbelohde capillary viscometer through a coarse, sintered-glass filter to separate any insoluble gel in the rubber solution. The relative viscosity data (η_{rel}) was reported as the viscosity relative to pure solvent.

2.7.5 Thermogravimetric Analysis (TGA)

Thermogravimetric analysis (TGA) of the samples before and after hydrogenation was performed on a Perkin-Elmer Pyris Diamond TG/DTA. The temperature was raised under a nitrogen atmosphere from room temperature to 700°C at a constant heating rate of 10°C/min. The flow rate of nitrogen gas was 50 mL/min. The initial decomposition temperature (T_{id}) and the temperature at the maximum of mass loss rate (T_{max}) were evaluated. In the presence of thermo-oxidative atmosphere, air was used at the flow rate of 50 mL/min. and weight loss of rubber samples at 300°C in 60 min. was investigated.

2.7.6 Differential Scanning Calorimetry (DSC)

Differential scanning calorimetry (DSC) of the samples was carried out on a Mettler Toledo DSC 822. The instrument signal is derived from the temperature difference between the sample and the reference. 10 mg rubber samples in a crimped aluminium pan were cooled to -100°C with liquid nitrogen and then heated at a constant rate of $20^{\circ}\text{C}/\text{min}$ to 0°C . The glass transition temperature was calculated from the midpoint of the base-line shift of the DSC thermogram.

2.7.7 Cure Characterization

The optimum cure time for vulcanization of rubbers was investigated using a Monsanto Rheometer MDR 2000. Test specimen size was approximately 1.5 cm x 1.5 cm x 5 mm. The test temperature was 150°C for natural rubber and 160°C for hydrogenated natural rubber and EPDM rubber.

2.7.8 Dynamic Mechanical Analysis (DMA)

Dynamic mechanical properties such as storage modulus and loss modulus of the starting rubber and hydrogenated samples after the vulcanization process were examined using a GABO QUALIMETER EPLEXOR 25N with tension mode. The temperature scan was run at an oscillation frequency of 10 Hz with a heating rate of $2^{\circ}\text{C}/\text{min}$. The vulcanized rubber samples were cut as strips with 10 mm width, 2.7 mm thickness and 10 mm length.

2.7.9 Mechanical Properties

The mechanical properties in terms of tensile strength and hardness of vulcanized rubber were evaluated. The tensile strength of all vulcanized rubber samples was carried out on a Universal Testing Machine (LLOYD model LR5K) at 500 mm/min of the cross-head speed. This test method followed the standard method ASTM D 412. The elongation of specimens was obtained from the extensometer. The testing specimens were cut using a die C and the average of three specimens was considered as the representative value. The method for hardness testing followed ASTM D 2240. The hardness results were performed using a Durometer Hardness System Model 716 and shore A was used for hardness measurement.

2.7.10 Ozone Resistance Test

The test of ozone resistance followed the standard method ISO 1431/1 – 1980 (E) for vulcanized rubber samples. The specimens were cut to a size of 2.5 cm x 8.0 cm x 2.7 mm. Samples of rubbers were exposed in an ozone cabinet (HAMPDEN, Northampton, England) at 40°C to a ozone atmosphere of 50 pphm (part per hundred million). Before exposure to ozone, the specimens were stretched by 20% using specimen holder for a 48 h in the absence of light and ozone – free atmosphere. The results of ozone cracking were observed at 3, 6, 24, 27 and 48 hr. The cracking on rubber surfaces was examined by using an optical microscope and a CCD camera.

2.8 Degree of Hydrogenation Determination

The final degree of hydrogenation of each experiment was evaluated using ¹H-NMR spectroscopy. The lump peak area for the saturated protons (-CH₂- and -CH₃) in the range of 0.8 – 2.3 ppm and the unsaturated protons peak area at 5.2 ppm were measured in order to calculate the %hydrogenation using eq. (2.1):

$$\% \text{Hydrogenation} = \frac{A - 7B}{A + 3B} \times 100 \quad (2.1)$$

where A is the lump peak area of saturated protons and B is peak area of unsaturated protons. An example for the %hydrogenation calculation is illustrated in Appendix B.

The data obtained from the automated gas uptake apparatus consisted of three outputs: reaction time in seconds, total gas uptake in millimoles, and reaction temperature. Data files were exported to a Microsoft Excel program for calculation. The total hydrogenation level measured by ¹H-NMR spectroscopy was used to confirm the total gas uptake. The gas uptake data were converted to the percent double bond conversion (x) using the known maximum extent of reaction. An apparent reaction rate constant (k') was provided by the slope of a plot of ln(1-x) versus time. The slope of the plot was determined by linear regression.

CHAPTER 3

HYDROGENATION OF NATURAL RUBBER IN THE PRESENCE OF $\text{OsHCl}(\text{CO})(\text{O}_2)(\text{PCy}_3)_2$

Natural rubber (NR) in the commercial market is totally dominated by *Hevea Brasiliensis*, which is an important industrial material utilized in many applications such as tires, gloves, footwear, belts, cables etc. The major component of NR identified from FTIR and NMR studies is polyisoprene in a *cis*-1,4 configuration ca. 94%. The unique composition of NR structure involves proteins, which are believed to bring about its characteristic properties. Due to the unsaturation of the carbon-carbon double bonds of the isoprene backbone, NR degrades when exposed to sunlight, ozone, oxygen and long term heating. Hydrogenation is one type of chemical modification, which reduces the amount of unsaturation and thus changes the properties of the diene polymer toward greater stability against thermal and oxidative degradation (Singha et al. 1997; Sarkar et al. 1997).

The mononuclear osmium complex, $\text{OsHCl}(\text{CO})(\text{O}_2)(\text{PCy}_3)_2$, has been shown to be a very effective catalyst for the hydrogenation of acrylonitrile-butadiene copolymers (NBR) (Parent et al., 1998a) and synthetic *cis*-1,4-polyisoprene (PIP) (Charmodusit et al., 2003) with up to 99% conversion within 15-30 minutes at moderate conditions. However, NR and polyisoprene are rather difficult to hydrogenate using conventional catalysts due to the steric constraint of the isopropyl group in the rubber chain. Singha et al. (1997) reported the hydrogenation of NR in the presence of $\text{RhCl}(\text{PPh}_3)_3$. It was found that the quantitative hydrogenation was only obtained after 22 h using a very high loading of catalyst (1.91 mM / NR 0.50 g). Thus, the $\text{RhCl}(\text{PPh}_3)_3$ catalyst system appears to be rather ineffective for NR hydrogenation.

The purpose of the present work were to study the kinetics and optimize the process of NR hydrogenation catalyzed by $\text{OsHCl}(\text{CO})(\text{O}_2)(\text{PCy}_3)_2$. The effect of catalyst concentration ($[\text{Os}]$), rubber concentration ($[\text{C}=\text{C}]$), hydrogen pressure (P_{H_2}), and reaction temperature was studied using a two-level factorial design and univariate kinetic experiments. The results from univariate experiments

were used to propose a catalytic mechanism for the hydrogenation process. The effects of the addition of some acids and nitrogen containing substances on the rate of hydrogenation were also investigated.

3.1 Structure Characterization Using FTIR and NMR Spectroscopy

The structure of hydrogenated natural rubber (HNR) is similar to the structure of an alternating ethylene-propylene copolymer. FTIR spectra of NR before and after hydrogenation are illustrated in Figure 3.1. The characteristic FTIR spectrum of HNR product indicated that the C=C stretching (1660 cm^{-1}) and olefinic C-H bending (836 cm^{-1}) disappeared while the intensity of the peak at 735 cm^{-1} attributed to $-(\text{CH}_2)_3-$ increased. For NR and HNR with impurities (proteins), the weak transmittance bands at 3280 cm^{-1} and 1530 cm^{-1} which are characteristic vibrations of $>\text{N-H}$ and $>\text{N-C=O}$ (Aik-Hwee et al., 1992) remained after the hydrogenation process.

Figure 3.2 shows a comparison of the $^1\text{H-NMR}$ spectra of NR and HNR. The characteristic $^1\text{H-NMR}$ signal attributed to $-\text{CH}_3$ (1.6 ppm), $-\text{CH}_2-$ (2.0 ppm) and olefinic protons (5.1 ppm), disappeared and the new signals, saturated $-\text{CH}_3$ (0.8 ppm) and $-\text{CH}_2-$ (1.2 ppm), were observed after the hydrogenation process. The actual degree of hydrogenation for each experiment could be calculated from the peak area at 5.1 ppm and the summation of peak areas between 0.8 and 2.0 ppm as described in Chapter 2 and Appendix B.

The $^{13}\text{C- NMR}$ spectra of NR before and after hydrogenation process are illustrated in Figure 3.3. The peaks at 135.3 and 125.1 ppm for olefinic carbons disappeared and four new peaks emerged at 37.6, 32.9, 24.6 and 19.9 ppm which are attributed to $\text{C}_{\alpha\gamma}$, $-\text{CH-}$, $\text{C}_{\beta\beta}$ and $-\text{CH}_3$ carbons, respectively upon hydrogenation of NR (Singha et al., 1997).

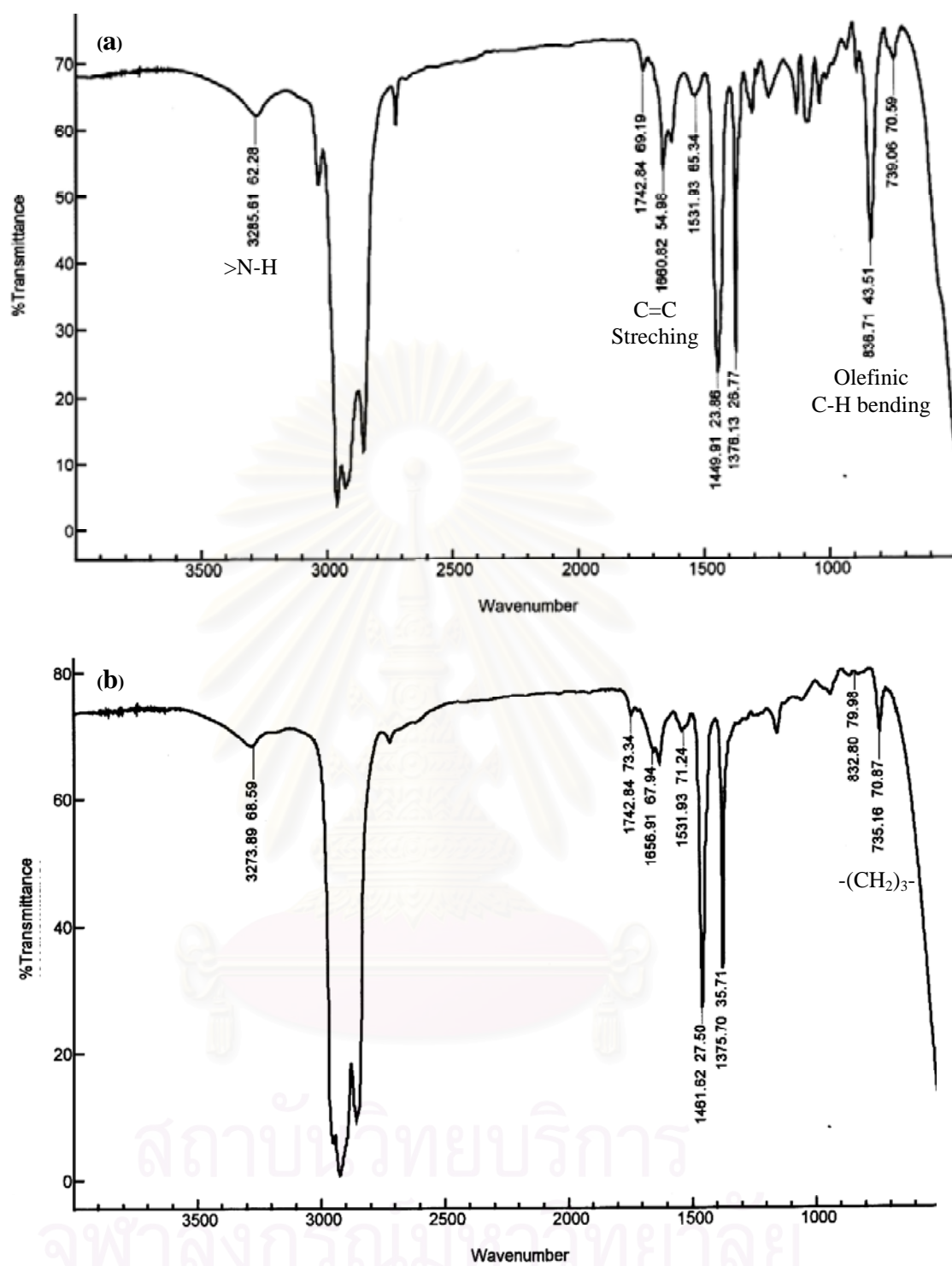


Figure 3.1 FTIR spectra of (a) NR and (b) HNR catalyzed by $\text{OsHCl}(\text{CO})(\text{O}_2)(\text{PCy}_3)_2$.

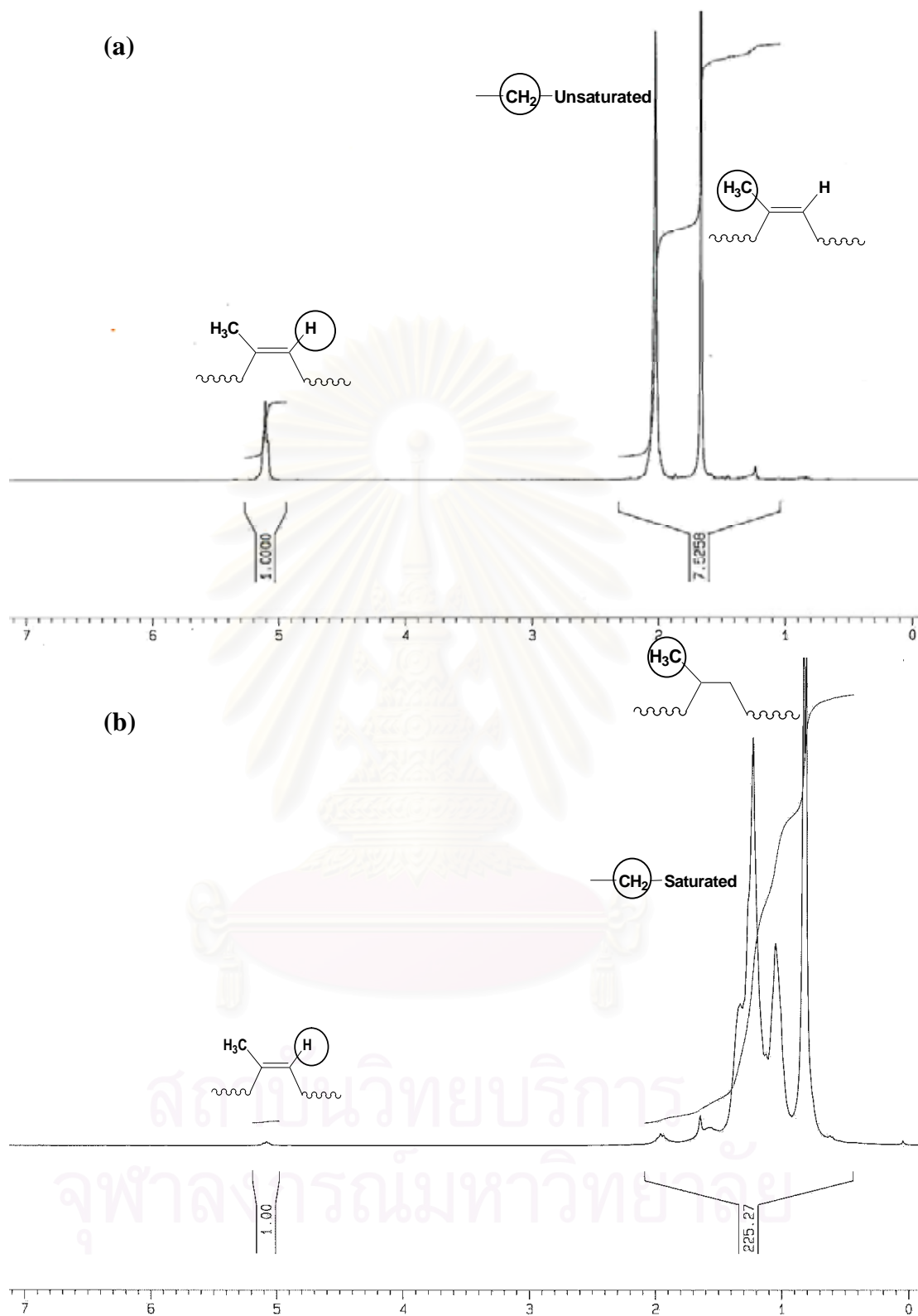


Figure 3.2 $^1\text{H-NMR}$ spectra of (a) NR and (b) HNR catalyzed by $\text{OsHCl}(\text{CO})(\text{O}_2)(\text{PCy}_3)_2$.

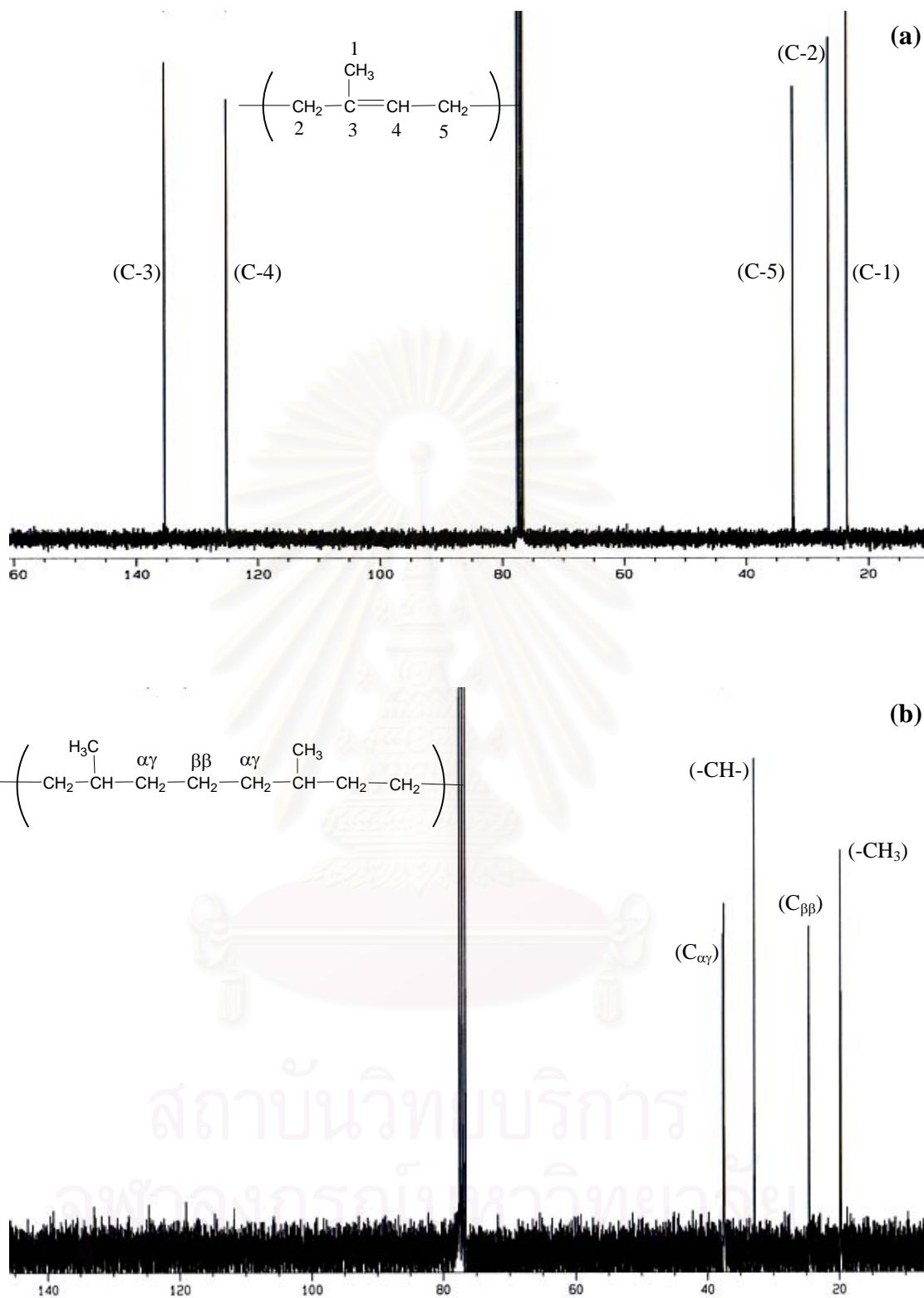


Figure 3.3 ^{13}C -NMR spectra of (a) NR and (b) HNR catalyzed by $\text{OsHCl}(\text{CO})(\text{O}_2)(\text{PCy}_3)_2$.

3.2 Kinetic Experimental Design for Natural Rubber Hydrogenation

All the kinetic data for the NR hydrogenation using $\text{OsHCl}(\text{CO})(\text{O}_2)(\text{PCy}_3)_2$ as catalyst was obtained using the automated gas-uptake apparatus. The initial experimental work was conducted by using a factorial design of experiments to find the main effects for the system and then univariate experiments were carried out to investigate the effect of each factor individually. Figure 3.4 shows the olefin conversion profiles and corresponding \ln plots for the NR hydrogenation carried out in the gas uptake apparatus. The reaction rate equation corresponds to a pseudo first order reaction rate model with respect to double bond concentration, $[\text{C}=\text{C}]$, as shown in eq.(3.1):

$$-\frac{d[\text{C}=\text{C}]}{dt} = k'[\text{C}=\text{C}] \quad (3.1)$$

where k' , the pseudo-first-order rate constant, was calculated from the slope of the straight line portion of the first order \ln plot of the gas-uptake data where x was the olefin conversion. The $\ln(1-x)$ versus time curves for NR hydrogenation exhibited good straight line behavior during the initial stages of the reaction and then deviated as the rate decreased. This result was different from the data observed for the hydrogenation of synthetic *cis*-1,4-polyisoprene (PIP) (Charmondusit et al., 2003) where the $\ln(1-x)$ versus time curves were linear to very high conversions. Presumably, the impurities in NR played a role in reducing the catalytic activity as the reaction progressed; therefore, the \ln plot data deviated from the linear model. However, the reaction data was close to the linear model for hydrogenation when higher catalyst concentrations were used as the relative amount of the catalyst deactivated to overcome the effect of impurities was not that significant compared to the total amount of catalyst used.

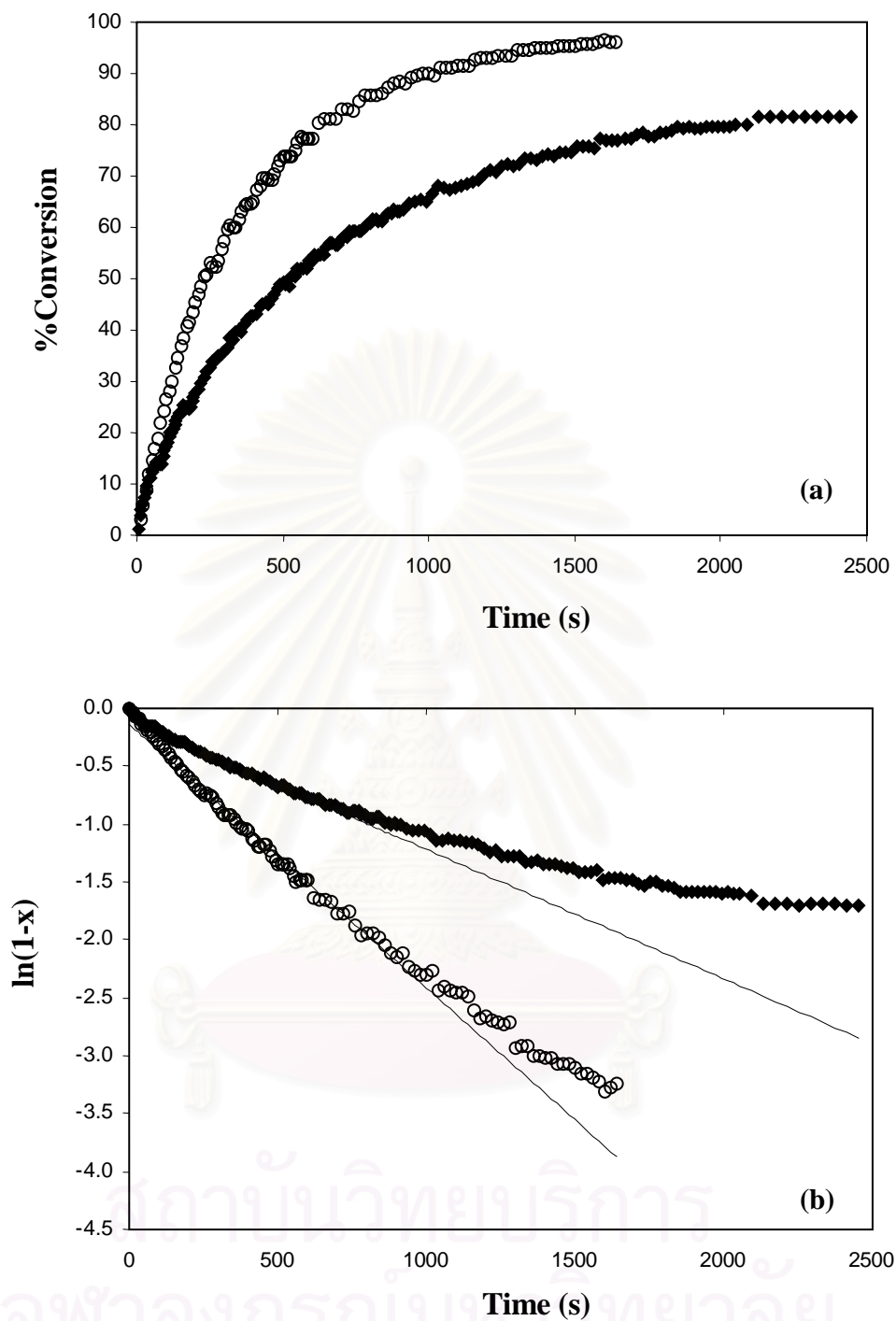


Figure 3.4 Hydrogenation profile of NR obtained from gas uptake apparatus: (a) olefin conversion profiles and (b) first-order \ln plot (----- model from linear regression). $[\text{Os}] = 60 \mu\text{M}$ (\blacklozenge) and $100 \mu\text{M}$ (\circ); $[\text{C}=\text{C}] = 260 \text{ mM}$; $P_{\text{H}_2} = 6.9 \text{ bar}$; $T = 140^\circ\text{C}$ in monochlorobenzene.

3.2.1 Statistical Analysis Using Two-Level Factorial Design Experiments

Factorial designs are generally used for experimental systems involving several factors in order to study the main effects and joint effects of factors on the response (Montgomery, 2001). Two-level factorial design experiments are widely used to screen the influence of each reaction factor. In this work, the principal factors, which had an effect on the k' and catalytic cycle of $\text{OsHCl}(\text{CO})(\text{O}_2)(\text{PCy}_3)_2$, were $[\text{Os}]$, $[\text{C}=\text{C}]$ and P_{H_2} . When two-level factorial design was applied to calculate the effect of parameters in the experiment, the levels of factors may be arbitrarily called “low (-1)” and “high (+1)”. The range of $[\text{Os}]$, $[\text{C}=\text{C}]$ and P_{H_2} were 60 - 120 μM , 260 - 392 mM and 6.9 - 41.3 bar, respectively as shown in Table 3.1. The reaction temperature was kept constant at 140°C. Yate’s algorithm was applied to investigate the main effects and interaction effects on the rate constant derived from the experimental data (Mason et al., 1989). Tables 3.2 and 3.3 represent the results of Yate’s algorithm calculation and the calculation of effects and standard errors for the 2^3 factorial design. The results in Table 3.3 indicate that $[\text{Os}]$ and $[\text{C}=\text{C}]$ had a profound influence on the rate of hydrogenation; while, the effect of P_{H_2} was moderate on the system over the selected range. Due to the fact that the low level of the hydrogen pressure selected was still relatively high for this catalyst system as seen from univariate experiments presented later, it became an important factor for natural rubber hydrogenation when the hydrogen pressure was lower than 6.9 bar. This finding is discussed later for the univariate experiments. The $[\text{Os}]$ and P_{H_2} had a positive effect which implies that the rate of hydrogenation increased with an increase in the $[\text{Os}]$ and P_{H_2} . In contrast, $[\text{C}=\text{C}]$ showed a large negative effect on the rate constant. It can be postulated that the impurities in the rubber might be giving rise to this effect on the rate of hydrogenation. The binary interactions, $[\text{Os}]*[\text{C}=\text{C}]$, $[\text{Os}]*P_{\text{H}_2}$ and $[\text{C}=\text{C}]*P_{\text{H}_2}$, also affected the hydrogenation rate but the three-factor interaction ($[\text{Os}]*[\text{C}=\text{C}]*P_{\text{H}_2}$) was not highly significant.

Table 3.1 Results from 2³ Factorial Design Experiment for NR Hydrogenation

Exp.	[Os] (μM)	[C=C] (mM)	P _{H₂} (bar)	Temperature (°C)	k' x 10 ³ (s ⁻¹)
1	60	259.9	6.8	140	1.12
2	60	259.8	6.8	140	0.96
3	120	259.8	6.8	140	3.13
4	120	259.8	6.8	140	2.86
5	60	392.4	7.0	140	0.72
6	60	392.3	6.9	140	0.56
7	120	392.3	6.9	140	0.98
8	120	392.3	6.9	140	1.18
9	60	259.8	41.4	140	1.08
10	60	259.8	41.4	140	1.26
11	120	259.7	41.4	140	3.71
12	120	259.8	41.4	140	3.83
13	60	392.4	41.2	140	1.02
14	60	392.3	41.0	140	1.04
15	120	392.2	41.2	140	1.83
16	120	392.2	41.3	140	2.04

Conditions: T = 140°C in monochlorobenzene.

สถาบันวิทยบริการ
จุฬาลงกรณ์มหาวิทยาลัย

Table 3.2 Yate's Algorithm Calculation of the 2^3 Factorial Experiment

Exp.	Design Matrix Variables			Ave. k' (s^{-1})	Algorithm			Divisor	Estimate	Identification
	[Os]	[C=C]	P_{H_2}		(1)	(2)	(3)			
1	-1	-1	-1	0.00104	0.00404	0.00576	0.01366	8	0.00171	Average
2	1	-1	-1	0.00300	0.00172	0.00791	0.00590	4	0.00148	[Os]
3	-1	1	-1	0.00064	0.00494	0.00240	-0.00429	4	-0.00107	[C=C]
4	1	1	-1	0.00108	0.00297	0.00351	-0.00321	4	-0.00080	[Os]*[C=C]
5	-1	-1	1	0.00117	0.00196	-0.00232	0.00215	4	0.00054	P_{H_2}
6	1	-1	1	0.00377	0.00044	-0.00198	0.00111	4	0.00028	[Os]* P_{H_2}
7	-1	1	1	0.00103	0.00260	-0.00152	0.00034	4	0.00009	[C=C]* P_{H_2}
8	1	1	1	0.00194	0.00091	-0.00170	-0.00018	4	-0.00005	[Os]*[C=C]* P_{H_2}

สถาบันวิทยบริการ
จุฬาลงกรณ์มหาวิทยาลัย

Table 3.3 Calculation of Effects and Standard Errors for 2^3 Factorial Design Experiment

Effect	Estimate \pm Standard Error
Average	0.00171 \pm 3.16E-05
Main Effects	
Catalyst Concentration, [Os]	0.00148 \pm 6.32E-05
Rubber Concentration, [C=C]	-0.00107 \pm 6.32E-05
Hydrogen Pressure, P_{H_2}	0.00054 \pm 6.32E-05
Two-Factor Interaction	
[Os]*[C=C]	-0.00080 \pm 6.32E-05
[Os]* P_{H_2}	0.00028 \pm 6.32E-05
[C=C]* P_{H_2}	0.00009 \pm 6.32E-05
Three-Factor Interaction	
[Os]*[C=C]* P_{H_2}	-0.00005 \pm 6.32E-05

3.2.2 Univariate Kinetic Experiments

The statistical experiments described above provide only information on the significance of the factors. In order to determine how each variable affects the hydrogenation rate, the univariate experiments of the central composite design of the parameters were carried out individually in order to determine their influence on the hydrogenation rate as shown in Figure 3.5 – 3.8. The results of these experiments are summarized in Table 3.4.

Table 3.4 Univariate Kinetic Data of NR Hydrogenation Catalyzed by $\text{OsHCl}(\text{CO})(\text{O}_2)(\text{PCy}_3)_2$

Exp.	[Os] (μM)	[C=C] (mM)	P_{H_2} (bar)	Temp. ($^\circ\text{C}$)	%Hydrogenation		$k' \times 10^3$ (s^{-1})	η_{rel}
					10 min	20 min		
1	40	259.8	6.9	140	37.1	54.5	0.58	-
2	60	259.9	6.9	140	53.6	70.7	1.12	-
3	60	259.8	6.9	140	50.9	69.7	0.96	-
4	80	259.9	6.9	140	69.8	86.7	1.83	-
5	100	259.8	6.9	140	77.5	93.0	2.28	8.50
6	120	259.8	6.9	140	84.5	94.6	2.79	-
7	120	259.8	6.9	140	83.1	90.2	2.86	-
8	40	259.8	27.6	140	38.6	55.1	0.60	7.12
9	60	259.9	27.6	140	49.4	70.0	1.01	7.65
10	80	259.8	27.6	140	68.8	85.8	2.02	7.63
11	100	259.9	27.6	140	79.1	92.7	2.53	8.18
12	100	259.9	27.6	140	77.9	91.4	2.45	-
13	120	259.9	27.6	140	87.1	97.5	3.64	8.43
14	40	259.9	41.4	140	38.8	56.7	0.62	-
15	60	259.8	41.4	140	52.1	72.1	1.08	-
16	60	259.8	41.4	140	59.6	76.4	1.26	-
17	80	258.9	41.4	140	68.2	86.3	1.99	-
18	100	259.7	41.4	140	78.5	92.7	2.49	8.52
19	120	259.7	41.4	140	87.7	97.3	3.71	-
20	120	259.8	41.4	140	88.5	98.2	3.83	-
21	100	259.9	2.1	140	61.6	75.5	1.46	-
22	100	259.8	3.4	140	69.0	81.2	1.79	7.26
23	100	259.7	5.2	140	74.2	89.5	1.99	6.57
24	100	259.8	13.8	140	78.0	92.3	2.53	7.40
25	100	259.9	55.2	140	69.0	86.6	1.96	7.57
26	100	259.7	55.2	140	63.2	82.5	1.66	-
27	100	259.8	68.9	140	68.2	86.2	1.58	-
28	100	259.7	68.9	140	66.1	84.5	1.47	-
29	100	64.9	27.6	140	94.1 (7.5 min)	-	8.34	9.21
30	100	97.6	27.6	140	96.7	97.0 (10.8 min)	7.72	9.88
31	100	129.9	27.6	140	96.3	97.5 (12.3 min)	6.28	9.25
32	100	194.9	27.6	140	92.0	97.6	4.06	8.70
33	100	326.0	27.6	140	68.2	85.2	1.84	8.39
34	100	392.2	27.6	140	72.7	88.0	1.88	-
35	100	441.2	27.6	140	35.8	55.5	0.64	-
36	100	259.8	27.6	125	34.6	53.1	0.58	-
37	100	259.7	27.6	130	63.4	82.0	1.49	-
38	100	259.7	27.6	135	68.2	87.1	1.78	-
39	100	259.8	27.6	145	90.5	97.2	4.19	-

*relative viscosity (η_{rel}) of NR = 7.54

3.2.2.1 Dependence on Catalyst Concentration

To study the influence of catalyst concentration on the rate of hydrogenation, the range of [Os] was varied between 40 and 120 μM at three levels of hydrogen pressure, 6.9, 27.6 and 41.4 bar. The rubber concentration was 260 mM at 140°C in monochlorobenzene. The influence of catalyst loading charged into the reaction system is illustrated in Figure 3.5. It can be seen that the reaction rate is linearly proportional to the total catalyst concentration at every hydrogen pressure. This implies that the NR hydrogenation exhibited the first-order behavior with respect to [Os]. This observation is consistent with the work of Andriollo et al. (1989) and Parent et al. (1998b) who suggested that the active complex is a mononuclear species. This figure also shows that the rate of PIP hydrogenation (Charmondusit et al., 2003) was higher than that of NR hydrogenation, which required higher loading of catalyst. It appears that impurities in NR decreased the activity of catalyst. Furthermore, the plots of NR hydrogenation exhibited a positive intercept on the [Os]-axis, while such was not the case for PIP hydrogenation. This suggests that in the case of NR hydrogenation some portion of catalyst, about 25 μM , was sacrificed during the reaction to quench impurities in the rubber.

3.2.2.2 Dependence on Rubber Concentration

The influence of NR concentration on the hydrogenation rate was studied over the range of 65 - 440 mM for which the initial catalyst concentration (100 μM), and reaction temperature (140°C) and hydrogen pressure (27.6 bar) were kept constant. The results of these experiments are displayed in Figure 3.6. These results indicate that the reaction rate decreased with an increase in rubber concentration. This figure also shows that the rate of PIP hydrogenation was constant when the rubber concentration was increased (Charmondusit et al., 2003). In general, the hydrogenation rates of PIP and styrene-butadiene rubber (SBR) (Parent et al., 1998b) are independent of the rubber concentration. In contrast, the hydrogenation rate of NBR decreased with increasing rubber concentration. The nitrile functional group within NBR is known to reversibly coordinate to $\text{OsHCl}(\text{CO})(\text{PCy}_3)_2$. Through σ -donation from the nitrogen lone pair, nitrile coordinates *trans* to the hydride to bind the metal center (Parent et al., 1998a). This behavior has also been observed for NBR

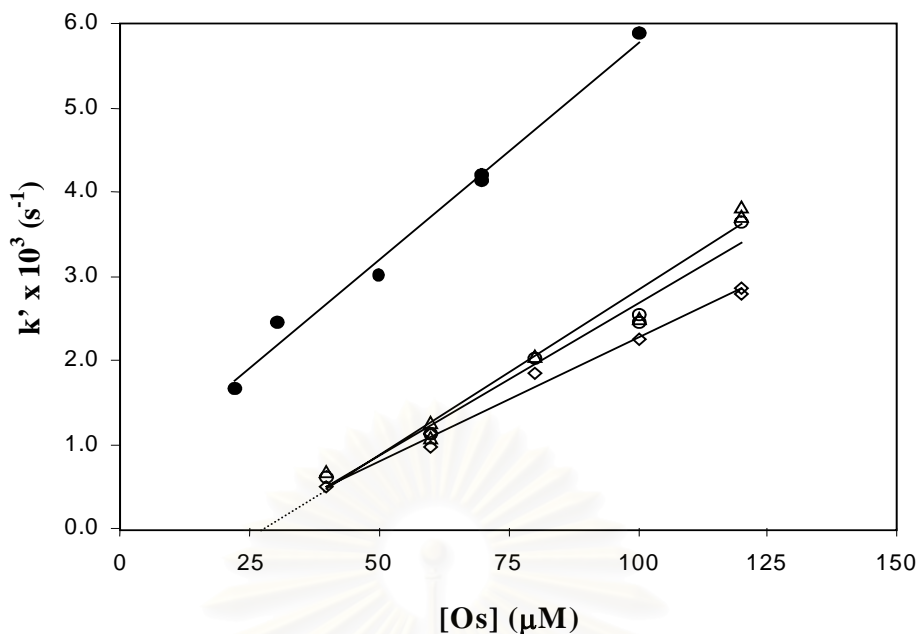


Figure 3.5 Effect of catalyst concentration on the rate of NR hydrogenation compared with PIP hydrogenation (Charmondusit et al., 2003). For NR: $[C=C] = 260$ mM; $P_{H_2} = 6.9$ (\diamond), 27.6 (\circ) and 41.4 (\triangle) bar; $T = 140^\circ\text{C}$ in monochlorobenzene. For PIP (\bullet): $[C=C] = 260$ mM; $P_{H_2} = 20.7$ bar and $T = 130^\circ\text{C}$ in toluene.

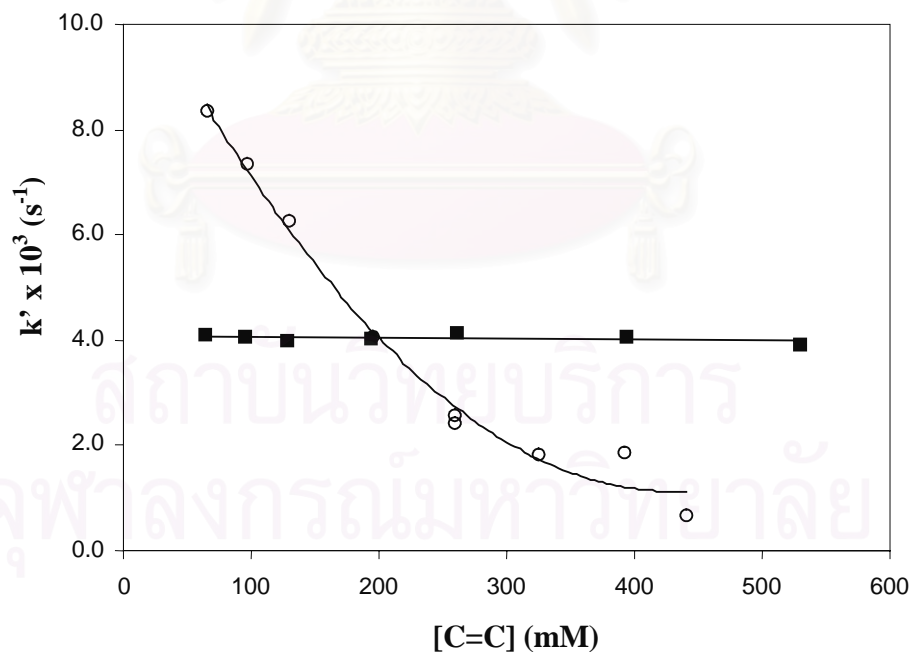


Figure 3.6 Effect of rubber concentration on the rate of NR hydrogenation compared with PIP hydrogenation (Charmondusit et al., 2003). For NR (\circ): $[Os]_T = 100$ μM ; $P_{H_2} = 27.6$ bar; $T = 140^\circ\text{C}$ in monochlorobenzene. For PIP (\blacksquare): $[Os] = 70$ μM ; $P_{H_2} = 20.7$ bar; $T = 130^\circ\text{C}$ in toluene.

hydrogenation catalyzed by $[\text{Rh}(\text{diene})(\text{NBD}_2)]^+$ (Mao and Rempel, 1998), $\text{RhCl}(\text{PPh}_3)_3$, $\text{RhH}(\text{PPh}_3)_4$ (Parent et al., 1996) and $\text{RuCl}(\text{CO})(\text{styryl})(\text{PCy}_3)_2$ (Martin et al., 1997). However, since NR does not contain any other complexing functional group, the reduction of the hydrogenation rate of NR is attributed to the influence of some impurities in the rubber. From Figure 1, FTIR spectrum of NR shows that proteins (bands 3280 and 1530 cm^{-1}) are the main impurities. These might compete with olefin for the metal coordination sites during the catalytic hydrogenation resulting in a certain level of catalytically inactive forms of the Os complex.

To gain further understanding about the effect of the inferent impurities in NR on the hydrogenation process, an attempt was made to model NR by using PIP with addition of hexylamine ($\text{CH}_3(\text{CH}_2)_4\text{CH}_2\text{NH}_2$) or hexadecylacrylamide ($\text{H}_2\text{C}=\text{CH}(\text{CO})\text{NHC}_{16}\text{H}_{33}$), both of which have nitrogen containing functional groups akin to the functional groups present in proteins. Table 3.5 shows the effect of added nitrogen substances on the catalytic activity in PIP hydrogenation. The reaction conditions were 260 mM of rubber concentration, 40 μM of catalyst concentration, 13.8 bar of hydrogen pressure at 130°C in toluene. It was found that hexylamine caused a drastic decrease in activity of $\text{OsHCl}(\text{CO})(\text{O}_2)(\text{PCy}_3)_2$. Hexylamine has an amine group, which is an electron donating species, so hexylamine can form bonds easily with the osmium centre. However, for hexadecylacrylamide, the lone pair of electrons of the nitrogen atom can be delocalized between nitrogen and $-\text{C}=\text{O}$; therefore, hexadecylacrylamide does not easily coordinate with the osmium centre. The results of the addition of nitrogen containing substances agree with the results of the factorial study and the univariate experiments, which indicate that the hydrogenation rate decreased due to the increase with rubber loading and impurities.

Table 3.5 Effect of Nitrogenous Substances on Hydrogenation Rate of Synthetic *Cis*-1,4-Polyisoprene (PIP)

Exp.	Substance	[Substance]* (mM)	[Substance]/[Os]	$k' \times 10^3$ (s ⁻¹)
1	None	-	-	2.96
2	Hexylamine	1.29	32.3	0.37
3	Hexadecylacrylamide	1.05	26.3	2.44

Condition: [Os] = 40 μ M, [C=C] = 260 mM and P_{H_2} = 13.8 bar at 130°C in toluene.

*The substance concentration was based on the maximum of nitrogen content in NR in grade STR-5L (0.60%).

3.2.2.3 Dependence on Hydrogen Pressure

According to the unique behavior of $OsHCl(CO)(O_2)(PCy_3)_2$ to form multiple hydride species, the hydrogenation of diene polymers such as NBR (Parent et al., 1998a) and PIP (Charmondusit et al., 2003) catalyzed by $OsHCl(CO)(O_2)(PCy_3)_2$ was found to exhibit a second-order dependence on the hydrogen pressure at low pressures which then tended to a zero-order behavior at high hydrogen pressure. However, for NBR hydrogenation in the presence of the $RhCl(PPh_3)_3$ system, it was found that the order of reaction with respect to hydrogen pressure shifted from a first to zero order behavior with increasing hydrogen pressure (Parent et al., 1996), while a first order behavior in hydrogen pressure is maintained over a considerable range of hydrogen pressure for the Ru complex, $RuHCl(CO)(PCy_3)_2$ system (Martin et al., 1997). For NR hydrogenation catalyzed with $OsHCl(CO)(O_2)(PCy_3)_2$, the rate of reaction is a function of hydrogen pressure. In order to investigate the dependence of the hydrogenation rate on the hydrogen pressure, a series of experiments were carried out from 2.1 to 68.9 bar at 140°C in monochlorobenzene. The catalyst concentration and rubber concentration were 100 μ M and 260 mM, respectively. The results shown in Figure 3.7(a) demonstrate that the rate of NR hydrogenation exhibited first order with respect to the hydrogen pressure from 2.1 to 6.9 bar and then shifted toward zero order dependence when the hydrogen pressure was 13.8 to 41.4 bar. The reaction rate of NR hydrogenation was diminished when the hydrogen pressure was higher than 41.4 bar. This first-order dependence at low hydrogen pressure (2.1 – 6.9 bar) was

shown by plotting $1/P_{H_2}$ versus hydrogenation rate as illustrated in Figure 3.7(b). It can be seen that the curve in this figure is linearly proportional to $1/P_{H_2}$. This shift in $[H_2]$ order in NR hydrogenation showed a different behavior from the hydrogenation of NBR (Parent et al., 1998b) and PIP (Charmondusit et al., 2003). The reason for the reduction of NR hydrogenation rate dependence on hydrogen pressure will be discussed later in the section of mechanistic interpretation of kinetic data.

3.2.2.4 Dependence on Reaction Temperature

A series of experiments were carried out over the range of 125 to 145°C. The reaction conditions were maintained constant at 100 μ M of catalyst concentration, 260 mM initial rubber concentration and 27.6 bar of hydrogen pressure. The Arrhenius plot is shown in Figure 3.8a. The apparent activation energy calculated from a least squares regression analysis of $\ln(k')$ versus $1/T$ was 122.76 kJ/mol providing evidence that the experiments were performed without mass-transfer limitation. The activation energy of NR hydrogenation is higher than that of PIP hydrogenation (109.32 kJ/mol) (Charmondusit et al., 2003). Based on the corresponding Eyring equation (eq. 3.2 cited in Tangthongkul, 2003), the apparent activation enthalpy and entropy were estimated as 119.37 kJ/mol and -7.83 J/mol K, respectively as shown in Figure 3.8b.

$$k = \frac{k_B T}{h} e^{\frac{-\Delta H^\ddagger}{RT}} e^{\frac{\Delta S^\ddagger}{R}} \quad (3.2)$$

where k_B is Boltzmann's constant (1.381×10^{-23} J/K) and h is Planck constant (6.626×10^{-34} J/s).

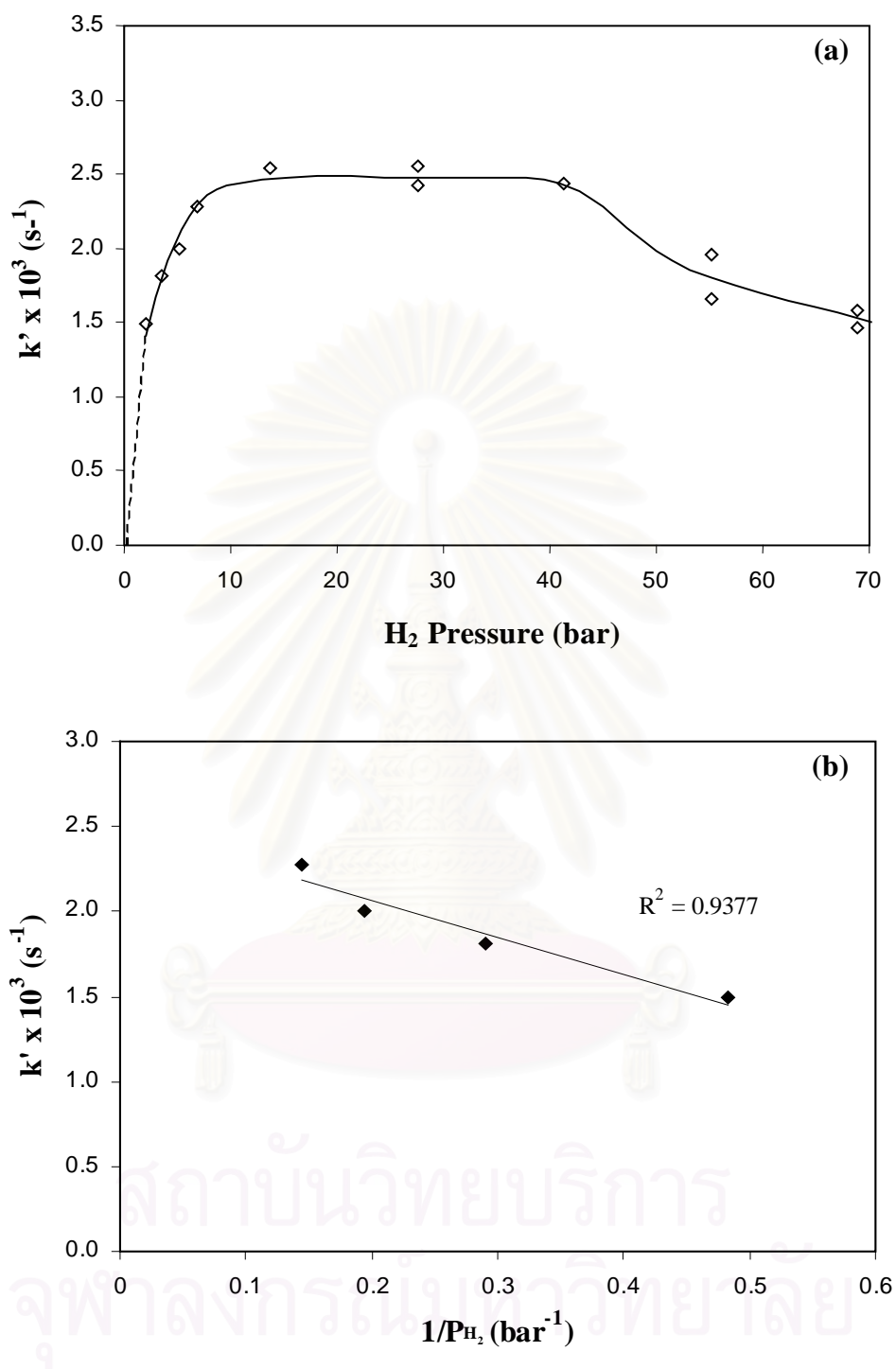


Figure 3.7 (a) Effect of hydrogen pressure on the rate of NR hydrogenation and (b) the plot of $1/P_{\text{H}_2}$ versus the rate constant (2.1-6.9 bar). $[\text{Os}] = 100 \mu\text{M}$; $[\text{C}=\text{C}] = 260 \text{ mM}$; $T = 140^\circ\text{C}$ in monochlorobenzene.

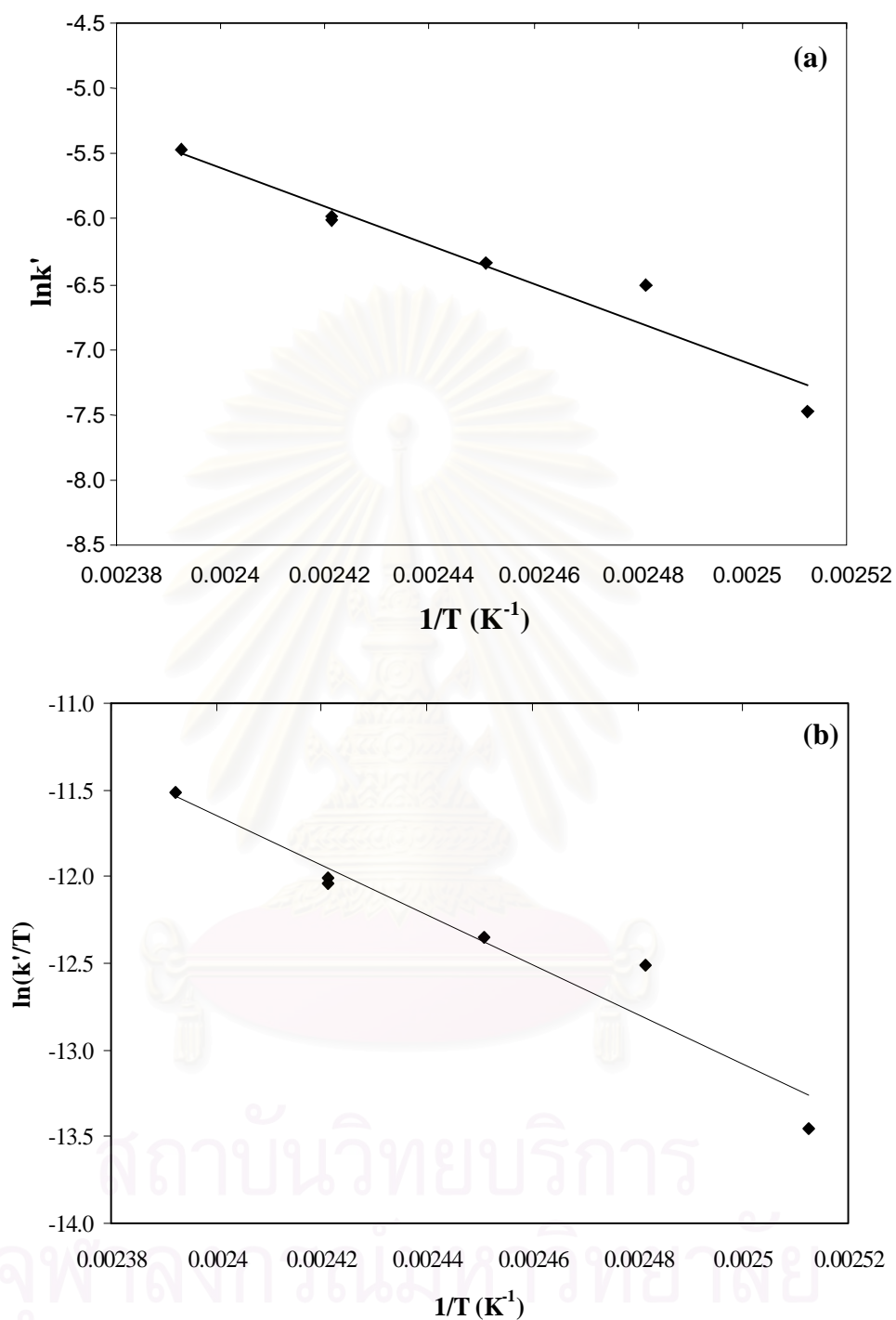


Figure 3.8 (a) Arrhenius plots and (b) Eyring plot for the NR hydrogenation.

$[\text{Os}] = 100 \mu\text{M}$; $[\text{C}=\text{C}] = 260 \text{ mM}$ and $P_{\text{H}_2} = 27.6 \text{ bar}$.

3.2.2.5 Dependence on Solvents

The effect of different solvents on the NR hydrogenation was investigated at 100 μM of catalyst concentration, 260 mM initial rubber concentration and 27.6 bar of hydrogen pressure at 140°C. The results of these experiments are presented in Table 3.6. It is obvious that solvent plays an important role in the hydrogenation reaction. Thus, the solvent should have sufficient coordinating power to facilitate dissociation of a tricyclohexylphosphine ligand in the catalytic cycle of the hydrogenation, but it should not be too strong to obstruct displacement by alkene. Ketone solvents such as methyl ethyl ketone (MEK) and butanone were not used since $\text{OsHCl}(\text{CO})(\text{O}_2)(\text{PCy}_3)_2$ has been reported to be not active in these solvents (Parent et al., 1998b). From Table 3.6, it was found that the rate constant increased with increasing solvating power of solvent in the order: tetrahydrofuran \cong chlorobenzene > toluene > xylene.

Table 3.6 Effect of Solvent on the NR Hydrogenation

Solvent	$k' \times 10^3$ (s^{-1})	Time for 60% Conversion (min)
Tetrahydrofuran	2.54	4.7
Monochlorobenzene	2.50	5.8
Toluene	0.55	30.0
Xylene	0.49	35.3

Condition: $[\text{Os}] = 100 \mu\text{M}$, $[\text{C}=\text{C}] = 260 \text{ mM}$ and $P_{\text{H}_2} = 27.6 \text{ bar}$ at 140°C

3.2.3 Effect of Acid Addition on the Catalytic Activity

There have been some research reports on acid addition to improve the catalytic activity for olefinic type hydrogenation reactions. Guo and Rempel (1997) discovered that carboxylic acids increased the catalytic activity for the hydrogenation of a NBR emulsion catalyzed by $\text{RuCl}(\text{CO})(\text{styryl})(\text{PCy}_3)_2$. It was suggested that carboxylic acids were very effective in preventing the poisoning of catalyst by impurities in emulsion systems. Yi et al. (2000) also reported that the addition of acids with weakly coordinating anions such as trifluoromethanesulfonic acid (HOTf) and tetrafluoroboric acid – dimethyl ether complex ($\text{HBF}_4 \cdot \text{OEt}_2$) enhanced the reaction rate of alkene hydrogenation catalyzed by $\text{RuH}(\text{CO})(\text{Cl})(\text{PCy}_3)_2$. They found that the increase in catalytic activity of $\text{RuH}(\text{CO})(\text{Cl})(\text{PCy}_3)_2/\text{acid}$ system might be due to the selective entrapment of the phosphine ligand and the formation of a highly active 14-electron ruthenium-monophosphine species. However, $\text{HBF}_4 \cdot \text{OEt}_2$ cannot be employed in the gas-uptake apparatus because of its low flash point (-42°F) and flammability. In this work, the role of the acids, 3-chloropropionic acid (3-CPA) and *p*-toluenesulfonic acid (*p*-TSA), on NR and PIP hydrogenation were studied and the results obtained are presented in Tables 3.7 – 3.8 and Figures 3.9 – 3.10.

The conversion profiles in Figure 3.9 indicate that the addition of 3-CPA increased the rate of NR hydrogenation. Figure 3.10(a) shows the effect of 3-CPA concentration on the rate of hydrogenation. It was found that this acid was effective when NR was dissolved in toluene. The rate of hydrogenation increased when the acid concentration was increased from 0.30 to 6.39 mM, then diminished and leveled off at an acid concentration above 6.39 mM. When monochlorobenzene was used as solvent, the rate of hydrogenation decreased with increase in acid concentration and also leveled off. It is possible that the acid can easily dissociate to an anion in a more polar solvent, which may cause the decrease in catalytic activity.

The effect of *p*-TSA on the rate of NR hydrogenation is illustrated in Figure 3.10(b). The results are different from the 3-CPA system in that the rate of hydrogenation increased with increasing acid concentration in both solvents and the hydrogenation rates tend to be decreased when the *p*-TSA concentration was more than 3.01 mM in toluene and 2.00 mM in monochlorobenzene. The drastic decrease in

hydrogenation rate at high loading of p-TSA can be explained in that p-TSA is a stronger acid than 3-CPA and can easily dissociate to the *p*-toluenesulfonic anion, which may decrease the efficiency of catalyst.

The results obtained from addition of these acids for hydrogenation of PIP in toluene and monochlorobenzene are represented in Table 3.8. It was found that the addition of these acids has an adverse effect on the hydrogenation rate. For hydrogenation in toluene, the rates decreased slightly and in monochlorobenzene, the rates decreased drastically. Although, this result cannot be explained for PIP hydrogenation, the role of acids in the NR hydrogenation may partially be due to the possible neutralization of the impurities in the rubber.

Table 3.7 Effect of Acid Types and Acid Concentration on the Rate of NR Hydrogenation

Solvent	Acid	[Acid] (mM)	[Acid]/[Os]	k'x10 ³ (s ⁻¹)	%Hydrogenation		η _{rel}
					10 min	20 min	
Toluene	-	-	-	0.63	32.6	49.5	-
	3-CPA	0.30	3	1.06	51.8	70.6	-
		0.83	8	1.64	68.2	87.5	-
		1.16	12	1.83	68.6	88.7	-
		2.06	21	2.16	77.4	91.1	-
		6.39	64	2.36	77.0	94.3	-
		10.07	101	2.10	77.2	92.0	-
		15.03	150	2.03	73.9	90.4	-
	p-TSA	0.19	2	1.09	51.9	72.2	-
		0.53	5	3.49	90.8	96.5	7.84
		1.03	10	3.52	87.1	97.1	8.03
		3.01	30	3.77	88.4	97.8	7.82
		5.96	60	2.93	76.4	93.3	7.47
-		-	-	2.51	80.3	92.8	8.18
Monochlorobenzene	-	-	-	2.51	80.3	92.8	8.18
	3-CPA	0.73	7	2.21	77.6	92.7	-
		1.02	10	1.79	68.7	89.3	-
		3.07	31	1.82	69.6	89.1	-
		9.77	98	1.95	72.4	92.0	-
		16.11	161	1.99	72.8	91.6	-
	p-TSA	0.20	2	2.97	84.1	97.1	-
		0.50	5	3.95	92.0	98.9	-
		1.06	11	4.03	92.1	97.6	-
		2.00	20	4.00	91.9	98.1	-
		4.00	40	1.75	78.6	90.5	-
		6.00	60	0.87	57.1	71.4	-
		-	-	-	-	-	-
-		-	-	-	-	-	-

Condition: [Os] = 100 μM, [C=C] = 260 mM and P_{H₂} = 27.6 bar at 140°C

Table 3.8 Effect of Acid Addition on the Hydrogenation Rate of Synthetic *Cis*-1,4-Polyisoprene

Solvent	Acid	[Acid] (mM)	[Acid]/[Os]	$k' \times 10^3$ (s ⁻¹)	%Hydrogenation	
					10 min	20 min
Toluene	-	-	-	2.96	80.4	96.6
	3-CPA	0.82	20	2.46	73.2	93.8
	p-TSA	0.80	20	2.50	76.2	93.8
Monochlorobenzene	-	-	-	3.03	83.1	95.7
	3-CPA	0.82	20	1.69	72.5	87.6
		3.36	84	1.59	64.6	82.6
		6.33	158	1.00	55.2	74.1
	p-TSA	0.80	20	0.96	65.8	80.8

Condition: [Os] = 40 μ M, [C=C] = 260 mM and P_{H_2} = 13.8 bar at 130°C

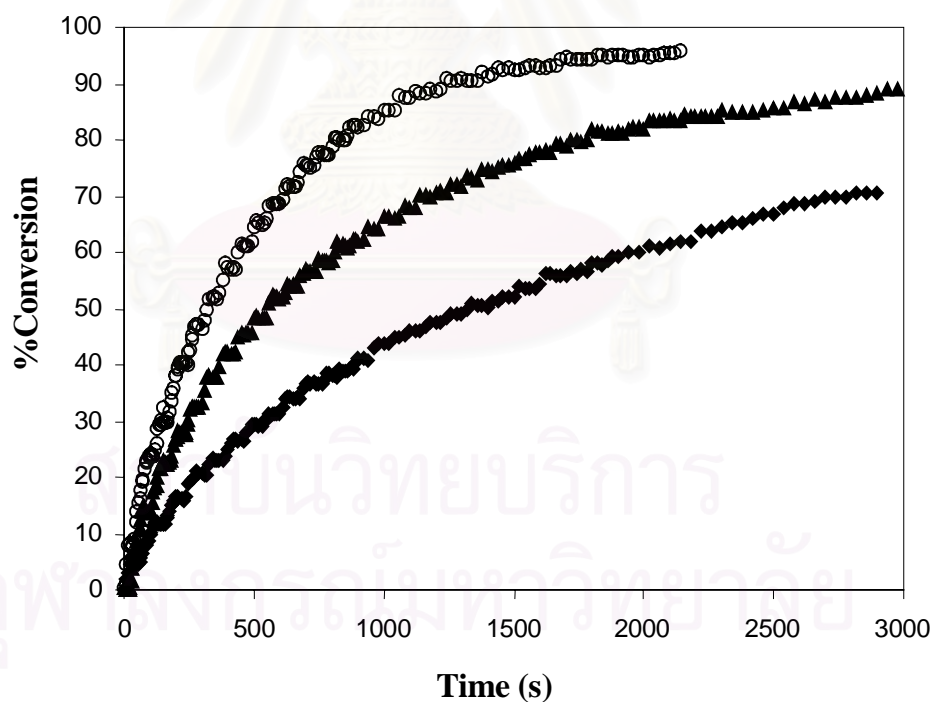


Figure 3.9 NR hydrogenation conversion profiles of non-acid addition (\blacklozenge) and acid addition systems: [3-CPA]/[Os] = 3/1 (\blacktriangle) and [3-CPA]/[Os] = 12/1 (\circ). [Os] = 100 μ M; [C=C] = 260 mM; P_{H_2} = 27.6 bar; T = 140°C in toluene.

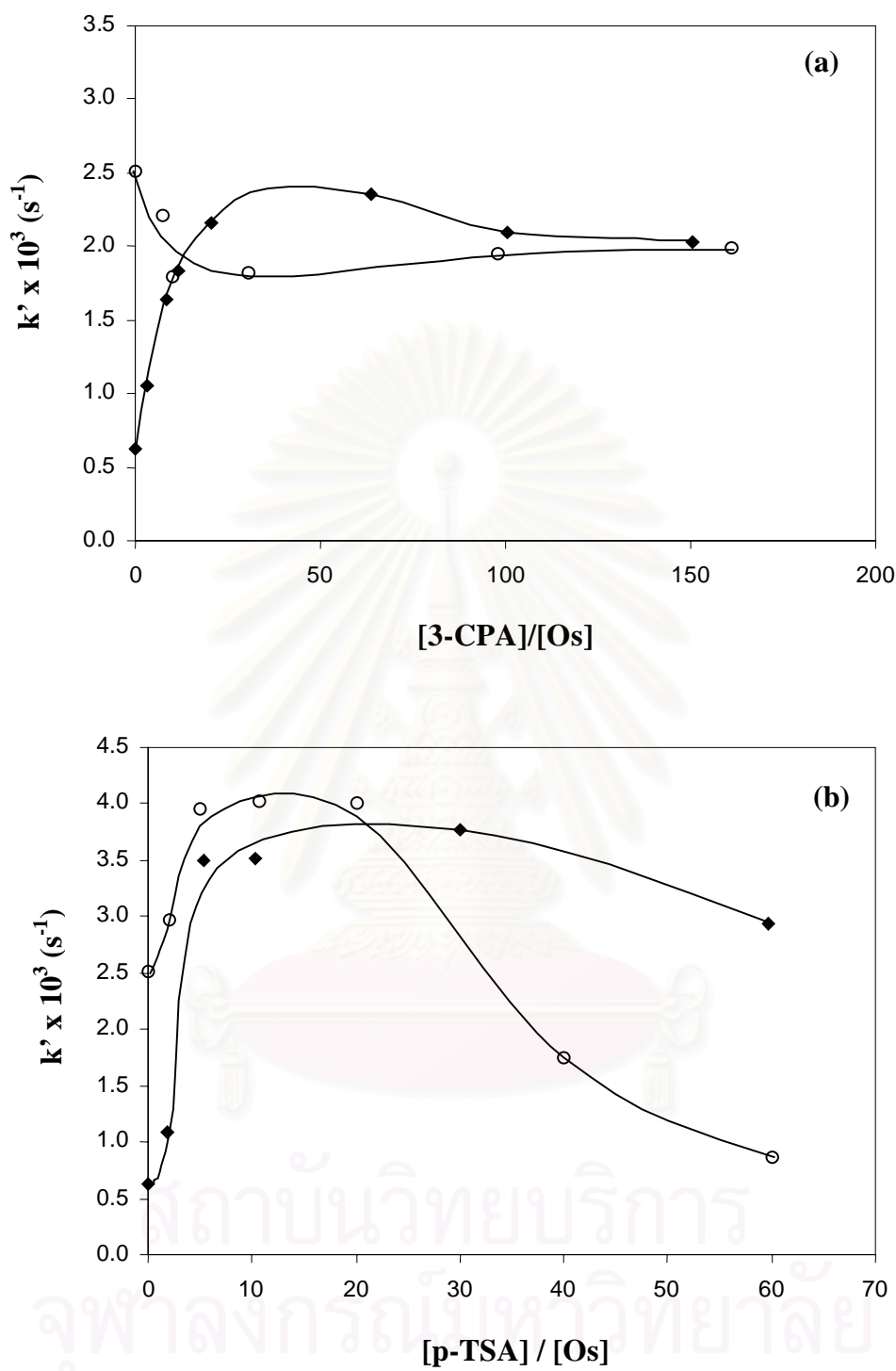


Figure 3.10 Effect of acid type and acid concentration on the NR hydrogenation: (a) the effect of 3-chloropropionic and (b) the effect of p-toluenesulfonic acid in toluene (\blacklozenge) and monochlorobenzene (\circ). $[\text{Os}] = 100 \mu\text{M}$; $[\text{C}=\text{C}] = 260 \text{ mM}$ and $P_{\text{H}_2} = 27.6 \text{ bar}$.

3.3 Mechanistic Interpretation of the Kinetic Data

A catalytic pathway is developed from inferences on the kinetic data and electron counting schemes. The catalytic cycle of $\text{OsHCl}(\text{CO})(\text{O}_2)(\text{PCy}_3)_2$ for NR hydrogenation illustrated in Figure 3.11 is inferred from the observed kinetic data. The catalytic cycle for polymer hydrogenation catalyzed by $\text{OsHCl}(\text{CO})(\text{O}_2)(\text{PCy}_3)_2$ has been proposed in the earlier work on NBR (Parent et al., 1998b) and PIP hydrogenation (Charmondusit et al., 2003).

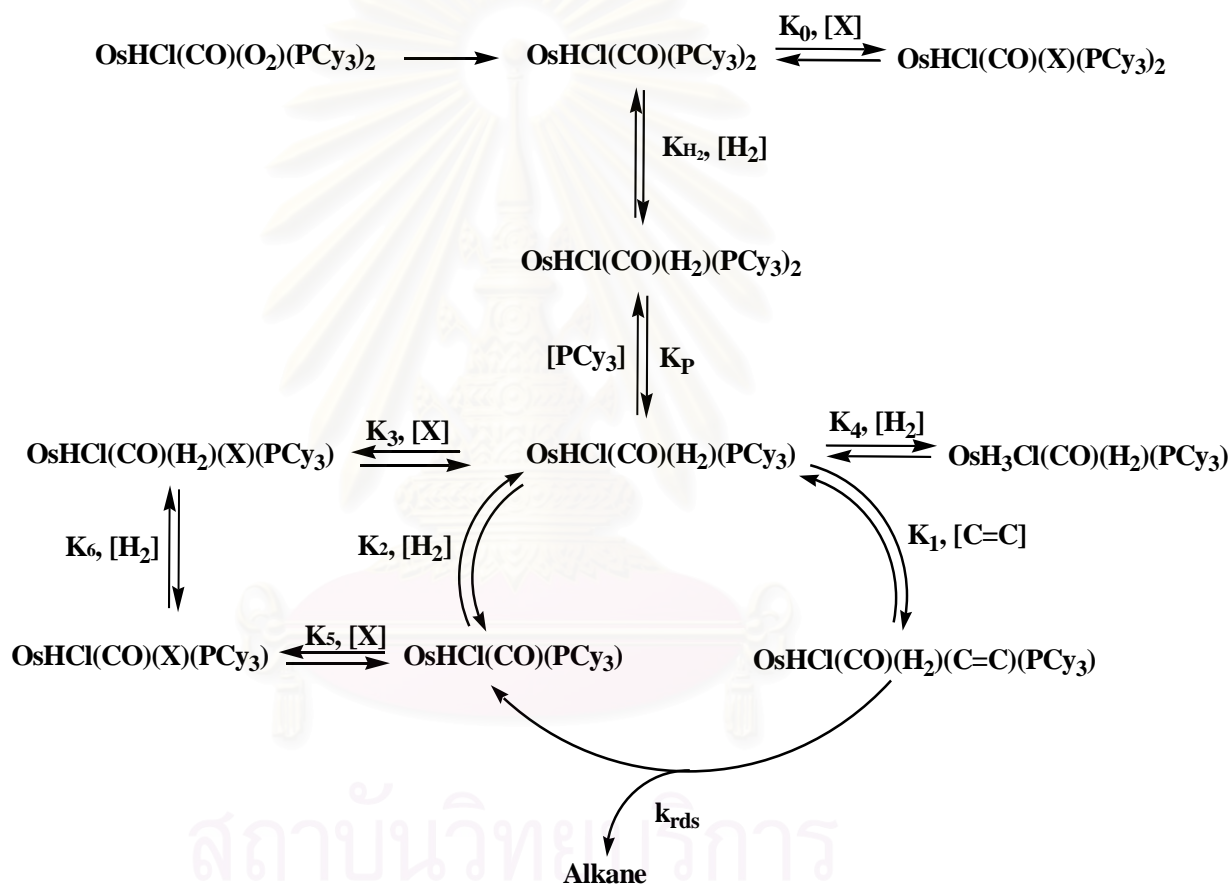
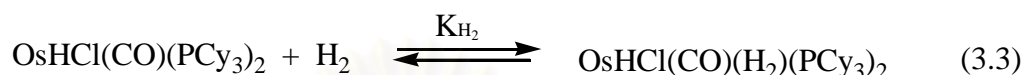
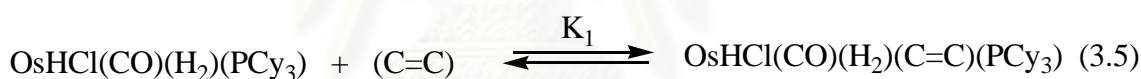


Figure 3.11 Proposed catalytic mechanism for NR hydrogenation in the presence of $\text{OsHCl}(\text{CO})(\text{O}_2)(\text{PCy}_3)_2$.

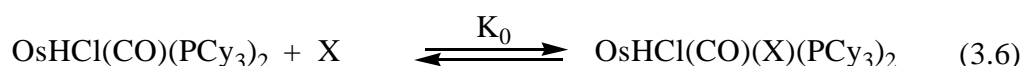
When the O₂ adducted catalyst precursor complex is employed in the hydrogenation system, OsHCl(CO)(O₂)(PCy₃)₂ is activated by O₂ dissociation to produce the five-coordinate analogue, OsHCl(CO)(PCy₃)₂, which is an active species. According to its coordinative unsaturation, a molecule of H₂ coordinates to OsHCl(CO)(PCy₃)₂ by η² coordination as shown in eq.(3.3).

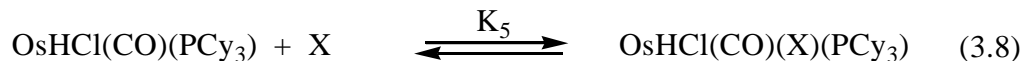
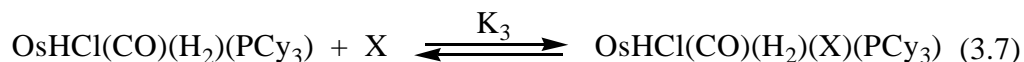


The complex formed in eq. (3.3) subsequently dissociates into a monophosphine complex (Parent et al., 1998a) which then reacts with carbon-carbon double bond of NR to produce OsHCl(CO)(H₂)(C=C)(PCy₃) as shown in eq. (3.4) and (3.5), respectively.

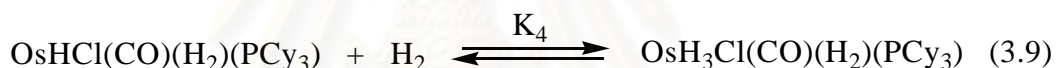


From the observed inverse behaviors with respect to the rubber concentration and high hydrogen pressure (> 41.4 bar), it appears that there are effective competitions between carbon-carbon double bond and impurities coordination or a second hydrogen molecule. The effect of impurities (X) in NR on the hydrogenation rate can be compared to the effect of the nitrile functional group, which inhibits the catalytic activity in NBR hydrogenation. Whereas the impurities inside NR are dominated by proteins, the amine group of proteins is an electron donating species that may react with intermediate species, OsHCl(CO)(PCy₃)₂, OsHCl(CO)(H₂)(PCy₃) or OsHCl(CO)(PCy₃), and then deactivate the catalysts. Eq. (3.6), (3.7) and (3.8) illustrate three possible pathways of impurities coordination that could inhibit the catalytic activity.





Unlike the shift in second- to zero-order behavior dependence on hydrogen pressure in the hydrogenation of NBR (Parent et al., 1998b) or PIP (Charmondusit et al., 2003) catalyzed by $\text{OsHCl}(\text{CO})(\text{O}_2)(\text{PCy}_3)_2$, the kinetic data of NR hydrogenation in the presence of this Os catalytic precursor showed the shift in first- to zero-order dependence on the low hydrogen pressure and then the inverse behavior appeared when hydrogen pressure exceeded 41.4 bar. It is possible that NR hydrogenation required only 1 molecule of H_2 to generate the hydrogenated product. The second hydrogen molecule may react with $\text{OsHCl}(\text{CO})(\text{H}_2)(\text{PCy}_3)$ to form the stable 18-electron catalytic species, $\text{OsH}_3\text{Cl}(\text{CO})(\text{H}_2)(\text{PCy}_3)$, as illustrated in eq. (3.9).



Parent et al. (1998b) reported that the observed kinetic isotope effect is involved with the cleavage of a bond to hydrogen in the rate-determining reaction. The rate expression for olefin hydrogenation is assumed from the coordination of olefin onto an Os-H bond or by a reductive elimination of an osmium-alkyl to produce the saturated product as shown in eq. (3.10).

$$-\frac{d[\text{C}=\text{C}]}{dt} = k_{\text{rds}}[\text{OsHCl}(\text{CO})(\text{H}_2)(\text{C}=\text{C})(\text{PCy}_3)] \quad (3.10)$$

A material balance on the osmium complex charged into the system given by eq. (3.11) is a function of the total amount of osmium ($[\text{Os}]_{\text{T}}$).

$$\begin{aligned} [\text{Os}]_{\text{T}} = & [\text{OsHCl}(\text{CO})(\text{H}_2)(\text{C}=\text{C})(\text{PCy}_3)] + [\text{OsHCl}(\text{CO})(\text{H}_2)(\text{PCy}_3)] + [\text{OsHCl}(\text{CO})(\text{PCy}_3)_2] \\ & + [\text{OsHCl}(\text{CO})(\text{H}_2)(\text{PCy}_3)_2] + [\text{OsHCl}(\text{CO})(\text{X})(\text{PCy}_3)_2] + [\text{OsHCl}(\text{CO})(\text{PCy}_3)] \\ & + [\text{OsHCl}(\text{CO})(\text{H}_2)(\text{X})(\text{PCy}_3)] + [\text{OsHCl}(\text{CO})(\text{X})(\text{PCy}_3)] + [\text{OsH}_3\text{Cl}(\text{CO})(\text{H}_2)(\text{PCy}_3)] \end{aligned} \quad (3.11)$$

Every osmium complex species concentration term in eq. (3.11) can be converted in terms of $\text{OsHCl}(\text{CO})(\text{H}_2)(\text{C}=\text{C})(\text{PCy}_3)$ using the equilibria defined in Figure 3.11 and then can be substituted into eq.(3.10) to provide the resulting rate law as shown in eq.(3.12). Derivation of the expression is shown in Appendix C.

$$-\frac{d[\text{C}=\text{C}]}{dt} = \frac{k_{\text{rds}} K_1 K_2 K_p K_{\text{H}_2} [\text{Os}]_T [\text{H}_2] [\text{C}=\text{C}]}{K_2 K_p K_{\text{H}_2} [\text{H}_2] (1 + K_1 [\text{C}=\text{C}]) + K_p K_{\text{H}_2} (1 + K_2 K_3 [\text{X}] [\text{H}_2] + K_3 [\text{X}] + K_2 K_4 [\text{H}_2]^2) + K_2 [\text{PCy}_3] (1 + K_{\text{H}_2} [\text{H}_2] + K_0 [\text{X}])} \quad (3.12)$$

The rate law equation of NR hydrogenation catalyzed by catalyst precursor, $\text{OsHCl}(\text{CO})(\text{O}_2)(\text{PCy}_3)_2$, indicates that the reaction exhibited a first order dependence on osmium concentration and an inverse behavior with respect to rubber concentration due to the impurities in NR. According to the observed kinetic data, the rate of NR hydrogenation exhibited a first-order dependence at low hydrogen pressure. The order of reaction with respect to hydrogen shifted to a zero-order dependence when hydrogen pressure was varied over the range of 13.8 to 41.4 bar. Above 41.4 bar, the term of $K_2 K_4 [\text{H}_2]^2$ in eq. (3.12) was more significant so that the rate of NR hydrogenation showed an inverse behavior on hydrogen.

3.4 Relative Viscosity of Hydrogenated Natural Rubber

Although FTIR or NMR spectroscopy can detect the level of hydrogenation, these techniques are not sensitive enough to investigate side reactions such as degradation and crosslinking during the hydrogenation reaction. Dilute solution viscometry is used to monitor the changes of molecular weight. The viscosity of a dilute NR and HNR solutions relative to pure solvent (η_{rel}) provides a simple and effective means of measuring the consequences of degradation of samples. Over the range of conditions investigated ($[\text{Os}] = 20 - 40 \mu\text{M}$, $P_{\text{H}_2} = 3.5 - 55.2 \text{ bar}$, $[\text{C}=\text{C}] = 64.9 - 326.0 \text{ mM}$ and $[\text{p-TSA}]/[\text{Os}] = 5 - 60$ at 140°C), the results of the relative viscosity of some HNR samples are summarized in Tables 3.4 and 3.7. Figures 3.12(a) – 3.12(d) illustrate the effect of $[\text{Os}]$, $[\text{C}=\text{C}]$, P_{H_2} and the molar ratio of $[\text{p-TSA}]/[\text{Os}]$ on the relative viscosity of HNR. It was found that the relative viscosity of NR was 7.54 while the relative viscosity of HNR varied over the range of 7.12 - 9.88, showing dependence on the reaction condition, degree of hydrogenation and

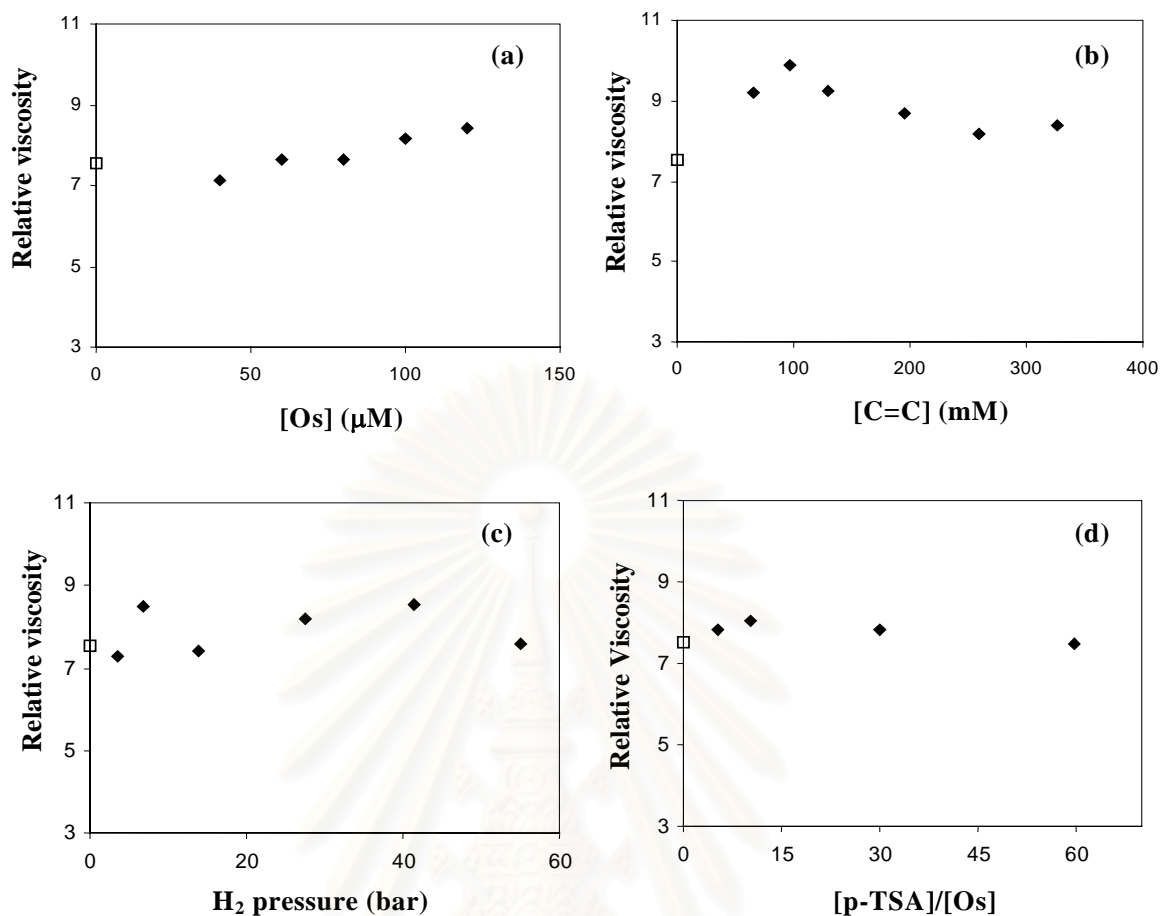


Figure 3.12 (a) Relative viscosity (η_{rel}) of HNR as a function of total metal loading (72.7 - 98.3% hydrogenation): $P_{H_2} = 27.6$ bar, $[C=C] = 260$ mM, $T = 140^\circ C$; (b) Relative viscosity of HNR as a function of rubber concentration (95 - 98% hydrogenation): $[Os] = 100 \mu M$, $P_{H_2} = 27.6$ bar, $T = 140^\circ C$; (c) Relative viscosity of HNR as a function of hydrogen pressure (93 - 96% hydrogenation): $[Os] = 100 \mu M$, $[C=C] = 260$ mM, $T = 140^\circ C$; (d) Relative viscosity of HNR as a function of acid-catalyst ratio (95 - 98% hydrogenation): $[Os] = 100 \mu M$, $[C=C] = 260$ mM, $P_{H_2} = 27.6$ bar, $T = 140^\circ C$ in toluene (Relative viscosity of NR (\square) = 7.54).

reaction time. The relative viscosity results of HNR are different from that of hydrogenated PIP (Charmondusit et al., 2003), which has a fairly constant relative viscosity with varying $[Os]$, $[C=C]$ and P_{H_2} . Figure 3.12(a), 3.12(c) and 3.12(d) show that the relative viscosity of HNR samples were not changed significantly when $[Os]$, P_{H_2} and $[p-TSA]/[Os]$ increased. For the effect of rubber concentration (Figure 3.12(b)), the relative viscosity of samples hydrogenated at low rubber concentration (64.9 - 129.9 mM) was greater than that of samples hydrogenated at higher rubber loading. This might be explained on the basis that when the catalyst loading is relatively high to the amount of polymer, it is possible to present a higher degree of crosslinking or branching of polymer chain. Similar results were observed for NBR hydrogenation catalyzed by $[Ir(cod)(PCy_3)(py)]PF_6$ (Hu, 2000).



CHAPTER 4

HYDROGENATION OF NATURAL RUBBER IN THE PRESENCE OF $[\text{Ir}(\text{cod})(\text{PCy}_3)(\text{py})]\text{PF}_6$

Chemical modification of polymers is a postpolymerization process to produce polymers with desirable properties that are not accessible by general polymerization (McManus and Rempel, 1995). Hydrogenation, one form of the chemical modification, has been used to reduce the saturation of diene polymers in order to enhance their thermal and oxidative resistance of the polymers. Hydrogenation can be provided by catalytic or non-catalytic methods. Due to disadvantages of non-catalytic methods which often lead to side reactions (Nang, et al., 1976), catalytic hydrogenation has been increasingly studied. Although heterogeneous catalysts such as $\text{Pd}/\text{Al}_2\text{O}_3$, Pd/CaCO_3 and Pd/BaSO_4 can be used as catalysts for hydrogenation of polymers (Chang and Huang, 1998; Cassano et al., 1998), homogeneous catalysts are more favorable for hydrogenation of unsaturated homo diene based polymers as well as diene based copolymers with sensitive functional groups such as $-\text{CN}$ or CO_2H . Homogeneous catalysts generally have higher selectivity and they are not susceptible to macroscopic diffusion problems (Bhaduri and Mukesh, 2000). Homogeneous catalysts for hydrogenation of diene-base polymers have been generally dominated by complexes of group VIII transition metals in the second row of the periodic table such as rhodium, ruthenium and palladium complexes.

As for the potential of transition metals in the third row of the periodic table, it has previously been generally felt that they have less catalytic activity than those of the second row. However, iridium-based catalysts have been shown to be efficient catalysts for hydrogenation of alkenes (Crabtree, 1979). The judicious choices of a suitable metal-ligand system, solvent and choice of reaction condition may lead to highly efficient catalysts. Crabtree et al. (1977) discovered that the use of chlorinated solvents which are non-coordinating solvents such as CHCl_3 , $\text{C}_6\text{H}_5\text{Cl}$ and CH_2Cl_2 enhanced the catalytic activity of iridium catalysts, whereas $[\text{Ir}(\text{cod})\text{L}_2]\text{PF}_6$ and $[\text{Ir}(\text{cod})\text{L}(\text{py})]\text{PF}_6$, while non-coordinating solvents such as benzene, toluene or hexane were unsuccessful in promoting the activity of the iridium catalyst because

only catalytically inactive precipitates were formed under hydrogen. The chlorinated solvents were reported to be the only viable solvents for catalytic hydrogenation with these cationic iridium catalysts, presumably since they have high polarity but negligible coordinating power (Crabtree, 1979). They found that these iridium catalysts showed much smaller rate differences between mono-, di-, tri- and tetra-substituted alkenes. Another advantage, which differs from other catalysts, of these iridium catalysts is that both the precursors and the catalyst themselves are stable to other oxidizing reagents, such as O₂ or EtI generally rapidly deactivate all other hydrogenation catalysts.

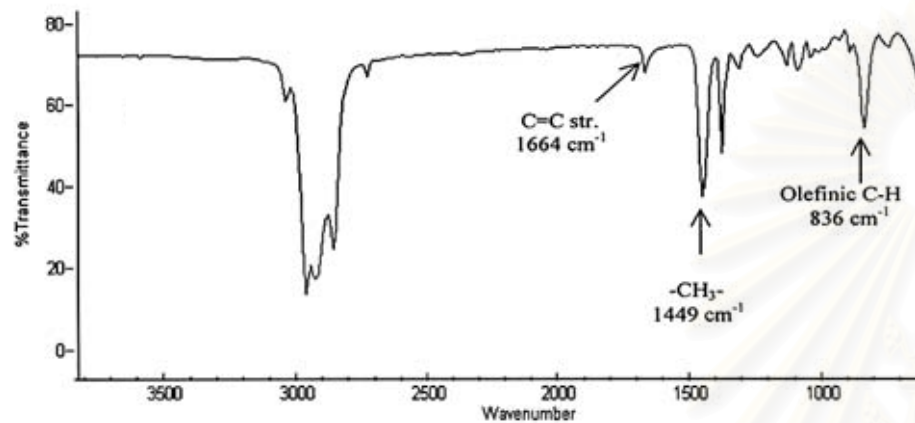
There are some previous research reports on the hydrogenation of diene - based polymers catalyzed by iridium catalysts. Gilliom (1989) studied the catalytic hydrogenation of polybutadiene and butadiene-styrene triblock copolymer by using polymer entrained [Ir(cod)(PMePh₂)₂]₂PF₆ as a catalyst in the absence of solvent under moderate conditions. Hu (2000) studied the kinetics of the hydrogenation of nitrile-butadiene rubber using [Ir(cod)(PCy₃)(py)]PF₆ in solution. Charmondusit (2002) has also used this iridium complex to hydrogenate synthetic *cis*-1,4-polyisoprene in solution and proposed a catalytic mechanism for this system.

In the present study, the goal of the research was to study the hydrogenation of natural rubber catalyzed by [Ir(cod)(PCy₃)(py)]PF₆ and compare the results with those of synthetic *cis*-1,4-polyisoprene hydrogenation examined by Charmondusit (2002). The effect of reaction parameters on the hydrogenation rate such as catalyst concentration, rubber concentration, hydrogen pressure and reaction temperature were investigated and the reaction mechanisms of natural rubber and synthetic *cis*-1,4-polyisoprene hydrogenation were proposed. The effect of the addition of some acids on the hydrogenation rate was also observed.

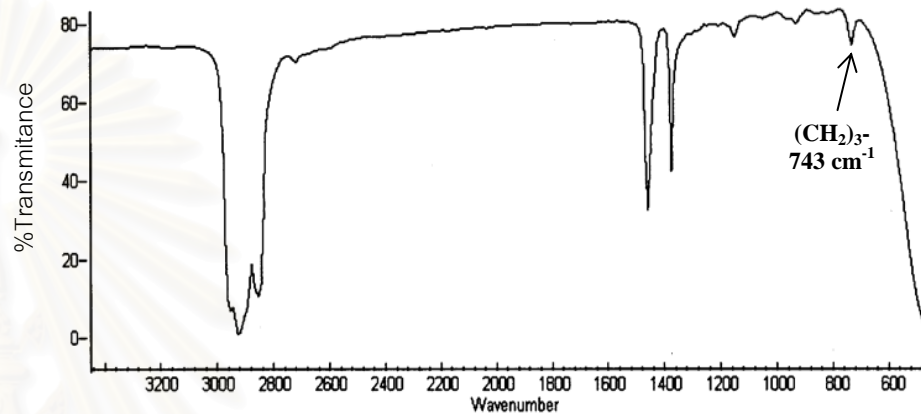
4.1 Structure characterization using FTIR and NMR spectroscopy

The structure of synthetic *cis*-1,4-polyisoprene (PIP) and natural rubber (NR) before and after hydrogenation process was preliminarily characterized by infrared spectroscopy (FTIR) as shown in Figure 4.1. The structures of hydrogenated natural rubber (HNR) and hydrogenated *cis*-1,4-polyisoprene (HPIP) are similar to an alternating ethylene-propylene copolymer. The characteristic FTIR peaks of both hydrogenated rubbers show that the absorption bands corresponding to the C=C stretching, olefinic C-H bending and $-(CH_2)_3-$ are located at 1664, 836 and 739 cm^{-1} , respectively. The characteristic signals of unsaturation, 1664 and 836 cm^{-1} , disappeared in the hydrogenated rubbers while an intense signal appeared at 739 cm^{-1} due to saturated carbon formed through hydrogenation. For FTIR spectrum of NR, the weak transmittance bands at 3285 cm^{-1} ($>N-H$) and 1531 cm^{-1} ($>N-C=O$) (Aik-Hwee et al., 1992) remained constant after hydrogenation.

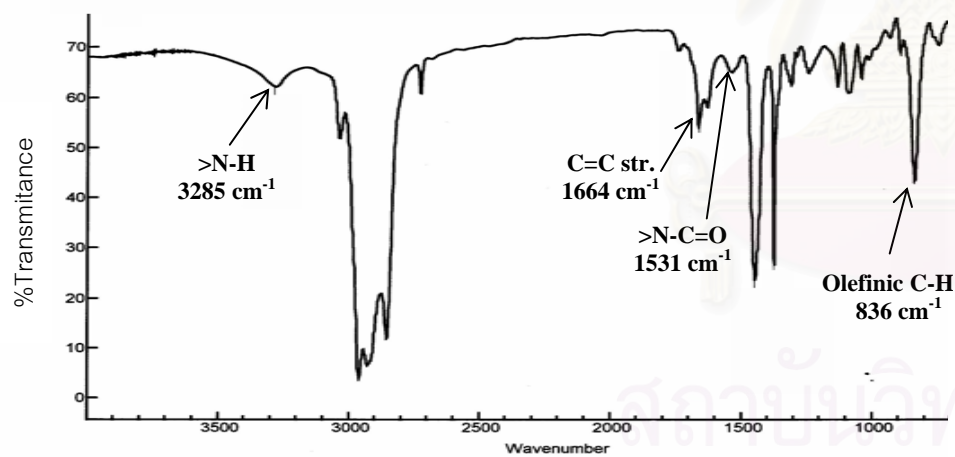
1H -NMR spectroscopy was used to investigate the actual degree of hydrogenation in each sample. The 1H -NMR spectra of PIP and NR before and after the hydrogenation reaction are shown in Figure 4.2. As can be observed, there is a sizeable reduction in the olefinic proton signal at 5.1 ppm after the hydrogenation process, which confirms that the carbon-carbon double bond in PIP and NR was hydrogenated. The aliphatic proton signals at 0.8 and 1.2 ppm, attributed to saturated $-CH_3$ and $-CH_2-$ groups, show a strong increment due to the chemical transformation of double bonds upon saturation. The actual degree of hydrogenation could be calculated from the peak area at 5.1 ppm and the summation of peak area between 0.8 and 2.0 ppm as described in Chapter 2 and Appendix B.



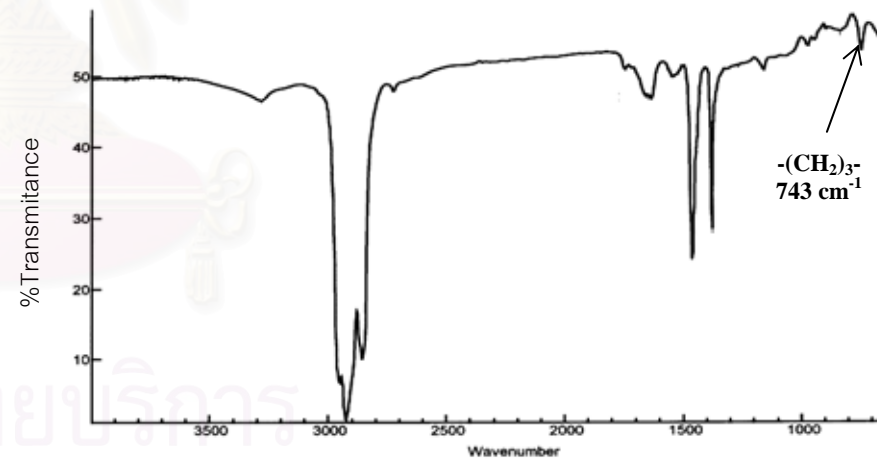
(a) PIP



(b) HPIP



(c) NR



(d) HNR

Figure 4.1 FTIR spectra of PIP and NR before and after hydrogenation catalyzed by $[\text{Ir}(\text{cod})(\text{PCy}_3)(\text{py})]\text{PF}_6$.

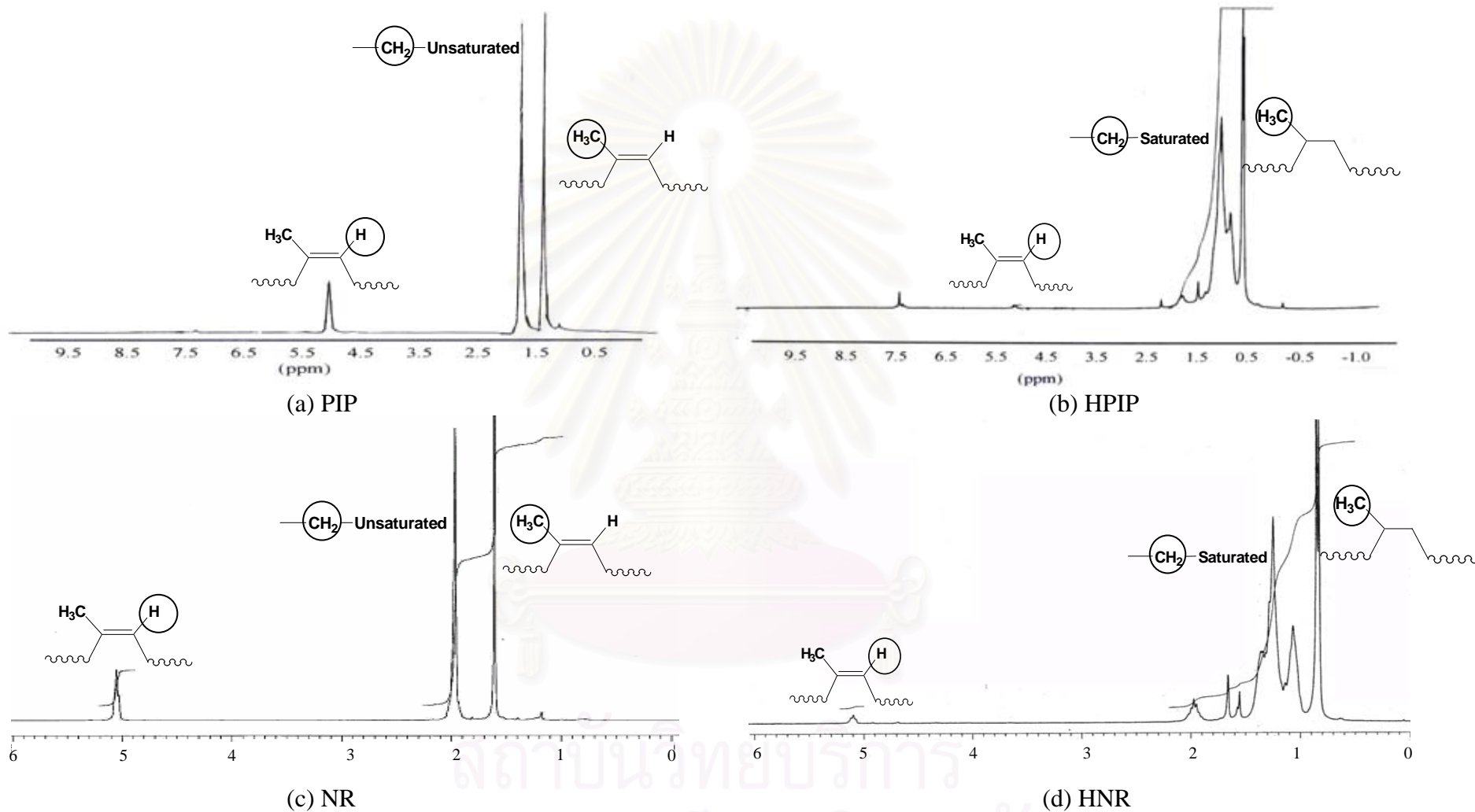


Figure 4.2 ^1H -NMR spectra of PIP and NR before and after hydrogenation catalyzed by $[\text{Ir}(\text{cod})(\text{PCy}_3)(\text{py})]\text{PF}_6$.

4.2 Kinetic Experiments of Natural Rubber Hydrogenation Compared with Synthetic *Cis*-1,4-Polyisoprene Hydrogenation

All the kinetic data for NR hydrogenation in the presence of the homogeneous catalyst, $[\text{Ir}(\text{cod})(\text{PCy}_3)(\text{py})]\text{PF}_6$, were obtained using an automated gas-uptake apparatus. Kinetic experiments conducted by using a two-level factorial design was studied for PIP hydrogenation (Charmondusit, 2002) in order to screen the main and interaction effects of the system and the results were used to predict the possible effect from the parameters on the NR hydrogenation. Univariate experiments were carried out to investigate the effect of each factor individually. All kinetic data were collected under a constant, high pressure of hydrogen, with vigorous mixing. Therefore, $[\text{H}_2]$ was assumed to be in equilibrium with the gaseous pressure and remained constant during the course of the reaction. Consequently, the reaction could be approximated as a pseudo-first-order reaction:

$$-\frac{d[\text{C} = \text{C}]}{dt} = k'[\text{C} = \text{C}] \quad (4.1)$$

where k' is the pseudo-first-order rate constant. Figure 4.3(a) shows represent the plots of conversion versus time for the hydrogenation reaction of PIP and NR. The hydrogen consumption plot indicates that the reaction was apparently first-order in the olefinic substrate, according to eq (4.1). Eq.(4.2) is further expressed in terms of the conversion of unsaturated double bonds (extent of hydrogenation), x , as

$$\ln(1 - x) = -k't \quad (4.2)$$

where t is the reaction time. Figure 4.3(b) shows a linear plot of $\ln(1-x)$ versus time plots for PIP and NR hydrogenation. The pseudo-first-order rate constant was then readily determined from the slope of the corresponding curve. The difference between the \ln plot of PIP hydrogenation and that of NR hydrogenation was that the initial phase of NR hydrogenation was slower. Presumably, the catalyst may have needed time to be dissolved in the natural rubber solution and/or some impurities in NR might retard the rate of reaction in the initial period as they were scavenged by some of catalyst.

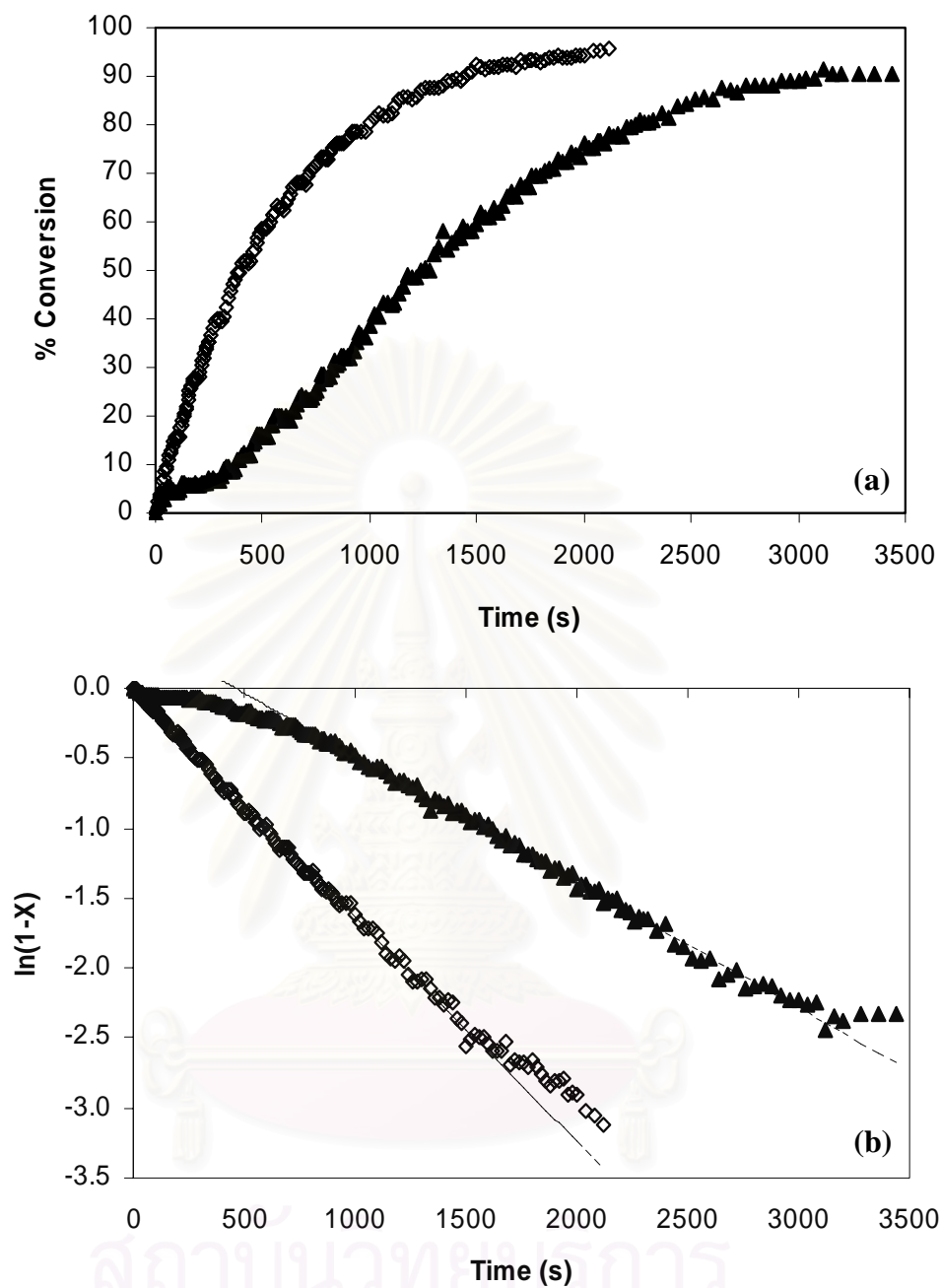


Figure 4.3 Hydrogenation profile of PIP and NR obtained from gas uptake apparatus: (a) olefin conversion profiles and (b) first-order \ln plot (----- model from linear regression). PIP hydrogenation (\diamond): $[\text{Ir}] = 90 \mu\text{M}$, $[\text{C}=\text{C}] = 259.8 \text{ mM}$; $P_{\text{H}_2} = 27.6 \text{ bar}$ at 130°C and NR hydrogenation (\blacktriangle): $[\text{Ir}] = 105 \mu\text{M}$, $[\text{C}=\text{C}] = 151.9 \text{ mM}$; $P_{\text{H}_2} = 27.6 \text{ bar}$ at 140°C in monochlorobenzene.

The statistical analysis for PIP hydrogenation in the presence of $[\text{Ir}(\text{cod})(\text{PCy}_3)(\text{py})]\text{PF}_6$ determined by Charmondusit (2002) was summarized here in order to use it as a preliminary study for the NR hydrogenation. A two-level factorial design analysis was applied to investigate the significance of interaction between factors, which affected the hydrogenation rate and the catalytic reaction mechanism. The three main factors of interest were catalyst concentration, rubber concentration and hydrogen pressure. The response for each variable was the rate constant. The levels of factors might be arbitrarily called “low (-)” and “high (+)”. The range for $[\text{Ir}]$, $[\text{C}=\text{C}]$ and P_{H_2} was 80 to 100 μM , 246 to 500 mM, and 20.7 to 34.5 bar, respectively in monochlorobenzene at a constant reaction temperature of 130°C. The results show that $[\text{Ir}]$ and P_{H_2} had a positive influence on the rate of hydrogenation; while, $[\text{C}=\text{C}]$ exhibited a negative result, which is possible due to some impurities such as residual catalyst additives in the polymerization process which can reduce the catalytic efficiency of the iridium catalyst in the hydrogenation process. The binary interactions, $[\text{Ir}]*P_{\text{H}_2}$, $[\text{Ir}]*[\text{C}=\text{C}]$ and $P_{\text{H}_2}*[\text{C}=\text{C}]$, and three-factor interaction, $[\text{Ir}]*P_{\text{H}_2}*[\text{C}=\text{C}]$, were not highly significant.

Although the results of the 2^3 factorial design summarized above are unable to explore fully a wide region in the factor space, they can indicate major trends and help to determine a promising direction for further experimentation. The univariate components of the central composite design augment the factorial study by exploring how each factor influences the hydrogenation rate in isolation. The experimental factors are varied one at a time, with the remaining factors held constant. This method provides an estimation of the effect of a single variable at selected set of fixed conditions of the other variables. In this section, the results from univariate experiments for NR hydrogenation were compared to those previously obtained for PIP hydrogenation (Charmondusit, 2002). The results for the NR hydrogenation experiments are summarized in Table 4.1. The compared kinetic data for the hydrogenation of PIP and NR are presented in Figure 4.4 – 4.7.

Table 4.1 Kinetic Results of Univariate Experiments for NR Hydrogenation Catalyzed by [Ir(cod)(PCy₃)(py)]PF₆

Expt.	[Ir] (μM)	[C=C] (mM)	P _{H₂} (bar)	Temp. ($^{\circ}\text{C}$)	%Hydrogenation at 40 min.	k'x10 ³ (s ⁻¹)	η_{rel}
1	50	152.04	27.6	140	31.0	0.12	
2	65	151.96	27.6	140	45.5	0.39	8.28
3	85	151.94	27.8	140	67.9	0.64	7.81
4	105	151.94	27.8	140	81.6	0.90	8.11
5	105	152.01	27.6	140	84.6	0.85	
6	125	151.92	27.7	140	73.9	1.02	8.94
7	125	151.97	27.9	140	88.8	1.13	
8	145	152.01	27.6	140	94.3	1.36	8.99
9	165	151.96	27.6	140	93.8 (35.7 min.)	1.39	
10	105	151.98	7.0	140	48.2	0.24	
11	105	151.99	14.0	140	66.8	0.46	7.03
12	105	151.88	41.4	140	82.5	1.15	9.70
13	105	151.88	55.1	140	94.4 (37.7 min.)	1.43	9.81
14	105	152.02	69.2	140	96.4 (38.7 min.)	1.66	
15	105	100.10	27.8	140	94.6 (35.3 min.)	1.58	8.53
16	105	200.03	27.6	140	57.0	0.57	7.48
17	105	259.76	27.6	140	39.8	0.43	7.79
18	105	300.02	27.8	140	15.9	0.15	
19	105	151.99	27.6	130	28.4	0.58	
20	105	151.98	27.6	135	44.5	0.80	
21	105	151.94	27.6	145	86.8	1.13	
22	105	151.96	27.4	150	89.6 (26.3 min.)	1.91	

Solvent: Monochlorobenzene

Relative viscosity (η_{rel}) of NR = 7.32

4.2.1 Effect of Catalyst Concentration

The effect of catalyst concentration on PIP and NR hydrogenation was investigated by varying the catalyst concentration as shown in Figure 4.4. The range of catalyst concentration for hydrogenation of PIP (246 mM) was 30 to 150 μM at 130°C and the range of catalyst concentration for hydrogenation of NR (152 mM) was 50 to 165 μM at 140°C. The hydrogen pressure was constant at 27.6 bar in chlorobenzene for all experiments. The results suggest that a first-order dependence on catalyst concentration occurred below ca. 100 μM for PIP hydrogenation. The higher load of catalyst caused a zero-order dependence on catalyst concentration. A well-known side reaction, the dimerization of the coordinatively unsaturated catalytically active species to inactive complexes such as $[\text{H}_2\text{Ir}_2(\mu\text{-H})_3(\text{PCy}_3)_4]\text{PF}_6$ (Dickson, 1985), might be employed to interpret this phenomena (Crabtree and Davis, 1986). NR hydrogenation catalyzed by $[\text{Ir}(\text{cod})(\text{PCy}_3)(\text{py})]\text{PF}_6$ also exhibited a first order dependence on the catalyst precursor loading, which implied that the active complex is a mononuclear species. Figure 4.4 also shows the comparison of catalytic activity of Ir complex for PIP and NR hydrogenation. The observation indicated that the NR hydrogenation system required the higher loading of catalyst; although, the rubber concentration of NR (152 mM) was less than that of PIP (246 mM). It can be presumed that impurities in NR might reduce the catalytic activity; thus, some portion of catalyst about 50 μM appears to be sacrificed due to removal of impurities. This behavior with respect to catalyst concentration is similar to that observed for the NR hydrogenation catalyzed by $\text{OsHCl}(\text{CO})(\text{O}_2)(\text{PCy}_3)_2$ which also exhibited a decrease in catalytic activity with an increase in the rubber concentration.

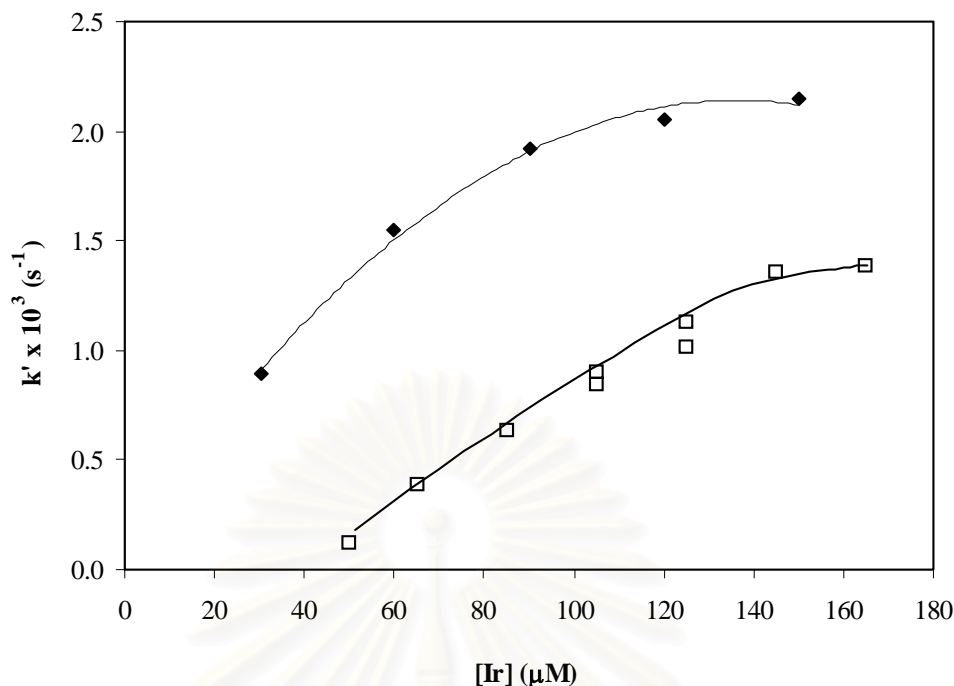


Figure 4.4 Effect of catalyst concentration on hydrogenation rate. PIP hydrogenation (Charmondusit, 2002) (◆): $P_{H_2} = 27.6$ bar, $[C=C] = 246$ mM; $T = 130^\circ\text{C}$ and NR hydrogenation (□): $P_{H_2} = 27.6$ bar, $[C=C] = 152$ mM; $T = 140^\circ\text{C}$.

4.2.2 Effect of Hydrogen Pressure

The order with respect to $[H_2]$ for the hydrogenation of acrylonitrile-butadiene rubber (NBR) in the presence of $RhCl(PPh_3)$ showed a first- to zero-order dependence as the system pressure increased (Parent et al., 1996), while a second- to zero-order behavior in hydrogen pressure was found in the system catalyzed by $OsHCl(CO)(O_2)(PCy_3)_2$ (Parent et al., 1998a). To investigate the dependence of the hydrogenation rate on the hydrogen pressure for the NR and PIP hydrogenation, series of experiments were carried out from 13.8 to 55.2 bar ($[Ir] = 90$ μM , $[C=C] = 246$ mM at 130°C in monochlorobenzene) for PIP hydrogenation and 7.0 to 69.2 bar ($[Ir] = 105$ μM , $[C=C] = 152$ mM at 140°C in monochlorobenzene) for NR hydrogenation. Plots of the rate constant versus hydrogen pressure of both rubbers are fairly linear, as shown in Figure 4.5 suggesting that the rate of hydrogenation was first-order with respect to the hydrogen pressure. The first order rate dependence implies that primarily a single reaction pathway is probably involved in the reaction of the unsaturation of the polymer with hydrogen. If more than one process were involved,

the relative contribution of each pathway should change with varying hydrogen pressure, and thus the dependence might deviate from the first order behavior observed. A similar behavior of first-order rate dependence on hydrogen pressure was also observed in the hydrogenation of NBR using this iridium complex (Hu, 2000).

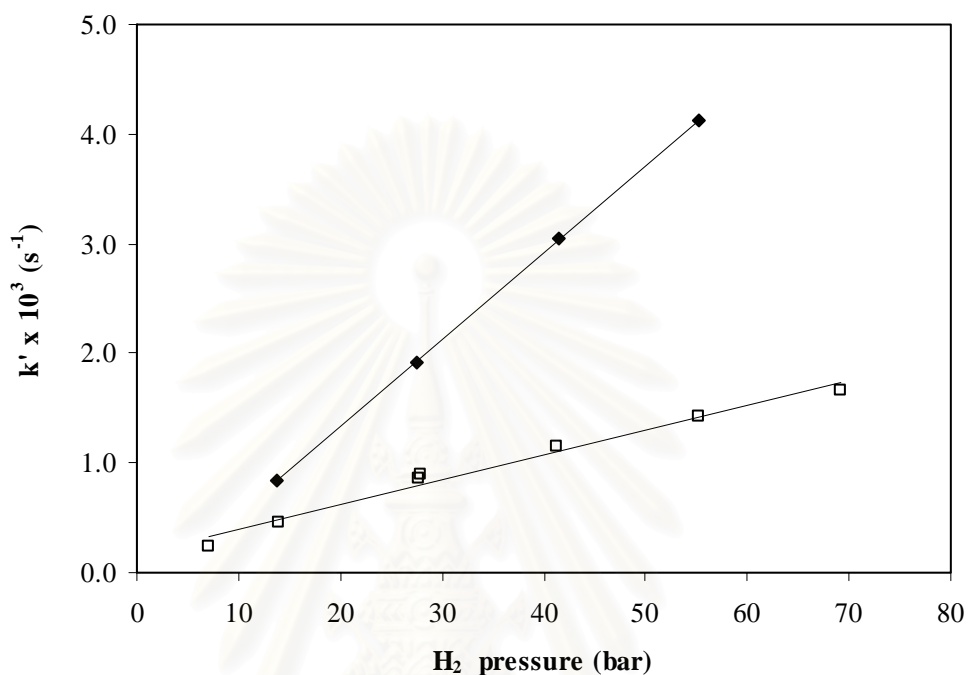


Figure 4.5 Effect of hydrogen pressure on hydrogenation rate. PIP hydrogenation (Charmondusit, 2002) (◆): [Ir] = 90 μ M; [C=C] = 246 mM; T = 130°C and NR hydrogenation (□): [Ir] = 105 μ M; [C=C] = 152 mM; T = 140 °C.

สถาบันวิทยบริการ
จุฬาลงกรณ์มหาวิทยาลัย

4.2.3 Effect of Rubber Concentration

The influence of rubber concentration on the hydrogenation rate was studied over the range of 163-500 mM ($[\text{Ir}] = 90 \mu\text{M}$, $P_{\text{H}_2} = 27.6 \text{ bar}$ at 130°C in monochlorobenzene) for PIP hydrogenation and 100-300 mM ($[\text{Ir}] = 105 \mu\text{M}$, $P_{\text{H}_2} = 27.6 \text{ bar}$ at 140°C in monochlorobenzene) for NR hydrogenation. The results for the comparison are shown in Figure 4.6. This results indicate that the hydrogenation activity was essentially unaffected by the amount of *cis*-1,4-polyisoprene. The conversion profiles for PIP hydrogenation that were first-order with respect to $[\text{C}=\text{C}]$ were, by definition, independent of the amount of olefin charged to the reactor. This agrees with the observations of *cis*-1,4-polyisoprene and styrene-butadiene copolymer (SBR) hydrogenation using the osmium system in which the $\text{C}=\text{C}$ concentration has no effect on the hydrogenation rate (Charmondusit et al., 2003; Parent et al., 1998a). Unlike the case of PIP hydrogenation, the relationship between the apparent rate constant and $\text{C}=\text{C}$ concentration in NR hydrogenation revealed that the reaction rate has an inverse rate behavior with an increase in the rubber loading. Crabtree et al. (1977) reported that iridium complexes, $[\text{Ir}(\text{cod})\text{L}(\text{py})]\text{PF}_6$ and $[\text{Ir}(\text{cod})\text{L}_2]\text{PF}_6$, were sensitive to a number of functional groups such as amines, which totally deactivate the catalysts via deprotonation reaction. Consequently, proteins which constitute a major impurity in NR likely lower the catalytic activity of $[\text{Ir}(\text{cod})(\text{PCy}_3)(\text{py})]\text{PF}_6$ by the amine content in the protein structure. The influence of impurities in NR drastically decreased the efficiency of the Ir complex; thus, it was necessary to reduce the concentration of NR or increase the reaction temperature in order to obtain a suitable reaction rate for the kinetic study. The effect of rubber concentration on the reaction rate of NR hydrogenation was similar to the hydrogenation of rubber with an interacting functional group such as the nitrile group in NBR. There are a number of reports showing that the activity of rhodium, ruthenium, osmium and iridium complexes was inhibited by coordination of nitrile functional group with the metal center of the complexes (Hu, 2000; Parent et al., 1998b; Parent et al., 1996; Martin et al., 1997).

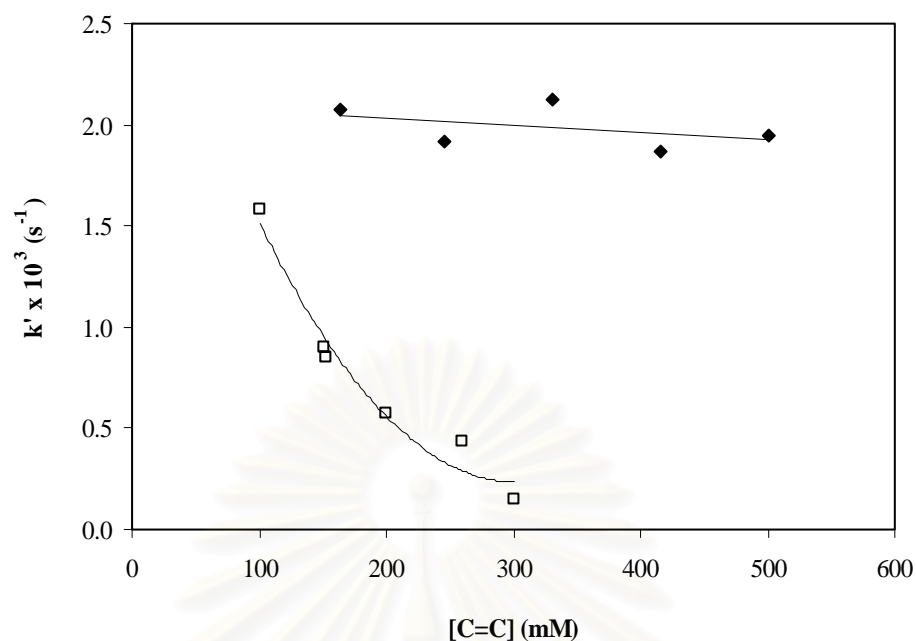


Figure 4.6 Effect of rubber concentration on hydrogenation rate. PIP hydrogenation (Charmondusit, 2002) (◆): $[\text{Ir}] = 90 \mu\text{M}$; $P_{\text{H}_2} = 27.6 \text{ bar}$; $T = 130^\circ\text{C}$ and NR hydrogenation (□): $[\text{Ir}] = 105 \mu\text{M}$; $P_{\text{H}_2} = 27.6 \text{ bar}$; $T = 140^\circ\text{C}$.

4.2.4 Effect of Reaction Temperature

A series of experiments were carried out over the temperature range of 120 to 140°C ($[\text{Ir}] = 90 \mu\text{M}$, $[\text{C}=\text{C}] = 246 \text{ mM}$ and $P_{\text{H}_2} = 27.6 \text{ bar}$ in monochlorobenzene) for PIP hydrogenation and 130 to 150°C ($[\text{Ir}] = 105 \mu\text{M}$, $[\text{C}=\text{C}] = 152 \text{ mM}$ and $P_{\text{H}_2} = 27.6 \text{ bar}$ in monochlorobenzene) for NR hydrogenation. The effect of temperature on the rate constant of hydrogenation for both rubbers can be represented by an Arrhenius plot as shown in Figure 4.7a. The linear plot indicates that a single rate-determining step is operative within the kinetic mechanism. The activation energy calculated from least squares regression analysis of $\ln(k')$ versus $1/T$ was 79.8 kJ/mol for PIP hydrogenation and 75.6 kJ/mol for NR hydrogenation. This provides further evidence that the kinetic data were obtained without mass transfer limitation and the diffusion of the reactants was not a rate-determining factor under these conditions. Hydrogenation at higher temperature exhibited a faster reaction rate and led to a higher efficiency. Although the hydrogenation rates of PIP

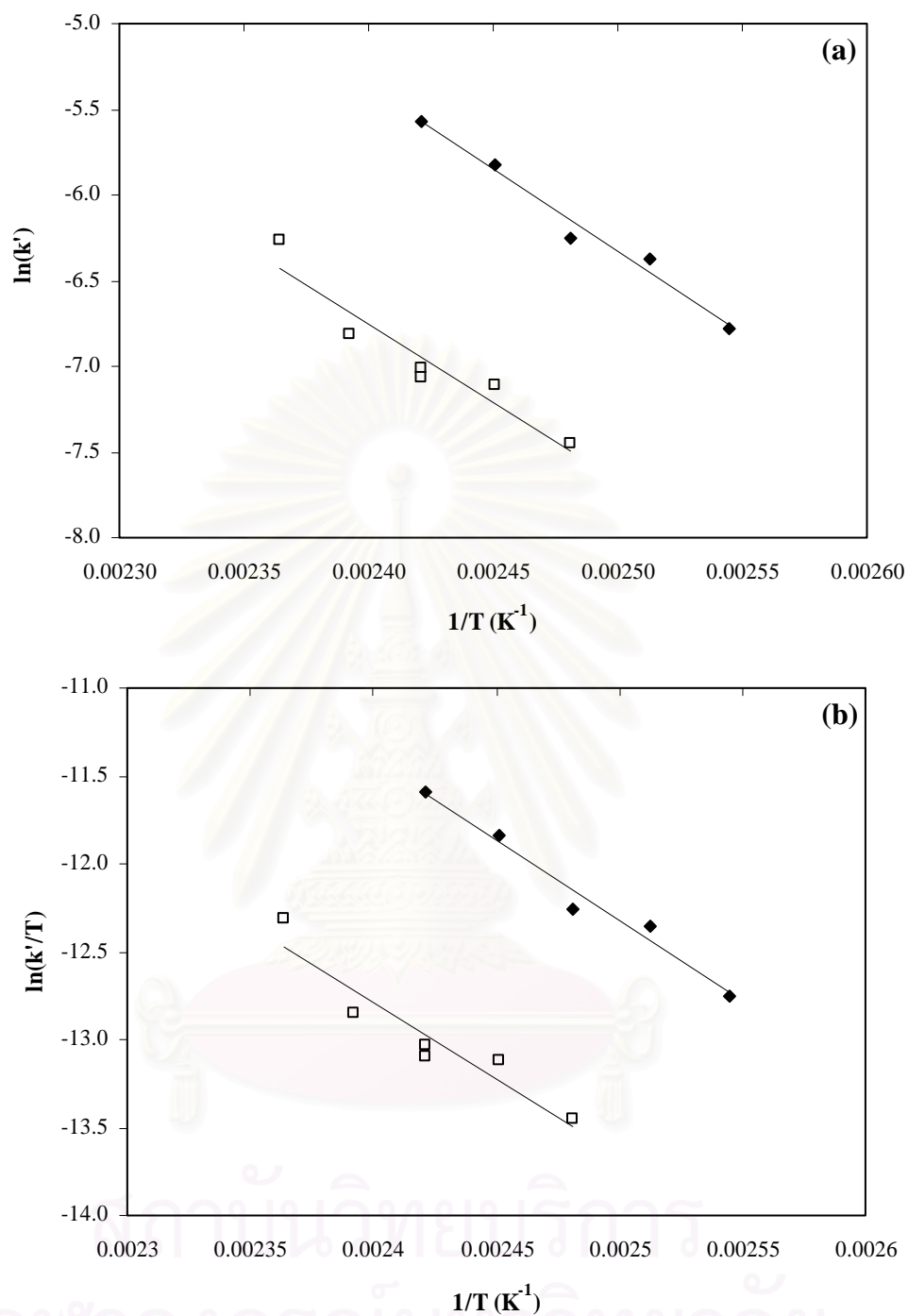


Figure 4.7 (a) Arrhenius plot and (b) Eyring plot for PIP and NR hydrogenation. PIP hydrogenation (Charmondusit, 2002) (\blacklozenge): $[\text{Ir}] = 90 \mu\text{M}$; $P_{\text{H}_2} = 27.6 \text{ bar}$; $[\text{C}=\text{C}] = 246 \text{ mM}$; $T = 120\text{-}140^\circ\text{C}$ and NR hydrogenation (\square): $[\text{Ir}] = 105 \mu\text{M}$; $P_{\text{H}_2} = 27.6 \text{ bar}$; $[\text{C}=\text{C}] = 152 \text{ mM}$; $T = 130\text{-}150^\circ\text{C}$.

and NR catalyzed by $\text{OsHCl}(\text{CO})(\text{O}_2)(\text{PCy}_3)_2$ were faster than that of the system in the presence of $[\text{Ir}(\text{cod})(\text{PCy}_3)(\text{py})]\text{PF}_6$, the apparent activation energy of the hydrogenation using Ir catalyst was lower than that of the system catalyzed by Os complex (109.3 kJ/mol for PIP hydrogenation (Charmondusit et al., 2003) and 122.8 kJ/mol for NR hydrogenation). It can be noted that the hydrogenation catalyzed by the Ir catalyst was less sensitive to reaction temperature than for the Os system. The Eyring equation was used to calculate the apparent activation enthalpy and entropy for the reaction. The Eyring plot presented in Figure 4.7b shows the enthalpy as 76.4 kJ/mol for PIP hydrogenation and 72.2 kJ/mol for NR hydrogenation. The entropy of activation for hydrogenation of PIP and NR was -108.9 and -130.6 J/mol K, respectively.

4.2.5 Effect of Solvents

The effect of different solvents on the hydrogenation rate of PIP and NR in the presence of Crabtree's catalyst was investigated at base conditions: $[\text{Ir}] = 90 \mu\text{M}$, $P_{\text{H}_2} = 27.6 \text{ bar}$, $[\text{C}=\text{C}] = 246 \text{ mM}$ at 130°C for PIP hydrogenation and $[\text{Ir}] = 105 \mu\text{M}$, $P_{\text{H}_2} = 27.6 \text{ bar}$, $[\text{C}=\text{C}] = 152 \text{ mM}$ at 140°C for NR hydrogenation. The results of these experiments are presented in Table 4.2. It shows that chlorinated solvents, chlorobenzene, dichloromethane, dichlorobenzene and trichlorobenzene, are viable solvents for catalytic hydrogenation of PIP and NR with this cationic iridium catalyst while the coordinating solvent, tetrahydrofuran, cannot be used as the solvent for this Ir catalytic system, in contrast to Rh (Crabtree, 1979) or Os (Charmondusit et al., 2003) catalysts. Crabtree et al. (1979) studied alkene hydrogenation catalyzed by $[\text{Ir}(\text{cod})\text{L}_2]\text{PF}_6$ and $[\text{Ir}(\text{cod})\text{L}(\text{py})]\text{PF}_6$ where (cod) was 1,5-cyclooctadiene and L was tertiary phosphine and found that noncoordinating solvents like toluene, benzene or hexane also could be inappropriate solvents since only catalytically inactive precipitates were formed under hydrogen. However, these Ir complexes were very active in noncoordinating solvents containing a chlorine atom except for 1,1-dichloroethylene and carbon tetrachloride since they failed to dissolve the Ir catalysts under a hydrogen atmosphere (Crabtree et al., 1977). In addition, the results shown in Table 4.2 indicate that the hydrogenation of both rubbers showed a slight difference in reaction rate with a different amount of chlorine atoms in the chlorinated solvents

Table 4.2 Effect of Solvent on Hydrogenation of *Cis*-1,4-Polyisoprene and Natural Rubber

Solvent	PIP Hydrogenation (Charmondusit, 2002)		NR Hydrogenation	
	$k' \times 10^3$ (s^{-1})	Final %Hydrogenation	$k' \times 10^3$ (s^{-1})	Final %Hydrogenation
	Chlorobenzene	1.92	98.1 (~35 min)	0.85
Tetrahydrofuran	0.80	75.8 (~1 h)	-	-
Dichloromethane	2.16	96.6 (~30 min)	-	-
Dichlorobenzene	1.73	97.1 (~40 min)	0.74	93.8 (~1.5 h)
Trichlorobenzene	2.21	97.4 (~30 min)	0.59	85.8 (~1.2 h)

4.2.6 Effect of Acid Addition on the Catalytic Activity

Acid addition has been found in some instances to enhance the catalytic activity of olefinic hydrogenation catalysts. Guo et al. (1997) reported that carboxylic acids increased the catalytic activity for the hydrogenation of an NBR emulsion catalyzed by $RuCl(CO)(styryl)(PCy_3)_2$. They suggested that the carboxylic acids were very effective in preventing the poisoning of the catalyst by impurities in the emulsion system. Yi et al. (2000) also investigated that the addition of acids with weakly coordinating anions such as trifluoromethanesulfonic acid (HOTf) and tetrafluoroboric acid-dimethyl ether complex ($HBF_4 \cdot OEt_2$) which increased the rate of alkene hydrogenation using $RuH(CO)(Cl)(PCy_3)_2$. They surmised that the increase in catalytic activity of this Ru catalytic species might be due to the selective entrapment of the phosphine ligand and the formation of a highly active 14-electron ruthenium-monophosphine species. In the case of NR hydrogenation, Charmondusit (2002) study and the results of acid addition presented in Chapter 3 show that the rate of NR hydrogenation in the presence of $OsHCl(CO)(O_2)(PCy_3)_2$ can be increased by adding some acids such as 3-chloropropionic acid (3-CPA) and *p*-toluenesulfonic acid (*p*-TSA). However, this behavior was not observed for PIP hydrogenation. Thus, it might be explained that the positive role of acids in the NR hydrogenation may be primarily due to possible neutralization of bases entities present in the rubber. For the

system of NR hydrogenation catalyzed by $[\text{Ir}(\text{cod})(\text{py})(\text{PCy}_3)]\text{PF}_6$, the role of acids, 3-CPA and p-TSA, on the hydrogenation of PIP and NR were studied and the results obtained are presented in Figure 4.8 and Table 4.3. The effect of acid addition on the hydrogenation rate of PIP and NR in the presence of Crabtree's catalyst was carried out at base conditions: $[\text{Ir}] = 60 \mu\text{M}$, $P_{\text{H}_2} = 27.6 \text{ bar}$, $[\text{C}=\text{C}] = 246 \text{ mM}$ at 130°C for PIP hydrogenation and $[\text{Ir}] = 105 \mu\text{M}$, $P_{\text{H}_2} = 27.6 \text{ bar}$, $[\text{C}=\text{C}] = 152 \text{ mM}$ at 140°C for NR hydrogenation.

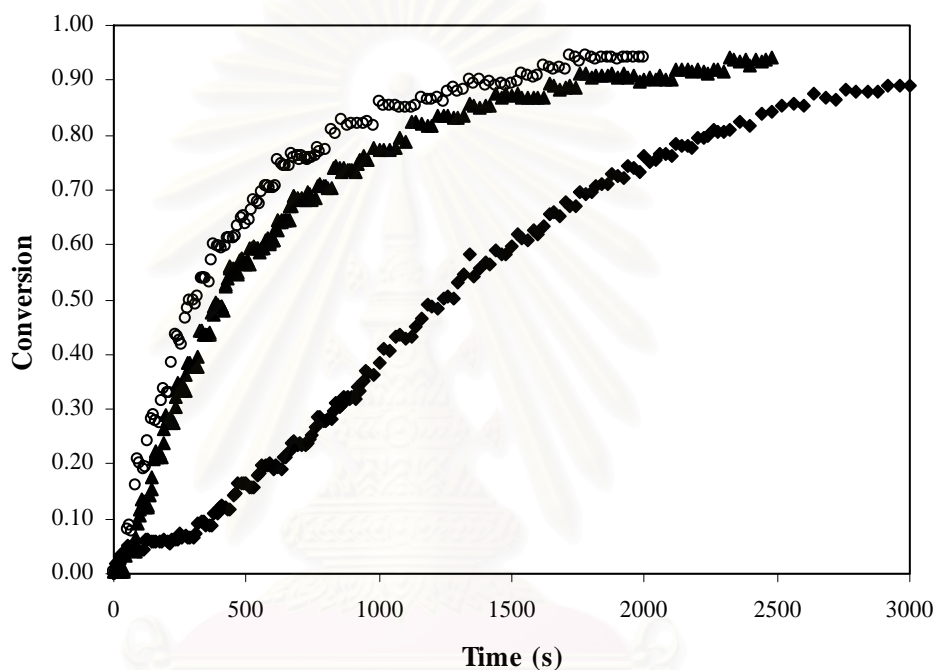


Figure 4.8 Comparison NR hydrogenation conversion profiles between non-acid addition (◆) and acid addition systems: $[\text{3-CPA}]/[\text{Ir}] = 21/1$ (▲) and $[\text{p-TSA}]/[\text{Ir}] = 20/1$ (○). $[\text{Ir}] = 105 \mu\text{M}$; $[\text{C}=\text{C}] = 152 \text{ mM}$; $P_{\text{H}_2} = 27.6 \text{ bar}$; $T = 140^\circ\text{C}$ in monochlorobenzene.

Table 4.3 Effect of Acid Addition on the Rate of Hydrogenation of *Cis*-1,4-Polyisoprene and Natural Rubber

Exp.	Rubber	Acid	[Acid] mM	[Acid]/[Ir]	%Hydrogenation at 20 min.	k' x 10 ³ (s ⁻¹)
1	PIP	-	-	-	81.9	1.48
2	PIP	p-TSA	0.60	9.9	88.1	1.78
3	PIP	3-CPA	0.63	10.6	89.3	1.85
4	NR	-	-	-	60.9	0.85
5	NR	p-TSA	0.53	5.0	74.2	1.37
6	NR	p-TSA	1.05	10.0	85.4	1.90
7	NR	p-TSA	2.11	20.1	86.4	2.10
8	NR	p-TSA	4.20	40.0	91.9	2.22
9	NR	3-CPA	0.56	5.3	79.6	1.56
10	NR	3-CPA	1.43	13.6	81.2	1.59
11	NR	3-CPA	2.22	21.1	81.8	1.57

Solvent: Monochlorobenzene

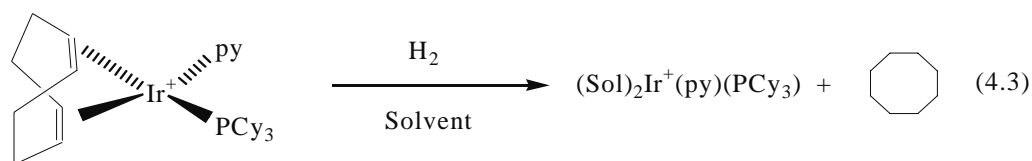
The conversion profiles in Figure 4.8 indicate that the addition of 3-CPA and p-TSA enhanced the rate of NR hydrogenation. The results of 3-CPA for the Ir system were different from the Os system as described in Chapter 3 in that the addition of 3-CPA exhibited a slower rate of hydrogenation when catalyzed by Os complex in monochlorobenzene. To investigate the role of acids on the NR hydrogenation in the presence of [Ir(cod)(py)(PCy₃)]PF₆, 3-CPA and p-TSA were also added to the PIP solution. It was found that the acid addition could slightly increase the rate of PIP hydrogenation. Therefore, it is possible that the acid addition might promote the catalytic activity of [Ir(cod)(PCy₃)(py)]PF₆ by preventing the poisoning of the catalyst by proteins present in NR or other residual impurities from the polymerization process for PIP. However, it cannot be concluded that the role of acid entrapped the PCy₃ of catalyst because Hu (2000) reported that a peak for free PCy₃ dissociated from the catalyst precursor at 10 ppm was not present in the ³¹P-NMR spectrum at 70°C, which indicated that no appreciable dissociation of the PCy₃

ligand occurred. However, the carboxylic acids have been known to increase the catalytic activity of the catalyst for the NR hydrogenation as shown in the previous chapter and in Charmondusit study (2002). An overload of these acids in the system might partially or totally deactivate Ir complexes, presumably by coordination (Crabtree et al., 1977).

4.3 Reaction Mechanism and Rate Law

The catalytic pathway of olefinic hydrogenation in the presence of Crabtree's catalyst and its analogues has been investigated. Hydrogenation of diene polymers catalyzed by homogeneous catalysts consists of many intermediate complexes. Thus, the manner in which to propose the catalytic mechanism for the hydrogenation of diene polymers is based on inference of kinetic data and electron counting schemes. The catalytic cycles of $[\text{Ir}(\text{cod})(\text{PCy}_3)(\text{py})]\text{PF}_6$ for the hydrogenation of PIP and NR are illustrated in Figure 4.9 and 4.10, respectively.

Crabtree et al. (1979) reported that $[\text{Ir}(\text{cod})(\text{PR}_3)(\text{py})]\text{PF}_6$ ($\text{PR}_3 = \text{PCy}_3, \text{P-}i\text{-Pr}_3$) reacts with H_2 at 0°C in CH_2Cl_2 in the presence of excess cyclooctadiene (cod) to obtain the *cis*-dihydrido-diolefin complexes. They had no evidence that $[\text{IrH}_2(\text{cod})(\text{PR}_3)(\text{py})]\text{PF}_6$ can be formed by the direct activation of H_2 by $[\text{Ir}(\text{cod})(\text{PR}_3)(\text{py})]\text{PF}_6$ in the absence of excess (cod) since pyridine, a donor ligand, inhibited H_2 addition to $[\text{Ir}(\text{cod})(\text{PCy}_3)(\text{py})]\text{PF}_6$ which was different from other donor ligands that favored H_2 addition to the metal center. However, the active catalyst can be formed in the presence of H_2 and a noncoordinating solvent, presumably via reduction of cyclooctadiene to cyclooctene (coe) and ultimately to cyclooctane (coa) as shown in eq. (4.3). It is particularly effective for the reduction of highly substituted alkenes since the $[\text{Ir}(\text{py})(\text{PCy}_3)]^+$ fragment is not very bulky (Dickson, 1985; Crabtree, 2001).



This 12-electron active species, $[\text{Ir}(\text{py})(\text{PCy}_3)]^+$, reacts with the H_2 molecule to generate the dihydrido iridium complex, $[\text{Ir}(\text{H}_2)(\text{py})(\text{PCy}_3)]^+$. The substrate double bond coordinates to the dihydrido catalyst. Then, the hydrogen is transferred to the pi-olefin complex to obtain an alkyl complex. The alkyl complex was cleaved by a transferred hydride to form hydrogenated polymer and to regenerate the cationic active species.

According to the proposed reaction mechanism, the hydrogenation of PIP and NR catalyzed by iridium complex is provided by the following rate expression:

$$-\frac{d[\text{C}=\text{C}]}{dt} = k_3 [\text{Ir}(\text{H}_2)(\text{C}=\text{C})(\text{py})(\text{PCy}_3)]^+ \quad (4.4)$$

A material balance on the active species of iridium charged to the hydrogenation system of PIP as shown in Figure 4.9 is given by eq. (4.5):

$$[\text{Ir}]_T = [\text{Ir}(\text{H}_2)(\text{C}=\text{C})(\text{py})(\text{PCy}_3)]^+ + [\text{Ir}(\text{H}_2)(\text{py})(\text{PCy}_3)]^+ + [\text{Ir}(\text{py})(\text{PCy}_3)]^+ \quad (4.5)$$

The effect of impurities (X) in NR on the hydrogenation rate can be compared to the effect of the nitrile functional group, which inhibits the catalytic activity in NBR hydrogenation (Hu, 2000). It is possible that impurities in NR might coordinate with unsaturated active species of catalyst to reduce the hydrogenation activity as shown Figure 4.10. A material balance on the active species of the Ir catalyst for the NR hydrogenation is expressed in eq. (4.6).

$$[\text{Ir}]_T = [\text{Ir}(\text{H}_2)(\text{C}=\text{C})(\text{py})(\text{PCy}_3)]^+ + [\text{Ir}(\text{H}_2)(\text{py})(\text{PCy}_3)]^+ + [\text{Ir}(\text{py})(\text{PCy}_3)]^+ + [\text{Ir}(\text{X})(\text{py})(\text{PCy}_3)]^+ + [\text{Ir}(\text{H}_2)(\text{X})(\text{py})(\text{PCy}_3)]^+ \quad (4.6)$$

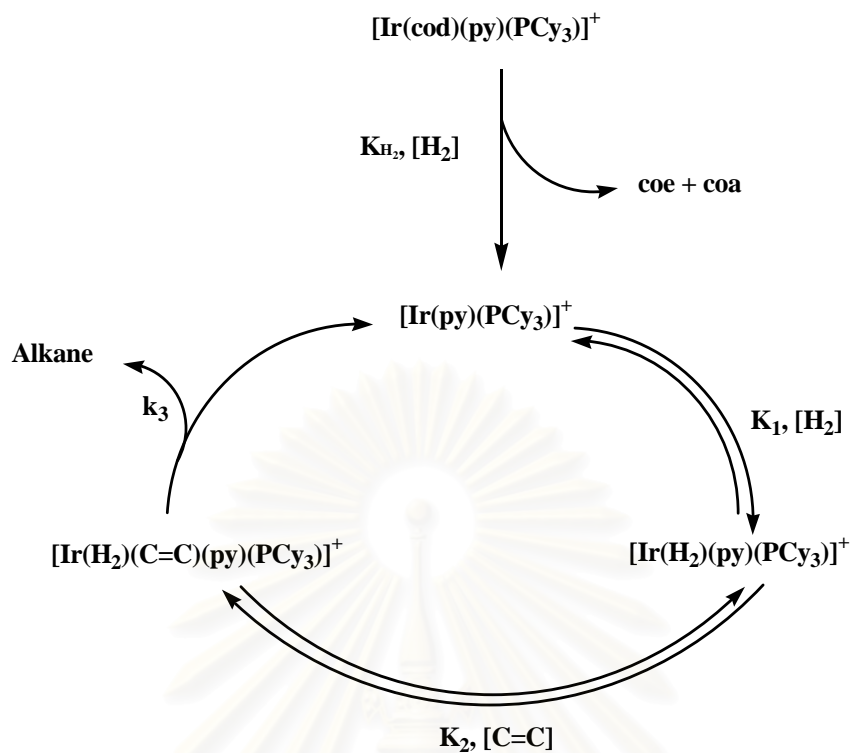


Figure 4.9 Proposed catalytic mechanism for PIP hydrogenation in the presence of $[\text{Ir}(\text{cod})(\text{py})(\text{PCy}_3)]\text{PF}_6$.

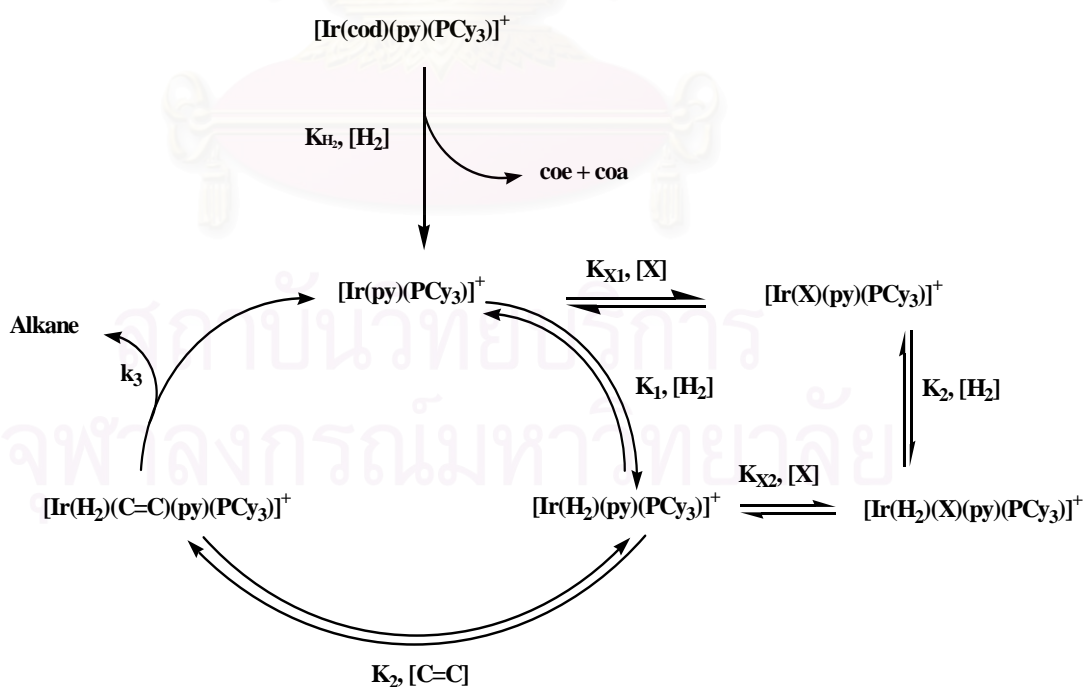


Figure 4.10 Proposed catalytic mechanism for NR hydrogenation in the presence of $[\text{Ir}(\text{cod})(\text{py})(\text{PCy}_3)]\text{PF}_6$.

Every iridium complex species concentration term in eq. (4.5) and (4.6) can be expressed in terms of $[\text{Ir}(\text{H}_2)(\text{C}=\text{C})(\text{py})(\text{PCy}_3)]^+$ using the equilibria defined in Figure 4.9 or 4.10 and then can be substituted into eq. (4.4) to provide the resulting rate law as shown in eq. (4.7) for PIP hydrogenation and eq. (4.8) for NR hydrogenation. Derivation of the expression is shown in Appendix C.

$$-\frac{d[\text{C}=\text{C}]}{dt} = \frac{k_3 K_1 K_2 [\text{Ir}]_T [\text{C}=\text{C}] [\text{H}_2]}{1 + K_1 [\text{H}_2] (1 + K_2 [\text{C}=\text{C}])} \quad (4.7)$$

$$-\frac{d[\text{C}=\text{C}]}{dt} = \frac{k_3 K_1 K_2 [\text{Ir}]_T [\text{C}=\text{C}] [\text{H}_2]}{1 + K_{X1} [\text{X}] + K_1 [\text{H}_2] (1 + K_2 [\text{C}=\text{C}] + K_{X2} [\text{X}])} \quad (4.8)$$

Although the rate expression would suggest that there would be a zero order dependence on $[\text{H}_2]$, the kinetic observation indicated that the hydrogenation rate was a first order with respect to hydrogen pressure. It can be presumed that K_1 , K_2 and K_{X2} were very small for the range of the reaction conditions and substrate concentration used in this study. The reaction was found to exhibit a first order response of k' on $[\text{Ir}]$ at low concentration of catalyst and shift to zero order at higher concentration of catalyst due to the possible dimerization of the catalyst as discussed previously. For NR hydrogenation, the effect of impurities in NR is an important factor in reducing the rate of hydrogenation. The rate expression, eq. (4.8), shows that the rate of NR hydrogenation decreased with rubber concentration since such resulted in an increase in the amount of impurities present.

สถาบันวิทยบริการ
จุฬาลงกรณ์มหาวิทยาลัย

4.4 Relative Viscosity of Hydrogenated Rubbers

One of the major problems associated with the modification of polymers are side reactions such as, chain degradation and crosslinking, which often accompany the desirable modification reaction. These side reactions result in a change in the chain length of the parent macromolecules during the chemical modification process. Although FTIR or $^1\text{H-NMR}$ spectroscopy is the usual technique to evaluate the degree of hydrogenation, these methods are not sufficient to detect these side reactions, crosslinks and degradation, which cause the undesirable properties. Therefore, the degree of polymer crosslinking must be inferred indirectly from molecular weight measurements. Dilute solution viscosity has been used to monitor the shifts in molecular weight that are created by crosslinking, branching or degradation. The viscosity of a dilute PIP and NR solution before and after the hydrogenation process relative to pure solvent (η_{rel}) provides a simple and effective means of measuring the consequences of crosslinking, branching and degradation of samples.

The effect of catalyst concentration, polymer concentration, and hydrogen pressure on the relative viscosity of PIP and NR after the hydrogenation process compared with an inherent viscosity is shown in Table 4.4 and Figure 4.11. Over the range of conditions investigated, (PIP ($\eta_{\text{rel}} = 4.48$): $[\text{Ir}] = 30\text{-}150\ \mu\text{M}$, $[\text{C}=\text{C}] = 163\text{-}500\ \text{mM}$ and $P_{\text{H}_2} = 13.8\text{-}52.2\ \text{bar}$ at 130°C and NR ($\eta_{\text{rel}} = 7.32$): $[\text{Ir}] = 65\text{-}145\ \mu\text{M}$, $[\text{C}=\text{C}] = 100\text{-}260\ \text{mM}$ and $P_{\text{H}_2} = 13.8\text{-}55.1\ \text{bar}$ at 140°C), the relative viscosity of both hydrogenated rubbers were somewhat higher than that of PIP and NR. The increase in the relative viscosity suggests that no degradation occurred during the catalytic hydrogenation reaction. Since relative viscosity of HPIP remained constant, it can be concluded that a very small amount of residual $\text{C}=\text{C}$ remained after the hydrogenation reaction and also possibly crosslinking did not affect the hydrogenation process (Charmondusit, 2002; Parent et al., 2001).

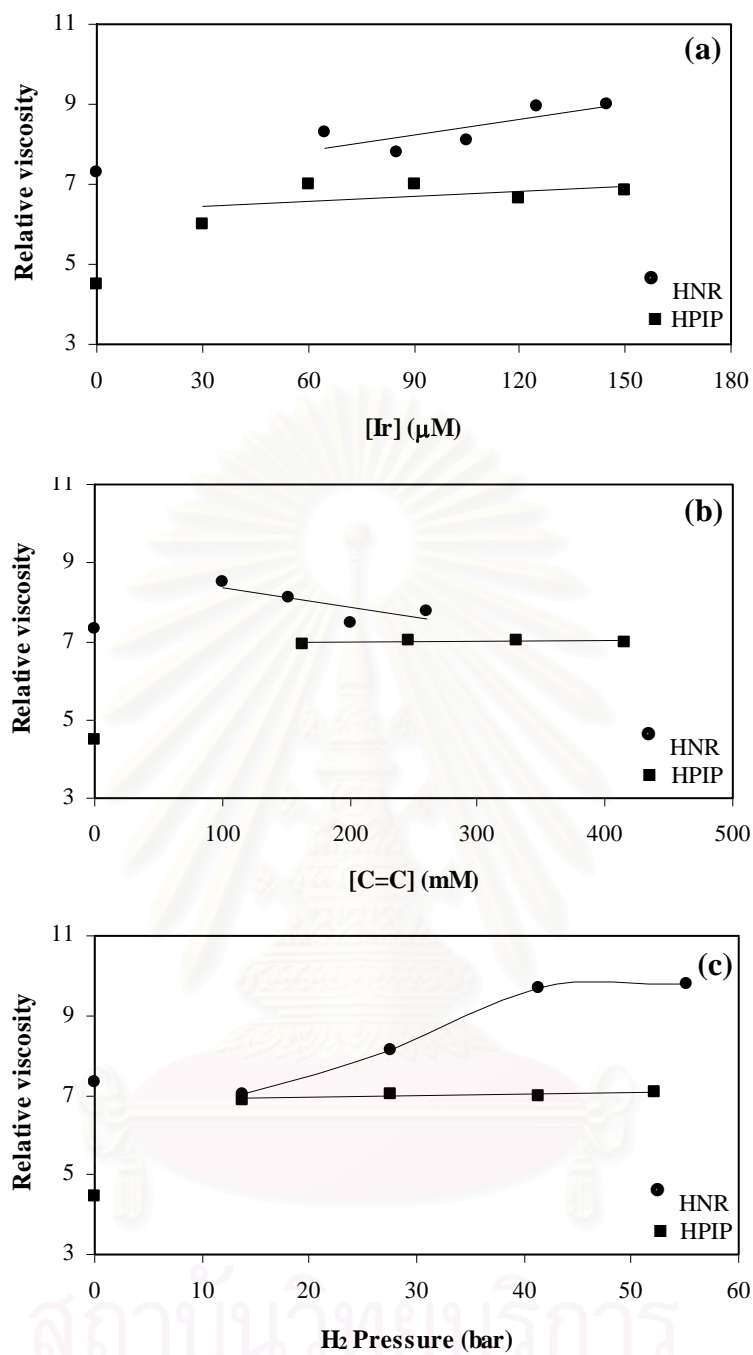


Figure 4.11 (a) Relative viscosity as a function of total metal loading, HPIP: $P_{\text{H}_2} = 27.6$ bar; $[\text{C}=\text{C}] = 246$ mM; $T = 130^\circ\text{C}$ and HNR: $P_{\text{H}_2} = 27.6$ bar; $[\text{C}=\text{C}] = 152$ mM; $T = 140^\circ\text{C}$. (b) Relative viscosity as a function of polymer loading, HPIP: $[\text{Ir}] = 90$ μM ; $P_{\text{H}_2} = 27.6$ bar; $T = 130^\circ\text{C}$ and HNR: $[\text{Ir}] = 105$ μM ; $P_{\text{H}_2} = 27.6$ bar; $T = 140^\circ\text{C}$. (c) Influence of hydrogen pressure on relative viscosity, HPIP: $[\text{Ir}] = 90$ μM ; $[\text{C}=\text{C}] = 246$ mM; $T = 130^\circ\text{C}$ and HNR: $[\text{Ir}] = 105$ μM ; $[\text{C}=\text{C}] = 152$ mM; $T = 140^\circ\text{C}$.

For NR hydrogenation, Figure 4.11 shows that the relative viscosity of hydrogenated natural rubber (HNR), varied over the range of 7.03 – 9.81, and is dependent on the reaction conditions, degree of hydrogenation and reaction time. The relative viscosity of HNR samples was higher when samples were hydrogenated at high catalyst loading or low rubber concentration. This might be explained on the basis that when the catalyst loading is relatively high compared with the amount of polymer, it is possible to present a higher degree of crosslinking or branching of polymer chain. Similar results were observed for NBR hydrogenation catalyzed by this Ir complex (Hu, 2000). For the effect of hydrogen pressure, it was found that the relative viscosity of HNR increased with hydrogen pressure. It is not clear as to what causes this phenomenon; however, it is possible that higher hydrogen pressure might promote a gel formation for this hydrogenation system.



CHAPTER 5

THERMAL ANALYSIS OF HYDROGENATED NATURAL RUBBER

Diene polymers such as acrylonitrile-butadiene copolymers, styrene-butadiene copolymers as well as natural rubber are susceptible to thermal and oxidative degradation due to the amount of unsaturated carbon-carbon double bonds in their structure. Nowadays, the need for greater polymer stability in many industrial applications has become more severe. Thus, chemical modification to saturate carbon-carbon double bonds is an important method to improve the structure of diene-based polymers to have higher heat-resistance performance.

Hydrogenation, one method of chemical modification, changes physical properties of elastomers because of changes in thermal properties such as glass transition temperature and thermal stability which are the inherent properties of each elastomer. Glass transition temperature and decomposition temperature can be evaluated from differential scanning calorimetry (DSC) and thermogravimetric analysis (TGA), respectively. The advantages of these methods are that the samples in the various forms, solid, liquid or gel, can be studied over a wide range of temperature programs and they require a small amount of sample (ca. 0.1 μg – 10 mg). Moreover, the sample can be investigated under any atmospheres such as air, helium or nitrogen.

There have been some research studies on the thermal properties of hydrogenated rubbers. Bhattacharjee et al. (1992) found that the glass transition temperature of hydrogenated nitrile-butadiene rubber catalyzed by palladium acetate was gradually decreased when the level of hydrogenation increased because of increased chain flexibility on hydrogenation. Sarkar et al. (1997) studied the degradation of hydrogenated styrene-butadiene rubber (HSBR) at high temperature under both aerobic and anaerobic aging conditions. The results from TG/DTG indicated that HSBR degraded in a single stage, whereas SBR degradation showed two stages of weight loss under a nitrogen atmosphere. It is possible that the initial decomposition step of SBR was accompanied by thermal isomerization to change *trans*- to *cis*- configuration, cyclization and volatilization. The final step of

decomposition of SBR and the single decomposition step of SBR might be performed from main chain scission.

This chapter focuses on the investigation of thermal properties of hydrogenated natural rubber by thermal analysis techniques and then comparison of the results with those obtained for natural rubber and ethylene-propylene copolymer (EPDM). The thermal properties of interest were glass transition temperature studied by DSC and thermal degradation temperature of polymers examined by TGA. The kinetics of polymer degradation was also implemented.

5.1 Glass Transition Temperature

Glass transition temperature (T_g) is one of the most important parameters for characterizing a polymer system. Consequently, the determination of the T_g is usually one of the first analyses performed on a polymer system. Generally, a polymer may be amorphous, crystalline, or a combination of both. The T_g is a transition related to the motion in the amorphous region of the polymer. Below the T_g , an amorphous polymer can be said to have characteristics of a glass, while it becomes more rubbery above the T_g . The glass transition temperature is usually determined by differential scanning calorimetry (DSC) (Sandler et al., 1998).

In this research work, the glass transition temperature of natural rubber was investigated before and after the hydrogenation process. It was also compared with synthetic *cis*-1,4-polyisoprene (PIP) and ethylene-propylene copolymer (EPDM: Sumitomo 505A). The results and DSC thermograms of hydrogenated natural rubber (HNR) samples at various degrees of hydrogenation are presented in Table 5.1 and Figure 5.1. DSC thermograms of HNR samples catalyzed by $\text{OsHCl}(\text{CO})(\text{O}_2)(\text{PCy}_3)_2$ (HNROs) and $[\text{Ir}(\text{cod})(\text{PCy}_3)\text{py}]\text{PF}_6$ (HNRIr) indicate a one step base-line shift. This suggests that the HNR samples have a single glass transition temperature. It can also suggest that no side reactions occurred during the catalytic hydrogenation process. In addition, the glass transition temperature of HNR was slightly increased with an increase in the level of hydrogenation. It can be concluded that the hydrogenation does not affect the glass transition temperature of NR; consequently, the HNR product still has high rubbery property. A similar observation

Table 5.1 Analysis of Glass Transition Temperature and Decomposition Temperature of Rubber Samples under the Nitrogen Atmosphere

Rubber	%Hydrogenation	T _g (°C)	T _{id} (°C)	T _{max} (°C)
EPDM*	-	-44.6	452.7	470.7
PIP	-	-58.9	359.2	384.1
NR	-	-62.3	357.2	380.9
HNROs**	37.9	-63.2	366.5	392.5
	52.2	-63.0	390.4	423.3
	79.1	-61.9	420.5	451.2
	91.9	-60.5	433.5	462.1
	99.7	-59.6	447.5	469.2
HNRIr***	91.3	-60.9	430.7	459.7

* The ethylene-propylene copolymer (EPDM) has the ratio of ethylene/propylene as 50/50 and 9.5% of diene content.

** NR Hydrogenation was catalyzed by OsHCl(CO)(O₂)(PCy₃)₂.

*** NR Hydrogenation was catalyzed by [Ir(cod)(PCy₃)(py)]PF₆.

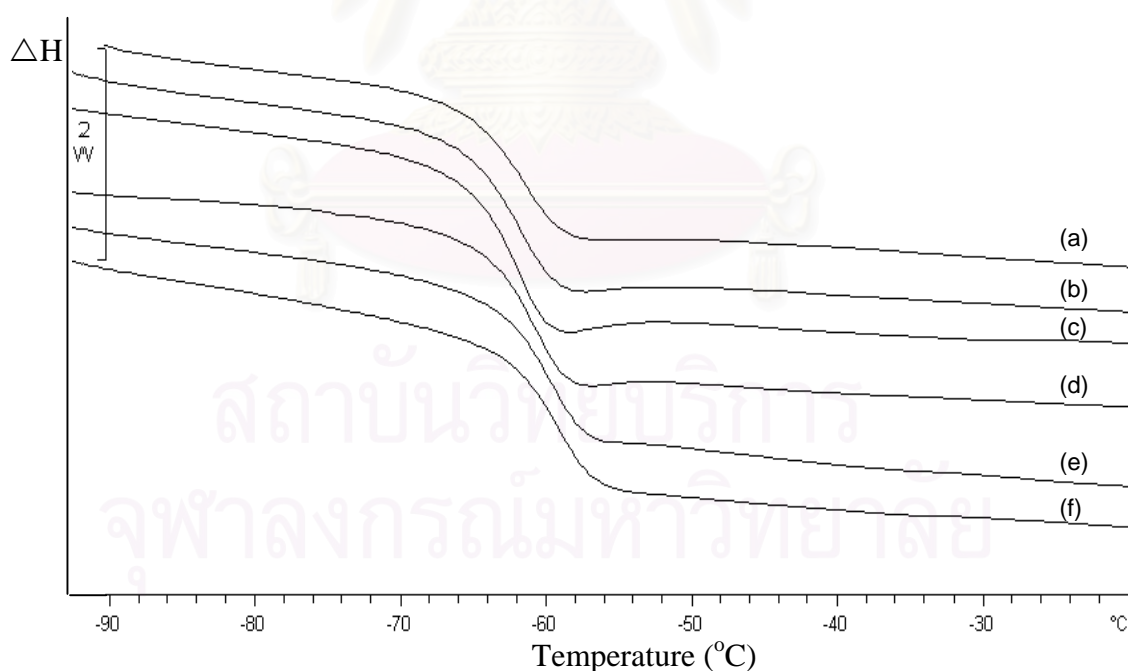


Figure 5.1 DSC thermograms of NR and HNR catalyzed by OsHCl(CO)(O₂)(PCy₃)₂ at various % hydrogenation. (a) 0.0%; (b) 37.9%; (c) 52.2%; (d) 79.1%; (e) 91.9% and (f) 99.7%.

was also made by Singha et al. (1997) for HNR obtained using the $\text{RhCl}(\text{PPh}_3)_3$ catalytic hydrogenation system.

5.2 Decomposition Temperature

Thermal stability means the ability of a material to maintain the required properties such as strength, toughness, or elasticity at a desired temperature. A detailed understanding how polymers break down on heating is important in the design and use of materials for a particular application. Thermogravimetric analysis (TGA) uses heat to drive reactions and physical changes in materials. TGA can directly record the mass change due to dehydration, decomposition, or oxidation of a polymer with time and a given temperature (Sandler et al., 1998).

To study how the decomposition temperature is related to the structure of NR modified by the hydrogenation reaction, the results of decomposition temperature of NR and HNR under the oxidative and non-oxidative atmosphere are shown in Tables 5.2 and 5.1, respectively. In the presence of nitrogen (non-oxidative) atmosphere, Table 5.1 and Figure 5.2 indicate that the polymer degradation is an overall one-step reaction because the TG curve of the samples is one-step and provides smooth weight loss curves. The initial decomposition temperature (T_{id}) was determined from the intersection of two tangents at the onset of the decomposition temperature. The maximum decomposition temperature (T_{max}) of each sample was obtained from the peak maxima of the derivative of TG curves. The results provided in Table 5.1 show that both T_{id} and T_{max} of HNR samples increased with an increase in the reduction of carbon-carbon double bond in the NR. Therefore, the hydrogenation can improve the thermal stability of NR by converting the weak π bond within NR to the stronger C-H σ bond (Charmondusit, 2002). On comparison with standard EPDM, it was found that T_{id} and T_{max} of the completely hydrogenated NR were close to those of EPDM. It can be concluded that the structure of HNR provides a facile entry and alternative method to alternating ethylene-propylene copolymers.

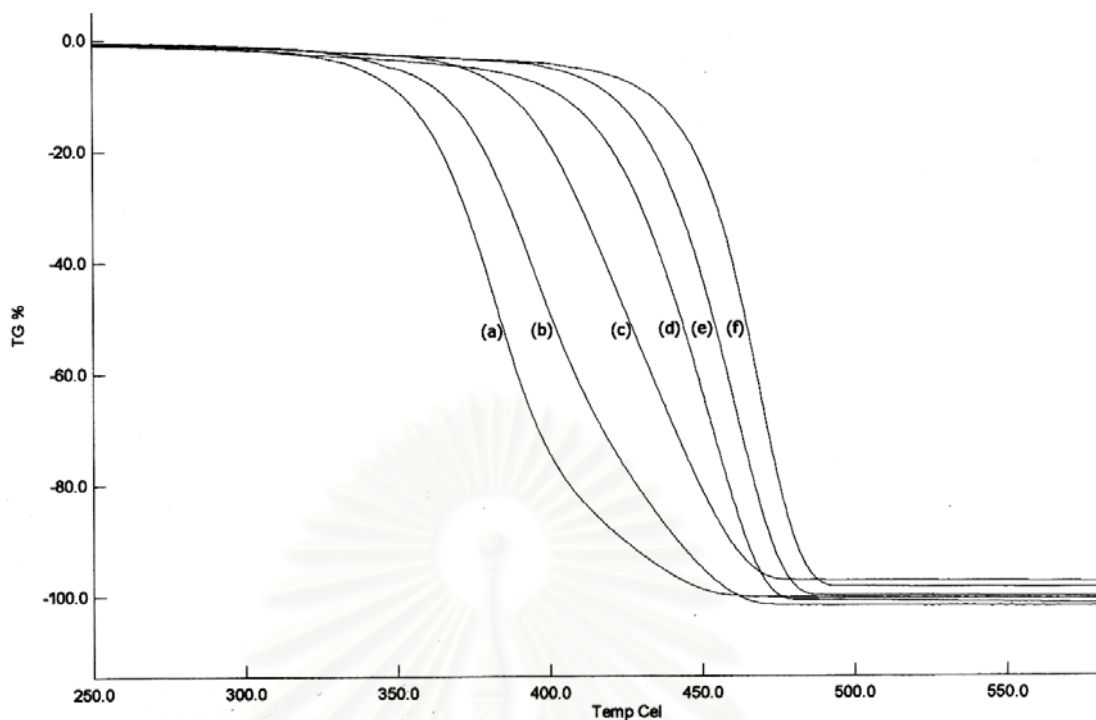


Figure 5.2 TGA thermograms of NR and HNR catalyzed by $\text{OsHCl}(\text{CO})(\text{O}_2)(\text{PCy}_3)_2$ at various % hydrogenation. (a) 0.0%; (b) 37.9%; (c) 52.2%; (d) 79.1%; (e) 91.9% and (f) 99.7%.

The degradation of NR and HNR under thermo-oxidative degradation was also carried out by using air at a 50 mL/min flow rate and a $10^\circ\text{C}/\text{min}$ heating rate. The % mass loss at 300°C in 60 min. of each rubber was recorded as shown in Table 5.2. These results indicate that the EPDM and HNR have a % mass loss less than NR. It confirms that hydrogenation can improve the structure of NR so that it can be used in the presence of high temperature and an oxidative atmosphere. Although HNR has the higher thermal stability than NR, the decomposition temperature and % mass loss at high temperature of HNR are still higher than that of EPDM. It is possible that the position of carbon-carbon double bond in HNR is in the backbone structure, whereas the unsaturation unit of EPDM is a pendent group and its main structure is still saturated. Thus, the HNR can still be more easily deteriorated from heat or oxidative agents than EPDM.

Table 5.2 % Mass Loss of Isothermal Degradation of Rubbers Under Nitrogen and Air Atmosphere

Sample	% Mass Loss at 300°C in 60 Min.
Nitrogen atmosphere	
NR	12.23
HNR*	3.22
EPDM**	1.03
Air atmosphere	
NR	26.82
HNR*	15.23
EPDM**	6.83

* HNR = 95.2% hydrogenation at 140°C.

** EPDM = Keltan 314 with 8% of diene content.

5.3 Decomposition Kinetics by Thermogravimetry Analysis

The test method followed the ASTM E 1641 – 99 in order to evaluate the activation energy of degradation of rubbers under a nitrogen atmosphere by using thermogravimetric technique based on the assumption that the decomposition obeys first-order kinetics. This activation energy may be used to calculate thermal endurance and estimate the lifetime of the rubber at a certain temperature. The investigation of decomposition kinetics is carried out under a series of heating rates. In this experiment, the results for determining the activation energy of decomposition of NR, HNR and EPDM were carried out by using five heating rates: 3, 5, 10, 15 and 20°C/min as shown in Figure 5.3 (a) - 5.5 (a). The degradation temperature of each % mass loss: 5, 10, 15 and 20% was recorded and summarized in Table 5.3. It indicates that the higher heating rate caused the higher resistance of thermal degradation. This may be due to the oxidation of the surface, which serves as a shield for the bulk of polymers. In the case of slower heating rate, the polymer chain will move more freely and completely so that the heat can pass further into the bulk of polymer and then degradation begins earlier. The Arrhenius activation energy can be calculated from a plot of the logarithm of heating rate versus the reciprocal of the absolute temperature at constant conversion level as indicated in Figure 5.3 (b) – 5.5 (b). The least-squares

Table 5.3 Results of Decomposition Temperature at Constant % Mass Loss at Various Heating Rate

Sample	Heating rate (°C/min)	Degradation Temperature at Constant % Mass Loss (°C)			
		5%	10%	15%	20%
NR	3	324.2	335.3	341.6	346.4
	5	322.0	339.6	347.2	353.0
	10	334.3	351.4	359.2	364.5
	15	339.9	358.4	366.9	371.4
	20	349.6	364.1	372.0	376.7
HNR*	3	396.7	412.1	418.2	423.2
	5	400.5	418.2	425.8	430.9
	10	407.9	426.8	434.9	440.4
	15	418.1	436.0	443.7	449.3
	20	425.6	444.0	450.9	456.5
EPDM**	3	420.2	427.4	431.0	434.0
	5	424.1	433.4	438.1	441.7
	10	440.6	448.1	452.4	455.5
	15	448.3	456.1	460.3	463.3
	20	454.2	462.3	466.6	469.5

* HNR = 95.6% hydrogenation at 140°C.

** EPDM= Keltan 314 with 8% of diene content.

สถาบันวิทยบริการ
จุฬาลงกรณ์มหาวิทยาลัย

method was used for fitting a straight line to these data without weighting factors and the slope can be determined from eq. (5.1)

$$\text{slope} = \frac{\Delta(\log\beta)}{\Delta(1/T)} \quad (5.1)$$

where β is the heating rate (K/min) and T is the absolute temperature (K) at constant % mass loss. The estimation of the activation energy can be calculated from eq. (5.2) and a value of 0.457/K for b in this first iteration.

$$E = -\left(\frac{R}{b}\right) * \frac{\Delta(\log\beta)}{\Delta(1/T)} \quad (5.2)$$

where E is defined to Arrhenius activation energy (J/mol), R is the gas constant (8.314 J/mol K) and b is an approximation derivative in Appendix IV. Then, the value of E/RT_c was calculated (where T_c is the temperature at constant % mass loss for the heating rate closet to the midpoint of the experimental heating rate) and used for estimating the new value of b . The example of this calculation is shown in Appendix D. The heating rate nearest the midpoint of the experimental heating rates was selected to calculate the pre-exponential factor (A) using eq. (5.3). The value of the exponent, a , is obtained from Table D-2 in Appendix D.

$$A = -\left(\frac{\beta'}{E_r}\right) * R * \ln(1-\alpha) * 10^a \quad (5.3)$$

where α is the mass loss value (% mass loss/100). The reaction rate constant of degradation can be evaluated from eq. (5.4).

$$k = Ae^{-E_a/RT} \quad (5.4)$$

The summary of non-isothermal kinetic parameters is shown in Table 5.4.

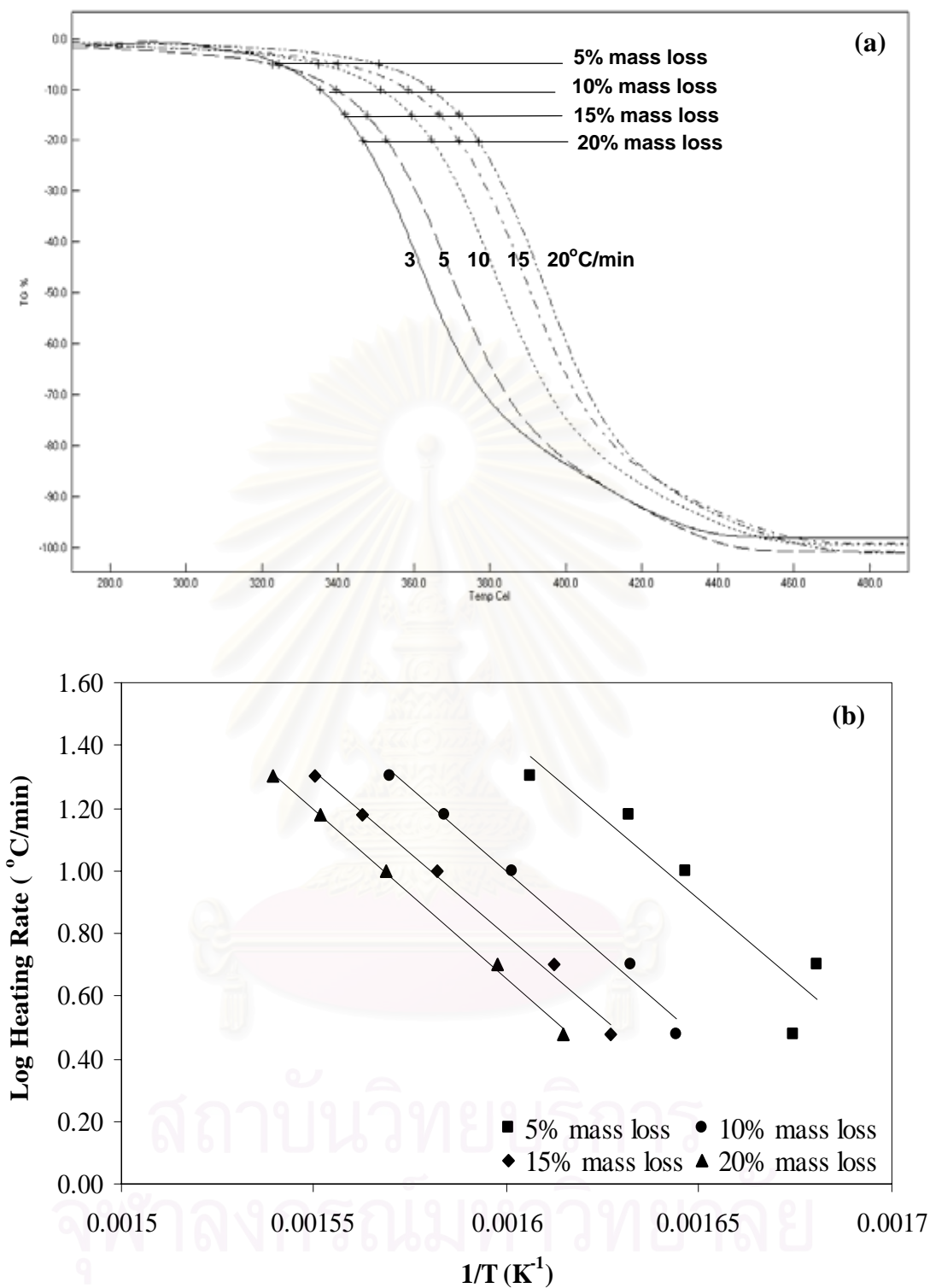


Figure 5.3 (a) Nonisothermal kinetics and (b) Arrhenius plot of heating rate versus the reciprocal decomposition temperature of NR.

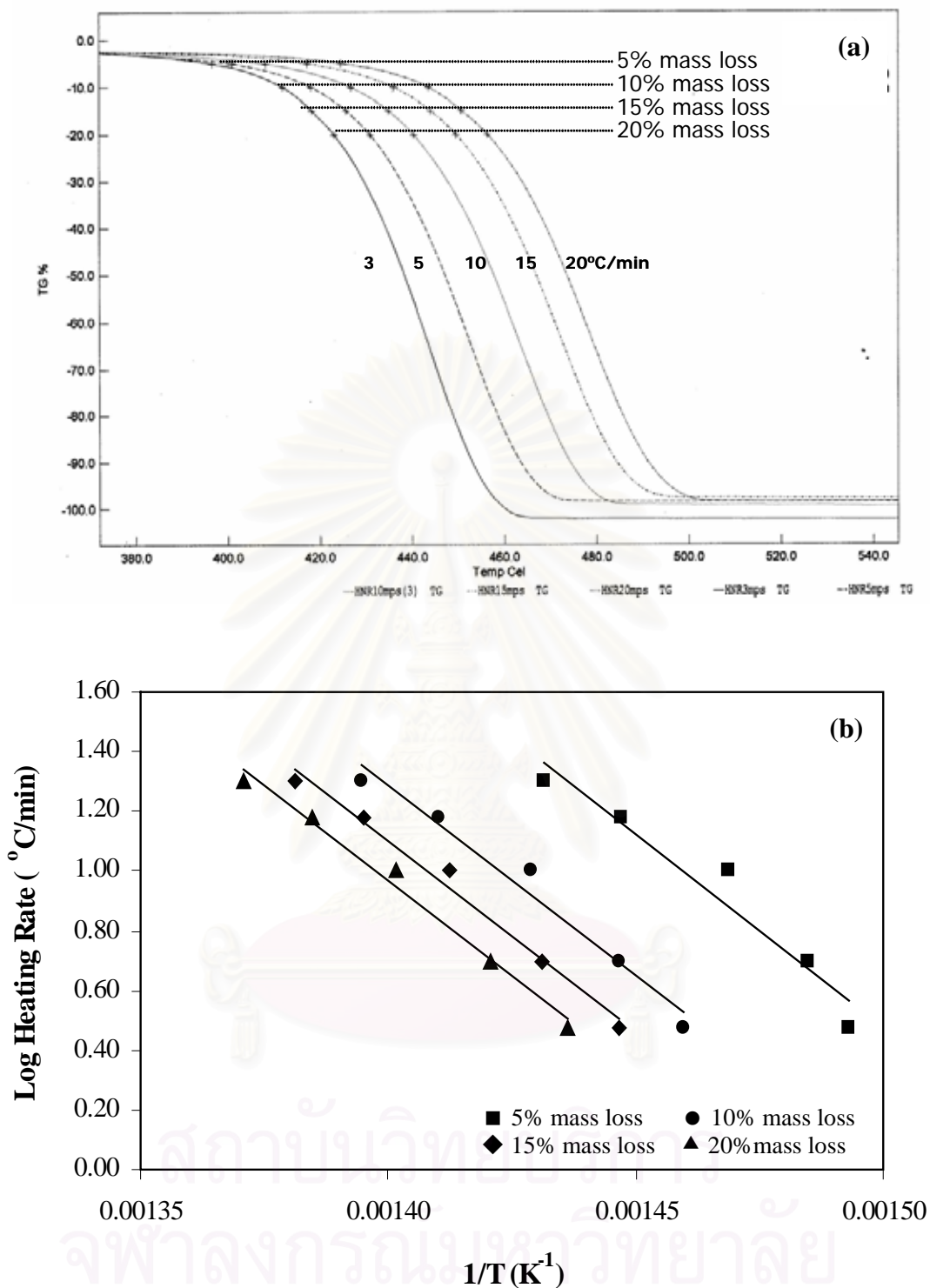


Figure 5.4 (a) Nonisothermal kinetics and (b) Arrhenius plot of heating rate versus the reciprocal decomposition temperature of HNR (95.6% hydrogenation).

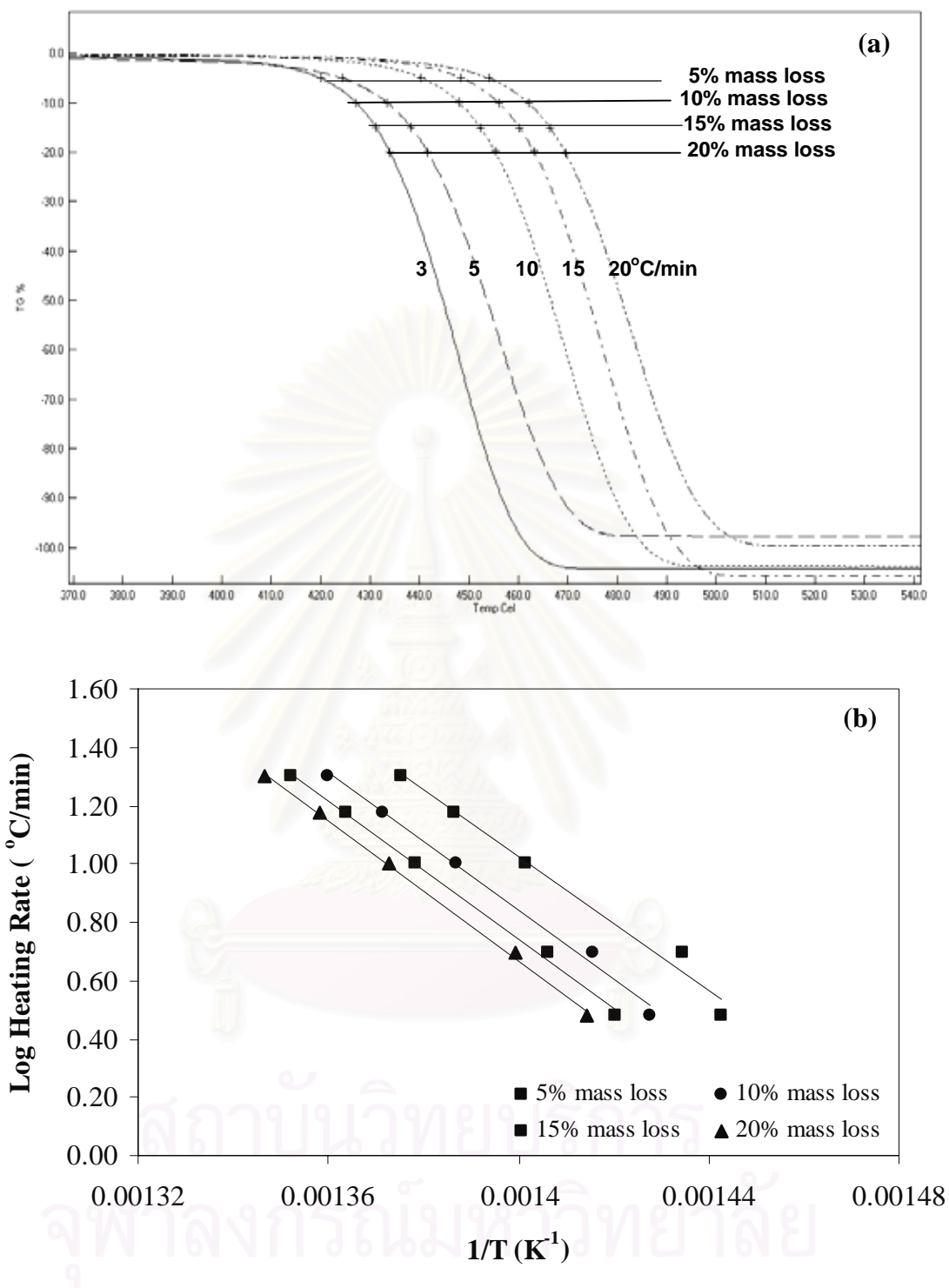


Figure 5.5 (a) Nonisothermal kinetics and (b) Arrhenius plot of heating rate versus the reciprocal decomposition temperature of EPDM (Keltan 314).

Table 5.4 Values of Non-Isothermal Kinetic Parameters for the Thermal Degradation of Rubbers

Sample	Kinetic Parameters	% Mass Loss			
		5	10	15	20
NR	Arrhenius activation energy (E_a , kJ/mol)	187.92	194.96	189.59	196.93
	Pre-exponential factor (A , min^{-1})	4.83E+14	1.35E+14	4.52E+14	1.88E+14
	Rate constant (k , min^{-1})	0.033	0.066	0.098	0.138
HNR	Arrhenius activation energy (E_a , kJ/mol)	234.13	232.15	233.65	232.48
	Pre-exponential factor (A , min^{-1})	2.99E+16	1.34E+16	1.67E+16	1.36E+16
	Rate constant (k , min^{-1})	0.033	0.063	0.096	0.129
EPDM	Arrhenius activation energy (E_a , kJ/mol)	206.36	213.55	214.61	218.80
	Pre-exponential factor (A , min^{-1})	3.36E+13	1.62E+14	2.38E+14	5.67E+14
	Rate constant (k , min^{-1})	0.026	0.055	0.084	0.116

The results from Table 5.4 indicate that the Arrhenius activation energy of HNR was intensely higher than that of NR and slightly higher than that of EPDM. It means that HNR required more energy to break down the chemical bond due to the greater saturation in the structure. However, the rate of thermal decomposition of HNR was similar to NR for every % mass loss, while the thermal decomposition rate of EPDM was slower. It is possible that the backbone structure of EPDM is saturated, so it has more thermal stability than HNR, which has the residual carbon-carbon double bond in its main chain structure.

CHAPTER 6

PHYSICAL AND MECHANICAL PROPERTIES OF HYDROGENATED NATURAL RUBBER

From the previous chapter, it was seen that the hydrogenation improved the thermal stability of natural rubber (NR) by reducing the carbon double bond in its structure. Furthermore, a study of vulcanization behavior and basic mechanical properties of hydrogenated natural rubber (HNR) is required to understand its performance for commercial utilization.

The measurement of any technological properties of HNR in the earlier research work was precluded due to the limited scale of its preparation (Bhowmick and Stephens, ed., 1988). Consequently, in order to measure such properties in the current study, NR hydrogenation in a 2-liter reactor was carried out to produce a sufficient quantity of HNR for determination of the mechanical properties. The molecular weight and molecular weight distribution of HNR were also investigated. The mechanical properties such as tensile strength and hardness and the ozone resistance of vulcanized HNR were studied and compared with vulcanized NR and commercial EPDM rubber.

6.1 Hydrogenation of Natural Rubber in 2-Liter Batch Reactor

Although the small volume reactor of the gas uptake apparatus is capable of providing high olefin conversion profiles, it may become untenable for the large scale production. The investigation of the physical properties of rubber requires using a large amount of sample. Therefore, the hydrogenation of NR in a 2-litre batch reactor was performed to provide an adequate quantity of hydrogenated sample (ca. 50 g/batch). The results for the NR hydrogenation obtained from the 2-liter reactor are summarized in Table 6.1 and Figure 6.1.

The results of the initial study in Table 6.1 indicate that the speed of agitation and the form of catalyst (solid catalyst or catalyst solution) affected the rate of NR hydrogenation. A suitable agitation speed was one important factor to achieve the desired level of hydrogenation over a limited reaction time. It can be seen that the NR

hydrogenation using a solid catalyst required a higher speed of agitation to provide an effective dispersion of the catalyst in the rubber solution. In contrast, the solution catalyst hydrogenation – method, which the solid catalyst was pre-dissolved in toluene was more advantageous during at the beginning stage of the reaction because the catalyst solution was easily dispersed in the rubber solution. However, the level of hydrogenation realized by the catalyst solution method was lower than that of the solid catalyst method during the final period of reaction. It is possible in the solution catalyst method that some portion of the catalyst was deactivated during the preparation of catalyst solution.

Based on the experimental results in Chapter 3 and Chapter 4, both the catalysts, $\text{OsHCl}(\text{CO})(\text{O}_2)(\text{PCy}_3)_2$ and $[\text{Ir}(\text{cod})(\text{PCy}_3)(\text{py})]\text{PF}_6$, were effective for NR hydrogenation. The addition of acid in the NR hydrogenation process has shown that 3-chloropropionic acid (3-CPA) and *p*-toluenesulfonic acid (*p*-TSA) enhanced the hydrogenation rate by preventing the poisoning of catalysts due to impurities present in NR. From the results shown in Figure 6.1, for the NR hydrogenation catalyzed by Os/3-CPA system, it is seen that higher than 90% conversion was achieved within 4 h. and the rubber product obtained was white. Although the hydrogenation rate catalyzed by Os/*p*-TSA was higher than that by Os/3-CPA, the rubber product color was brown. For the NR hydrogenation catalyzed by the Ir/*p*-TSA system, the hydrogenation rate was low and only 40% conversion was achieved in 4 h. It is possible that $[\text{Ir}(\text{cod})(\text{PCy}_3)(\text{py})]\text{PF}_6$ is more sensitive to being deactivated by the amine functional groups in the protein structure present in NR than in the case for $\text{OsHCl}(\text{CO})(\text{O}_2)(\text{PCy}_3)_2$. The obtained rubber product was also brown. The colors of NR and HNR are also shown in Figure 6.2.

Table 6.1 Effect of Agitation Speed and Form of Catalyst on %Hydrogenation

Sample	Form of Catalyst	Agitator Speed (rpm)	%Hydrogenation			
			1 h	2 h	3 h	4 h
1	solid	400	21.9	56.1	81.2	95.0
2	solution	400	54.7	70.2	77.3	86.0
3	solid	600	67.8	82.4	84.6	92.1

Os = OsHCl(CO)(O₂)(PCy₃)₂ and 3-CPA = 3-chloropropionic acid

Conditions: [NR]/[Os] = 6398 and [3-CPA]/[Os] = 47, P_{H₂} = 27.6 bar at 140°C and in 1300 mL of toluene.

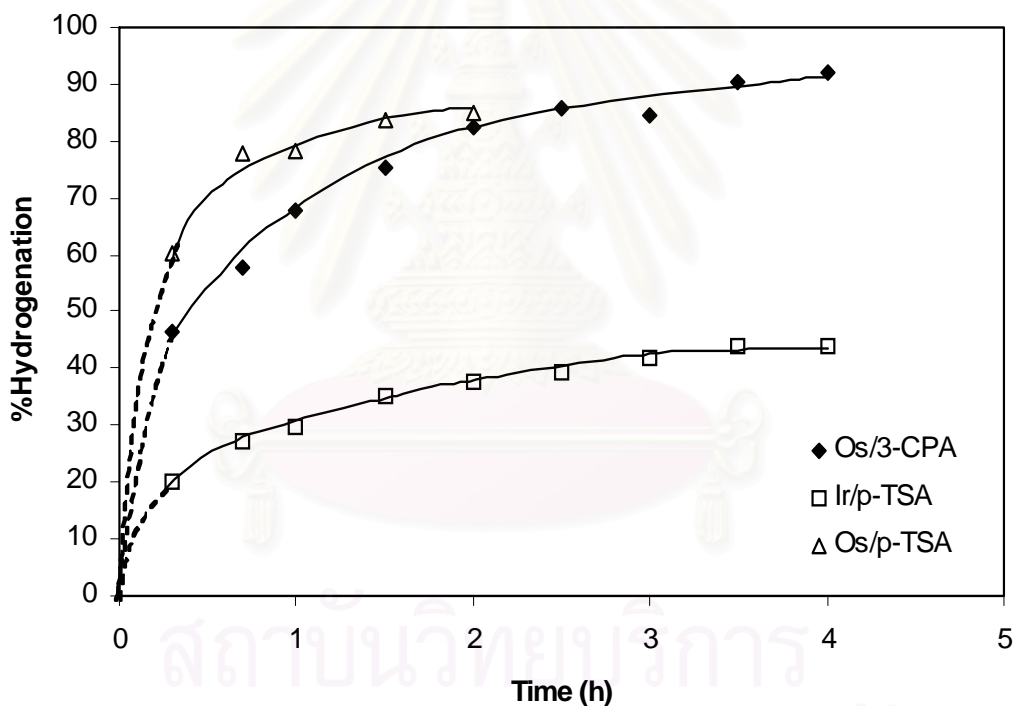


Figure 6.1 Effect of catalyst and acid types on %hydrogenation: Os/3-CPA: [NR]/[Os] = 6398 and [3-CPA]/[Os] = 47 in toluene; Ir/p-TSA: [NR]/[Ir] = 4976 and [p-TSA]/[Ir] = 40 in chlorobenzene; Os/p-TSA: [NR]/[Os] = 6398 and [p-TSA]/[Os] = 30 in toluene (P_{H₂} = 27.6 bar at 140°C).

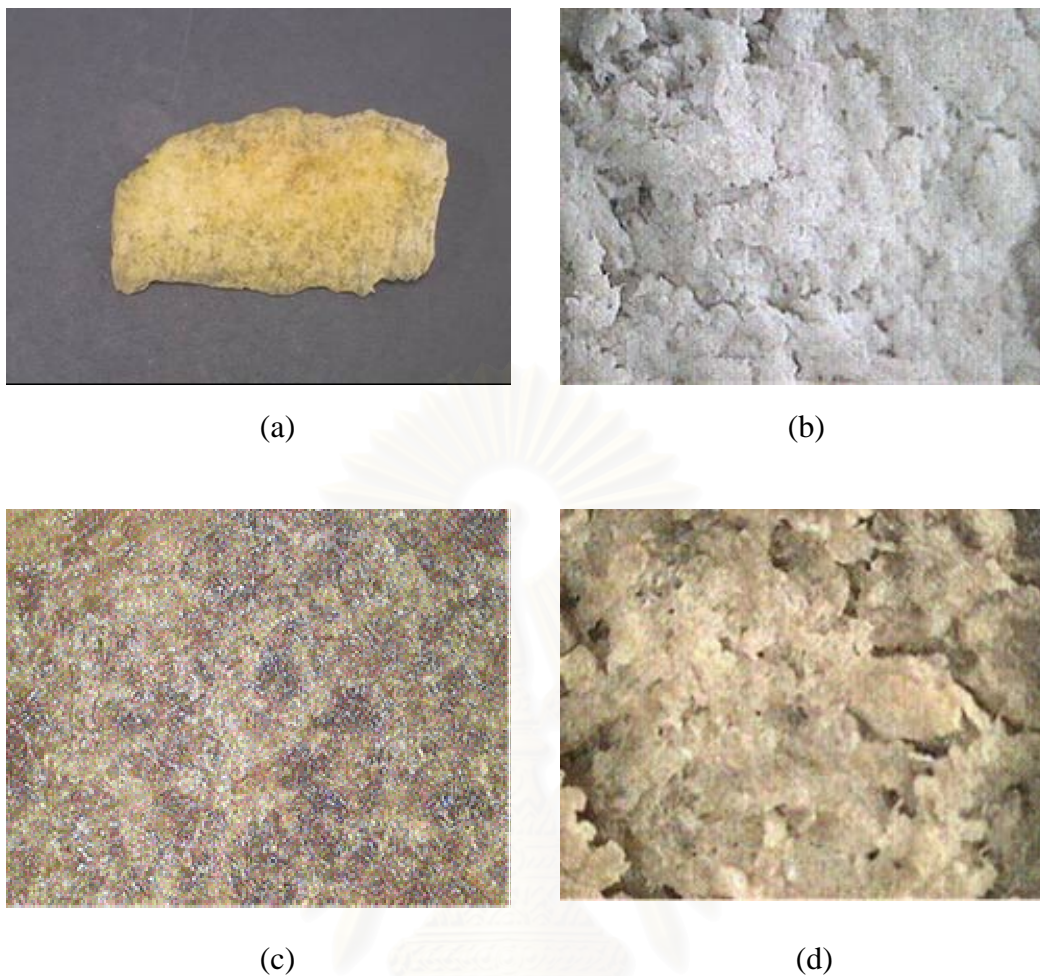


Figure 6.2 Surface color of hydrogenated natural rubber from each system ((b) – (d) captured by CCD camera): (a) natural rubber, (b) Os/3-CPA (82.1% hydrogenation), (c) Ir/p-TSA (43.9% hydrogenation) and (d) Os/p-TSA (85.0% hydrogenation).

สถาบันวิทยบริการ
จุฬาลงกรณ์มหาวิทยาลัย

6.2 Molecular Weight and Molecular Weight Distribution of Hydrogenated Natural Rubber

Molecular weight and molecular weight distribution are fundamental characteristics of a polymer material. Gel permeation chromatography (GPC) is a useful separation method for polymers and provides a measure of relative molecular weight (Sandler et al). Generally, rubber from *Hevea brasiliensis* is a high molecular weight polymer with broad molecular weight distribution. It also has been confirmed to have a bimodal distribution by GPC analysis (Tanaka, 1989).

The molecular weight and molecular weight distribution of NR and HNR were determined as presented in Table 6.2 and Figure 6.3. The hydrogenation conditions used in the 2-liter batch reactor were as follows: $[Os] = 97.3 \mu\text{M}$, $[C=C] = 622 \text{ mM}$ and $[3\text{-CPA}]/[Os] = 47$ at 27.6 bar of P_{H_2} and 140°C . The results in Table 6.2 indicate that the molecular weight of the soluble part of NR was significantly decreased due to high reaction temperature and long reaction time. However, the molecular weight of HNR at various % hydrogenation was not changed during hydrogenation process. The sample with high %hydrogenation (> 90% hydrogenation) has the same value of molecular weight as that of samples with lower %hydrogenation (61 and 83% hydrogenation). This indicates that the highly saturated structure has more resistance to thermal degradation than the unsaturated form. The similar results were also observed for PIP hydrogenation catalyzed by Ru complex (Tangthongkul, 2003). Due to the hydrogenation conditions, the gel content and molecular weight and polydispersity (M_w/M_n) of HNR was lower than that of NR. Consequently, the bimodal distribution of NR became nearly unimodal after the hydrogenation process as illustrated in Figure 6.3.

Table 6.2 Molecular Weight and Molecular Weight Distribution of Natural Rubber and Hydrogenated Natural Rubber at Various %Hydrogenation

Sample	%Hydrogenation	%Gel	Mn x 10 ⁶ (g/mol)	Mw x 10 ⁶ (g/mol)	Mw/Mn
NR	-	9.50	1.20	2.72	2.27 ± 0.07
HNR	61.23 (1 h)	3.86	0.62	1.19	1.93 ± 0.09
	83.17 (2 h)	3.16	0.56	1.06	1.89 ± 0.08
	92.07 (4 h)	0.86	0.58	1.09	1.88 ± 0.09

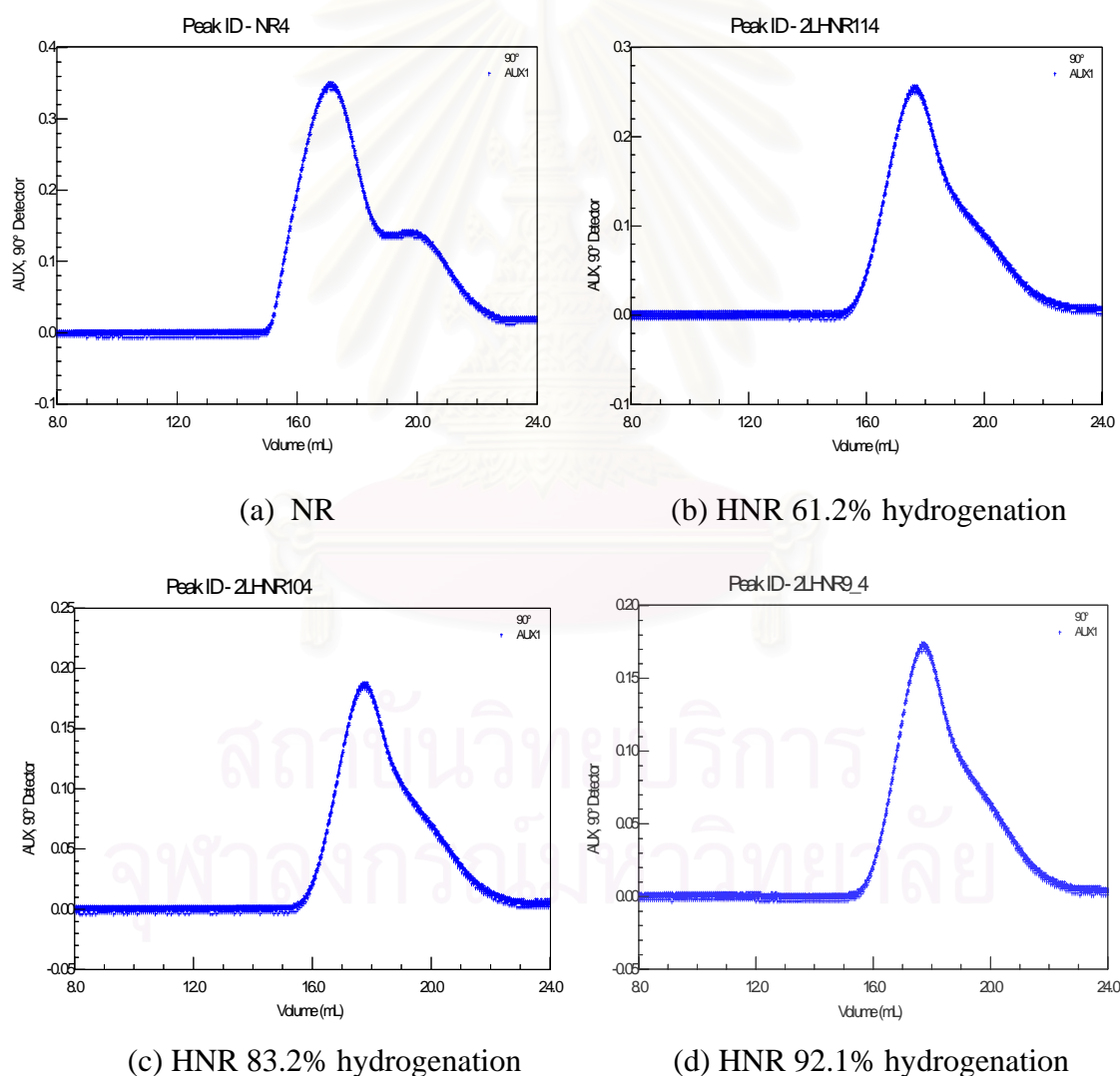


Figure 6.3 GPC chromatograms of natural rubber samples before and after hydrogenation at various %hydrogenation.

6.3 Blend and Vulcanization of Hydrogenated Natural Rubber

Vulcanization is a process to change rubber from essentially a plastic material to either an elastic or a hard material. Vulcanized rubber is highly elastic and resistant to plastic deformation. Normally, rubber mixed with vulcanizing agents and other chemicals such as an activator or fillers is vulcanized by heating at a temperature between 120 and 200°C in a mold of a desired shape and size (Stephens, ed., 1993). During vulcanization, the long chains of rubber molecules become crosslink by reactions with the vulcanizing agent to form a three – dimensional structure. The vulcanized rubber loses its tackiness and it has more resistance to deterioration normally caused by heat, light and aging (Morton, ed., 1999). Typically, vulcanization can be classified into four systems: sulfur vulcanization, sulfurless vulcanization, peroxide vulcanization and other systems, which make use of certain nonsulfur bifunctional compounds. The most common system used in general rubber industries is sulfur vulcanization because of the low cost of chemicals and ease of operation.

Due to the high saturation structure of some rubbers such as ethylene-propylene rubber (EPM), the vulcanization process of this rubber can be provided by peroxide curing instead of by the normal sulfur curatives. However, these peroxide cures are expensive, malodorous and difficult to handle on standard rubber equipment (Morton, ed., 1999). Because of the outstanding performance of EPM in terms of resistance to heat, oxygen and ozone, ethylene-propylene diene polymer (EPDM) has been developed in order to use the sulfur vulcanization process. Hydrogenated natural rubber (HNR) is also a highly saturated polymer similar to EPDM; although, the structure of HNR is an alternating ethylene-propylene copolymer while EPDM is a random structure. Therefore, the vulcanization system used for EPDM can also be used for HNR. Basically, the combination of two or three types of accelerators can be used for vulcanization of EPDM such as thiazole accelerator (2-mercaptobenzothiazole (MBT), dibenzothiazole disulfide (MBTS), or etc.) in combination with a thiuram and/or a dithiocarbamate (Morton, ed., 1999).

6.3.1 Blend of Rubbers with Curing Agent

In this work, 15 g of HNR was blended with curing agents at 100°C by using a mixer, Brabender Plasticorder. It is impossible to blend HNR with other chemicals on a two – roll mill because HNR loses the tackiness and also has a peculiar characteristic of pulling out into fine threads when stretched. It was found that the addition of some plasticizers such as paraffinic oil was required to be incorporated in the HNR before adding the vulcanizing agents. The amount of paraffinic oil depended on the level of hydrogenation. The sample with low level of hydrogenation required the smaller amount of oil than that of HNR with higher saturation. The addition of excessive oil to HNR with low saturation caused a slippery surface and the blending became more difficult. The NR and EPDM with 100 parts paraffinic extender oil (Keltan 509x100) were blended with curing agents using the same method as that of HNR. Then, the four batches of rubber obtained from Brabender Plasticorder were compounded by using a two-roll mill at 70°C. The compounding formulations of the blends are presented in Table 6.3. The details of the blending step are given in Appendix E.

6.3.2 Cure Characterization and Color of Vulcanizates

The vulcanization characteristics of rubber are usually measured using a rheometer such as oscillating disk rheometer (ODR) to obtain a saving in time and complete information of vulcanization at a desired cure temperature. The rubber mixed with additives is held under pressure between heated plates surrounding a biconical rotor (Morton, ed., 1999). The small rotor oscillates through a small angle of arc. The oscillating resistance of the mixed rubber, which is a measure of modulus, is recorded as a function of time to give a characteristic cure curve.

Table 6.3 Formulation of Mixes for Vulcanization using Brabender Plasticorder

Components	Mix								
	1	2	3	4	5	6	7	8	9
	NR1	EPDM	HNR60	HNR80	HNR90	NR2	HNR94	NR/HNR90 (10/90)	NR/HNR90 (30/70)
NR	100	-	-	-	-	100	-	10	30
EPDM ^a	-	200	-	-	-	-	-	-	-
HNR60 (60±1%)	-	-	100	-	-	-	-	-	-
HNR80 (80±2%)	-	-	-	100	-	-	-	-	-
HNR90 (90±2%)	-	-	-	-	100	-	-	90	70
HNR94 (94±3%)	-	-	-	-	-	-	100	-	-
CBS ^b	-	-	-	-	-	1.2	1.2	-	-
MBT ^c	0.5	0.5	0.5	0.5	0.5	-	-	0.5	0.5
TMTD ^d	1.0	1.0	1.0	1.0	1.0	0.2	0.2	1.0	1.0
Paraffinic oil ^e	-	-	44.0	54.0	70.0	-	86.0	59.0	43.0
Ultrablend 6000 ^f	-	-	-	-	-	-	7.0	-	-

ZnO = 5.0 phr; Stearic acid = 2.0 phr and Sulfur = 2.0 phr.

Mixing temperature = 70°C for Mix 1, Mix 6, Mix 8 and Mix 9 and 100°C for Mix 2 – 5 and Mix 7.

^a Keltan 509x100 (8.7% diene content with 64% ethylene content and 100 parts paraffinic extender oil); ^c *N*-Cyclohexylbenzthiazylsulphenamide; ^d 2-Mercaptobenzothiazole; ^e Tetramethyl thiuram disulphide; ^f DN process PA 32T and ^g Tackifier.

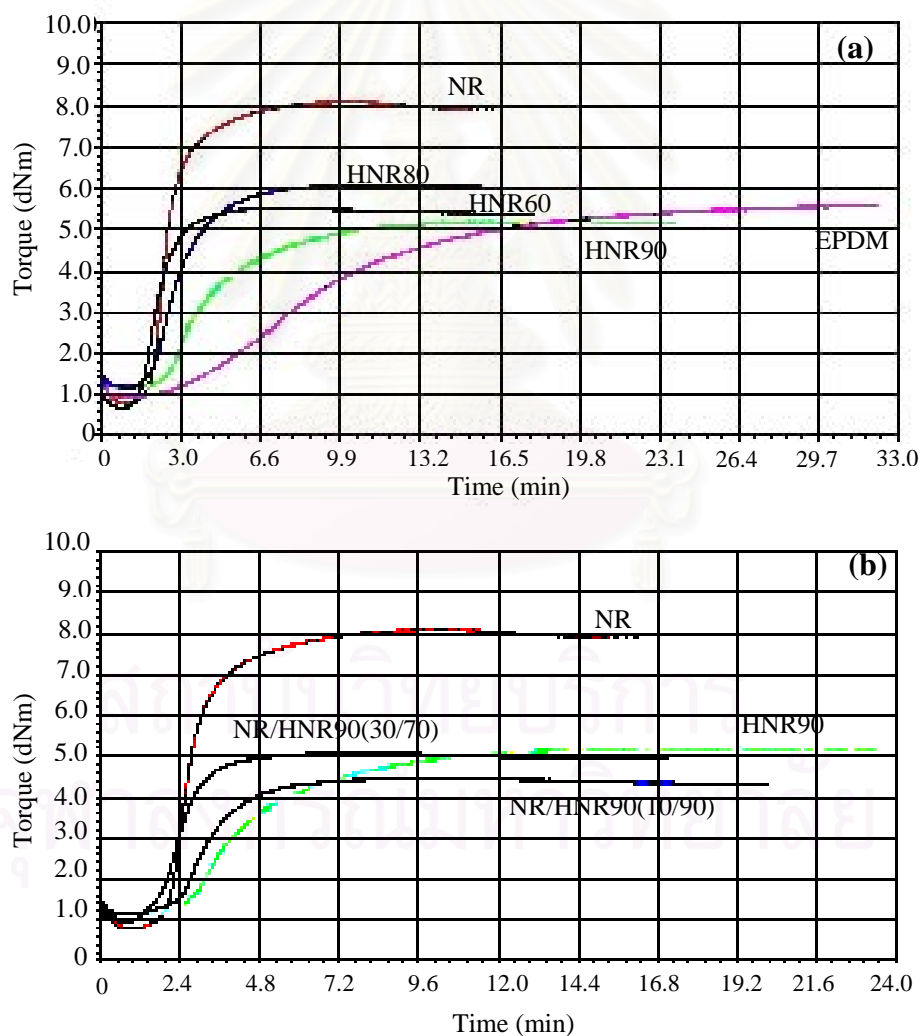
In this work, the curing system was divided to two types, MBT/TMTD and CBS/TMTD. The rheographs of rubbers vulcanized by MBT/TMTD are shown in Figure 6.4 and the cure characteristics of both cured systems are summarized in Table 6.4. The cure characteristics of EPDM and HNR were measured under higher cure temperature than that of NR. The results in Table 6.4 show that the HNR with low level of unsaturation required higher values of both scorch time (t_2) and optimum cure time (t_{95}). It was also found that the increase in the degree of hydrogenation tended to decrease the vulcanization rate. EPDM exhibited a longer optimum cure time than HNR90. It is possible that the higher oil content present for EPDM obstructed the access of additives to the rubber structure. In addition, the optimum cure time of rubber compound with higher content of TMTD was shorter because TMTD is an ultra – accelerator and vulcanizing agent (Blow, ed., 1982). The rubber compound (Mix8 – 9) shows the decreasing trends in scorch time and optimum cure time due to the high level of unsaturation in NR. However, the incorporation of saturated rubber with high diene rubber causes the cure – rate mismatch due to an imbalance in unsaturation level (Ghosh et al., 2001). It is possible that unvulcanized HNR90 exists in the vulcanized blend with NR.

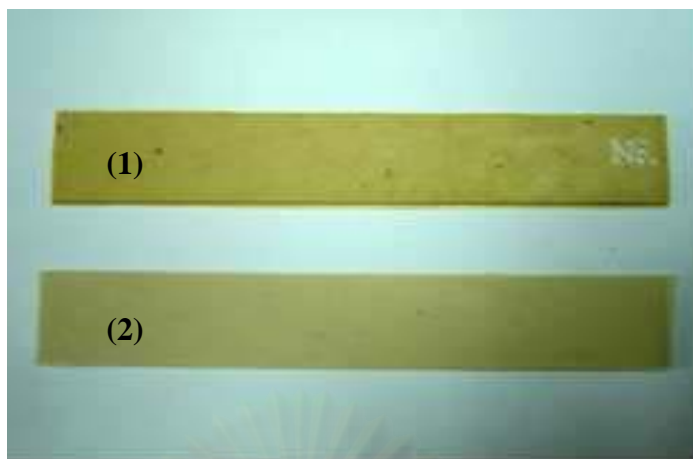
The curing system was found to have an effect on the color of vulcanizates as shown in Figure 6.5. The color of rubber vulcanized by CBS/TMTD was darker than MBT/TMTD system. The longer optimum cure time obtained from the CBS/TMTD system might be another factor, which effected the change of the color of vulcanized rubbers. This effect was apparent in the hydrogenated product.

สถาบันวิทยบริการ
จุฬาลงกรณ์มหาวิทยาลัย

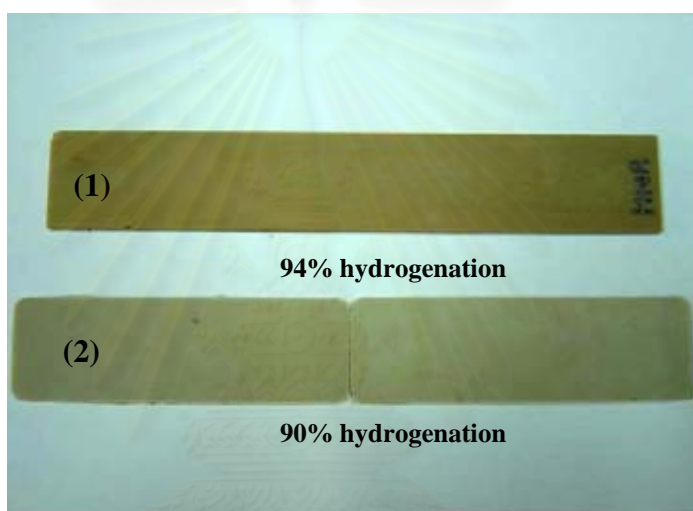
Table 6.4 Cure Characteristics of Vulcanizates Using Oscillating Disk Rheometer

Cure Properties	Mix								
	1	2	3	4	5	6	7	8	9
	NR1	EPDM	HNR60	HNR80	HNR90	NR2	HNR94	NR/HNR90 (10/90)	NR/HNR90 (30/70)
Cure temperature (°C)	150	160	160	160	160	150	160	160	160
Scorch time t_2 (min)	2.36	7.69	2.12	2.81	4.12	4.55	Not recorded	3.42	2.34
Optimum cure time T_{95} (min)	5.81	22.01	4.30	6.55	10.66	8.27	22.11	5.98	4.15

**Figure 6.4** Rheographs of vulcanizates: (a) pure rubbers and (b) rubber blends between HNR90 and NR.



(a) NR



(b) HNR

Figure 6.5 Color of vulcanized rubbers cured by (1) CBS/TMTD system and (2) MBT/TMTD system.

6.4 Mechanical Properties of Vulcanized Hydrogenated Natural Rubber

Mechanical properties of vulcanized NR, HNR and EPDM using MBT/TMTD as accelerators were measured in terms of tensile strength, ultimate elongation and hardness. The thin rubber sheets from the two – roll mill were pressed under pressure by compression molding at a temperature and time interval from the ODR study. The thickness of vulcanized sheets was ca. 2 mm. Then, the sheet was cut into standard specimens according to the ASTM test method. The results of mechanical properties are summarized in Table 6.5 and Figure 6.6. The mechanical properties of vulcanizates obtained from HNR and EPDM were retained after heat

aging. This indicated that HNR and EPDM are more resistant to heat due to the low saturation level in the rubber structures (Ghosh et al., 2001). However, the low content of carbon – carbon double bonds caused the poor mechanical properties of both HNR and EPDM. Nang et al. (1976) reported that the mechanical properties of vulcanizates from hydrogenated *cis*-1,4-polyisoprene (11.7 – 33.3% hydrogenation) produced by diimide reduction were lower than that of the starting material, owing to depolymerization during the hydrogenation reaction.

It can be noticed that the values of mechanical properties presented in Table 6.5 were quite low; especially, in the case of vulcanized NR. It can be explained that the shear force of the mixer Brabender Plasticorder was higher than that for the two-roll mill; thus, the chain scission of the rubber molecule might occur during the mixing process. In addition, vulcanized rubber sheets for the mechanical properties test might have some defects due to air bubbles in the sample because the amount of rubber mixed with curing agents was small and not high enough to make a rubber band around the roll of the two-roll mill. Therefore, air bubbles possibly remained inside the rubber before it was pressed in the compression mold.

Table 6.5 Physical Properties of Vulcanized Rubber Samples

Mix	Tensile Strength		Ultimate Elongation		Hardness	
	(MPa)		(%)		(Shore A)	
	Un-aged	Aged	Un-aged	Aged	Un-aged	Aged
1 (NR1)	3.05	1.90	309.6	154.0	43.3	46.6
2 (EPDM)	0.82	0.81	137.5	126.8	33.5	34.5
3 (HNR60)	0.57	0.51	64.3	44.6	34.2	34.6
4 (HNR80)	0.70	0.66	80.6	65.0	38.6	39.3
5 (HNR90)	0.69	0.64	102.4	81.3	36.5	36.5

Heat aging was done at 100°C for 22 h.

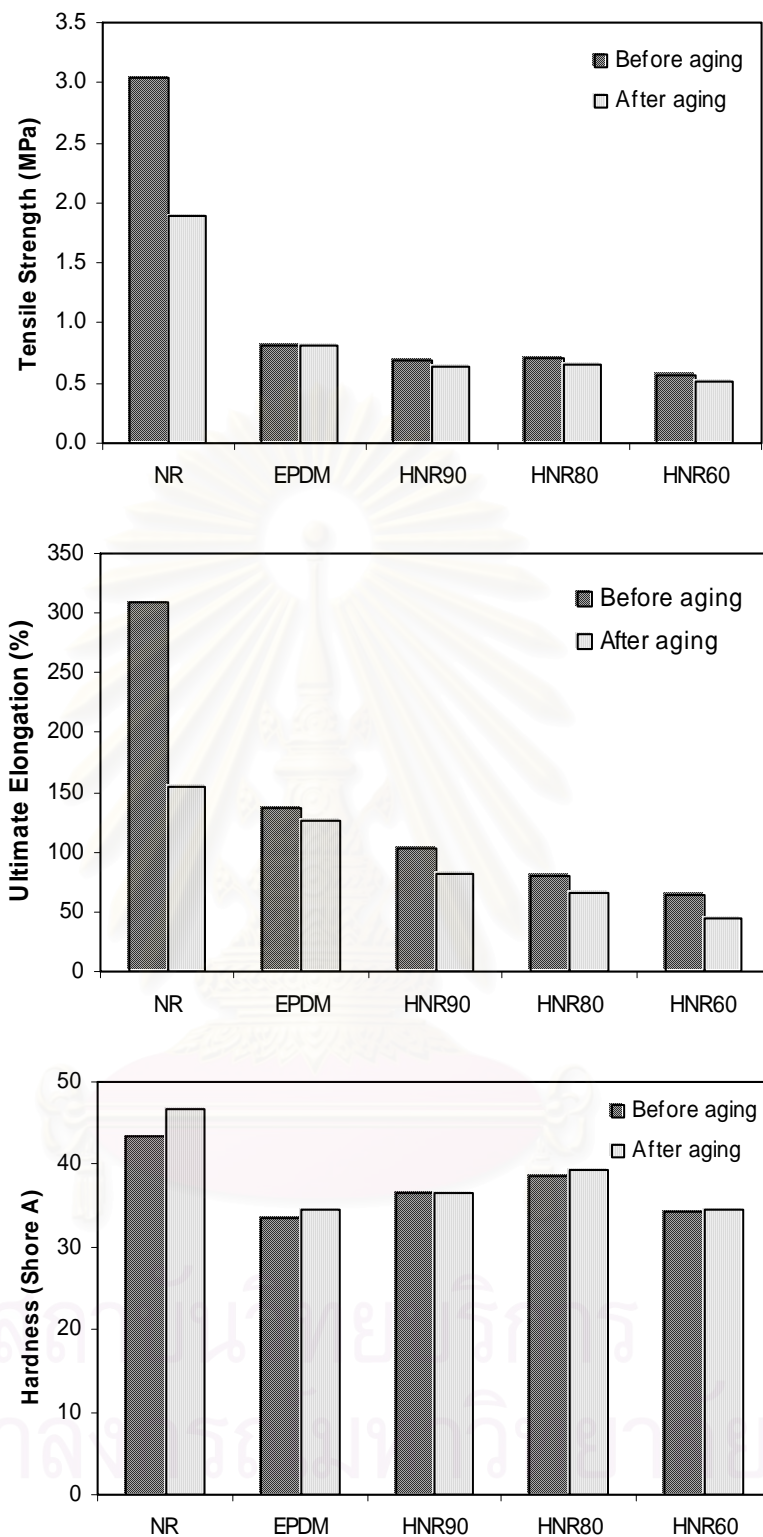


Figure 6.6 Mechanical properties before and after heat aging at 100°C for 22 h of hydrogenated natural rubber compared with natural rubber and EPDM (Keltan 509x100).

6.5 Dynamic Mechanical Properties of Vulcanized Hydrogenated Natural Rubber

Dynamic mechanical analysis (DMA) is a measurement to determine the elastic modulus of a material and its mechanical damping or energy dissipation characteristics as a function of frequency and temperature (Stuart, 2002). A specimen is subjected to some kind of cyclic deformation over a temperature or time scan. Various deformations can be used such as compressive, flexure, tension, torsion or bending. A sinusoidal stress introduced into the materials results in a sinusoidal deformation response which refers to dynamic storage or elastic modulus (E') and dynamic loss or viscous modulus (E''). E' means the energy stored and recovered during each cycle and it also indicates the stiffness of the material. E'' or damping factor or loss factor is related to energy dissipation in the system per cycle. It indicates the impact strength or ability of the system to absorb energy. Another factor called the loss angle is $\tan \delta$ determined from E''/E' (Cheremisinoff, ed., 1993).

The dynamic mechanical properties of vulcanizates from HNR, NR and EPDM (Keltan 509x100) were evaluated using tension mode of deformation over a temperature range of -100 to 50°C at a heating rate of 2°C/min and at a frequency of 10 Hz. Figure 6.7 shows the temperature dependence of storage modulus and the $\tan \delta$ of rubbers vulcanized by a MBT/TMTD curing system. The glass transition temperature (T_g) was obtained from the peak position of the $\tan \delta$ when plotted versus the temperature. The T_g at maximum $\tan \delta$ values including storage modulus (E') at 30°C for each vulcanized rubber are summarized in Table 6.6.

The results indicate that the storage modulus of all samples illustrated in Figure 6.7(a) decreased with increasing temperature. This tendency was very extreme around the transition region because of the increasing mobility of polymer chains when the temperature increases (Da Costa et al., 2002). The transition region after the onset of a sharp reduction in storage modulus related to the crystallinity of polymers. The results show that E' of EPDM in the transition region was higher than that of HNR; although, the structure of HNR is an alternating ethylene – propylene copolymer. The higher modulus of EPDM in the transition region is due to the higher content of ethylene segment (64%wt.) in its structure (Markovic et al., 2001). The comparison between HNR and EPDM indicates that the arrangement of monomers in

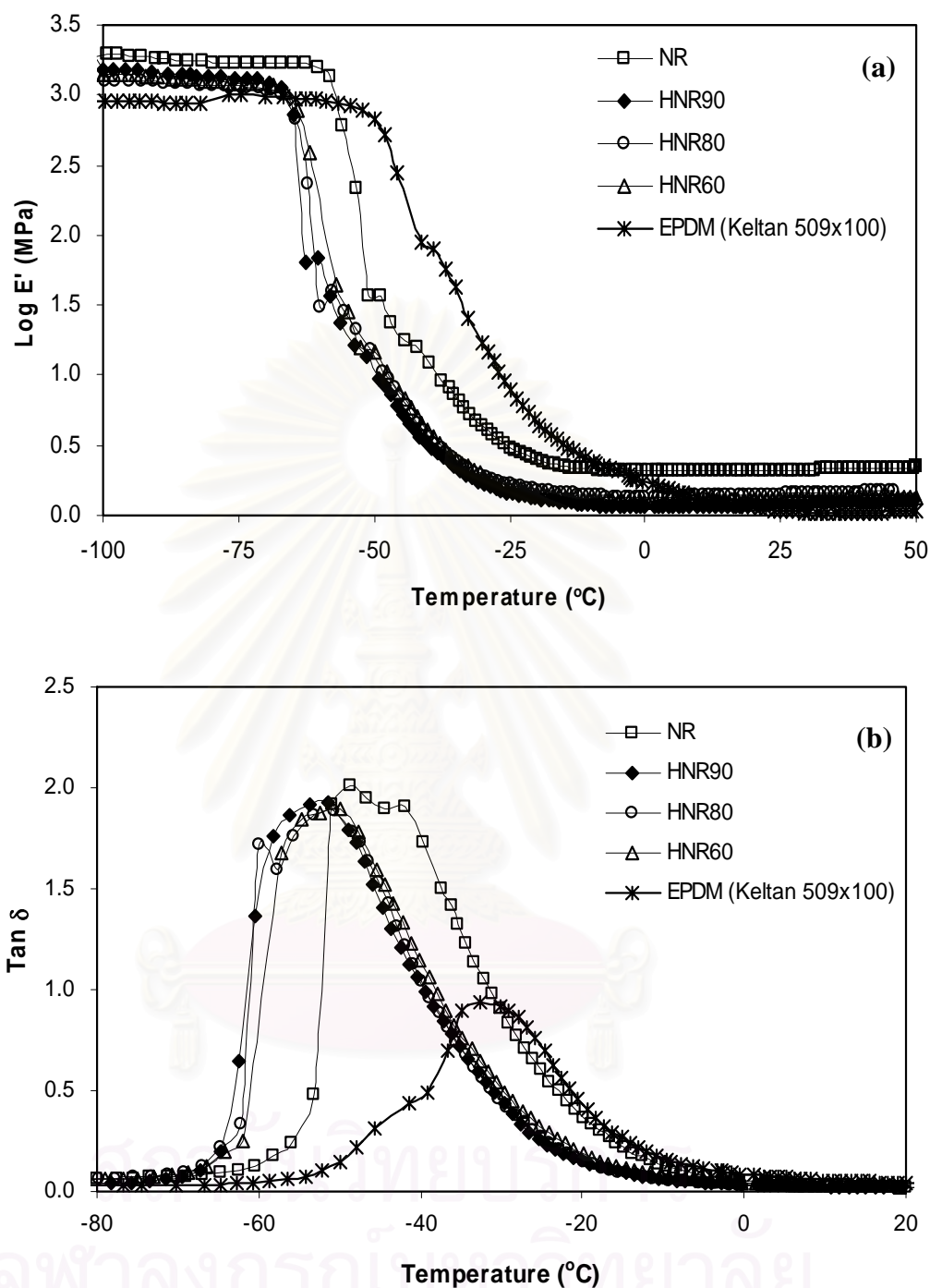


Figure 6.7 Temperature dependence of (a) the storage modulus (E') and (b) the loss tangent ($\tan \delta$) for hydrogenated natural rubber at various level of hydrogenation (ca. 60%, 80% and 90% hydrogenation) compared with natural rubber and EPDM after vulcanization using MBT/TMTD as accelerators.

the EPDM as a random ethylene – propylene copolymer is possible to have higher crystallinity than the alternating structure of HNR. For the comparison between NR and HNR, it was found that the storage modulus of NR in the region of transition decreased after the hydrogenation process. It can be noted that hydrogenation conditions such as high reaction temperature and long reaction time may cause a decrease in crystallinity of NR structure.

The exact value of T_g from the DMA technique can be evaluated from the onset of a sharp reduction in storage modulus if a plateau in the storage modulus before T_g is well defined. However, it is difficult to determine for some materials which have a broad region of storage modulus decline. Alternatively, the peak of either the loss modulus or $\tan \delta$ may be used to evaluate T_g of polymers; especially, the onset in the increase in the $\tan \delta$ is a good representative for the beginning of the change in the viscoelastic balance within the polymer system (Morrison cited in Cheremisinoff, ed., 1993). Figure 6.7(b) shows the dependence of the damping characteristics, measured from the $\tan \delta$ as a function of temperature. It can be seen that $\tan \delta$ is very low at sufficiently low temperature because the viscosity of rubbers is so high; thus, the movement of the polymer segment and the adjustment of their relative position can hardly take place during the dynamic experiment. When the temperature is increased, the damping curve goes through a maximum and then decreases. The maximum point of damping or $\tan \delta$ curve indicates the glass transition temperature, where the viscosity of the polymer decreases very rapidly and the molecular adjustments take place more easily so that the elastic modulus is decreased (Da Costa et al., 2002). The results from Figure 6.7(b) indicate that the T_g of HNR at various levels of hydrogenation was slightly lower than that of NR. In addition, the value of $\tan \delta$ of HNR and NR was not different, while the $\tan \delta$ of EPDM exhibited the lower value due to the higher ethylene content in EPDM which is related to high values of E' in the transition zone.

The strength of a polymer not only depends on its crystallinity, but it also relates to the crosslink density after the vulcanization process. The storage modulus behavior as a function of temperature for various structural changes in a polymer was reported by Soni (1991, cited in Cheremisinoff, ed., 1993: 176) as shown in Figure 6.8. It indicates that the plateau region of E' curves after the

transition zone exhibits the crosslink density of polymers. The storage modulus in the plateau region at 30°C of NR as reported in Table 6.6 was higher than that of HNR and EPDM. It means that NR has a higher crosslink density than HNR and EPDM.

Table 6.6 Value of T_g , $\tan \delta$ at T_g and Storage Modulus (E') at 30°C of Vulcanized Rubbers

Rubber	T_g (°C)	$\tan \delta$ at T_g	E' at 30°C (MPa)
NR	-48.6	2.01	2.12
HNR60	-50.0	1.90	1.30
HNR80	-50.8	1.88	1.43
HNR90	-51.4	1.93	1.22
EPDM (Keltan 509 x 100)	-32.6	0.94	1.05

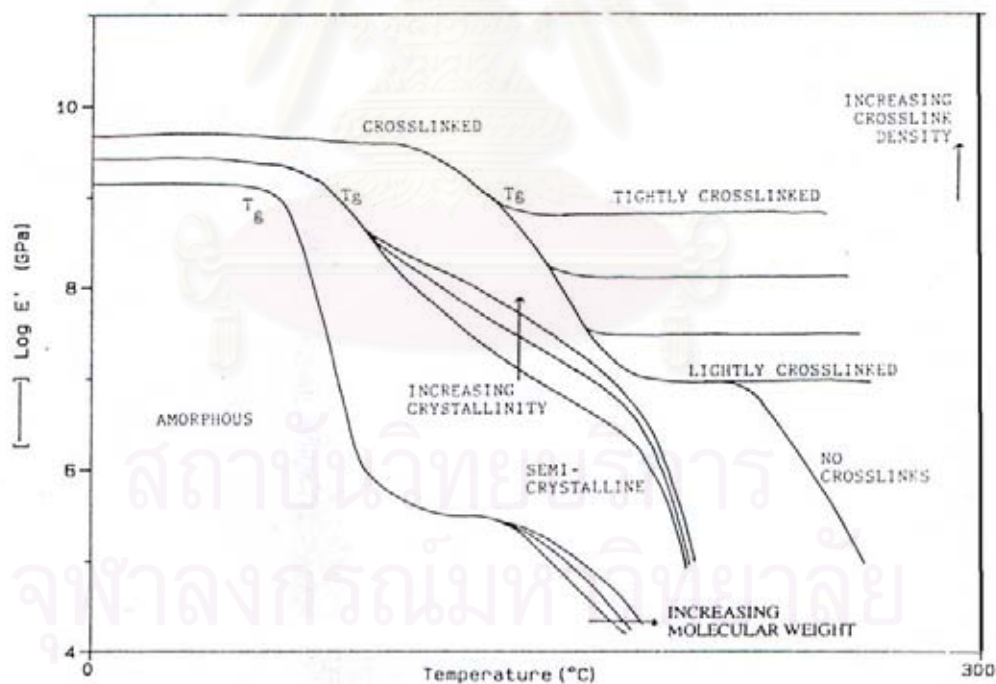


Figure 6.8 Storage modulus behaviors as the function of temperature for various structural changes in polymers (Soni, 1991 cited in Cheremisinoff, ed., 1993: 176).

6.6 Ozone resistance of Vulcanized Hydrogenated Natural Rubber

Many unsaturated rubbers are susceptible to degradation by heat, humidity, light, ozone, radiation etc. (Vinod et al., 2002). Nowadays, the ozone resistance of polymer products becomes of paramount importance because the atmospheric ozone concentration has gradually increased; especially, in industrialized areas (Allen et al., 2003). Ozone presented in the atmosphere at a concentration in the range of 0 – 7 parts per hundred million (pphm) can severely attack on non – resistant rubbers. The series of cracks on the rubber surface develop, over time, which are perpendicular to applied stress (Findik et al, 2004). The various possible reactions related to ozone attack or ozonolysis of diene – containing polymer are summarized as illustrated in Figure 6.9.

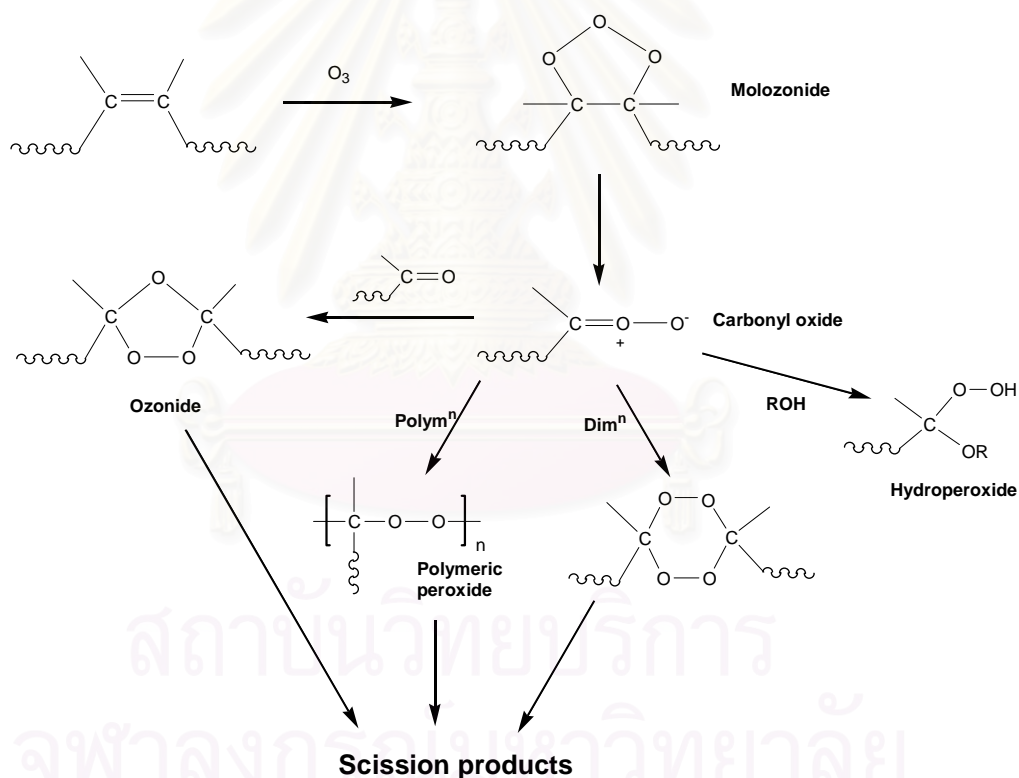


Figure 6.9 Possible reactions following ozonolysis of a diene-containing polymer (Criegee, 1975 cited in Nor and Ebdon, 2000).

Ethylene-propylene rubbers (EPM and EPDM) have a completely saturated hydrocarbon main chain, so they have excellent ozone resistance and very good resistance to heat and oxidation. Although the incorporation of EPDM into a diene rubber such as NR results in a significant improvement in heat and ozone resistance, it has been found that the polymer blends generally exhibit poor mechanical properties due to imbalance incompatibility and phase separation which occur from dissimilarity in polarity of elastomers (Ghosh et al., 2001; El-Sabbagh et al., 2003). To improve the ozone resistance of unsaturated polymers, an attempt has been made to reduce the C=C unsaturation of some elastomers such as acrylonitrile-butadiene rubber (NBR) and styrene-butadiene rubber (SBR) via a hydrogenation reaction. For the case of NR, the structure of NR after the hydrogenation process results is an alternating ethylene-propylene copolymer which is believed to have better ozone resistance.

For the study of the properties of HNR, the hydrogenation of NR catalyzed by $\text{OsHCl}(\text{CO})(\text{O}_2)(\text{PCy}_3)_2$ was carried out in 2-liter reactor. Then, the vulcanized rubbers were investigated for ozone resistance. The vulcanizate of HNR at various levels of hydrogenation were exposed in a HAMPDEN ozone cabinet at 40°C in an atmosphere of 50 ppm by volume of ozone concentration for 3, 6, 24, 27 and 48 h. Before exposure to the ozone atmosphere, the specimens were stretched by 20% in the absence of light for 48 h. The test method follows the ISO 1431 Part 1 and The Physical Testing Standards of Rubbers by Nishi and Nagano (1983). A lens of magnification of about 7 times was used to detect the appearance of cracking. A type of ozone cracking on the rubber surface of each specimen was classified according to Table 6.7. After exposure to the ozone atmosphere at the same condition, the cracking of HNR, NR and EPDM was compared as shown in Table 6.8, Figure 6.10 and 6.11. The test samples having been stretched by 20% strained were exposed to ozonized air in the absence of light to assess the ozone resistance. Characteristic cracking on the surface of the rubber is not observed unless a deformation under stress is imposed during exposure as illustrated in Figure 6.10a and 6.10b.

Table 6.7 Classification of Cracking on Rubber Surface (Nishi and Nagano, 1983)

Number of Cracking	Size and Depth of Cracking
A: a small number of cracking	1. That which cannot be seen with eyes but can be confirmed with 10 times magnifying glass. 2. That which can be confirmed with naked eyes.
B: a large number of cracking	3. That which is deep and comparatively long (below 1 mm). 4. That which is deep and long (above 1 mm and below 3 mm).
C: numberless cracking	5. That which is about to crack more than 3 mm or about to sever.

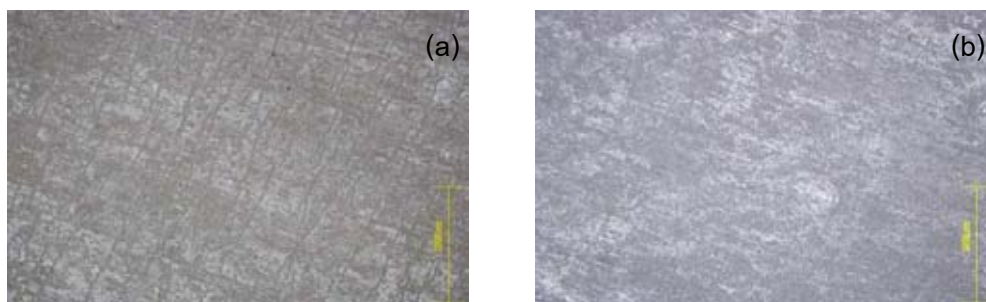
Table 6.8 Ozone Cracking of Vulcanized HNR Compared with NR and EPDM

Rubber	Type of Curing Agents	Type of Cracking				
		3 h	6 h	24 h	27 h	48 h
NR	CBS/TMTD	nc	A-3	A-4	-	B-5
EPDM1	CBS/TMTD	nc	nc	nc	-	nc
HNR94	CBS/TMTD	nc	nc	A-3	-	A-4
NR	MBT/TMTD	nc	C-3	C-3	C-3	C-3
EPDM2	MBT/TMTD	nc	nc	nc	nc	nc
HNR60	MBT/TMTD	nc	nc	C-3	C-3	C-5
HNR80	MBT/TMTD	nc	nc	C-3	C-3	C-5
HNR90	MBT/TMTD	nc	nc	C-3	C-3	C-5
NR/HNR90 (10/90)	MBT/TMTD	nc	C-3	C-3	C-4	C-5
NR/HNR90 (30/70)	MBT/TMTD	nc	C-3	C-3	C-4	C-4

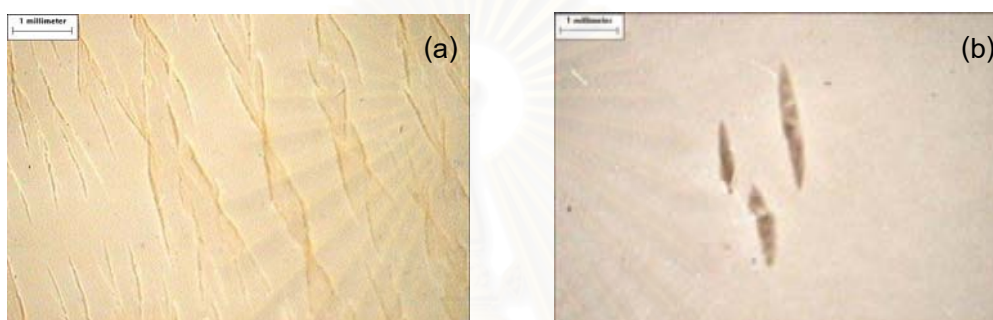
*nc = The number of cracking appeared on the surface of specimens.

**All codes in this table follow the information in Table 6.7.

*** EPDM1 = Keltan 314; EPDM2 = Keltan 509x100.



Before strain (captured by light optical microscope)



After strain of 20% (captured by CCD camera)

Figure 6.10 Surface of rubbers vulcanized by CBS/TMTD curing system after exposure to ozone at 40°C for 48 h: (a) NR and (b) HNR at 94±3% hydrogenation.

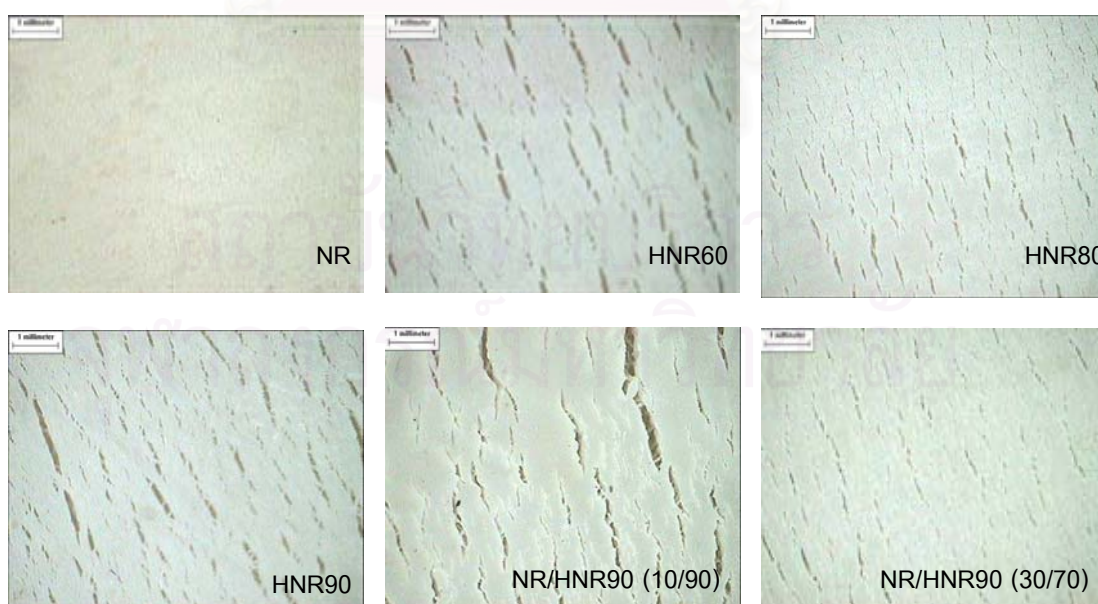
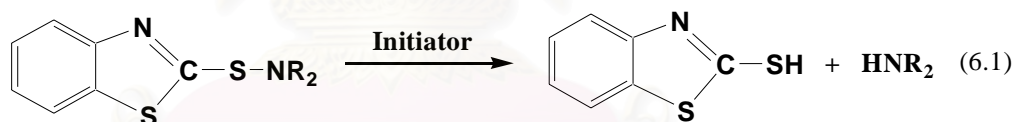
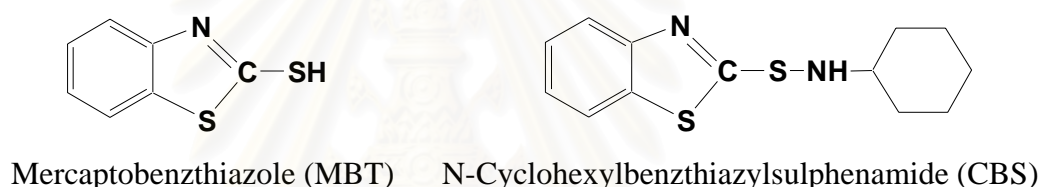


Figure 6.11 Surface of rubbers vulcanized by MBT/TMTD curing system after exposure to ozone for 48 h (captured by CCD camera).

Normally, ozone attacks the unsaturation in hydrocarbon unsaturated polymers by the cleavage of bonds between sp^2 or sp carbon atoms (Allen et al., 2003). Thus, hydrogenated rubbers have been expected to have excellent ozone resistance as well as EPDM, which has a saturated backbone chain. However, the results presented in Table 6.9, Figure 6.10 and Figure 6.11 indicate that the significant cracking appeared on the surface of HNR specimens; although, the level of hydrogenation achieved was more than 90%. It is possible that the residual catalyst, $\text{OsHCl}(\text{CO})(\text{O}_2)(\text{PCy}_3)_2$, residual carbon-carbon double bond and the curing system used are important factors related to the ozonolysis of hydrogenated specimens. Figure 6.10 and Figure 6.11 show that HNR samples vulcanized by the CBS/TMTD system have higher resistance to ozone than by the MBT/TMTD curing system. The structure of MBT and CBS is illustrated as follows:



The plausible mechanism of sulphenamide decomposition in the vulcanization process is shown in eq. 6.1 (Stephens, ed., 1993). The decomposition of sulphenamide generates MBT and amine, presumably gaining the hydrogen from the rubber (Roberts, ed.). It is possible that this amine inhibits the catalytic activity for side reactions such as oxidation of the residual osmium complex used as the catalyst for the hydrogenation process. This was consistent with the results in Table 3.5. In the MBT/TMTD curing system, cracking was apparent on the surface of the specimens for NR and HNR90. It can be explained that the residual osmium complex in HNR90 might catalyze the oxidation of NR in the rubber compound; so the cracking appeared within 6 h of exposure to the ozone atmosphere. This phenomenon also occurred in HNR with high %hydrogenation, HNR90, because of the remaining C=C bonds in its

backbone structure. Thus, a removal process of residual catalysts is required after hydrogenation to avoid the effect of side reactions.



สถาบันวิทยบริการ
จุฬาลงกรณ์มหาวิทยาลัย

CHAPTER 7

CONCLUSIONS AND RECOMMENDATIONS

7.1 Conclusions

7.1.1 Hydrogenation of Natural Rubber Catalyzed by $\text{OsHCl}(\text{CO})(\text{O}_2)(\text{PCy}_3)_2$

$\text{OsHCl}(\text{CO})(\text{O}_2)(\text{PCy}_3)_2$ was found to be an efficient catalyst precursor for natural rubber hydrogenation in chlorobenzene. The kinetic studies showed that the hydrogenation reaction was first order with respect to catalyst concentration, which implied that the active complex was a mononuclear species. In contrast, an increase in rubber concentration reduced the catalytic activity. It is possible that impurities in natural rubber could coordinate to the metal centre to cause the inverse dependence on rubber concentration. The unique behavior of NR hydrogenation catalyzed by $\text{OsHCl}(\text{CO})(\text{O}_2)(\text{PCy}_3)_2$ was first-order with respect to hydrogen pressure which diminished to an inverse behavior dependence at high hydrogen pressure. The hydrogenation rate was dependent on reaction temperature and the activation energy of this process was 122.8 kJ/mol. In addition, the role of carboxylic acid and sulfonic acid in rubber hydrogenation suggested that these acids could assist in helping to prevent the poisoning of $\text{OsHCl}(\text{CO})(\text{O}_2)(\text{PCy}_3)_2$ by the impurities present in natural rubber.

7.1.2 Hydrogenation of Natural Rubber Catalyzed by $[\text{Ir}(\text{cod})(\text{PCy}_3)(\text{py})]\text{PF}_6$

In monochlorobenzene, $[\text{Ir}(\text{COD})(\text{PCy}_3)(\text{py})]\text{PF}_6$ was an effective catalyst for the hydrogenation of natural rubber. The kinetic results indicated that the hydrogenation was first order on hydrogen pressure and first to zero order with respect to catalyst concentration. The reaction rate implied that the active complex is mononuclear at low catalyst concentration and that a side reaction such as dimerization of the Ir catalyst might be occurring at high catalyst loading. The impurities in natural rubber caused the hydrogenation rate to have an inverse behavior

with respect to rubber concentration. The apparent activation energy of the hydrogenation of natural rubber was calculated to be 75.6 kJ/mol. The proposed mechanism and the rate expression for hydrogenation of natural rubber in the presence of $[\text{Ir}(\text{COD})(\text{PCy}_3)(\text{py})]\text{PF}_6$ were consistent with the kinetic data. The relative viscosity of the hydrogenated products indicated that there was probably no degradation for the hydrogenated rubber. However, crosslinking or branching might occur at high hydrogen pressure during the natural rubber hydrogenation.

7.1.3 Thermal Analysis of Hydrogenated Natural Rubber

Differential scanning calorimetry and thermogravimetric analysis were used to characterize the thermal properties of natural rubber and its hydrogenated products. It was found that the degradation temperature of hydrogenated natural rubber increased with increasing level of hydrogenation; while the glass transition temperature of natural rubber after hydrogenation was not different. This demonstrates that hydrogenation increases the thermal stability of natural rubber without affecting its glass transition temperature. The activation energy of decomposition of rubbers was evaluated by using thermogravimetric analysis. The results showed that the higher heating rate caused the higher resistance of thermal degradation due to the oxidation of the surface, which serves as a shield for the bulk of the polymers. The Arrhenius activation energy of natural rubber was lower than that of hydrogenated natural rubber and EPDM. This indicates that hydrogenated natural rubber and EPDM require more energy to break down the chemical bond because of the higher saturation in the structure. However, the rate constant of decomposition of hydrogenated natural rubber was higher than that of EPDM. It is possible that the EPDM backbone with saturated structure has higher thermal stability than hydrogenated natural rubber, which still has some residual carbon-carbon double bonds in its main chain structure.

7.1.4 Physical and Mechanical Properties of Hydrogenated Natural Rubber

The vulcanization of hydrogenated natural rubber compared with natural rubber and commercial EPDM was investigated. The cure characteristics of the rubbers were evaluated by using an oscillating disk rheometer (ODR). The results showed that the hydrogenated natural rubber and EPDM required a higher cure temperature to obtain the appropriate cure time. The optimum cure time of hydrogenated natural rubber increased with increasing level of hydrogenation due to the lower content of carbon-carbon double bonds in its structure. The color of vulcanized rubbers was affected by the curing agents. The color of vulcanizates from CBS/TMTD curing system was darker than that of MBT/TMTD system.

The mechanical properties of vulcanizates from hydrogenated natural rubber and EPDM were not all that different after heat aging at 100°C for 22 hr. This implies that these rubbers are more resistant to heat than natural rubber because of the low saturation level in the backbone chain. The dynamic mechanical properties of vulcanizates indicate that the crystallinity and crosslink density of hydrogenated natural rubber were lower than that of natural rubber, while its glass transition temperature was slightly different from natural rubber.

For the ozone resistance test, the vulcanized hydrogenated natural rubber exhibited cracking on the surface of the specimens; even though, 90% hydrogenation was achieved. The residual carbon double bond, residual osmium catalyst and curing agents are possible factors related to the ozone cracking of hydrogenated rubber. The residual catalyst in the hydrogenation process may catalyze the ozonolysis and caused the cracking on the rubber surface. It was also found that the hydrogenated natural rubber vulcanized by the CBS/TMTD system exhibited less cracking than did the MBT/TMTD system. It was believed that the amine, which was dissociated from the CBS during vulcanization could retard the reactivity of residual osmium catalyst during ozonolysis.

7.2 Recommendations

A further study of the hydrogenation of natural rubber should be concerned with the following aspects:

1. Inhibitor for Osmium Catalyst after Hydrogenation Process

Due to the ozonolysis produced from the residual osmium complex in hydrogenated natural rubber, the amine generated from CBS during vulcanization process has been observed to retard the reactivity of catalyst for ozonolysis reaction. For further research work, other chemicals which may inhibit or stop the activity of catalyst after hydrogenation process should be investigated.

2. Applications of Hydrogenated Natural Rubber

The hydrogenated natural rubber exhibited good resistance to thermal degradation. However the thermal and mechanical properties had to be improved. Other applications of this novel polymer such as grafting or blending with other polymers should be further studied. In addition, the miscibility of blending between hydrogenated natural rubber and other polymers such as polyethylene or polypropylene should also be investigated.

3. Reduction and Recovery of Solvent from Hydrogenation Process

The present hydrogenation process requires the use of a large amount of solvent to dissolve the solid rubber and catalyst. Therefore, the minimization and recovery of solvent used in the hydrogenation process should be further studied to reduce the cost of the operation.

REFERENCES

- Aik-Hwee, E., Tanaka, Y. and Seng-Neon, G. FTIR studies on amino groups in purified *Hevea* rubber. J. Nat. Rubber. Res. 7(2) (1992): 152 – 155.
- Allen, N. S., Edge, M., Mourelatou, D., Wilkinson, A., Liauw, C. M., Parellada, M. D., Barrio, J. A. and Quiteria, V. R. S. Influence of ozone on styrene-ethylene-butylene-styrene (SEBS) copolymer. Polym. Degrad. Stab. 79 (2003): 297 – 307.
- Allen, P. W. and Bristow, G. M. The gel phase in natural rubber. J. Appl. Polym. Sci. 7 (1963): 603 – 615.
- Andriollo, A., Esteruelas, M. A., Meyer, U., Oro, A. L., Delgado, R. A., Sola, E., Valero C. and Werner, H. Kinetic and mechanistic investigation of the sequential hydrogenation of phenylacetylene catalyzed by OsHCl(CO)(PR₃)₂ [PR₃ = PMe-*t*-Bu₂ and P-*i*-Pr₃]. J. Am. Chem. Soc. 111 (1989): 7431 – 7437.
- Bhaduri, S. and Mukesh, D. Homogeneous Catalysis Mechanisms and Industries Applications. (n.p.): Wiley & Sons, 2000.
- Bhattacharjee, S., Bhowmick, A. K. and Avasthi, B. N. Hydrogenation of epoxidized natural rubber in the presence of palladium acetate catalyst. Polymer. 34 (1993): 5168 – 5173.
- Bhattacharjee, S., Bhowmick, A. K. and Avasthi, B. N. Preparation of hydrogenated nitrile rubber using palladium acetate catalyst: its characterization and kinetics. J. Polym. Sci. Part A: Polym. Chem. 30 (1992): 471 – 484.
- Bhowmick, A. K. and Stephens, H. L., eds. Handbook of Elastomers. New York and Basel: Marcel Dekker, 1988.

- Blow, C. M. and Hepburn, C. Rubber Technology and Manufacture. London: Butterworth Scientific, 1982.
- Brydson, J. A. Rubbery materials and their compounds. Essex, England: Elsevier Ltd., 1988.
- Cassano, G. A., Valles, E. M. and Quinzani, L. M. Structure of partially hydrogenated polybutadienes. Polymer. 39 (1998): 5573 – 5577.
- Chang, J. R. and Huang, S. M. Pd/Al₂O₃ catalysts for selectivity hydrogenation of polystyrene-*block*-polybutadiene-*block*-polystyrene thermoplastic elastomers. Ind. Eng. Chem. Res. 37 (1998): 1220 – 1227.
- Charmondusit, K. Hydrogenation of cis-1,4-poly(isoprene) and natural rubber catalyzed by OsHCl(CO)(O₂)(PCy₃)₂ and [Ir(COD)py(PCy₃)]PF₆. Doctoral dissertation, Department of Chemical Technology, Faculty of Science, Chulalongkorn University, 2002.
- Charmondusit, K., Prasassarakich, P., McManus, N. T. and Rempel, G. L. Hydrogenation of cis-1,4-poly(isoprene) catalyzed by OsHCl(CO)(O₂)(PCy₃)₂. J. Appl. Polym. Sci. 89 (2003): 142 – 152.
- Crabtree, R. H. and Davis, M. W. Directing effects in homogeneous hydrogenation with [Ir(cod)(PCy₃)(py)]PF₆. J. Org. Chem. 51 (1986): 2655 – 2661.
- Crabtree, R. H. and Morris, G. E. Some diolefin complexes of iridium (I) and a *trans*-influence series for the complexes [IrCl(cod)L]. J. Organometallic Chem. 135 (1977): 395 – 403.
- Crabtree, R. H. The Organometallic Chemistry of the Transition Metals. New York: John Wiley & Sons, 2001.

- Crabtree, R. H., Felkin H., Fillebeen-Khan, T. and Morris, G. E. Dihydridoiridium diolefin complexes as intermediates in homogeneous hydrogenation. J. Organometallic Chem. 168 (1979): 183 – 195.
- Crabtree, R. H., Felkin, H. and Morris, G. E. Cationic iridium diolefin complexes as alkene hydrogenation catalysts and the isolation of some related hydrido complexes. J. Organometallic Chem. 141 (1977): 205 – 215.
- Crabtree, R. Iridium compounds in catalysis. Acc. Chem. Res. 12 (1979): 331 – 338.
- Cheremisinoff, N. P. ed. Elastomer Technology Handbook. Boca Raton: CRC Press Inc., 1993.
- Da Costa, H. M., Visconte, L. L. Y., Nunes, R. C. R. and Furtado, C. R. G. Mechanical and dynamic mechanical properties of rice husk ash – filled natural rubber compounds. J. Appl. Polym. Sci. 83 (2002): 2331 – 2346.
- Delgado, R. A. S., Rosales, M., Esteruelas, M. A. and Oro, L. A. Homogeneous catalysis by osmium complexes. A review. J. Mol. Cat. A: Chem. 96 (1995): 231 – 243.
- Dickson, R. S. Homogeneous Catalysis with Compounds of Rhodium and Iridium. Dordrecht, Netherlands: D. Reidel, 1985.
- El-Sabbagh, S. H., Compatibility study of natural rubber and ethylene-propylene diene rubber blends. Polymer Testing. 22 (2003) 93 – 100.
- Esteruelas, M. A. and Werner, H. Five- and six-coordinate hydrido(carbonyl)-ruthenium (II) and –osmium (II) complexes containing triisopropylphosphine as ligand. J. Organometallic Chem. 303 (1986): 221 – 231.
- Esteruelas, M. A., Sola, E., Oro, L. A., Meyer, U. and Werner, H. Coordination of H₂ and O₂ to [OsHCl(CO)(PiPr₃)₂]: A catalytically active M(η^2 -H₂) complex. Chem. Int. Ed. Engl. 27 (1988): 1563 – 1564.

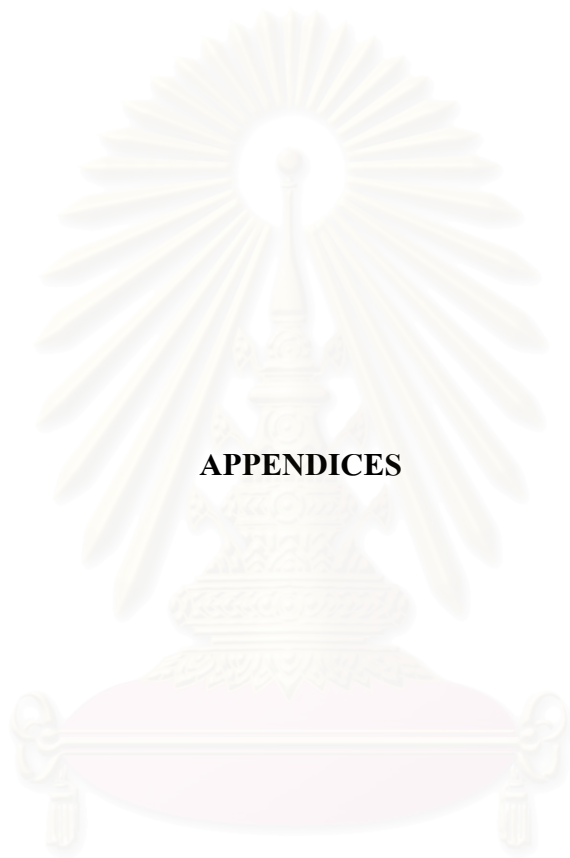
- Findik, F., Yilmaz, R. and Koksall, T. Investigation of mechanical and physical properties of several industrial rubbers. Material & Design, 2004 (In Press).
- Gan, S. N., Subramaniam, N. and Yahya, R. Hydrogenation of natural rubber using nickel 2-ethylhexanoate catalysts in combination with triisobutylaluminum. J. Appl. Polym. Sci. 59 (1996): 63 – 70.
- Gilliom, L. R. Catalytic hydrogenation of polymers in the bulk. Macromolecules. 22 (1989): 662 – 665.
- Gilliom, L. R. Observation of a reaction front in the bulk catalytic hydrogenation of a polyolefin. Macromolecules. 25 (1992): 6066 – 6068.
- Guo, X. Y. and Rempel, G. L. Catalytic hydrogenation of nitrile-butadiene copolymer emulsion. J. Appl. Poly. Sci. 65 (1997): 667 – 675.
- Ghosh, A. K., Debnath, S. C., Naskar, N. and Basu D. K. NR – EPDM covulcanization: A novel approach. J. Appl. Poly. Sci. 81 (2001): 800 – 808.
- Harwood, H. J., Russell, D. B., Verthe, J. J. A. and Zymonas, J. Diimide as a reagent for the hydrogenation of unsaturated polymers. Makromol. Chem. 163 (1973): 1 – 12.
- Hu, J. Catalytic hydrogenation of nitrile butadiene rubber using [Ir(COD)(PCy₃)(py)]PF₆ catalyst. Master thesis, Department of Chemical Engineering, Faculty of Engineering, University of Waterloo, 2000.
- Koch, S., Kempermann, Th. and Sumner, J., eds. Manual for the Rubber Industry. Germany: Bayer AG, 1993.
- Mango, L. A., Lenz, R. W. Hydrogenation of unsaturated polymers with diimide. Makromol. Chem. 163 (1973): 13 – 36.

- Mao T. F. and Rempel, G. L. Catalytic hydrogenation of acrylonitrile-butadiene copolymers by a series of osmium complexes. J. Mol. Cat. A: Chem. 153 (2000): 63 – 73.
- Mao, T. F. and Rempel, G. L. Catalytic hydrogenation of nitrile-butadiene copolymers by cationic rhodium complexes. J. Mol. Cat. A: Chem. 135 (1998): 121 – 132.
- Mark, J. E., Erman, B. and Eirich, F. R. Science and Technology of Rubber. San Diego: Academic Press, 1994.
- Markovic, M. G., Choudhury, N. R., Dimopoulos, M. and Matison, J. Macromolecular modification of EPDM: wettability, miscibility, and morphology study. J. Appl. Polym. Sci. 80 (2001): 2647 – 2661.
- Martin, P., McManus, N. T. and Rempel, G. L. A detailed study of the hydrogenation of nitrile-butadiene rubber and other substrates catalyzed by Ru (II) complexes. J. Mol. Cat. A: Chem. 126 (1997) 115 – 131.
- Mason, R. L.; Gunst, R. F. and Hess, L. H. Statistical Design and Analysis of Experiments. New York: John Wiley & Sons, 1989.
- McManus, N. T. and Rempel, G. L. Chemical modification of polymers: catalytic hydrogenation and related reactions. Rev. Macromol. Chem. Phys. C35(2) (1995): 239 – 285.
- Moers, F. G. A new hydridocarbonyl complexes of osmium (II). J. Chem. Soc., Chem. Commun. (1971): 79.
- Moers, F. G. Ruthenium (II) and osmium (II) complexes of tricyclohexylphosphine. J. Coord. Chem. 13 (1984): 215 – 219.

- Mohammadi, N. A. and Rempel, G. L. Control, data acquisition and analysis of catalytic gas – liquid mini slurry reactors using a personal computer. Comput. Chem. Eng. 11 (1987): 27 – 35.
- Mohammadi, N. A. and Rempel, G. L. Homogeneous Catalytic Hydrogenation of Polybutadiene. J. Mol. Cat. A. 50 (1989): 259 – 275.
- Montgomery, D. C. Design and Analysis of Experiments. New York: John Wiley & Sons, 2001.
- Morton, M., ed. Rubber Technology. New York: Van Nostrand Reinhold Company, 1987.
- Morton, M., ed. Rubber Technology. Dordrecht: Kluwer Academic Publishers, 1999.
- Nang, T. D., Katabe, Y. and Minoura, Y. Diimide reduction of cis-1,4-polyisoprene with *p*-toluenesulphonylhydrazide. Polymer. 17 (1976): 117 – 120.
- Nishi, T. and Nagano, F. The Physical Testing Standards of Rubber. Rubber Research Centre. Document No. 117 (1983): 114 – 121.
- Nor, H. M. and Ebdon, J. R. Ozonolysis of natural rubber in chloroform solution part 1. A study by GPC and FTIR spectroscopy. Polymer 41 (2000): 2359 – 2365.
- Parent, J. S., McManus, N. T. and Rempel, G. L. RhCl(PPh₃)₃ and RhH(PPh₃)₄ catalyzed hydrogenation of acrylonitrile – butadiene copolymers. Ind. Eng. Chem. Res. 35 (1996): 4417 – 4423.
- Parent, J. S., McManus, N. T., Rempel, G. L., Power, W. P. and Marder, T. B. Ligand exchange processes of OsHCl(CO)(L)(PR₃)₂ (L = vacant, H₂, R'CN, O₂; R = Cy, *i*-Pr). J. Mol. Cat. A: Chem. 135 (1998a): 285 – 293.

- Parent, J. S., McManus, N. T. and Rempel, G. L. OsHCl(CO)(O₂)(PCy₃)₂-Catalyzed hydrogenation of acrylonitrile-butadiene copolymers. Ind. Eng. Chem. Res. 37 (1998b): 4253 – 4261.
- Parent, J. S., McManus, N. T. and Rempel, G. L. Selectivity of the OsHCl(CO)(O₂)(PCy₃)₂ catalyzed hydrogenation of nitrile-butadiene rubber. J. Appl. Polym. Sci. 79 (2001): 1618 – 1626.
- Rao, P. V. C., Upadhyay, V. K. and Pillai, S. M. Hydrogenation of polybutadiene catalyzed by RuCl₂(PPh₃)₃ and a structural study. Eur. Polym. J. 37 (2001): 1159 – 1164.
- Roberts, A. D. ed. Natural Rubber Science and Technology. Oxford: Oxford University Press, 1988.
- Sandler, S. R., Karo, W., Bonesteel, J. A. and Pearce, E. M. Polymer Synthesis and Characterization. A Laboratory Manual. (San Diego: Academic Press, 1998), pp.108 – 130, 140 – 147.
- Sarkar, M. D., Mukunda, P. G., De, P. P. and Bhowmick, A. K. Degradation of hydrogenated styrene-butadiene rubber at high temperature. Rubber Chem. Tech. 70(1997): 855 – 870.
- Schulz, D. N., Turner, S. R. and Golub, M. A. Recent advances in the chemical modification of unsaturated polymers. Rubber Chem. Tech. 55 (1982): 809 – 859.
- Singha N. K., De, P. P. and Sivaram, S. Homogeneous catalytic hydrogenation of natural rubber using RhCl(PPh₃)₃. J. Appl. Polym. Sci. 66 (1997): 1647 – 1652.
- Stephens, H. L., ed. Intermediate Rubber Technology Textbook Part II. (n.p.) 1993.

- Stork, G. and Kahne, D. E., Stereocontrol in homogeneous catalytic hydrogenation via hydroxyl group coordination. J Am. Chem. Soc. 105 (1983): 1072 – 1073.
- Stuart, B. H. Polymer Analysis. West Sussex: John Wiley & Sons, 2002.
- Tanaka, Y. Structural characterization of natural polyisoprenes: solve the mystery rubber based on structural study. Rubber Chem. Tech. 74 (2001): 355 – 375.
- Tanaka, Y. Structure and biosynthesis mechanism of natural polyisoprene. Prog. Polym. Sci. 14 (1989): 339 – 371.
- Tangpakdee, J. and Tanaka, Y. Characterization of sol and gel in *Hevea* natural rubber. Rubber Chem. Tech. 70 (1997): 707 – 713.
- Tangthongkul, R. Hydrogenation of synthetic rubber cis-1,4-polyisoprene and natural rubber catalyzed by ruthenium (II) complex. Doctoral dissertation, Department of Chemical Technology, Faculty of Science, Chulalongkorn University, 2003.
- Thai Rubber Association. World Rubber Statistics [online]. Available from: http://www.thainr.com/stat/world_stat_pro.html [2003, May 4].
- Vinod, V. S., Varghese, S. and Kuriakose, B. Degradation behaviour of natural rubber – aluminium powder composites: effect of heat, ozone and high energy radiation. Polym. Degrad. Stab. 75 (2002): 405 – 412.
- Yi, C. S., Lee, D. W. and He, Z. Acid-promoted homogeneous hydrogenation of alkenes catalyzed by the ruthenium-hydride complex $(PCy_3)_2(CO)(Cl)RuH$: evidence for the formation of 14-electron species from the selective entrapment of the phosphine ligand. Organometallics. 19 (2000): 2909 – 2915.



APPENDICES

สถาบันวิทยบริการ
จุฬาลงกรณ์มหาวิทยาลัย

Appendix A

The Overall Compositions of Rubbers

Table A-1 Properties of Standard Thai Rubber 5L (STR-5L)

Parameter	Limit
Dirt, retained on 44 μ aperture (max, % wt.)	0.04
Ash (max, % wt.)	0.40
Nitrogen (max, % wt.)	0.60
Volatile matter (max, % wt.)	0.80
Initial Plasticity, P0	35
Plasticity Retention Index, PRI (min.)	60
Color Lavibond Scale, individual value (max.)	6.0

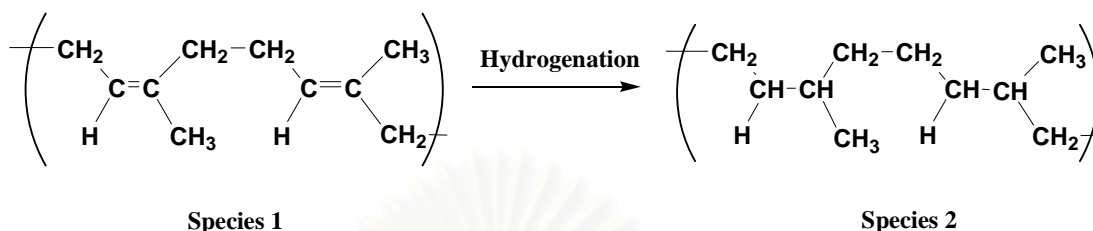
Table A-2 Properties of Ethylene-Propylene-Diene Copolymer

Properties	Typical Values	
	Keltan 509x100	Keltan 314
Type of termonomer	ENB*	ENB
Content of termonomer (% wt.)	8.7	8.0
Ethylene content (% wt.)	64	52
Oil content (% wt.)	50	0
Molecular weight distribution	Medium	Broad
Mooney viscosity	48	33
ML(1+4) 125°C (MU)		

* Ethylidenenorbonene

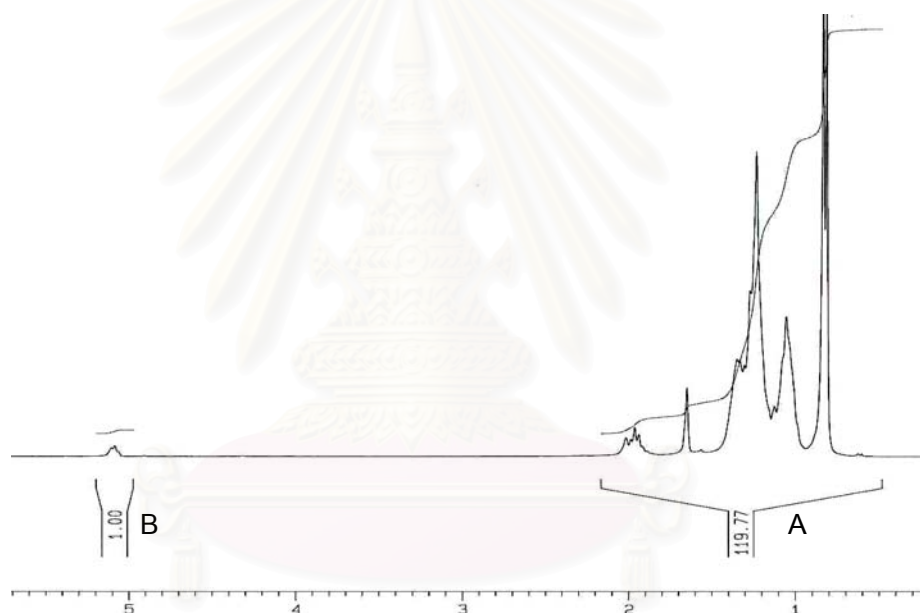
Appendix B

Calculation of % Hydrogenation



Proton of repeating unit except =CH in Species 1 = 7 protons

Proton of repeating unit in Species 2 = 10 protons



A = Peak area except at 5.2 ppm

B = Peak area at 5.2 ppm

C = Peak area of saturated $-\text{CH}_2-$ and $-\text{CH}_3$

$$A = 10C + 7B$$

$$C = \frac{A - 7B}{10}$$

Total peak area = Peak area of saturated $-\text{CH}_2-$ and $-\text{CH}_3$ + Peak area at 5.2 ppm

$$= \frac{A - 7B}{10} + B$$

$$= \frac{A + 3B}{10}$$

%Hydrogenation = [(Peak area of sat. -CH₂- and -CH₃)/(Total peak area)] x 100

$$= \frac{\left(\frac{A - 7B}{10}\right)}{\left(\frac{A + 3B}{10}\right)} \times 100$$

$$= \frac{A - 7B}{A + 3B} \times 100$$

For example: A = 119.77 and B = 1.00

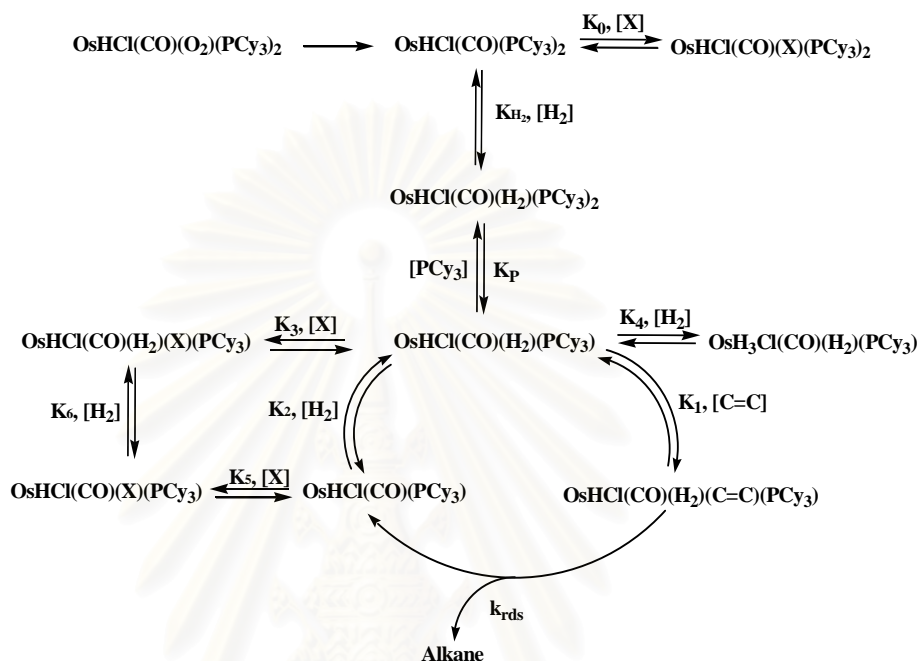
$$\begin{aligned} \text{\%Hydrogenation} &= \frac{119.77 - 7(1.00)}{119.77 + 3(1.00)} \times 100 \\ &= 91.85\% \end{aligned}$$

สถาบันวิทยบริการ
จุฬาลงกรณ์มหาวิทยาลัย

Appendix C

Derivation of the Rate Law from the Proposed Kinetic Model

1) Hydrogenation of natural rubber catalyzed by $\text{OsHCl}(\text{CO})(\text{O}_2)(\text{PCy}_3)_2$



Using the steady state assumption for reaction intermediates, the following equilibria define the concentration of each catalytic species related the rate determining step.

$$-\frac{d[\text{C}=\text{C}]}{dt} = k_{\text{rds}} [\text{OsHCl}(\text{CO})(\text{H}_2)(\text{C}=\text{C})(\text{PCy}_3)] \quad (1.1)$$

$$[\text{OsHCl}(\text{CO})(\text{H}_2)(\text{PCy}_3)] = \frac{[\text{OsHCl}(\text{CO})(\text{C}=\text{C})(\text{PCy}_3)]}{K_1[\text{C}=\text{C}]} \quad (1.2)$$

$$[\text{OsHCl}(\text{CO})(\text{H}_2)(\text{PCy}_3)_2] = \frac{[\text{OsHCl}(\text{CO})(\text{H}_2)(\text{C}=\text{C})(\text{PCy}_3)][\text{PCy}_3]}{K_1 K_p [\text{C}=\text{C}]} \quad (1.3)$$

$$[\text{OsHCl}(\text{CO})(\text{PCy}_3)_2] = \frac{[\text{OsHCl}(\text{CO})(\text{H}_2)(\text{C}=\text{C})(\text{PCy}_3)][\text{PCy}_3]}{K_1 K_p K_{\text{H}_2} [\text{C}=\text{C}][\text{H}_2]} \quad (1.4)$$

$$[\text{OsHCl}(\text{CO})(\text{X})(\text{PCy}_3)_2] = \frac{K_0[\text{X}][\text{OsHCl}(\text{CO})(\text{H}_2)(\text{C}=\text{C})(\text{PCy}_3)][\text{PCy}_3]}{K_1 K_p K_{\text{H}_2} [\text{C}=\text{C}][\text{H}_2]} \quad (1.5)$$

$$[\text{OsHCl}(\text{CO})(\text{PCy}_3)] = \frac{[\text{OsHCl}(\text{CO})(\text{H}_2)(\text{C}=\text{C})(\text{PCy}_3)]}{K_1 K_2 [\text{H}_2][\text{C}=\text{C}]} \quad (1.6)$$

$$[\text{OsHCl}(\text{CO})(\text{X})(\text{PCy}_3)] = \frac{K_5[\text{X}][\text{OsHCl}(\text{CO})(\text{H}_2)(\text{C}=\text{C})(\text{PCy}_3)]}{K_1 K_2 [\text{H}_2][\text{C}=\text{C}]} \quad (1.7)$$

$$[\text{OsHCl}(\text{CO})(\text{H}_2)(\text{X})(\text{PCy}_3)] = \frac{K_3[\text{X}][\text{OsHCl}(\text{CO})(\text{H}_2)(\text{C}=\text{C})(\text{PCy}_3)]}{K_1 [\text{C}=\text{C}]} \quad (1.8)$$

$$[\text{OsH}_3\text{Cl}(\text{CO})(\text{H}_2)(\text{PCy}_3)] = \frac{K_4[\text{H}_2][\text{OsHCl}(\text{CO})(\text{H}_2)(\text{C}=\text{C})(\text{PCy}_3)]}{K_1 [\text{C}=\text{C}]} \quad (1.9)$$

A material balance on the osmium charged to the system yields:

$$\begin{aligned} [\text{Os}]_T = & [\text{OsHCl}(\text{CO})(\text{H}_2)(\text{C}=\text{C})(\text{PCy}_3)] + [\text{OsHCl}(\text{CO})(\text{H}_2)(\text{PCy}_3)] + [\text{OsHCl}(\text{CO})(\text{PCy}_3)_2] \\ & + [\text{OsHCl}(\text{CO})(\text{H}_2)(\text{PCy}_3)_2] + [\text{OsHCl}(\text{CO})(\text{X})(\text{PCy}_3)_2] + [\text{OsHCl}(\text{CO})(\text{PCy}_3)] \\ & + [\text{OsHCl}(\text{CO})(\text{H}_2)(\text{X})(\text{PCy}_3)] + [\text{OsHCl}(\text{CO})(\text{X})(\text{PCy}_3)] + [\text{OsH}_3\text{Cl}(\text{CO})(\text{H}_2)(\text{PCy}_3)] \end{aligned} \quad (1.10)$$

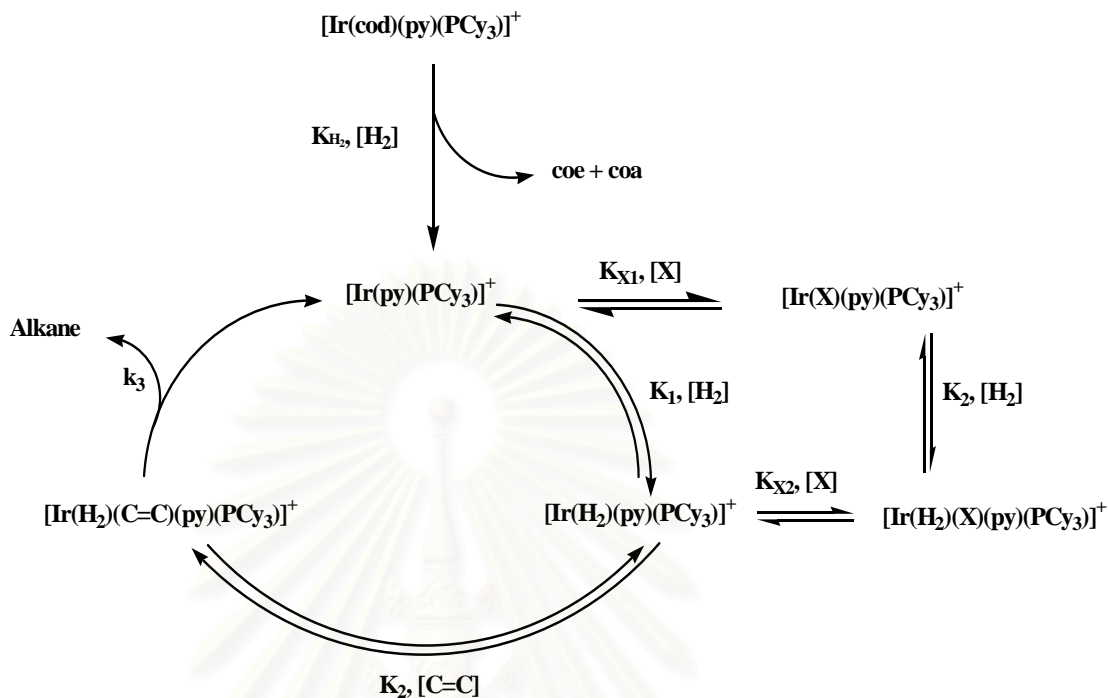
The osmium species in eq. (1.10) are substituted by eq. (1.2) to eq. (1.9) as shown in eq. (1.11).

$$[\text{Os}]_T = A \left\{ \frac{K_2 K_p K_{\text{H}_2} [\text{H}_2] (1 + K_1 [\text{C}=\text{C}] + K_2 [\text{PCy}_3] (1 + K_{\text{H}_2} [\text{H}_2] + K_0 [\text{X}] + K_p K_{\text{H}_2} (1 + K_5 [\text{X}] + K_2 K_3 [\text{H}_2][\text{X}] + K_2 K_4 [\text{H}_2]^2))}{K_1 K_2 K_p K_{\text{H}_2} [\text{H}_2][\text{C}=\text{C}]} \right\} \quad (1.11)$$

$$\text{Given } A = [\text{OsHCl}(\text{CO})(\text{H}_2)(\text{C}=\text{C})(\text{PCy}_3)]$$

The relationship of the hydrogenation rate to the operating conditions can be derived by substitution of eq. (1.11) into eq. (1.1) which is the rate determining step of the process.

$$-\frac{d[\text{C}=\text{C}]}{dt} = \frac{k_{\text{rds}} K_1 K_2 K_p K_{\text{H}_2} [\text{Os}]_T [\text{H}_2][\text{C}=\text{C}]}{K_2 K_p K_{\text{H}_2} [\text{H}_2] (1 + K_1 [\text{C}=\text{C}] + K_p K_{\text{H}_2} (1 + K_2 K_3 [\text{X}][\text{H}_2] + K_5 [\text{X}] + K_2 K_4 [\text{H}_2]^2) + K_2 [\text{PCy}_3] (1 + K_{\text{H}_2} [\text{H}_2] + K_0 [\text{X}])} \quad (1.12)$$

2) Hydrogenation of natural rubber catalyzed by $[\text{Ir}(\text{cod})(\text{PCy}_3)(\text{py})]\text{PF}_6$ 

From the steady state assumption for intermediates, the concentrations of each catalytic species can be expressed in term of $[\text{Ir}(\text{H}_2)(\text{C}=\text{C})(\text{py})(\text{PCy}_3)]^+$ in the rate determining equation as shown in eq. (2.1).

$$-\frac{d[\text{C}=\text{C}]}{dt} = k_3 [\text{Ir}(\text{H}_2)(\text{C}=\text{C})(\text{py})(\text{PCy}_3)]^+ \quad (2.1)$$

$$[\text{Ir}(\text{H}_2)(\text{py})(\text{PCy}_3)]^+ = \frac{[\text{Ir}(\text{H}_2)(\text{C}=\text{C})(\text{py})(\text{PCy}_3)]^+}{K_2 [\text{C}=\text{C}]} \quad (2.2)$$

$$[\text{Ir}(\text{py})(\text{PCy}_3)]^+ = \frac{[\text{Ir}(\text{H}_2)(\text{C}=\text{C})(\text{py})(\text{PCy}_3)]^+}{K_1 K_2 [\text{C}=\text{C}] [\text{H}_2]} \quad (2.3)$$

$$[\text{Ir}(\text{X})(\text{py})(\text{PCy}_3)]^+ = \frac{K_{X1} [\text{X}] [\text{Ir}(\text{H}_2)(\text{C}=\text{C})(\text{py})(\text{PCy}_3)]^+}{K_1 K_2 [\text{C}=\text{C}] [\text{H}_2]} \quad (2.4)$$

$$[\text{Ir}(\text{H}_2)(\text{X})(\text{py})(\text{PCy}_3)]^+ = \frac{K_{X2} [\text{X}] [\text{Ir}(\text{H}_2)(\text{C}=\text{C})(\text{py})(\text{PCy}_3)]^+}{K_2 [\text{C}=\text{C}]} \quad (2.5)$$

A material balance on the iridium charged to the system yields:

$$[\text{Ir}]_T = [\text{Ir}(\text{H}_2)(\text{C}=\text{C})(\text{py})(\text{PCy}_3)]^+ + [\text{Ir}(\text{H}_2)(\text{py})(\text{PCy}_3)]^+ + [\text{Ir}(\text{py})(\text{PCy}_3)]^+ \\ + [\text{Ir}(\text{X})(\text{py})(\text{PCy}_3)]^+ + [\text{Ir}(\text{H}_2)(\text{X})(\text{py})(\text{PCy}_3)]^+ \quad (2.6)$$

The iridium species in eq. (2.6) are substituted by eq. (2.2) to eq. (2.5) as shown in eq. (2.7).

$$[\text{Ir}]_T = [\text{Ir}(\text{H}_2)(\text{C}=\text{C})(\text{py})(\text{PCy}_3)] \left[\frac{\text{K}_1[\text{H}_2](1 + \text{K}_2[\text{C}=\text{C}] + \text{K}_{x_2}[\text{X}] + 1 + \text{K}_{x_1}[\text{X}])}{\text{K}_1\text{K}_2[\text{C}=\text{C}][\text{H}_2]} \right] \quad (2.7)$$

The relationship of the hydrogenation rate to the operating conditions can be derived by substitution of eq. (2.7) into eq. (2.1). The rate law of reaction is illustrated in eq. (2.8).

$$-\frac{d[\text{C}=\text{C}]}{dt} = \frac{k_3\text{K}_1\text{K}_2[\text{Ir}]_T[\text{C}=\text{C}][\text{H}_2]}{1 + \text{K}_{x_1}[\text{X}] + \text{K}_1[\text{H}_2](1 + \text{K}_2[\text{C}=\text{C}] + \text{K}_{x_2}[\text{X}])} \quad (2.8)$$

สถาบันวิทยบริการ
จุฬาลงกรณ์มหาวิทยาลัย

Appendix D

Calculation of Decomposition Kinetic Parameters by Thermogravimetry

This calculation follows the method in ASTM E 1641 – 99 to determine the kinetic parameters such as Arrhenius activation energy and preexponential factor by thermogravimetry, based on the assumption that the decomposition obeys first-order kinetics. Hydrogenated natural rubber with 95.6% conversion obtained by using $\text{OsHCl}(\text{CO})(\text{O}_2)(\text{PCy}_3)_2$ as the catalyst is used for an example.

- (1) Record the degradation temperatures at 10% of constant mass loss at different heating rate as showed in Figure D-1 and Table D-1.

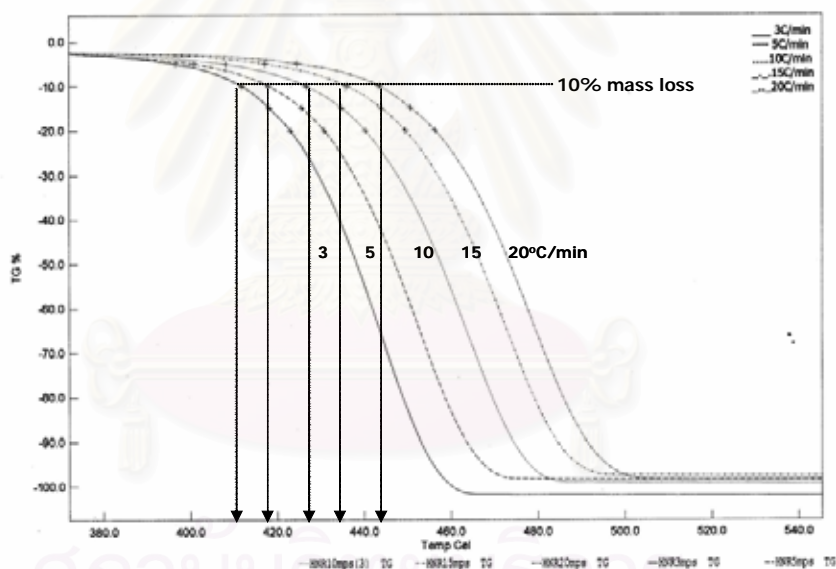


Figure D-1 Mass loss curves of hydrogenated natural rubber with 95.6% hydrogenation at various heating rates.

Table D-1 Degradation Temperatures of Hydrogenated Natural Rubber with 95.6% Hydrogenation at Various Heating Rates

Heating Rate (°C/min)	3	5	10	15	20
Degradation Temperature (°C)	412.1	418.2	426.8	436.0	444.0

- (2) Plot the logarithm of the heating rate expressed as Kelvin per min versus the reciprocal of the absolute degradation temperature obtained from (1) at which the conversion level was reached. A straight line as shown in Figure D-2 should result.

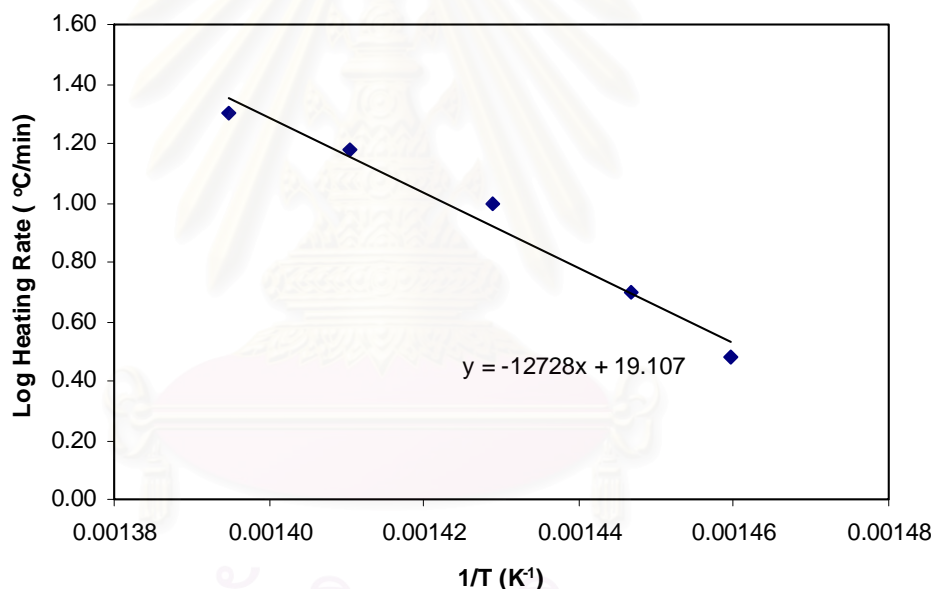


Figure D-2 Arrhenius plot of heating rate versus degradation temperature at the constant %mass loss.

- (3) Use the least-squares method fit a straight line to these data and determine the slope of this line.

$$\begin{aligned} \text{From data of (1): Slope} &= \frac{\Delta(\log\beta)}{\Delta(1/T)} \text{ where } \beta \text{ is the heating rate.} \\ &= -12728 \end{aligned}$$

- (4) Calculate an estimation of the activation energy (E) as shown in eq. (D-1), making use of the value of slope obtained from (3).

$$E = -\left(\frac{R}{b}\right)\left(\frac{\Delta(\log\beta)}{\Delta(1/T)}\right) \quad (\text{D-1})$$

where R = gas constant, 8.314 J/(mol*K)

b = approximation derivative from Table D-2

(use b = 0.457/K on first iteration)

$$E = -\left(\frac{8.314}{0.457}\right)(-12728) = 231554.91 \text{ J/mol}$$

- (5) Calculate the value for E/RT_c where T_c = the temperature at constant for the heating rate closet to the midpoint of the experimental heating rates.

$$T_c = 426.8^\circ\text{C} (699.8^\circ\text{C})$$

$$E/RT_c = 231554.91 / (8.314 \times 699.8)$$

$$= 39.80$$

- (6) Estimate a new value of b from the Table D-2 and resubmit this value to eq. (D-1).

$$\text{new } b = 0.45584$$

$$E = -\left(\frac{8.314}{0.45584}\right)(-12728)$$

$$= 232144.16 \text{ J/mol}$$

- (7) Repeat (5) and (6) until the activation energy change by less than 1%.

$$E \text{ for this example} = 232.15 \text{ kJ/mol}$$

$$E/RT_c = 39.90$$

Table D-2 Numerical Integral Constants (ASTM E 1641 – 99)

E/RT	a	$b(1/K)$
8	5.3699	0.5398
9	5.8980	0.5281
10	6.4167	0.5187
11	6.928	0.511
12	7.433	0.505
13	7.933	0.500
14	8.427	0.494
15	8.918	0.491
16	9.406	0.488
17	9.890	0.484
18	10.372	0.482
19	10.851	0.479
20	11.3277	0.4770
21	11.803	0.475
22	12.276	0.473
23	12.747	0.471
24	13.217	0.470
25	13.686	0.469
26	14.153	0.467
27	14.619	0.466
28	15.084	0.465
29	15.547	0.463
30	16.0104	0.4629
31	16.472	0.462
32	16.933	0.461
33	17.394	0.461
34	17.853	0.459
35	18.312	0.459
36	18.770	0.458
37	19.228	0.458
38	19.684	0.456
39	20.141	0.456
40	20.5967	0.4558
41	21.052	0.455
42	21.507	0.455
43	21.961	0.454
44	22.415	0.454
45	22.868	0.453
46	23.321	0.453
47	23.774	0.453
48	24.226	0.452
49	24.678	0.452
50	25.1295	0.4515
51	25.5806	0.4511
52	26.0314	0.4508
53	26.4820	0.4506
54	26.9323	0.4503
55	27.3823	0.4500
56	27.8319	0.4498
57	28.2814	0.4495
58	28.7305	0.4491
59	29.1794	0.4489
60	29.6281	0.4487

- (8) Calculate the pre-exponential factor, A, using eq. (D-2) and the value of exponent, a, obtained from Table D-2.

$$A = -\left(\frac{\beta'}{E}\right) * R * \ln(1 - \alpha) * 10^a \quad (\text{D-2})$$

where α = conversion value of decomposition

$$a = 20.551$$

$$\begin{aligned} A &= -\left(\frac{10}{232154.34}\right) * 8.314 * \ln(1 - 0.1) * 10^{20.551} \\ &= 1.34 \times 10^{16} \end{aligned}$$

- (9) Calculate the rate constant of decomposition, k.

$$\begin{aligned} k &= A e^{-E/RT_c} = (1.34 \times 10^{16}) e^{-232154.34 / (8.314 \times 699.8)} \\ &= 0.063 \text{ min}^{-1} \end{aligned}$$

สถาบันวิทยบริการ
จุฬาลงกรณ์มหาวิทยาลัย

Appendix E

Steps of Rubber Blending

Table E-1 Steps of Blending for Each Formulation in Brabender Plasticorder

Components	Time of Components Addition into Mixer (min.)					
	Mix1	Mix2	Mix3 – 5	Mix6	Mix7	Mix8 – 9*
	NR1	EPDM	HNR	NR2	HNR94	NR/HNR90
Adding rubber	0	0	0	0	0	0 – 2
Paraffinic oil	No**	No	0	No	0	2
Ultrablend 6000	No	No	No	No	0	No
ZnO/ Stearic acid	5	1	2	5	6	5
MBT/TMTD or CBS/TMTD	7	3	4	7	8	7
S	9	4	6	9	10	9
Removing rubber	14	7	9	14	15	12

*Mix8 – 9 mixed NR with HNR90.

**No = No addition of that component.

สถาบันวิทยบริการ
จุฬาลงกรณ์มหาวิทยาลัย

Appendix F

Mechanical Properties of Vulcanizates

Table F-1 Tensile Strength of Vulcanizates

	NR		EPDM		HNR60		HNR80		HNR90	
	Unaged	Aged	Unaged	Aged	Unaged	Aged	Unaged	Aged	Unaged	Aged
Tensile	3.03	1.91	0.85	0.82	0.46	0.51	0.51	0.70	0.67	0.70
Strength	3.88	2.01	0.79	0.80	0.59	-	0.88	0.71	0.52	0.63
(MPa)	2.23	1.77	-	0.81	0.67	-	0.71	0.56	0.89	0.60
Means	3.05	1.90	0.82	0.81	0.57	0.51	0.70	0.66	0.69	0.64
S.D.	0.83	0.12	0.04	0.01	0.11	-	0.19	0.08	0.19	0.05

Table F-2 Ultimate Elongation of Vulcanizates

	NR		EPDM		HNR60		HNR80		HNR90	
	Unaged	Aged	Unaged	Aged	Unaged	Aged	Unaged	Aged	Unaged	Aged
Ultimate	302.5	155.3	148.4	118.0	38.0	44.6	56.5	69.2	112.3	80.1
Elongation	400.2	158.7	126.5	119.6	76.9	-	104.4	74.4	50.2	85.1
(%)	226.1	148.1	-	142.7	78.0	-	80.9	51.4	144.6	78.7
Means	309.6	154.0	137.5	126.8	64.3	44.6	80.6	65.0	102.4	81.3
S.D.	87.3	5.41	15.5	13.8	22.8	-	24.0	12.1	48.0	3.36

Table F-3 Hardness of Vulcanizates

	NR		EPDM		HNR60		HNR80		HNR90	
	Unaged	Aged	Unaged	Aged	Unaged	Aged	Unaged	Aged	Unaged	Aged
Hardness	42.6	46.5	33.1	33.8	33.9	34.5	38.4	39.3	36.4	36.0
(Shore A)	44.2	48.6	33.3	34.6	33.9	34.9	38.9	39.1	37.0	37.0
	43.8	46.3	33.5	34.1	34.1	34.0	38.6	39.5	35.9	36.6
	43.1	46.0	33.9	34.9	34.6	35.3	38.5	39.3	36.9	36.6
	42.6	45.5	33.6	34.9	34.3	34.4	38.5	39.4	36.3	36.1
Means	43.3	46.6	33.5	34.5	34.2	34.6	38.6	39.3	36.5	36.5
S.D.	0.72	1.19	0.30	0.49	0.30	0.50	0.19	0.15	0.45	0.41

สถาบันวิทยบริการ
จุฬาลงกรณ์มหาวิทยาลัย

VITA

Miss Napida Hinchiranan was born on October 15, 1978 in Bangkok, Thailand. She graduated with a Bachelor's degree of Science from Department of Chemical Technology, Faculty of Science, Chulalongkorn University in 2000. She has continued her study in Ph.D. program at Department of Chemical Technology, Faculty of Science, Chulalongkorn University since 2000 and finished her study in 2005.



สถาบันวิทยบริการ
จุฬาลงกรณ์มหาวิทยาลัย